Azeotropic Pressure Swing Distillation

vorgelegt von:

Dipl.-Ing. Andreas Klein
aus Berlin

Von der Fakultät III - Prozesswissenschaften
der Technischen Universität Berlin

zur Erlangung des akademischen Grades
Doktor der Ingenieurwissenschaften

- Dr. - Ing. -

genehmigte Dissertation.

Promotionsausschuß:
Vorsitzender: S. Enders
Gutachter: G. Wozny
Gutachter: E. Sørensen

Tag der wissenschaftlichen Aussprache: 14. April 2008

Berlin 2008
D83

I. Preface

Die vorliegende Arbeit entstand während meiner Tätigkeit als wissenschaftlicher Mitarbeiter am Fachgebiet Dynamik und Betrieb technischer Anlagen des Instituts für Prozess- und Verfahrenstechnik der Technischen Universität Berlin.

Bei meinem Doktorvater Professor Dr.-Ing. Günter Wozny möchte ich mich herzlich für die Betreuung, die wertvollen Anregungen und die Unterstützung bedanken. Er stand immer als Ansprechpartner zur Verfügung und gewährte mir stets einen großen wissenschaftlichen Gestaltungsspielraum.

Frau Dr. Eva Sørensen vom University College London danke ich für die Übernahme des Koreferats.

Frau Prof. Dr. Sabine Enders danke ich für die Übernahme des Prüfungsvorsitzes.

Besonderer Dank gilt Dr.-Ing. Jens-Uwe Repke für die Unterstützung und ausgezeichnete Zusammenarbeit.

Ich bedanke mich bei allen Freunden, Kollegen und Mitarbeitern für die freundliche und ausgezeichnete Zusammenarbeit und Unterstützung. Besonderer Dank gilt hier Marita Skupin für die Unterstützung im Technikum, Daniel Weissmann für die Unterstützung in Rechnerfragen, sowie der Werkstatt Dietmar Plotka, Max Zeidler und Lutz Heise, ohne die so manche Umbaumaßnahme nicht realisiert worden wäre und Inge Habisreitinger für Ihre Unterstützung in organisatorischen Fragen. Außerdem danke ich Mike und Gisela Palmer für das Korrekturlesen der Arbeit und die hilfreichen Tipps im Umgang mit der englischen Sprache.

Ohne den Einsatz der Studentinnen und Studenten, die im Rahmen von Praktika, Studien- und Diplomarbeiten und als Hilfskräfte mit mir zusammengearbeitet haben, wäre diese Arbeit in dieser Form nicht möglich gewesen. Ihnen gilt an dieser Stelle mein besonderer Dank.

Für die finanzielle Unterstützung sei der Max-Buchner Forschungsstiftung und dem Pipes-Programm gedankt.

Schließlich gilt mein größter Dank meiner Frau Haike und meinen Eltern, die mich mit viel Geduld und Liebe bei dieser Arbeit unterstützt haben.

Berlin, August 2008 Andreas Klein

Haike

und

meinen Eltern

II. List of symbols

Table II.1. Latin letters.

symbol	unit	description
A	[m²]	area
A, B, C, D	[-]	parameters for properties equation
A_i, B_i, C_i, D_i, E_i,	[-]	vapor pressure equation parameters
B	[mol]	bottom product
C_P	[J/kgK]	specific heat capacity
C_O	[-]	outflow parameter
C_{OW}	[-]	weir over flow parameter
D	[mol]	distillate amount
e	[-]	error
E	[-]	enhancement factor
f	[-]	function for data reconciliation (side condition)
F	[mol]	feed amount
F	[-]	F-factor
F_e	[-]	enhancement factor
$\dot{F}$	[mol/h]	feed flow rate
G	[-]	Lagrangian function
Δg_{ij}	[-]	NRTL interaction parameter
g	[m/s²]	earth gravity
h	[J/mol]	specific enthalpy
H	[J]	enthalpy
h^{LV}	[KJ/mol]	heat of vaporization
h_{ow}	[mm]	weir over height
h_f	[mm]	froth height
h_w	[mm]	weir height
HU	[mol]	hold up

Table II.1. Latin letters.

symbol	unit	description
K_p	[-]	gain
K_i	[-]	K-factor
$\dot{K}$	[mol/h]	stream on shell side (HP)
$\dot{L}$	[mol/h]	liquid flow rate
L	[mol]	liquid amount
l_w	[m]	weir length
level	[m]	level
M	[kg]	mass
$\tilde{M}$	[g/mol]	mol mass
$\dot{m}$	[kg/h]	mass stream
MT	[K]	MT-function
MX	[mol/mol]	MX-function
NC	[-]	number of components
P	[bar]	pressure
Δp	[mbar]	pressure drop
P_{0i}^{LV}	[bar]	vapor pressure
Δp_d	[mbar]	dry pressure drop
Δp_h	[mbar]	hydrostatic pressure drop
Δp_r	[mbar]	rest pressure drop
Δp_B	[mbar]	acceleration pressure
Δp_h	[mbar]	hydraulic pressure drop
Δp_a	[mbar]	acceleration pressure drop
Δp_{2ph}	[mbar]	two phase pressure drop
Q	[J]	energy
$\dot{Q}$	[kW/h]	energy amount
r	[J/mol]	heat of vaporization
R	[mol/h]	reflux stream
R_L	[-]	reflux ratio at the top of the column
R_V	[-]	reboil ratio at the bottom of the column
S	[-]	main function for data reconciliation
S	[-]	bubble formation factor
t	[h]	time
T	[K]	temperature
u(t)	[-]	system input
u	[J/mol]	internal energy
V	[mol]	vapor amount
$\dot{V}$	[mol/h]	vapor flow rate

Table II.1. Latin letters.

symbol	unit	description
V_G	[m³/kmol]	molar vapor volume
V_L	[l/kmol]	molar liquid volume
v_i^L	[m³/kmol]	molar volume (Wilson)
Vol	[m³]	volume
w	[m/s]	velocity
w(t)	[-]	reference
w	[kg/kg]	weight fraction
x	[mol/mol]	mol fraction (liquid phase)
x*	[-]	mass flow ratio $\frac{\dot{m}^V}{\dot{m}_{com}}$
X_m	[-]	Martinelli parameter
y	[mol/mol]	mol fraction (vapor phase)
y(t)	[-]	system output
z	[mol/mol]	mol fraction (feed)

Table II.2. Greek letters.

symbol	unit	description
α_{ij}	[-]	relative volatility; separation factor $\frac{K_i}{K_j} = \frac{y_i/x_i}{y_j/x_j}$
α_{film}	[W/m²K]	heat transfer coefficient of the film
α_{pipe}	[W/m²K]	heat transfer coefficient of the pipe
α_B	[W/m²K]	heat transfer coefficient, nucleate boiling part
α_C	[W/m²K]	heat transfer coefficient, convective part
α_{ij}	[-]	randomness parameter (NRTL)
γ_i	[-]	activity coefficient
δ_m	[-]	standard deviation
ε	[-]q	volumetric ratio $\frac{Vol^V}{Vol_{com}}$
ζ^V	[-]	resistance coefficient
η	[-]	tray efficiency by Murphree
η	[Pas]	viscosity
ϑ	[°C]	temperature
Λ_{ij}	[-]	parameter (Wilson)
λ	[-]	Lagrangian factor
λ	[W/mK]	thermal conductivity
$\Delta\lambda_{ji} - \lambda_{ii}$	[-]	Wilson interaction parameter
ν	[-]	reflux ratio

Table II.2. Greek letters.

symbol	unit	description
Π_{oi}	[-]	Pointing correction
ρ	[kg/m³]	density
σ	[N/m	surface tension
τ_{ij}	[-]	NRTL parameter
τ_R	[-]	reset time
φ_{0i}	[-]	fugacity coefficient of the pure substance
φ_i	[-]	fugacity coefficient
φ_{2ph}^{V}	[-]	correction factor hydrostatic pressure

Table II.3. Subscripts.

symbol	description
*	equilibrium state
2ph	two phase
az	azeotropic
B	bottom
boil	boiling point
tot	total / overall
cond	condenser
CW	cooling water
D	distillate
e	end of process
F	feed
film	liquid film
G	gas
HP	high pressure column
i	component, input stream
in	inlet
initial	initial state
inside	inside
inv	inverted
j	output streams
k	number of trays
K	shell side
L	liquid
linear	linear
loss	loss
LP	low or ambient pressure column
max	maximal
min	minimal
n	tray

Table II.3. Subscripts.

symbol	description
new	new value
old	old value
optimal	optimal
out	outlet
P	permeate
pipe	pipe (condenser, reboiler)
R	retentate
reb	reboiler
ref	reference
reg	regular
set	set point
stat	stationary
steel	steel
Σ	summation
V	vapor
val	validated
vap	vapor
W	wall

Table II.4. Dimensionless numbers.

symbol	description
Nu	Nusselt number
Re	Reynolds number
Pr	Prandtl number

Table II.5. Abbreviations.

symbol	description
AIB	advanced inverted batch
AIB4x	advanced inverted batch, with quad feed flow rate and column square area
NIB	normal inverted batch
NIBdF	normal inverted batch, with double feed flow rate and column square area
NIBeq	normal inverted batch, but the feed tank volume is equal to the feed volume flow rate
NIB4x	normal inverted batch, with quad feed flow rate and column square area
RB	regular batch with additional feed tank
RB-bB	regular batch with a big reboiler tank, with out additional tank at the bottom
RB-bBeq	same as RB-bB, but the feed tank volume is equal to the feed volume flow rate
RB-bB4x	same as RB-bB, but with quad capacity, this means a quad square column area, and a quad vapor volumetric flow rate

Table II.5. Abbreviations.

symbol	description
CHE	coupled heat exchanger
PSD	pressure swing distillation
PCS	process control system

1. Introduction

The distillation process is the most used thermal unit operation in industry. In 1992 in the US alone more than 40,000 rectification columns were in use [Humphrey & Seibert 1992], which constituted 7% of the whole energy demands of the USA (4.8 billion BTU - energy). The Office of Industrial Technology - USA sees an energy saving potential of up to 53 Mrd. BTU till 2020 with the help of useful research [Ozokwelu 2002, Porter 1995, Darton 1992]. Moreover 60 - 80 % of the energy demands of all thermal separation units for the production of chemical components are used for the distillation processes [Sattler & Feindt 1995]. Distillation is mainly applied for the treatment of main- and by-products of reactions, recycling of resources and also for the preparation of high and highest purity products. It is an application in the commodity chemical industry as well as in the fine and special chemical industry, as in the pharmaceutical and food industry.

Most of the mixtures have non-ideal behavior, so the separation will only be possible with a great complexity concerning plant, automation and equipment. The systematic feed back inside these systems makes the process control and automation very complex and the design of the system challenging. But the use of distillation columns for the separation of such non-ideal mixtures, especially the separation of homogenous azeotropic mixtures are common in the chemical industry [Hamad & Dunn 2002, Frank 1997]. In the past the research has added a lot of alternatives to the distillation, like membrane processes, adsorption processes (preparative chromatography)..., but in the future distillation will also be one of the main unit operations in thermal separation especially for the

separation of non-ideal liquid mixtures in big dimensions [Fair 1987, Widagdo & Seider 1996].

In the literature pressure swing distillation is often mentioned as an alternative process to the widely applied azeotropic or extractive distillation [Widagdo & Seider 1996]. However, despite the theoretical fundamental knowledge [Abu-Eishah & Luyben 1984], only a few very restricted experimental data have been published and so far the pressure swing distillation process is not well studied. Especially for the discontinuous operation (the batch operation) and here for the inverted batch process as I know, no experimental data have been published.

The pressure swing distillation (PSD) uses the dependency of azeotropic composition on the system pressure to break the azeotrope. The main advantages of these processes compared to the other is, that no additional substances (entrainer) have to be used. The PSD process can be operated in continuous or in discontinuous mode and also in semi-continuous mode [Phimister & Seider 2000]. For the continuous operation a heat integration is possible which can save energy, but it has a greater demand on automation. The discontinuous process is much simpler to control and operate. The discontinuous process has two main possible design concepts, the regular and the inverted batch operation. To get an idea which process structure is the most feasible for the separation an easy approach for a fast and simple decision making is needed.

This unit operation is not widely used in industry used but the PSD process has a high potential because of the possible energy savings (continuous process) and the simple process structure (discontinuous process).

The objective of this work is the analysis, evaluation and comparison of the discontinuous and the continuous operation concerning design, process control concepts, energy demands and complexity and feasibility, to expand the experimental data basis and the theoretical knowledge of the PSD process and to get industrial relevant data and better process understanding. To close the gaps and solve the problems mentioned above, the present work will first reduce the lack of missing experimental data and than discuss the different PSD processes in detail to get more knowledge of this unit operation.

The work is structured into the following parts. It starts with the state of the art with an overview of the publication and a description of the main process structures of the PSD process (**chapter 2**). In **chapter 3** a basic model and a rigorous dynamic model with start-up from cold and empty will be introduced and described in detail. These two approaches will first help finding the feasible batch structure for a given PSD case and second will give the possibility to design a good process control structure for the continuous process. It follows in **chapter 4** the experimental validation of the different models. That includes first experimental results for batch PSD processes as well as the validation of the start-up processes of the continuous totally heat integrated columns system. In **chapter 5** the continuous process will be analysed concerning possible process control concepts and process design concepts, which will also be evaluated. Here it can be shown that a process control concept can handle feed concentration changes into the other distillation region in a very stable way. The chapter ends with a detailed analysis of the start-up concepts. The main challenge lies in the coupling of the columns during start-up. To do so, heuristics were developed to start-up pressure swing column systems

including heat and mass integration. The discontinuous pressure swing distillation process is discussed in **chapter 6**. As well as for the continuous process the process control concepts and the process designs will be discussed and analyzed. The main improvement in inverted batch design is the introduction of the advanced batch structure. Furthermore the start-up of the batch processes is discussed. The focus lies here in the automatic switching of the controllers. The different batch design concepts will be compared in a simulations study using an analytical as well as the rigorous dynamic model. The comparison of both concepts, the continuous and the discontinuous process follows in **chapter 7**. The potential of the heat integration discussed for the pressure swing distillation leads to the idea to uses this concept with other unit operation as well. So in the last **chapter 8** a new way of using an energy integration concept for a Hybrid-process composed of a distillation and a pervaporation unit will be introduced, including a first feasibility study, also for the example of the homogenous azeotropic mixture acetonitrile / water as an alternative process concept to the pressure swing distillation process mainly discussed in this work. Finally in **chapter 9** a summary of all results and an outlook for further studies in the range of azeotropic separation is given.

In conclusion the main contributions from this work are the new experimental data for the continuous and especially for the discontinuous pressure swing distillation processes, the development and verification of a stable process control structure for the heat- and mass-integrated continuous process with energy savings up to 45%, the heuristically analysis of the start-up process of the coupled system including PCS visualization for the operator, the analytical method for a first and fast comparison of the regular and inverted batch process, the verification of a reasonable use of the inverted batch column in case of pressure swing distillation and the transfer of the heat integration concept to other separation processes like hybrid processes.

2. State of the art

The modern research on distillation concentrates mostly on the separation of non ideal mixtures with focus on the azeotropic separation [Widagdo & Seider 1996]. The separation of azeotropic mixtures with help of distillation is the most important unit operation in chemical and pharmaceutical industry and also in the pharmaceutical and the food industry. It is also used in the commodity chemical industry as well as in the fine and special chemical industry.

The literature focus on different unit operations for the separation of azeotropic mixtures, such as extractive distillation, azeotropic distillation, heterogeneous azeotropic distillation, vacuum distillation and the pressure swing distillation. Furthermore a combination of different unit operations is possible. These processes are called hybrid processes. It can be a combination of distillation and membrane. A detailed survey on azeotropic distillation concerning homogenous as well as heterogeneous azeotrops is done by Widagdo and Seider [Widagdo & Seider 1996]. An overview about different unit operations for the separation of azeotropic mixtures can be found in Sattler and Lei [Sattler & Feindt 1995, Lei et al. 2005]. An overview about azeotropic mixtures which can be separated especially with the pressure swing process can be found in [Lei et al. 2005, Frank 1997, Horsely & Gould 1973].

The main topic of this work is the separation of homogenous azeotropic mixtures by pressure swing distillation (PSD). The PSD can be operated in three different modes, the discontinuous (batch) mode, the semi-continuous mode, and the continuous mode [Phimister & Seider 2000, Phimister & Seider 2001]. In the literature the pressure swing distillation process is called an very energy-

consuming process against the other unit operation with use of an entrainer, but with help from the energy integration the pressure swing distillation process can become an economically reasonable solution [Gmehling & Kolbe 1992].

In this chapter the different possible distillation processes for the separation of an azeotropic mixture will be introduced. Followed by a detailed description of the pressure swing process. It ends with an introduction on the topic of start-up operation strategies of distillation columns. Other unit operations for the separation of azeotropic mixtures will not be addressed in this work.

2.1 Separation of azeotropic mixtures

To separate close boiling mixtures, there is a need of an increasing number of stages in the column and an increasing reflux ratio, if the relative volatility $\alpha_{i,j}$ converge to one ($\alpha_{i,j} \rightarrow 1$). Then an economical reasonable separation is not possible with simple distillation. Especially the separation at the azeotropic point is not possible, because of the reason that the relative volatility $\alpha_{i,j}$ is equal to one. This means that the concentrations in each phase remains constant. A good definition of the azeotropic state is given by Rowlinson [Rowlinson 1969]:

„... an azeotropic state is defined as a state in which mass transfer occurs between phases while the composition of each phase remains constant, but not necessarily equal.“

A separation through the azeotropic point in one column can not be done. There is a need for different unit operation for such kind of problems. For a main classification of azeotropic distillation operation we can distinguish between unit operation with use of an entrainer (extractive distillation and azeotropic distillation) and without an entrainer (Vacuum distillation and pressure swing distillation). All these unit operations have in common that the azeotropic point is shifted in the liquid phase or erased [Sattler & Feindt 1995, Lei et al. 2005, Stichlmair & Fair 1998].

There exist three types of azeotropic mixtures, the heterogeneous and the low boiling and the high boiling homogeneous azeotropic mixtures. Homogeneous azeotrops have one liquid phase, heterogeneous azeotrops separate into two liquid phases at the azeotropic point. These mixtures have a miscibility gap (Fig. 2.1). For low-boiling (e.g. acetonitrile/water) azeotrops the azeotropic mixture is separated from the top of the column and the pure product from the bottom of the column. For high-boiling azeotrops it is the other way around. The product is at the top, the azeotropic mixture at the bottom of the column (e.g. water/nitric acid). The ten most produced basic products in Germany (methanol, benzene, toluene, xylene, acetic acid, ...) generate over 120 homogeneous azeotropic mixtures [VCI 2006, Ponton 2007], so there is a big industrial relevance for the separation of homogeneous azeotropic mixtures. In this work I will concentrate on low boiling azeotrops because most azeotrops - especially those encountered in solvent recycling applications - fall in this category [Frank 1997].

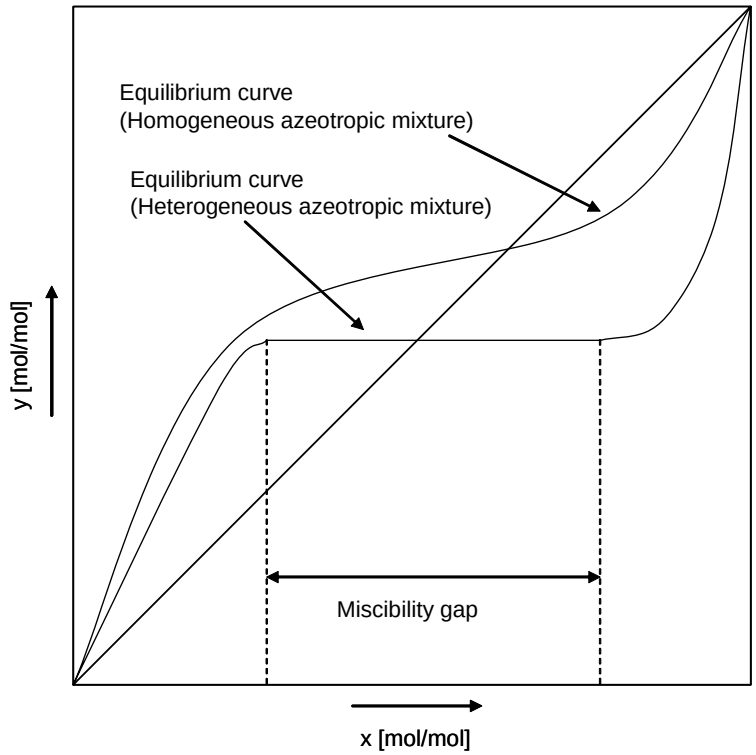

Fig. 2.1 Comparison of the equilibrium curves for a homogeneous and heterogeneous azeotropic mixture.

2.1.1 Extractive distillation

For the separation of homogeneous close boiling or azeotropic mixtures, *extractive distillation* could be used. A low volatile liquid is added to the mixture as an entrainer to increase the volatility over the whole concentration region by decreasing the partial pressure or the volatility of one component. The main problem of the process is the choice of the right entrainer. The entrainer has to fulfil many different properties. The boiling point of the entrainer must be much higher than the boiling points of the other components, it has to be thermal stable, cheap and non toxic, to mention only the main characteristics [Düssel & Warter 1998]. In general, it is difficult and expensive to use an entrainer because of the additional recycling process. This means additional investment and operation costs and a more complex automation (Fig. 2.2).

The newest type of *extractive distillation* uses ionic liquids as an entrainer. The main advantage of ionic liquids is the absence of its own vapor pressure, so it is easy to separate them from vaporizable liquids. Because of their saline character, they have a big influence on the phase equilibrium. It is much easier to shift azeotropic points or create miscibility gaps [Beste et al. 2005, Jork et al. 2004, Seiler et al. 2004].

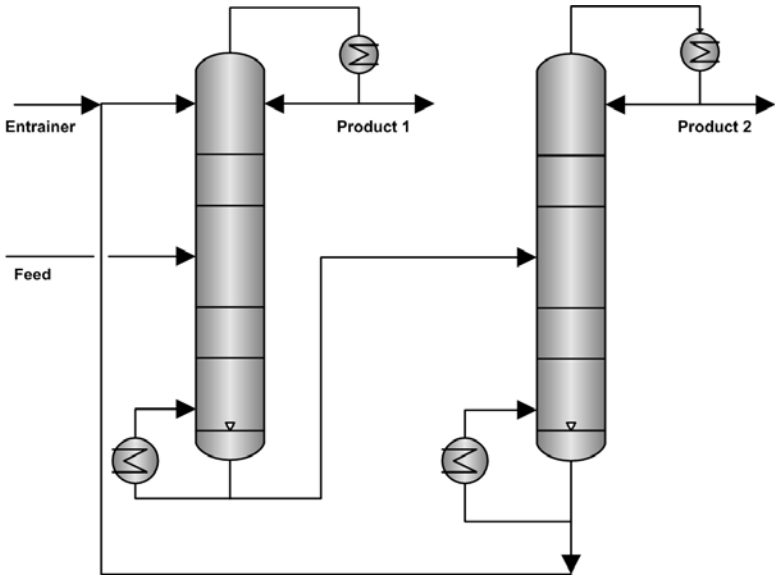

Fig. 2.2 Extractive distillation plant.

2.1.2 Azeotropic distillation

In contrast to the *extractive distillation* the *azeotropic distillation* uses an entrainer to create a heterogeneous low boiling azeotrope with one of the original components [Knapp & Doherty 1992, Lei et al. 2005]. In this case the phase separation of the condensed vapor is used. For this a decanter on top of the column is necessary. Both liquid phases have

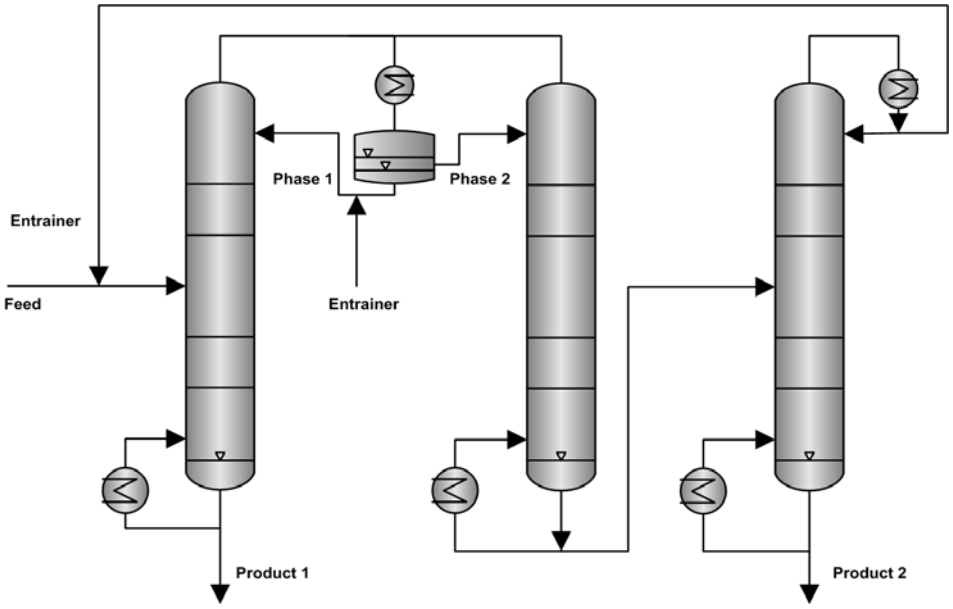

Fig. 2.3 Azeotropic distillation plant.

different concentrations of entrainer. For example the light phase has more entrainer with more low boiling liquid and in the other phase has more high boiling liquid inside. Each phase is

separated in a different column to get pure products and recycle of the entrainer at the same time. So in this constellation the process structure sketched in Fig. 2.3 will be used.

The main disadvantage of the *azeotropic distillation* against the *extractive distillation* is the higher energy demand because of the vaporization of the entrainer [Hoffmann 1964, Onken 1975, Doherty & Caldarola 1985, Lei et al. 2005].

2.1.3 Vacuum distillation

If it is possible to shift the azeotropic point with temperature change induced from a pressure change, a pressure reduction in the column can be used. The azeotropic point shifts to higher concentrations of the low boiling component and it is also possible to erase the azeotrope. The disadvantages of the *vacuum distillation* are mainly the costs of the process and the complexity of the process because of the vacuum, so it is not often used [Grassmann et al. 1997].

2.1.4 Other processes

One possibility is the use of a combination of different unit operations, called *hybrid processes* [Strube et al. 2004]. This means for example a combination of distillation and membrane process [Rautenbach & Vier 1996, Kreis & Gorak 2005, Zerry et al. 2005, Barakat et al. 2006, Klein et al. 2006]. These kind of processes are currently under development and a main topic of the research on thermal separation technology. It has a great potential for development. The *hybrid process* consisting of a distillation and a pervaporation will be discussed in the last chapter (chapter 8) as an additional application for a heat integrated process like the continuous pressure swing distillation.

Mixtures that have naturally a heteroazeotrope does not need any entrainer for the separation. The distillation column system is similar to that described in the section *Azeotropic distillation* without the entrainer recycle column. In this case without an entrainer the operation is called *Heteroazeotropic distillation* [Sattler & Feindt 1995].

Table 2.1. Literature overview on azeotropic separation (selection).

Topic	Reference
Azeotropic mixtures	Lei 2005, Sattler 1995, Frank 1997, Horley 1973, Ponton 2007
Azeotropic separation - general	Sattler 1995, Widagdo 1996, Lei 2005
Extractive distillation	Düssel 1998, Hoffmann 1964, Beste 2005, Seiler 2004, Luyben 2005
Azeotropic distillation	Knapp 1992, Hoffmann 1964, Onken 1975, Doherty 1985
Separation using additional salt	Furter 1972
Vacuum distillation	Grassmann 1997
Hybrid-process (membrane/ distillation)	Strube 2004, Rautenbach 1996, Kreis 2005, Zerry 2005, Sørensen 2006, Klein 2006
Pressure swing distillation - general	Phimister 2000, Phimister 2001, Lei 2005, Luyben 2005

The azeotropic composition can also be influenced be a non-mixable inert gas stream. The components of the mixture in vaporous condition go through the inert gas with different velocities. Therefore, a separation is possible. This separation process is called *diffusion distillation* [Sattler & Feindt 1995].

At least the azeotropic mixture can be erased by adding salt to the mixture, but, as well as for the processes with entrainer, the additional component has to recycled [Furter 1972].

The table 2.1 below gives an overview about the main references on the topic of azeotropic separation.

2.2 Pressure swing distillation

The pressure swing distillation (PSD) is a process for the separation of homogeneous azeotropic mixtures and is focused in this work and will be described now in detail.

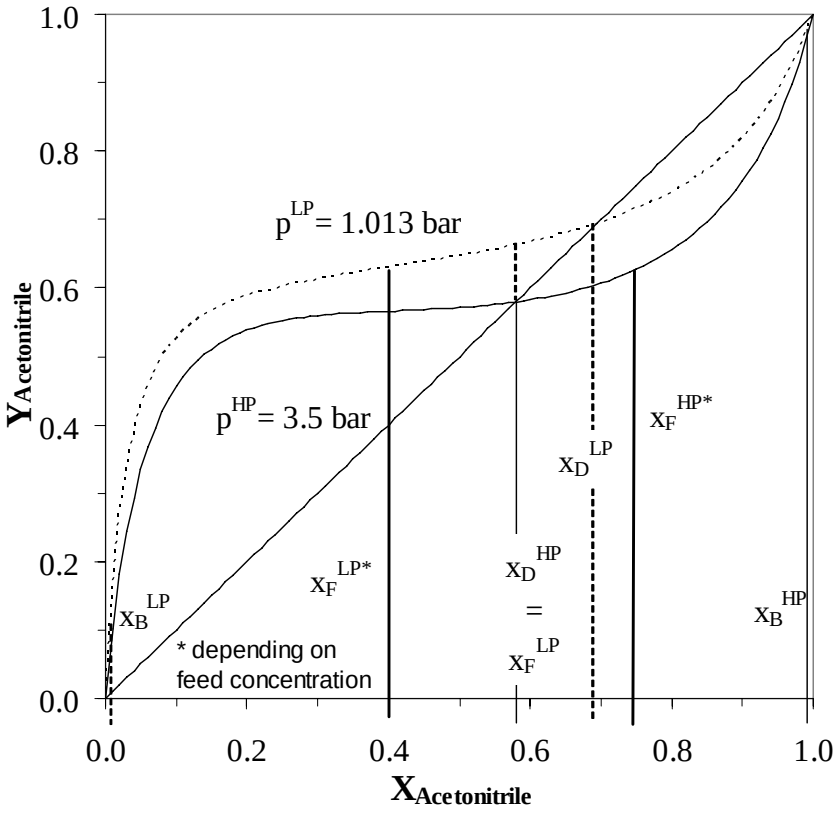

Fig. 2.4 T-x,y-diagram of the mixture acetonitrile-water at different pressures (pressure sensitivity of the azeotropic point), equilibrium and Antoine data from [Gmehling et al. 1981].

The PSD process uses the pressure sensitivity of the binary azeotropic point [Sattler & Feindt 1995, Lei et al. 2005]. If the pressure is increased, the azeotropic point shifts to lower concentrations of the low boiling component. So a separation of the azeotropic mixture

at different pressures is possible (Fig. 2.4)[1]. In this work the mixture acetonitrile/water is used as an example for a low-boiling homogeneous azeotropic mixtures.

Depending on the feed composition based on the component acetonitrile, the feed concentration could be lower or higher than the azeotropic point. The effect is that it is possible to get two different high-boiling products. If the feed concentration is lower than the azeotropic point, the bottom product is water and above the bottom product is acetonitrile. For the process structure this means that in the continuous case two columns operating at two different pressures are needed or in the discontinuous case one column operating at two different pressures in at least two loops. The operation of the different cases are described in detail later in this chapter.

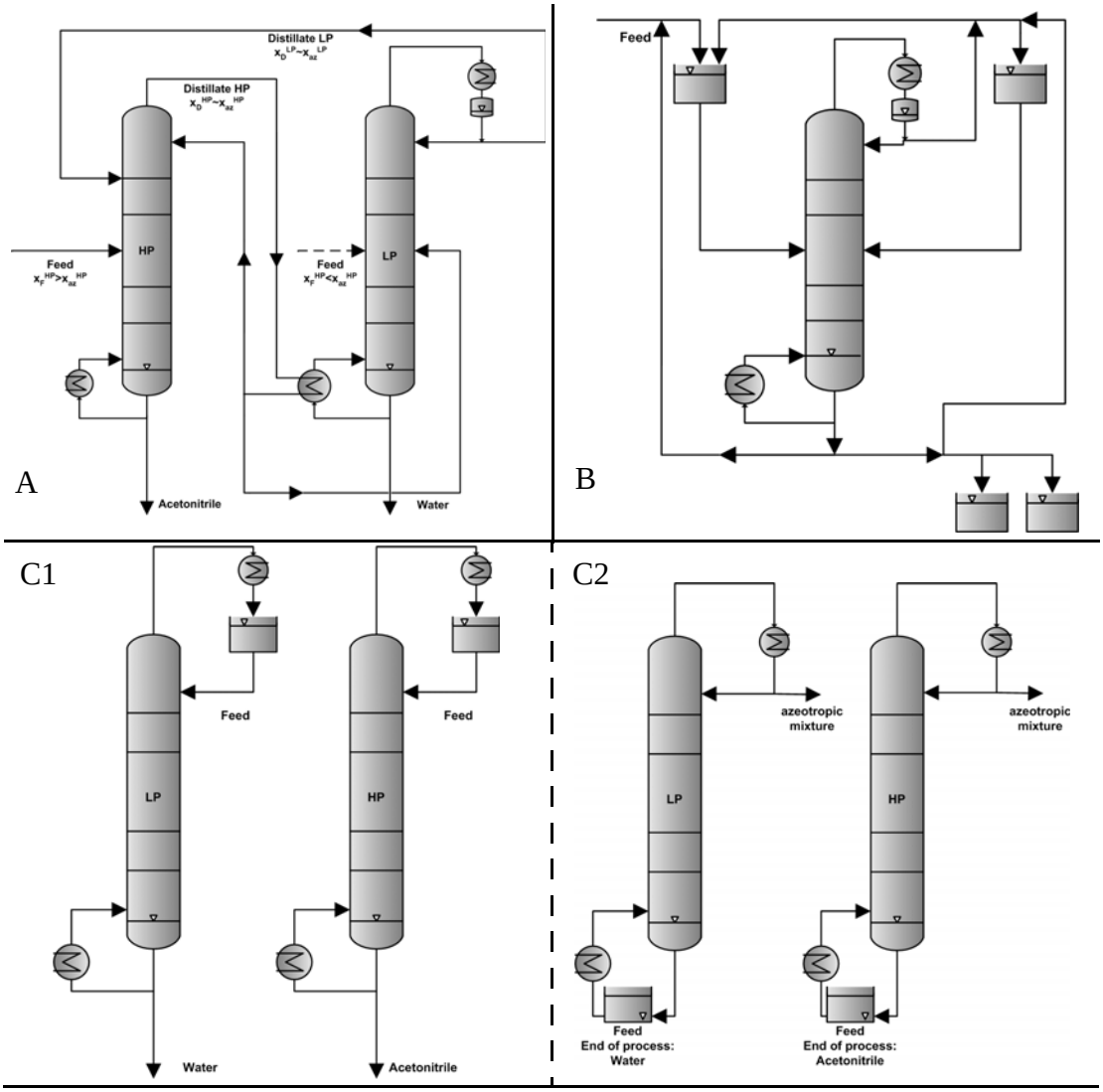

Fig. 2.5 Pressure swing distillation; A: continuous, B: semi continuous, C1: discontinuous (inverted), C2: discontinuous (regular).

1. The curves are calculated with gProms™ with the in chapter 3 introduced equilibrium model.

The main advantage of the PSD process is the process intensification which means an abdication of an entrainer and therefore a reduction of columns and stages for the recycling of the entrainer. Furthermore there is a possibility of heat integration for the continuous process. In this case the heat of the condenser of the high pressure column (HP) is used for heating up the low pressure column (LP). The disadvantages of the process are a higher complexity of the process and a more complex automation, therefore the development of applicable process control strategies are much more difficult. There is also a gap of experimental data in the literature and industrial applications are seldom published. An overview about industrial applications and PSD-suitable azeotropic mixtures is given in table 2.2. There is a big relevance for industry using this process. One possible reason why process designers do not consider PSD is that azeotropic data frequently are not available at non-atmospheric pressures and the generating of such data is expensive [Frank 1997]. To solve the problem of missing azeotropic data see the work of [Wasylkiewicz et al. 2003]. Wasylkiewicz and his co-author developed an algorithm that applies bifurcation theory together with an arc length continuation and a rigorous stability analysis. This method is a robust scheme for finding all homogeneous as well as heterogeneous azeotrops predicted by a thermodynamic model at a specified pressure. Also a lot of research is done to expand the thermodynamical properties data bases for pure components and mixtures [Gmehling et al. 1981, Ponton 2007, Gmehling 2004].

Table 2.2. Examples of PSD binary azeotrops [Lei et al. 2005, Frank 1997, Knapp & Doherty 1992, Horsely & Gould 1973][a].

azeotropic Mixture
tetrahydofuran (THF) / water[i]
acetonitrile / water[i]
methanol / methyl ethyl ketone (MEK)[i]
acetone / methanol[i]
ethanol / ethyl acetate[s]
benzene / isopropanol[s]
ethanol / 1,4-dioxane[s]
aniline / octane
phenol / butyl acetate
propanol / cyclohexane
methanol / ethyl acetate
MEK / benzene
propanol / toluene
acetic acid / toluene
carbon tetrachloride / ethyl acetate

a. i = industrial application; s = suitable mixture

Only one example for the separation of THF-water is found by [Abu-Eisha & Luyben 1984]. Abu-Eisha compares the energy demand of a non-energy integrated system with an energy integrated system. The result was a reduction of the energy demand by two. Furthermore, he

introduces a controller structure for the heat integrated system with use of an additional evaporator at the low pressure column. He does not use a complete heat integration as is done in this work. The different possibilities of heat integration and the process control strategies are the main part of chapter 5.1.

In spite of the theoretical knowledge [Abu-Eisha & Luyben 1984] reliable experimental studies cannot be found in the literature. This could be another reason why the pressure swing distillation is not used very often in industry. A good overview of the advantages of this process is also found in [Frank 1997] and [Lei et al. 2005].

In principle the pressure swing distillation can be operated in three different modes (Fig. 2.5), the continuous [Widagdo & Seider 1996, Abu-Eisha & Luyben 1984], the discontinuous [Robinson & Gilliland 1950, Mutjaba 2004] and the semi-continuous process [Phimister & Seider 2000, Phimister & Seider 2001]. The focus in this work is on the analysis and comparison of the continuous and the discontinuous processes. The discontinuous process can be divided into two different operation structures, the regular and the inverted batch structure. The different structure of the continuous and the discontinuous process will be described now in detail.

2.2.1 Continuous pressure swing distillation

Two columns are in operation for the continuous pressure swing distillation system at two different pressures (Fig. 2.4, Fig. 2.5-A). Feed streams with different concentrations have to be put into the suitable column, depending on the concentration under or above the azeotropic point. For concentrations under the azeotropic point, the feed is put into the low pressure column. For concentrations above the azeotropic point the feed has to be put into the high pressure column. In both columns pure product is withdrawn from the bottom, acetonitrile from the bottom of the high pressure column and pure water from the bottom of the low pressure column. At the top of the columns there are azeotropic mixtures with concentrations depending on the pressure in the column. Each distillate stream is recycled into the other column, so there is a mass integration between the columns. The respective distillation region of low and high pressure operation are overlapping.

Heat integration. Because of the pressure difference both columns can be coupled energetically. This means that the high pressure vapor stream at the top of the high pressure column is used to heat up the low pressure column at the bottom (Fig. 2.5-A). The main advantage of this coupling is an energy savings of up to 40% [Luyben & Cheng 1985]. This is a result which Löwe et al. also found for the separation of methanol-water in a heat integrated but not complete mass integrated column system [Löwe et al. 1999, Löwe & Wozny 2001a, Löwe 2001b]. The main disadvantage is the feed back streams of the distillate into the other column because of the back coupled system. The methanol-water system does not have these feed backs because it is not an azeotropic system, so there are no feed-back streams (recycle streams) between the columns necessary. Another application of the heat integration is the multi-component mixture separation to save energy and costs. The literature refers to the fact

that heat integrated pressure swing distillation is a very economic process [Sattler & Feindt 1995, Stichlmair & Fair 1998, Lang 1996].

But the integration reduces the degree of freedom. The control of the heat duty of the low pressure column is now not possible any more. So a much more complex process control strategy is needed. Keeping in mind the increasing of the energy prices these kind of energy saving can bring a real advantage despite the effort. The reduced degree of freedom can be avoided by introducing an additional reboiler for controlling purposes at the bottom of the LP column (see chapter 5.1.2.1).

The requirement for the energy integration is that the azeotropic point is pressure sensitive and the pressure difference between the two columns is high enough to have a satisfying temperature difference between the condenser of the high pressure column and the reboiler of the low pressure column. But as the boiling temperature difference of the pure components increases, the pressure difference must be increased proportionally to get the satisfying temperature difference in the coupled heat exchanger mentioned above.[1] The literature shows that the pressure swing distillation is most effective and economical with energy integration [Sattler & Feindt 1995, Stichlmair & Fair 1998, Lang 1996]. Research in the field of total energy coupled pressure swing operation, process control concepts of such processes including start-up and operation, evaluation of different design concepts and comparison of discontinuous structures is missing in the literature.

Process control. The operation of energy and mass integrated distillation columns have high demands on the process control concept as well as on the controller concept itself [Horwitz 1997]. Disturbances has to be illuminated as soon as possible to reduce the possibility of running of the process out of a stable operation. By leaving the operational range, for example, if the distillate concentrations are not absolute enough or if the pressure difference between low and high pressure column is too small or the feed concentration changes very much, the column system cannot be operated stably and the process has to be stopped. Early concentration measures and an optimal process control concept must be developed to have a processes that is controllable and stable against disturbances. Güttinger and Lee say that often coupled column systems will be influenced by oscillation and Multiple-Steady-States, so operation is therefore much more difficult [Güttinger et al. 1997, Lee et al. 1999]. First studies on the dynamic of such systems can be found in [Abu-Eisha & Luyben 1984] (partially heat integrated column system with additional reboiler). A general overview on the dynamics and control of distillation columns can be found in Skogestad [Skogestad 1992] who gives a critical survey about the most interesting ideas on this topic.

To summarize the facts described above, research is need to develop suitable process control concepts for a totally heat integrated pressure swing distillation column system using a rigorous experimentally validated model, to demonstrate that the PSD process is a appropriate alternative for the separation of homogeneous azeotropic mixtures.

1. normally a minimum temperature difference of $\Delta T = 5...10K$

2.2.2 Batch pressure swing distillation

The batch process is one of the best known distillation processes. It is mostly used in fine chemistry, for seasonal products, in the pharmaceutical, and in food industry, despite the competition of the continuous process [Sørensen 1994, Sørensen & Skogestad 1996, Mutjaba 2004]. Mainly the energy demand is much higher than for the continuous processes [Hasebe et al. 1999]. But if the whole producing costs are considered there could be an advantage of the discontinuous process compared to the continuous process [Oppenheimer & Sørensen 1997]. But one main advantage is that the process structure (one column) is much simpler than for a continuous operation and or flexible in the scope of product changes and also product amount changes.

The discontinuous process uses one column which is operated in two loops at different operation pressures (Fig. 2.5-C1/C2). In the first loop (e.g. atmospheric pressure) the mixture is added to the column and the high boiling component (component 1, high boiling) is drained at the bottom and the azeotropic mixture at the top. The process ends if the bottom purity runs out of specification and then the process stops. After that the pressure will be changed (e.g. high pressure). The pressure change leads to a shift of the azeotropic point and therefore of the azeotropic concentration at the top of the column. Now the other component (component 2, high boiling) will be drained from the bottom because the column operate in the other distillation region (Fig. 2.4). The azeotropic mixture (at a different pressure, means a different composition) will drained from the top of the column. The process ends, if the specification runs out of the set points.

The main disadvantage of the process is the unproductive times during the pressure change, which is normally very fast and during the filling and draining of the different tanks between the loops. For that changes up to 20 - 30 % of the process time are used [Phimister & Seider 2000]. Also an energy integration is not possible as is true for the continuous process. The main characteristic of the batch process is the cyclic filling and draining of the top and the bottom tanks which can be well controlled as mentioned in [Sørensen & Prenzler 1997]. Like the continuous process also the batch process is also discussed only on a theoretical bases in the literature up to now, and experimental data are missing. The only case is the separation of methanol-water, but this is not a homogeneous azeotropic mixture [Sørensen & Prenzler 1997]. No experimental data for the inverted batch process can be found in the open literature.

The regular batch process. The common discontinuous structure is the regular batch structure. In this case the feed is added to the bottom and the low boiling azeotropic mixture will be drained from the top, and the first high boiling component will be accumulated in the bottom tank (mostly reboiler). After pressure change and a pumping of the azeotropic mixture from the top tank to the bottom tank, the other component (high boiling) is accumulated at the bottom and the azeotropic mixture is drained from the top. In the LP-loop (low pressure or atmospheric pressure), the bottom product will be water and in the HP-loop (high pressure) the bottom product will be acetonitrile.

But the regular process must not be the optimal structure for the separation of homogenous azeotropic mixture. In the literature other structures are also discussed, such as the inverted, the

middle vessel [Hasebe et al. 1992, Hasebe et al. 1996] and the multivessel batch process [Wittgens & Skogestad 2000]. Warter et. al. compares the regular batch with the middle vessel batch processes and also conducted experiments [Warter & Stichlmair 2002, Warter et al. 2004]. He identifies for the regular batch a high thermal stress of the mixture and a high energy and time demand. These disadvantages can be avoided by use of the middle vessel batch. In our case the pressure swing operation with a binary mixture the middle vessel and the multivessel batch is not feasible in practical use [Gruetzmann et al. 2007]. But the inverted process can be a good alternative for the separation of such mixtures [Sørensen & Skogestad 1996] and will now be introduced.

The inverted batch process. In the inverted case the feed is added to a top tank and the product is drained from the bottom [Robinson & Gilliland 1950]. In contrast to the regular process the pure products will be drained from the bottom and not be accumulated. The azeotropic mixture will be accumulated at the top and that means that after the pressure change the feed (azeotropic mixture) does not have to be pumped into the feed tank. It is already in the right position. The process loop ends if the concentration on the bottom runs out of the set point, that means the maximum amount of product is withdrawn from the bottom. There are only theoretical results in the literature for zeotropic mixtures as well for azeotropic mixtures with or without an entrainer [Bernot et al. 1991, Sørensen & Skogestad 1996, Lelkes et al. 1998, Düssel & Warter 2000, Rev et al. 2003, Mutjaba 2004, Low & Sørensen 2005]. As fare as I know, the process is not used in industry, but it has a high potential.

2.2.3 Summary

As mentioned above, all possible PSD process concepts have been inadequately researched, mainly there are only theoretical references. Experimental data are missing, but because of the possible energy savings (continuous) and the simplicity of the process (discontinuous) and the demand of fine chemicals and complex separations, there is a great industrial relevance to research this topic in detail. This means a detailed modelling of the pressure swing distillation combined with a model validation (steady state and dynamic) to compare and evaluate the different possible structures. It is vitally important to get reliable results for the start-up operation, as well especially for the discontinuous process. The basics of the start-up operation for distillation columns will be introduced in the next section.

2.3 Start-up of distillation columns

To make the comparability of the different time limited looped batch processes possible, the analysis and modelling of the start-up process from cold and empty is essential. Without modelling the start-up it is very difficult to find consistent initial conditions for the inverted and the batch process. Especially the start-up time differ very much between the regular and the inverted batch process (chapter 6.2.1).

For the continuous process, the point of time where the coupling (heat and/or mass coupling) is realized, is the main challenge in starting up such a system. So also in this case the modelling of

the start-up is very important, because the coupling is a part of the start-up process. For future process optimization the start-up will also be an important part especially for the discontinuous process. The optimization of the different processes will not be part of this work.

In general the start-up operation is a complex time consuming unproductive and unsteady operation where a lot of product which does not fulfill the specifications is produced.

The start-up operation is an often discussed topic in the literature. In general the start-up process means the time between the cold and empty state and the steady state where all required specifications are reached. Ruiz et al. and Gani et al. described in their work the start-up operation could be divided into three phases [Ruiz et al. 1988, Gani et al. 1987]:

1. *Discontinuous phase*: The column is cold and empty or already has a certain temperature because of an attended heating or cooling. The liquid and vapor hold up is equal to zero at a respective pressure (vacuum pump, inert gas, open atmospheric column). During this phase feed is added into the system until the respective level in the reboiler is reached to switch on the reboiler heating. After the reboiler is heated up, the vapor rises up the column, condenses at the first tray with cold liquid, heats up the liquid and rises up to the next tray. If the vapor reaches the condenser, the discontinuous phase ends.
2. *Semi continuous phase*: When reflux is added, the trays above the feed input will be filled up. All streams inside the columns will be formed. This phase ends when all streams are formed, which means constant pressure drops on every tray.
3. *Continuous phase:* This phase is the change between the state variables into the steady state point until all products reach their specification.

The continuous phase is the most time-consuming phase and is therefore the most important one during the start-up operation as well as for an optimal start-up procedure. But also the discontinuous and the semi-continuous phase have a saving potential, because especially the pressure and the concentrations are mainly important for the coupling of the columns of the continuous system. This problem is discussed in detail in chapter 5.2.1.

The following is an overview about the main references in start-up operation. Reepmeyer et al. discusses in her work the start-up operation of reactive distillation columns (tray columns), with practical aspects and an in-between product recycle and as a main topic the catalyst input [Reepmeyer et al. 2003, Reepmeyer 2004a, Reepmayer et al. 2004b]. Forner et al. expanded these research on packed reactive distillation columns [Forner et al. 2007]. Other authors discuss the start-up of conventional columns without reaction from a pseudo heated-up state, with filled-up trays in equilibrium. This means you need Trial-and-Error methods to appreciate the initial state. Wang et al. discuss a single batch column with start-up from cold and empty [Wang et al. 2003]. Löwe et al. examined the start-up of a heat-integrated two-column system (methanol - water) without feed backs inside the column system concerning the mass flows from cold and empty [Löwe et al. 1999, Löwe & Wozny 2001a, Löwe 2001b]. The use of controller for the start-up process is done by Barolo et al. Because there are big changes during the start-up process, a use of linear controllers is not possible [Barolo et al. 1994]. A more complex system

has to be used. The work of Fabro et al. describes the start-up of a single column with help of controllers [Fabro et al. 2005]. The start-up of batch distillation columns is analyzed by Sørensen et al. on the topic of time optimal start-up operation. There a prefilling of the condenser with low boiling mixture is used to reduce the start-up time [Sørensen& Skogestad 1996]. Scenna describes the start-up of homogeneous azeotropic systems in one column, but with the focus on Multiple-Steady-States [Scenna et al. 2004]. Finally Tran did research on the topic of start-up of three phase distillation columns [Tran 2004].

Research on the field of start-up of PSD column systems and batch distillation columns for the separation of homogenuous azeotropic systems including the experimental validation is not mentioned in the literature. Moreover the analysis of the inverted batch column has not been done up to now.

The literature introduces different start-up concepts which will be introduced here shortly:

1. *Conventional start-up:* All steady state values will be set at the beginning of the start-up operation (heat duty, feed stream, reflux stream, distillate and bottom product concentrations). The start-up process ends when the steady state is reached.
2. *Strategy of total reflux:* There are different definitions under that topic. Ruiz and Barolo say simply that no distillate is drained from the column. That means that feed stream and bottom outlet are not equal to zero [Ruiz et al. 1988, Barolo & Trotta 1993]. Shinskey, Yamada et al., Kister and Ganguly define *total reflux* as a completely closed column after filling up, that means neither feed is pumped into the column nor distillate or bottom product is leaving the column [Shinskey 1977, Yamada et al. 1981, Kister 1990, Ganguly & Saraf 1993]. The start-up with total reflux is very uncomplicated and the most used strategy mentioned in the literature [Kister 1990].
3. *Time optimal strategy*: This strategy uses a higher heat duty or as an alternative increased manipulated values (depending on the hydrodynamic loading tolerance of the column). The switching point to the steady state values is calculated with help of the MT-function:

$$MT = \sum_{n=1}^{k} \left| T_n - T_n^{stat} \right|, \qquad \text{(eq. 2.1)}$$

with T_n = actual temperature on the tray n,

T_n^{stat} = steady state temperature on the tray n and

k = number of trays.

The function runs through a minimum, which indicates the optimal switching point [Yamadaet al. 1981, Yasuoka et al. 1987, Löwe 2001b]. As an alternative to the MT-function (eq. 2.1) the MX-function can be used as a switching criterion.

This function uses a concentration difference instead of the temperature difference and is often used for reactive distillation processes [Reepmeyer et al. 2002].

4. *Strategy of a total distillate draining at the top of the column:* In this strategy the column will be operated without a reflux stream. The switching point will also be calculated with help of the above described minimum of the MT- or MX-function [Kruse 1995]. With this strategy, time savings up to 50 - 70% compared to the conventional strategy are possible. Flender et al. has done the analytical derivation and expanded it for columns with side streams [Flender et al. 1997, Flender 1998].

The start-up of column system can be found in [Gani & Cameron 1987] without heat integration, but with a product stream from the first column to the second one (serial connection). Gani suggests the start-up of the single columns with total reflux and after that a coupling of the columns.

For a complete overview about the start-up literature see the next table:

Table 2.3. Literature overview on azeotropic separation (selection).

Topic	reference
Concepts and start-up of distillation columns	Ruiz 1988, Barolo 1993, Shinskey 1977, Yamada 1981, Kister 1990, Ganguly 1993, Yasuoka 1987, Löwe 2001b, Reepmeyer 2002, Flender 1997, Flender 1998, Kruse 1995a + 1995b, Wozny 2004
Non heat integrated columns	Gani 1987
Reactive distillation columns	Reepmeyer 2003, 2004a & 2004b; Forner 2007
Batch columns	Sørensen 1994, Wang 2003, Gruetzmann 2006
Heat integrated column system	Löwe 1999, 2001a, 2001b
Use of controllers during start-up	Barolo 1994, Fabro 2005
Multiple steady states and start-up of distillation columns	Scenna 2004
Start-up of a three phase distillation columns	Tran 2004
Divided wall column	Niggemann 2006

The work of Löwe is focused on the start-up of heat integrated distillation columns. Löwe discusses different coupling structures in concurrent and counter current flow direction (related to the flow of the energy and the masses), and pre-column and Petlyuk-connection, as well as feed split-connections (Fig. 2.6). A structure with mass and heat integration including feed backs as in the pressure swing operation (Fig. 2.5A) is not focused in her work [Löwe 2001b].

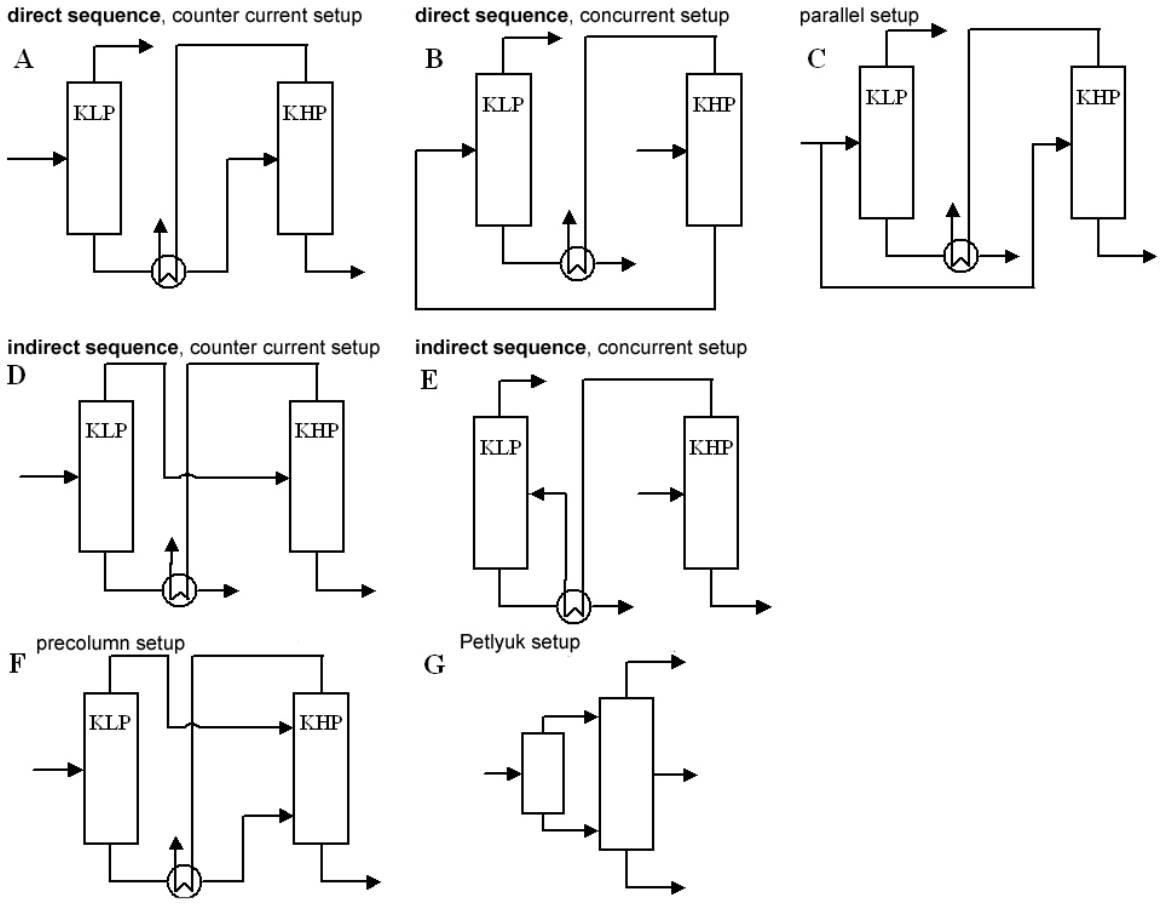

Fig. 2.6 Heat and mass integrated column systems [Löwe 2001b].

The main challenge in start-up of heat and mass integrated column systems with feedbacks is the difference in the azeotropic points only for different pressures and the possible missing feed input stream into the high pressure column (with the reboiler) in the case of feed concentrations lower than the azeotropic point. Especially the coupling time point has to be chosen well. The start-up strategy of the pressure swing distillation system is discussed in chapter 5.2.1.

2.4 Summary

This chapter distinguish the need of research in the field of pressure swing distillation by presenting the different distillation unit operations for the separation of azeotropic mixtures. The pressure swing distillation process is described in detail with the focus on the continuous and the discontinuous (batch) processes (regular and inverted). The last part deals with the theoretical background of the start-up process and motivates the modelling of the start-up. In the next chapter the models for the different not well researched PSD processes will be explained to analysis and compare the continuous and the discontinuous PSD processes in the following chapters.

3. Model

In this chapter the different mathematical models for the modelling and analysis of the different pressure swing processes will be introduced. Especially the differences and the commonalties will be described in detail. The literature introduces different kind of models for dynamic simulation of distillation columns. Rix gives in his work a detailed overview about methodical approaches and a classification of the modelling depth and modelling costs [Rix 1998].

A more complex model describes the process in much more detail, but the modelling costs increase significantly. There is a main model classification into simple model, reduced models, rigorous dynamic models, rate based models and nonlinear detailed models with increasing modelling costs (Fig. 3.1). In this work there are simple models (analytical analysis) and detailed rigorous equilibrium models used for the description of the processes. Each model satisfies the needs of the modelling depth for an optimal problem description. In particular the demands on accuracy and handling and computational time will be well satisfied. The use of rate-based models or models with a higher complexity are not necessary for the description of the different processes here as the model validation results will show. The model depth is quite enough for the simulation studies done in this work.

The chapter starts with the description of the analytical model of the discontinuous process on the base of the Rayleigh equations (simple model). After that the detailed rigorous equilibrium model will be introduced for the continuous and for the discontinuous process. In

particular, the coupled heat exchanger for energy integration will be introduced. In the last part of the chapter a detailed description of the start-up model from cold and empty follows.

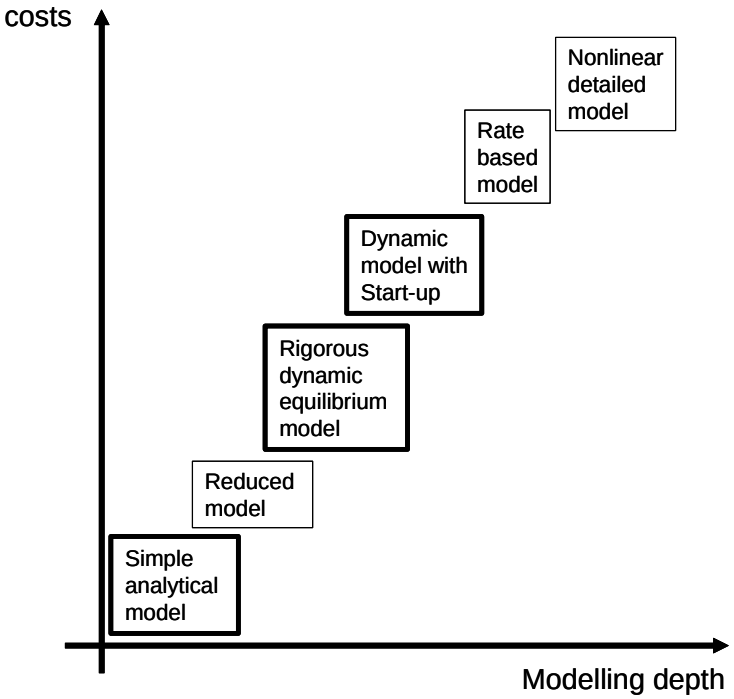

Fig. 3.1 Comparison of modelling costs in respect to modelling depth

3.1 An analytical view on the batch process

To get a short-cut method for the analysis and comparison of the two different discontinuous processes a simple model was developed. This approach makes a fast comparison of the regular with the inverted batch process possible, to decide which process will be the best separation solution for a given mixture. This approach is based on the well know Rayleigh equation [Stichlmair & Fair 1998].

The first part contains the calculation method for the regular process and after that the approach will be transferred for the inverted process. All concentration definitions are for the low boiling component.

Regular batch process. A multi stage discontinuous distillation process for a zeotropic binary mixture can be calculated with help of the mass and component balance (Fig. 3.2 and (eq. 3.1)).

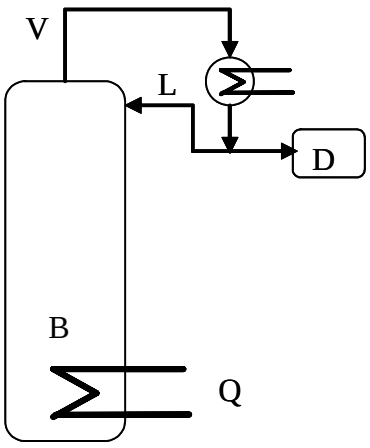

Fig. 3.2 Regular batch.

Mass balance:

$$dB = -dD. \qquad \text{(eq. 3.1)}$$

Component balance:

$$x_D dD + d(B \cdot x_B) = 0, \text{ with } x_D = const. \qquad \text{(eq. 3.2)}$$

This yields the *Rayleigh-equation*:

$$\frac{dB}{B} = \frac{dx_B}{x_D - x_B} \qquad \text{(eq. 3.3)}$$

Usually the distillate concentration x_D is a function of the separation factor (relative volatility) α_{12}, defined to

$$\alpha_{12} = \frac{y_1/x_1}{y_2/x_2} = \frac{K_1}{K_2}, \qquad \text{(eq. 3.4)}$$

the number of stages n, the reflux ratio $R_L = \frac{L}{D}$ and the bottom concentration x_B:

$$x_D = f(\alpha, x_B, R_L, n). \qquad \text{(eq. 3.5)}$$

Under the assumption of a constant distillate concentration the equation can be integrated to:

$$B_e = F \cdot \frac{x_D - x_F}{x_D - x_{B_e}}. \qquad \text{(eq. 3.6)}$$

For the comparison of the two batch processes (regular and inverted) the energy consumption can be a criterion for the decision which process is better. Other criteria are the costs or the batch time but in this case the minimal energy consumption is used.

The energy consumption for a batch column depends on the vapor stream:

$$\frac{dQ}{dt} = r \cdot \frac{dV}{dt}, \qquad \text{(eq. 3.7)}$$

were V is calculated with a variable reflux ratio R_L for the regular case. dQ is now calculated to:

$$dQ = d(D \cdot (R_L + 1) \cdot r). \qquad \text{(eq. 3.8)}$$

after differencing (eq. 3.6) and with $dD = -dB$ and r = constant, it yields to:

$$\frac{dQ}{r \cdot F} = (x_D - x_F) \cdot \frac{R_L + 1}{(x_D - x_B)^2} dx_B, \qquad \text{(eq. 3.9)}$$

with the Feed F:

$$B(t_0) = F. \qquad \text{(eq. 3.10)}$$

This equation must be integrated:

$$\frac{Q}{r \cdot F} = (x_D - x_F) \int_{x_F}^{x_{B_e}} \frac{R_L + 1}{(x_D - x_B)^2} dx_B. \qquad \text{(eq. 3.11)}$$

The changing reflux ratio depending on the bottom concentration x_B for an infinite number of trays can be calculated [Stichlmair & Fair 1998]:

$$R_L(x_B) = \frac{1}{(\alpha - 1)} \cdot \left(\frac{x_D}{x_B} \cdot \alpha \cdot \frac{1 - x_D}{1 - x_B} \right). \qquad \text{(eq. 3.12)}$$

The minimal necessary energy consumption relating to the overall heat of evaporation r and the molar feed F can be calculated with help of (eq. 3.11) and (eq. 3.12):

$$\frac{Q_{min}}{r \cdot F} = (x_D - x_F) \int_{x_F}^{x_{B_e}} \frac{1}{(x_D - x_B)^2} \cdot \left(\frac{1}{\alpha - 1} \cdot \left(\frac{x_D}{x_B} - \alpha \cdot \frac{1 - x_D}{1 - x_B} \right) + 1 \right) dx_B. \qquad \text{(eq. 3.13)}$$

For a constant α the integral can be solved:

$$\frac{Q_{min}}{r \cdot F} = \frac{x_D - x_F}{(\alpha - 1) \cdot x_D \cdot (1 - x_D)} \cdot \qquad \text{(eq. 3.14)}$$

$$\left\{ \alpha \cdot x_D \cdot \ln \frac{1 - x_F}{1 - x_{B_e}} - [(\alpha - 1) \cdot x_D + 1] \cdot \ln \frac{x_D - x_F}{x_D - x_{B_e}} + (1 - x_D) \cdot \ln \frac{x_F}{x_{B_e}} \right\}$$

To calculate the maximal possible rate of yield, the relative yield for the regular process is defined to:

$$\frac{D}{F} = \frac{x_F - x_{B_e}}{x_D - x_{B_e}}, \qquad \text{(eq. 3.15)}$$

which has to be changed to a function for x_{B_e} to get a function from (eq. 3.14) for $\frac{Q_{min}}{r \cdot F}\left(\frac{D}{F}\right)$.

With this function $\frac{Q_{min}}{r \cdot F}\left(\frac{D}{F}\right)$ the energy demand for a changing relative yield, which means a distillate to feed ratio in the regular case, can be calculated. This calculation is valid in general for binary mixtures under the following simplifications:

- constant distillate concentration,
- infinite number of trays,
- minimal energy consumption,
- ideal mixture (constant separation factor).

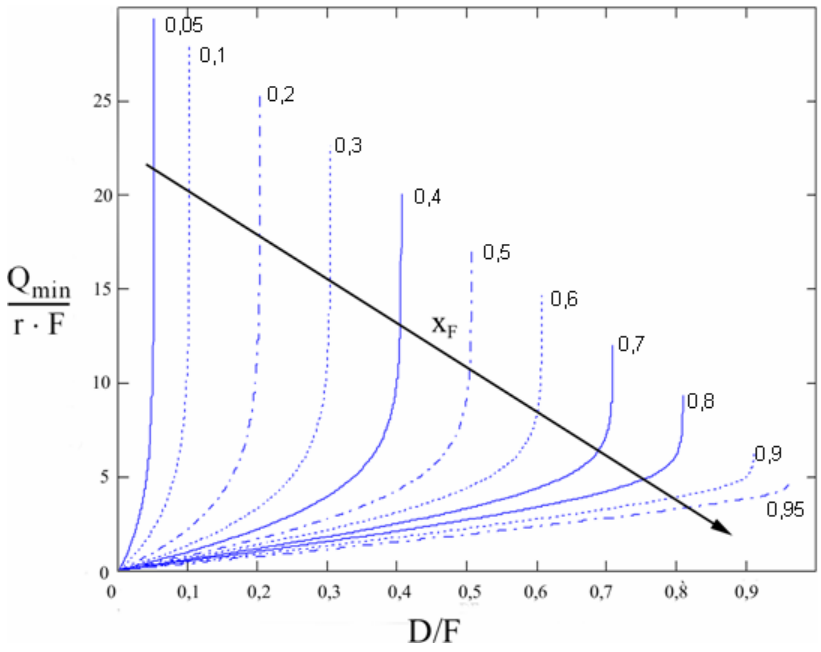

Fig. 3.3 Regular batch process zeotropic mixture, maximal recovery ($x_D = 0{,}99; \alpha = 2$).

In Fig. 3.3 the related energy consumption is shown over the relative yield. If the maximal relative yield is reached, the energy consumption goes to infinite. The figure shows as an example calculation results for a zeotropic binary mixture with a distillate concentration of 0.99 mol/mol and a constant separation factor of 2 for different feed concentrations. With an increasing of the feed concentration the relative yield also increases. The maximal relative yield can also be calculated much easier with:

$$\left.\frac{D}{F}\right|_{max} = \frac{x_F - x_{B,\,min}}{x_{D,\,set} - x_{B,\,min}}. \qquad \text{(eq. 3.16)}$$

But the interesting thing is, that the calculation with the Rayleigh equation has the same results for $\frac{Q_{min}}{r \cdot F}\left(\frac{D}{F}\right) \rightarrow \infty$; so it is consistent.

Inverted batch process. Now the analytical model for the inverted process will be presented which is based on the same derivation as the regular one. First the mass and component balance is formulated (Fig. 3.4).:

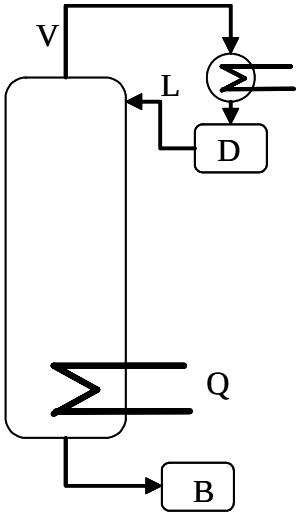

Fig. 3.4 Inverted process.

Mass balance:

$$dB = -dD. \qquad \text{(eq. 3.17)}$$

Component balance:

$$x_B dB + d(D \cdot x_D) = 0, \text{ with } x_B = const. \qquad \text{(eq. 3.18)}$$

This yields to:

$$\frac{dD}{D} = \frac{dx_D}{x_B - x_D}. \qquad \text{(eq. 3.19)}$$

Equation (eq. 3.19) can be integrated for a constant bottom concentration:

$$D_e = F \cdot \frac{x_B - x_F}{x_B - x_{D_e}}. \qquad \text{(eq. 3.20)}$$

Also in the inverted case the energy consumption is a function of the vapor amount:

$$dQ = r \cdot dV. \qquad \text{(eq. 3.21)}$$

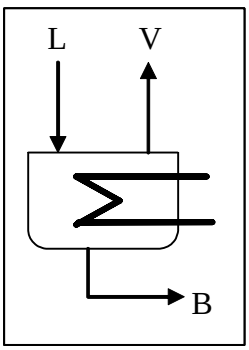

In analogy to the regular case the vapor amount can be calculated with help of the reflux ratio. In this case the reboil ratio is used:

$$R_V = \frac{V}{B}. \qquad \text{(eq. 3.22)}$$

The energy consumption can be now calculated for the inverted case:

$$dQ = d(R_V \cdot B \cdot r), \qquad \text{(eq. 3.23)}$$

with $-dD = dB$ it is

$$dQ = -d(R_V \cdot D \cdot r). \qquad \text{(eq. 3.24)}$$

The differencing of (eq. 3.20) in equation (eq. 3.24) and r = constant, yields to:

$$\frac{dQ}{r \cdot F} = R_V(x_D) \cdot \frac{x_B - x_F}{(x_B - x_D)^2} dx_D. \qquad \text{(eq. 3.25)}$$

For the calculation of the energy consumption in the inverted case the minimal reboil ratio is needed for an infinite number of trays and depending on the changing distillate concentration x_D:

$$R_V = \left(\frac{1}{1 - \frac{x_B}{x_D}} \cdot \left(\frac{\alpha}{1 + (\alpha - 1) \cdot x_D} - 1 \right) \right)^{-1}. \qquad \text{(eq. 3.26)}$$

With equation (eq. 3.25) it is:

$$\frac{Q_{min}}{r \cdot F} = \int_{x_{D_e}}^{x_F} \left[\left(1 - \frac{x_B}{x_D} \right) \cdot \frac{1 + (\alpha - 1) \cdot x_D}{(\alpha - 1) \cdot (1 - x_D)} \cdot \frac{x_B - x_F}{(x_B - x_D)^2} \right] dx_D . \qquad \text{(eq. 3.27)}$$

The integral will be also evaluated due to the relative yield. In this case the relative yield is defined to:

$$\frac{B}{F} = \frac{x_F - x_{D_e}}{x_B - x_{D_e}}, \qquad \text{(eq. 3.28)}$$

the ratio of the bottom amount to the feed amount. So the distillate concentration can be calculated to:

$$x_D = \frac{x_F - \left(\frac{B}{F} \cdot x_B \right)}{1 - \frac{B}{F}}. \qquad \text{(eq. 3.29)}$$

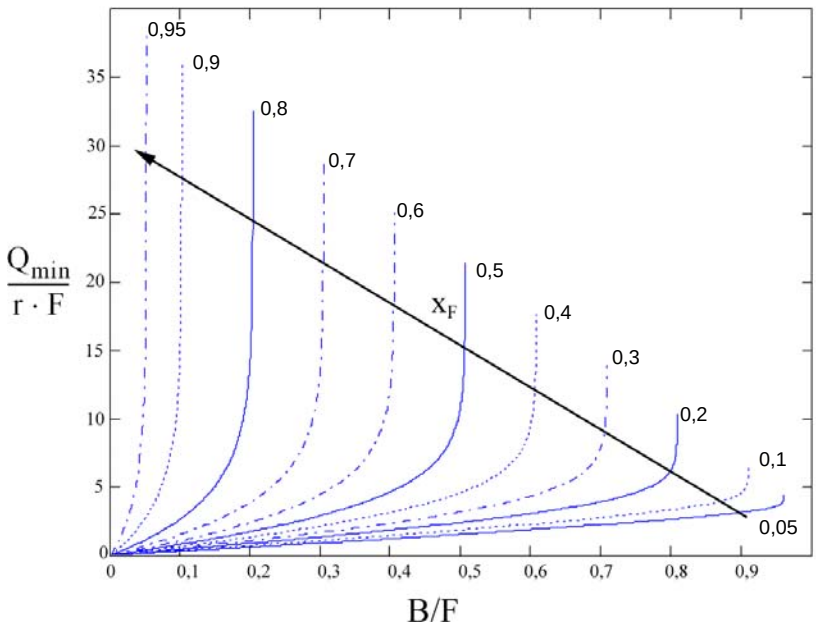

Fig. 3.5 Inverted batch, zeotropic mixture, maximal recovery ($x_B = 0{,}99; \alpha = 2$).

The energy consumption related to the heat of evaporation and the feed amount over the relative yield for the inverted process is shown in Fig. 3.5.

The relative yield is as maximal as for the regular case for infinite energy consumption for a given feed concentration. The maximal relative yield decreases with an increase of the feed concentration which is the opposite of the regular process.

For the inverted case there is also a much easier calculation for the maximal relative yield:

$$\left.\frac{B}{F}\right|_{max} = \frac{x_F - x_{D,max}}{x_{B,set} - x_{D,max}}. \qquad \text{(eq. 3.30)}$$

A detailed validation against the detailed model is done in chapter 6. The comparison of the regular and the inverted case on the base of this simplified model approach is done in chapter 6, too.

This calculation is valid in general for binary mixture under the following simplifications:

- constant bottom product concentration,
- infinite number of trays,
- minimal energy consumption,
- ideal mixture (constant separation factor, $\alpha_{12} = 2$).

Both analytic approaches for the regular and the inverted batch distillation can be used for the process synthesis.

3.2 Description of the equilibrium model

To describe the dynamics of pressure swing process, a much more detailed model than the above described one is needed. For the modelling of the discontinuous and the continuous process a detailed rigorous dynamic equilibrium model is developed in the commercial simulation software package gProms™ from PSE [PSE 2006]. The commercial simulation package has been used because it is able to handle discontinuities (switches between model equations during the iteration) as they occur in the developed model (start-up operation). The model contains the dynamic balances of the phase equilibriums, fluid dynamics, pressure drops, and heat transfers in each separation unit and process unit. With help of the modelling of the pressure drop and the heat transfer on every tray and in the units (reboiler, condenser and heat exchanger) the dynamic of the system especially for start-up and load changes can be calculated very well.

The chapter starts with the introduction of the general units for both cases (continuous and discontinuous) and after that the differences and characteristics of each case are illustrated in detail. The chapter ends with the description of the start-up model from cold and empty. All properties which are used in the model for the mixture acetonitrile - water are listed in the appendix (chapter A.4.1).

3.2.1 General units

The column is subdivided into main units which means an evaporator or column bottom unit, a column unit, and a condenser unit. Each unit has its own model and will be now described separately. The different Units and their location are shown in Fig. 3.6. The numbers in each unit indicates the chapter were the unit is described. All following model descriptions only take the dynamic model without start-up into account. The differences for modelling the start-up are described in chapter 3.3.

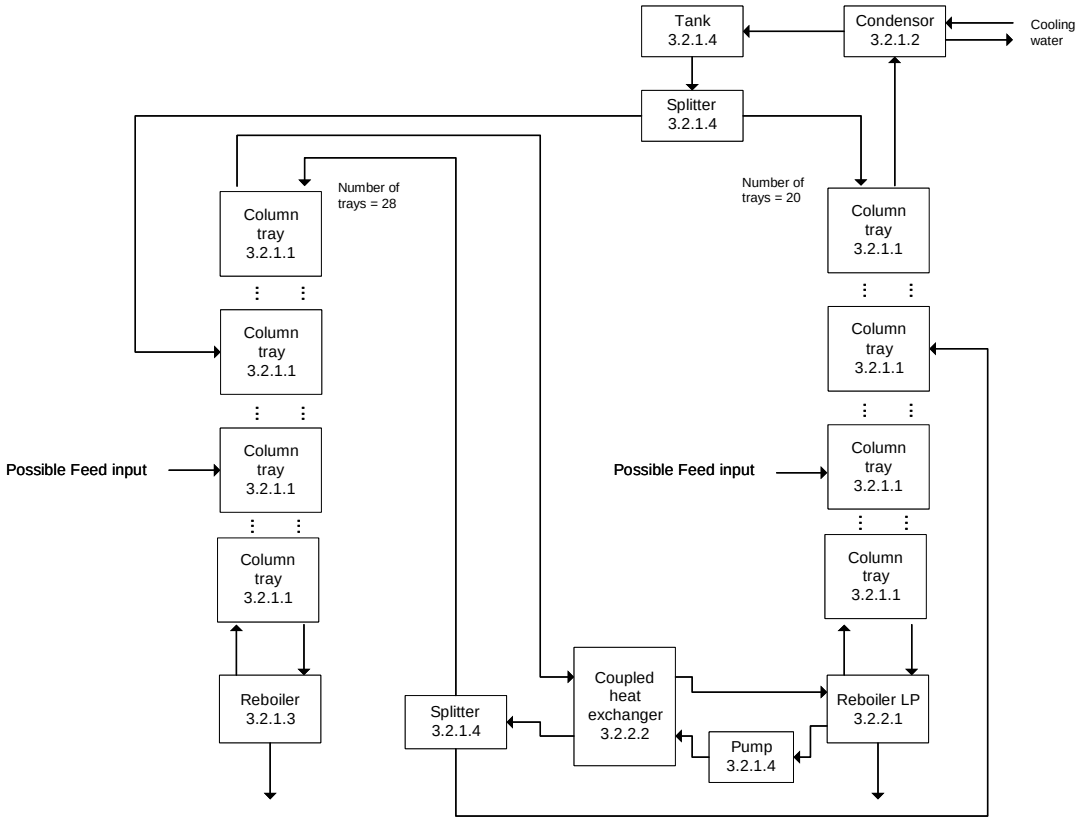

Fig. 3.6 Units of the equilibrium model and there location in the plant.

3.2.1.1 Column tray

Each tray is modeled separately. All these models together builds up the column model. Each tray is modelled as an ideal mixed tank. That means temperature, pressure, and concentration do not depend on a location in the „tank“, which means on the tray. Liquid and vapor phase are calculated fully dynamic and together. Both vapor and liquid hold-ups are taken into account. The tray is calculated following the fundamental sketch shown in (Fig. 3.7).

Assumptions:

- ideal mixed tank
- temperature, pressure concentration are locally independent on the tray
- liquid and vapor phase fully dynamic
- including heat losses over the column wall

- including pressure drop calculation
- tray efficiency by Murphree

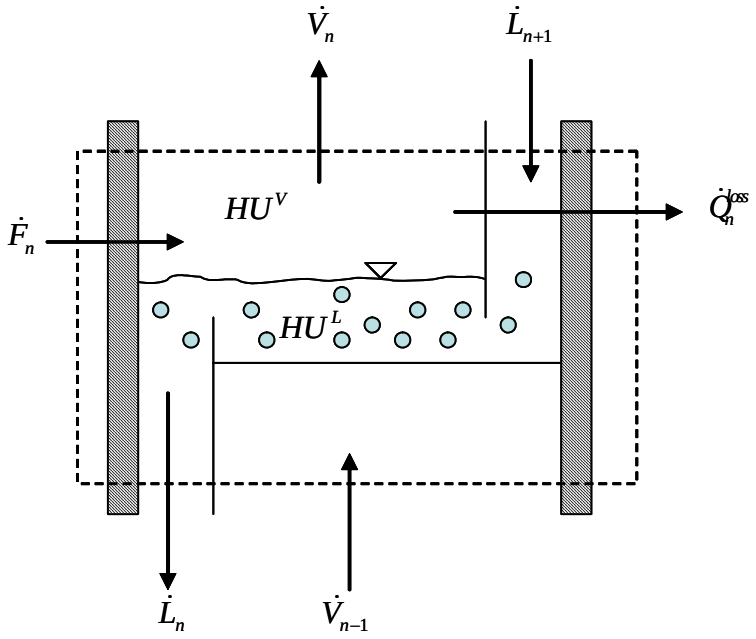

Fig. 3.7 Schematic figure of a column tray.

For one tray n the following main dynamic equation are given:

Overall mass balance: $$\frac{d(HU_n^L + HU_n^V)}{dt} = \dot{V}_{n-1} - \dot{V}_n + \dot{L}_{n+1} - \dot{L}_n + \dot{F}_n . \qquad \text{(eq. 3.31)}$$

Component balance:

$$\frac{d(HU_n^L \cdot x_{n,i} + HU_n^V \cdot y_{n,i})}{dt} ,$$

$$= \dot{V}_{n-1} \cdot y_{i,n-1} + \dot{V}_n \cdot y_{i,n} + \dot{L}_{n+1} \cdot x_{i,n+1} - \dot{L}_n \cdot x_{i,n} + \dot{F}_n \cdot z_{i,n}$$

with i = 1...NC. (eq. 3.32)

Energy balance:

$$\frac{dH_n}{dt} = \dot{V}_{n-1} \cdot h_{i,n-1}^V + \dot{V}_n \cdot h_{i,n}^V + \dot{L}_{n+1} \cdot h_{i,n+1}^L - \dot{L}_n \cdot h_{i,n}^L + \dot{F}_n \cdot h_{i,n}^F - \dot{Q}^{loss} ,$$

$$\text{with } H_n = HU_n^L \cdot u_n^L + HU_n^V \cdot u_n^V + (M_{steel} \cdot c_{p,steel} \cdot T)_n . \qquad \text{(eq. 3.33)}$$

The heat stored in the steel plate $(M_{steel} \cdot c_{p,steel} \cdot T)_n$ is calculated with the equilibrium temperature T_n on the tray. The vapor phase needs an additional *summation*:

$$\sum_{i=1}^{NC} y_{n,i} = 1 . \qquad \text{(eq. 3.34)}$$

Furthermore there is the assumption that in both phases liquid and vapor are in thermodynamical equilibrium on the tray and this means that the outlet streams are also in thermodynamical equilibrium.

Under the assumption that the pressures are always lower than 10 bar the pointing correction $\Pi_{oi,n}$ is negligible. Also the fugacity coefficient for the pure components to the fugacity coefficient for the component in the mixture can be set to one:

$$\varphi^{LV}_{oi,n} / \varphi_{i,n} = 1 . \qquad \text{(eq. 3.35)}$$

The *thermodynamic equilibrium* is:

$$x_{i,n} \cdot \gamma_{i,n} \cdot p^{LV}_{oi,n} = y^*_{i,n} \cdot p_n . \qquad \text{(eq. 3.36)}$$

This yields to the calculation of the k-factor, the ratio of the vapor to the liquid concentration:

$$K_{i,n}(T_n, p_n, x_{i,n}) \equiv \frac{y^*_{i,n}}{x_{i,n}} = \frac{\gamma_{i,n} \cdot p^{LV}_{oi,n}}{p_n} . \qquad \text{(eq. 3.37)}$$

For calculation of the activity coefficient a g^E-model is used (semi empirical Wilson-approach). The vapor pressure is calculated with the Antoine-equation. All equations and properties of the mixture and the substance can be found in chapter A.1 and the properties are from the Dechema Data Series [Gmehling et al. 1981] and ChemCAD [Chem 2000].

In reality there is mostly no mass equilibrium on the tray because of the contact time between the two phases and the non ideal mixing of them[1]. This deviation from the ideal behavior can be taken into account be using the *tray efficiency* by Murphree [Gmehling & Brehm 1996]. The tray efficiency calculates a new non ideal vapor concentration:

$$\eta_{n,i} = \frac{y_{n,i} - y_{n-1,i}}{y^*_{n,i}(x_{n,i}) - y_{n-1,i}} . \qquad \text{(eq. 3.38)}$$

$x_{n,i}$ and $y_{n,i}$ are the concentration of the phases leaving the tray and $y^*_{n,i}(x_{n,i})$ is the concentration of the vapor phase which is in equilibrium with $x_{n,i}$ calculated with the equilibrium equation. The tray efficiency is the ratio of the real concentration change on the tray to the maximal concentration change (equilibrium)[2].

The *pressure drop* on each tray consists of the dry pressure drop $\Delta p_{d,n}$, the hydrostatic pressure drop $\Delta p_{h,n}$ and the rest pressure drop $\Delta p_{r,n}$:

$$\Delta p_n \equiv \Delta p_{d,n} + \Delta p_{h,n} + \Delta p_{r,n} . \qquad \text{(eq. 3.39)}$$

1. The direct consequence is no thermal equilibrium on the tray. But this effect is much smaller and will be neglect.
2. For a binary mixture the tray efficiencies for both components are the same.

The equation for each pressure drop is described in the appendix (chapter A.2). The problem is a dynamic equation system with an index greater than one [Kreul et al. 1998, Unger et al. 1995, Gani & Cameron 1992] which is not solvable with gProms™. The system has to be reduced to an index to one. To solve this index problem the Francis-Weir-equation for the calculation of the *tray hydraulic* will be introduced.

The outflowing liquid stream L_n will be calculated against the weir length l_w and the weir over height h_{ow}, for more details see [Betlem et al. 1998, Stichlmair & Fair 1978, Lockett 1986]:

$$h_{ow} = \frac{C_{ow}}{g^{1/3}} \cdot \left(\frac{\tilde{M}^L}{l_w \cdot \rho_n^L} \cdot L_n \right)^{2/3}, \text{ with } \frac{C_{ow}}{g^{1/3}} = 750 \text{ follows:} \qquad \text{(eq. 3.40)}$$

$$L_n = \frac{\rho_n^L \cdot l_w}{\tilde{M}^L} \cdot \left(\frac{h_{ow}}{750} \right)^{1,5}. \qquad \text{(eq. 3.41)}$$

Here the weir over height h_{ow} is the difference between the liquid part of the froth height h_f and the weir height h_w:

$$h_{ow} = h_f - h_w . \qquad \text{(eq. 3.42)}$$

The F-factor, a measure of the vapor load, is calculated with the gas velocity w_n^V and vapor density ρ_n^V:

$$F_n = w_n^V \sqrt{\rho_n^V} . \qquad \text{(eq. 3.43)}$$

3.2.1.2 Condenser

The condenser model is valid for both condensers (HP top, LP top) of the continuous system for a non-heat-integrated operation, and also for the discontinuous system where only one column is used. The heat integrated operation uses only one condenser (LP top) described here and the coupled heat exchange (HP top) described later.

In (Fig. 3.8) three balance region are shown (shell side, wall, cooling water). The condensation of the distillate is on the shell side.

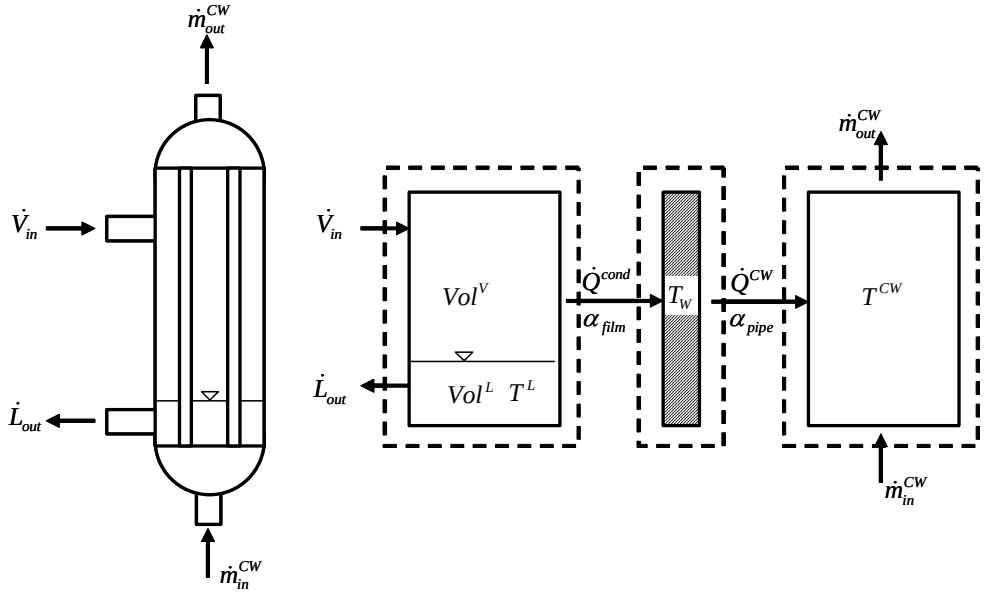

Fig. 3.8 Condenser model, based on [Rix 1998].

Shell side . For the shell side the following balances are used:

Overall mass balance: $$\frac{d(HU^L + HU^V)}{dt} = \dot{V}_{in} - \dot{L}_{out} \; . \qquad \text{(eq. 3.44)}$$

Component balance: $$\frac{d(HU^L \cdot x_i + HU^V \cdot y_i)}{dt} = \dot{V}_{in} \cdot y_{i,\,in} - \dot{L}_{out} \cdot x_{i,\,out} \; ,$$

with i = 1...NC. (eq. 3.45)

Energy balance: $$\frac{d(HU^L \cdot u^L + HU^V \cdot u^V)}{dt} = \dot{V}_{in} \cdot h_{in}^V - \dot{L}_{out} \cdot h_{out}^L - \dot{Q}^{cond} \; . \qquad \text{(eq. 3.46)}$$

The calculation of the thermodynamical equilibrium is done in analogy to the tray model (eq. 3.36) and (eq. 3.37), including the summation (eq. 3.34).

The following equation for the condenser outflow is used:

$$L_{out} = C_0 \cdot \sqrt{\frac{h_{ow}}{level}} \, . \qquad \text{(eq. 3.47)}$$

The heat flow inside the condenser $\dot{Q}^{cond}$ is calculated with help of the heat transfer coefficient α_{film}:

$$\dot{Q}^{cond} = \frac{Vol^V}{Vol_{tot}} \cdot \alpha_{film} \cdot A_{inside}(T^L - T^W) \, . \qquad \text{(eq. 3.48)}$$

The active surface for the heat transfer is defined as the outer surface of the pipes inside the condenser above the liquid level. The heat transfer of the accumulated liquid at the wall will be

neglected. The temperature difference is defined between the temperature in the liquid film T^L and the average of the wall temperature T^W (Fig. 3.8).

For the calculation of the heat transfer coefficient α_{film} the Nusselt relations of the film condensation are used [Nusselt 1916] and can be found in detail in (chapter A.3).

The pressure drop in the shell side is proportional to the square of the vapor stream V_{in} and will be calculated with the following equation:

$$\Delta p = \zeta^V \cdot V_{in}^2 \,. \qquad \text{(eq. 3.49)}$$

Wall. The heat transition through the wall is done with the energy balance around the wall of the pipe:

$$M^W \cdot c_p^W \cdot \frac{dT^W}{dt} = \dot{Q}^{cond} - \dot{Q}^{CW} \,. \qquad \text{(eq. 3.50)}$$

Cooling water side. On the cooling water side the equations for a one-phase forced convection is used. A dynamic balance is not necessary and also a calculation of the pressure drop is neglected because these values have no influence on the dynamic of the column. For a constant cooling water stream the energy balance is formulated:

$$M^{CW} \cdot c_p^{CW} \cdot \frac{dT^{CW}}{dt} = \dot{Q}^{CW} - \dot{M}^{CW} \cdot c_p^{CW} \cdot (T_{in}^{CW} - T_{out}^{CW}) \,, \qquad \text{(eq. 3.51)}$$

with an average cooling water temperature:

$$T^{CW} = \frac{1}{2}(T_{in}^{CW} - T_{out}^{CW}) \,. \qquad \text{(eq. 3.52)}$$

The heating stream which is accepted by the cooling water can be calculated in analogy to (eq. 3.48):

$$\dot{Q}^{CW} = \frac{Vol^V}{Vol_{tot}} \cdot \alpha_{pipe} \cdot A_{inside}(T^W - T^{CW}) \,. \qquad \text{(eq. 3.53)}$$

The calculations of the heat transfer coefficient α_{pipe} is done with the definition of Nu_{pipe} by Gnielinski (see chapter A.3) [Gnielinski 1994].

3.2.1.3 Column bottom (reboiler)

The column bottom and the reboiler is modelled together (Fig. 3.9).

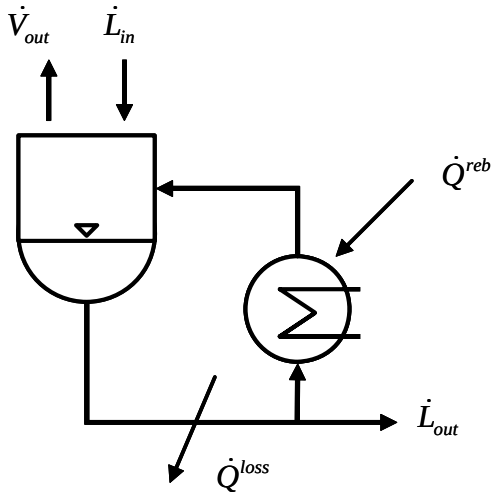

Fig. 3.9 Column bottom and reboiler model.

The bottom is modelled as an ideal separation stage which means that the phase equilibrium is calculated with (eq. 3.36) and (eq. 3.37).

There are the following balances:

Overall mass balance: $$\frac{d(HU^{L} + HU^{V})}{dt} = \dot{L}_{in} - \dot{V}_{out} - \dot{L}_{out}. \qquad \text{(eq. 3.54)}$$

Component balance: $$\frac{d(HU^{L} \cdot x_i + HU^{V} \cdot y_i)}{dt} = \dot{L}_{in} \cdot x_{i,\,in} - \dot{V}_{out} \cdot y_{i,\,out} - \dot{L}_{out} \cdot x_{i,\,out},$$

with i = 1...NC. (eq. 3.55)

Energy balance:

$$\frac{d(HU^{L} \cdot u^{L} + HU^{V} \cdot u^{V})}{dt} = \dot{L}_{in} \cdot h_{in}^{L} - \dot{V}_{out} \cdot h_{out}^{V} - \dot{L}_{out} \cdot h_{out}^{L} + \dot{Q}^{reb} - \dot{Q}^{lost}. \qquad \text{(eq. 3.56)}$$

Also the summation of the concentration is used (eq. 3.34). The reboiler has an electric heating which will be controlled. There is no heating steam used. Also the pressure drop in the reboiler will be neglected.

3.2.1.4 Additional units

This section describes the additional units splitter, pump and tank.

Splitter. The splitter model only consists of a steady state mass balance and an equation for the reflux calculation:

Mass balance: $L_{in} = D + R,$ (eq. 3.57)

Reflux: $R = \upsilon \cdot D.$ (eq. 3.58)

The following assumption are made:

- The device splits only the molar flow rate of the inlet stream between to outlet streams.
- Intensive parameters of the inlet streams are not changed by the splitter and are passed on to the outlet streams.

Pump. The unit pump consists of a pressure drop equation to model the pressure drop over the pump:

$$P_{in} = P_{out} + \Delta P . \qquad \text{(eq. 3.59)}$$

The following assumption are made:

- The pump alters only the pressure of the liquid passing through the device.
- All other properties of the passing liquid are assumed to remain unchanged.

Tank. The tank model consists of component balance, energy balance and a summation:

$$\textit{Component balance}: \frac{d(HU^{L} \cdot x_i)}{dt} = \dot{L}_{in} \cdot x_{i,\,in} - \dot{L}_{out} \cdot x_{i,\,out}, \quad \text{with } i = 1...NC. \qquad \text{(eq. 3.60)}$$

$$\textit{Energy balance:} \frac{d(HU^{L} \cdot u^{L})}{dt} = \dot{L}_{in} \cdot h_{in}^{L} - \dot{L}_{out} \cdot h_{out}^{L} . \qquad \text{(eq. 3.61)}$$

$$\textit{Summation}: \sum_{i=1}^{NC} y_{n,\,i} = 1 . \qquad \text{(eq. 3.62)}$$

The following assumption are made:

- Any amount of vapor present is negligible.
- The pressure in the tank is equal to that of the incoming liquid.
- Liquid hold up is perfectly mixed.
- Intensive properties of the hold up are equal to the outlet stream.

3.2.1.5 Controller model

The controller model uses the equation for a classic PI-controller:

$$\textit{Controller equation}: u(t) = K_P \cdot \left(e(t) + \frac{1}{\tau_R} \int_0^t e(t)dt \right), \qquad \text{(eq. 3.63)}$$

$$\text{with } e(t) = w(t) - y(t) . \qquad \text{(eq. 3.64)}$$

To reproduce the reality, boundaries for the control value are introduced:

$$u(t) = \text{min.-value, if } u(t) < \text{min.-value}, \qquad \text{(eq. 3.65)}$$

$$u(t) = \text{max.-value, if } u(t) > \text{max.-value}. \qquad \text{(eq. 3.66)}$$

Let's give an example: The heat duty of the reboiler only can be between zero and 50 kW, which sets the min.-value to zero and the max.-value to 50 kW. The controller now only operates between zero and 50 kW (Fig. 3.10).

```
  CASE ControllerState OF                                    # Boudaries
   WHEN ctrlNormal:                                          # Inside the boudaries
    OutputSignal = CalcSignal ;
   SWITCH TO ctrlLowSat IF CalcSignal < MinSignal ;
   SWITCH TO ctrlUpSat IF CalcSignal > MaxSignal ;
   WHEN ctrlLowSat:                                          # Lower than the boudaries
    OutputSignal = MinSignal ;
    SWITCH TO ctrlNormal
    IF CalcSignal >= MinSignal and  CalcSignal <= MaxSignal ;
   SWITCH TO ctrlUpSat IF CalcSignal > MaxSignal ;
   WHEN ctrlUpSat:                                           # Higher than the boudaries
    OutputSignal = MaxSignal ;
    SWITCH TO ctrlNormal
    IF CalcSignal >= MinSignal and  CalcSignal <= MaxSignal ;
   SWITCH TO ctrlLowSat IF CalcSignal < MinSignal ;
 END # CASE ControllerState inside Automatic
```

Fig. 3.10 gProms™ code to reproduce the real controller boundary in the model.

The controller can also have different states:

- *Automatic*: The controller is set to automatic and the equation (eq. 3.63) is used (Fig. 3.11-A).
- *Inactive*: The controller is inactive, control value $u(t) = 0$ (Fig. 3.11-B).
- *Manual:* The control value $u(t)$ is set to a constant value (e.g.: reboiler heat duty 15 kW) (Fig. 3.11-C).
- *Direct channel*: In this mode also (eq. 3.63) is used but the set value will be influenced by an other variable. The set point changes depending on the other variable (e.g.: infinite reflux at the top of the column: The distillate stream = the reflux stream back to the column, so the value of the distillate stream is the set point of the reflux stream controller) (Fig. 3.11-D).

To switch between the four different states a *trigger*/ *threshold* combination is used. To switch a controller from *inactive* to *automatic* for example depending on the reboiler level, the *trigger* is the level and the *threshold* is set to e.g. 60% level height. If the level height is higher or equal to the threshold the controller is switched to *automatic*. Keying times and dead times are not implemented in the controller model.

This controller model can be used for different kinds of column setups and control concepts. The model is used for the start-up of the discontinuous processes as well for start-up of the continuous processes.

```
WHEN Automatic:                                          # Controller automatic
  Error = SetPoint - Measurement ;                        # Error calculation
  $IntError = Error ;                                     # Integration action
  CalcSignal = Bias + Gain * (Error + IntError / ResetTime); # PI control law

  CASE ControllerState OF                                 # Boudaries
   WHEN ctrlNormal:                                       # Inside the boudaries
    OutputSignal = CalcSignal ;
   SWITCH TO ctrlLowSat IF CalcSignal < MinSignal ;
   SWITCH TO ctrlUpSat IF CalcSignal > MaxSignal ;
   WHEN ctrlLowSat:                                       # Lower than the boudaries
    OutputSignal = MinSignal ;
    SWITCH TO ctrlNormal
    IF CalcSignal >= MinSignal and  CalcSignal <= MaxSignal ;
   SWITCH TO ctrlUpSat IF CalcSignal > MaxSignal ;
   WHEN ctrlUpSat:                                        # Higher than the boudaries
    OutputSignal = MaxSignal ;
    SWITCH TO ctrlNormal
    IF CalcSignal >= MinSignal and  CalcSignal <= MaxSignal ;
   SWITCH TO ctrlLowSat IF CalcSignal < MinSignal ;
END # CASE ControllerState inside Automatic                                    A
```

```
WHEN Inactive:                                           # Controller inactive
 Error = 0 ;                                             # NO Error is calculated
 $IntError = 0 ;                                         # NO Integration action
 CalcSignal = 0 ;                                        # ZERO output is generated
 OutputSignal = CalcSignal ;                             # Propagate the zero signal
SWITCH TO Automatic IF Trigger >= Threshold ;
SWITCH TO Manual IF Trigger_man >= Threshold_man ;
SWITCH TO DirectChannel IF Trigger_dir >= Threshold_dir ;                      B
```

```
WHEN Manual:                                             # Controller is set manually
 Error = 0 ;                                             # NO Error is calculated
 $IntError = 0 ;                                         # NO Integration action
 CalcSignal = ManualValue ;                              # Output set to ManualValue
 OutputSignal = CalcSignal ;                             # Propagate the setting
SWITCH TO Automatic IF Trigger >= Threshold ;                                  C
```

```
WHEN DirectChannel:                                      # Controller direct channel
 Error = 0 ;                                             # NO Error is calculated
 $IntError = 0 ;                                         # NO Integration action
 CalcSignal = ChannelSource ;                            # Output set to ManualValue
 OutputSignal = CalcSignal ;                             # Propagate the setting
SWITCH TO Automatic IF Trigger >= Threshold ;                                  D
```

Fig. 3.11 gProms™ code of the different controller modes (A: automatic; B: inactive; C: manual; D: direct channel).

3.2.2 Specifics of the continuous column system model

Besides the condenser the rigorous continuous model consists of the reboiler and the column of the coupled heat exchanger, which is used as an additional unit for the heat integration between the high and the low pressure column. The next sketch shows the complete structure of the continuous model:

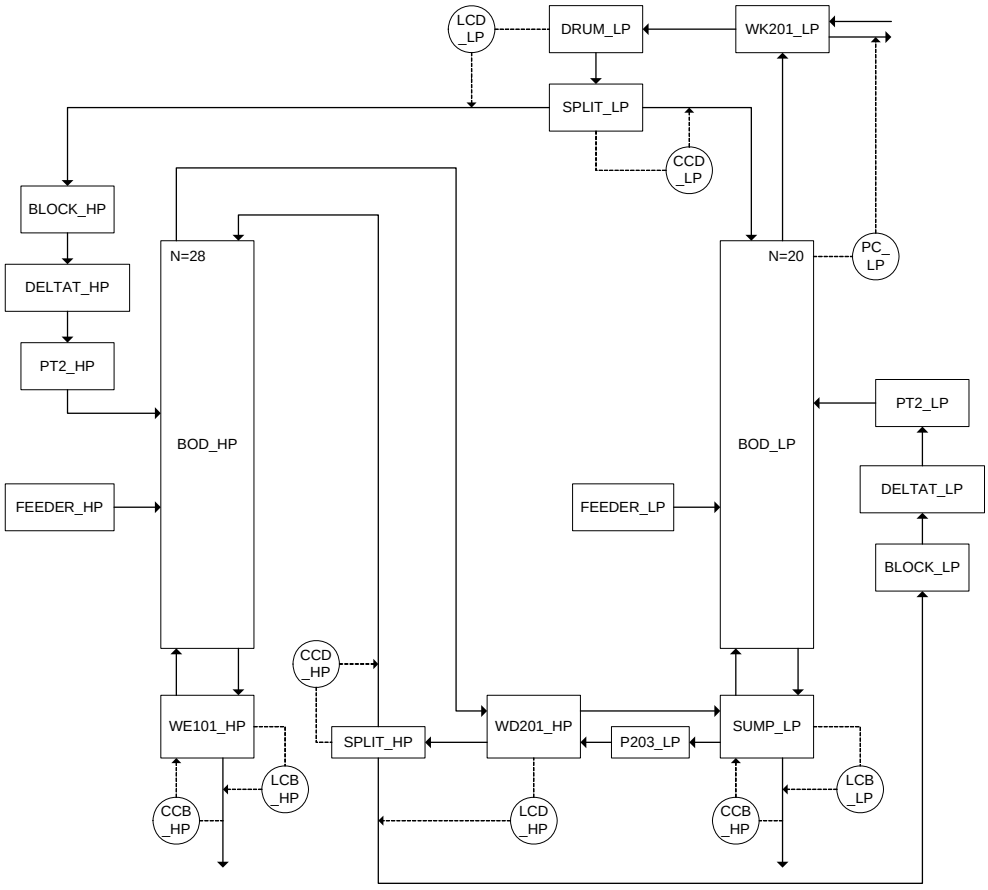

Fig. 3.12 Unit connection in gProms™ (one controller setup as an example).

The model consists of two columns, one for atmospheric pressure (LP) and one for high pressure (HP). The high pressure column has a reboiler, 28 trays (model is independend of tray number) and on the top the coupled heat exchanger as a condenser. This heat exchanger is also the reboiler of the low pressure column, which has 20 trays and a condenser at the top. A coupled heat exchanger means that the vapor of the high-pressure column heats up the bottom of the low-pressure column. Besides this heat integration the column system is also mass integrated, because the distillate streams from the top of each column go into the other column as a recycle stream (Fig. 3.12).

For process control concepts where an additional reboiler at the bottom of the LP-column is used, the HP-column has also an normal condenser at the top, to use the system without heat integration. In the next chapter the reboiler model of the LP column will be introduced, which is different from the model in (chapter 3.2.1.3).

The units listed in table 3.1 are used in the continuous model.

Table 3.1. Description of the gProms™ models and units.

UNIT in gProms™	description	model name in gProms™	chapter
SUMP_LP	bottom + reboiler LP	BOIL_ZU	chapter 3.2.2.1
BOD_LP	column with trays LP	DTRAYS_LP, consists of 20x DTRAY	chapter 3.2.1.1
FEEDER_LP	feed inlet LP	FEEDER	chapter 3.2.1.1
WK201_LP	condenser LP	KON	chapter 3.2.1.2
SPLIT_LP	splitter LP	SPLITTER	chapter 3.2.1.4
DRUM_LP	drum	DRUM	chapter 3.2.1.4
WE101_HP	reboiler HP	BOIL	chapter 3.2.1.3
BOD_HP	column with trays HP	DTRAYS_HP, consists of 28x DTRAY	chapter 3.2.1.1
FEEDER_HP	feed inlet HP	FEEDER	chapter 3.2.1.1
WD201_HP	coupled heat exchanger HP	BOIL_KOPP	chapter 3.2.2.2
SPLIT_HP	splitter HP	SPLITTER	chapter 3.2.1.4
P203_LP	pump	PUMPE	chapter 3.2.1.4
TANK1-3	tanks for the batch structure	DRUM	chapter 3.2.1.4
CCB_HP	concentration controller bottom HP column	PI_CTRL_AMI	chapter 3.2.1.5
LCB_HP	level controller bottom HP column	PI_CTRL_AMI	chapter 3.2.1.5
CCD_HP	concentration controller distillate HP column	PI_CTRL_AMI	chapter 3.2.1.5
LCD_HP	level controller distillate HP column	PI_CTRL_AMI	chapter 3.2.1.5
PC_HP	pressure controller HP column	PI_CTRL_AMI	chapter 3.2.1.5
CCB_LP	concentration controller bottom LP column	PI_CTRL_AMI	chapter 3.2.1.5
LCB_LP	level controller bottom LP column	PI_CTRL_AMI	chapter 3.2.1.5
CCD_HP	concentration controller distillate LP column	PI_CTRL_AMI	chapter 3.2.1.5
LCD_HP	level controller distillate LP column	PI_CTRL_AMI	chapter 3.2.1.5
PC_LP	pressure controller LP column	PI_CTRL_AMI	chapter 3.2.1.5

3.2.2.1 Reboiler model (LP-column)

The reboiler of the LP-column consists of the column bottom, the electric heater and the coupled heat exchanger, this means in practice a combination of two tanks with the column bottom.

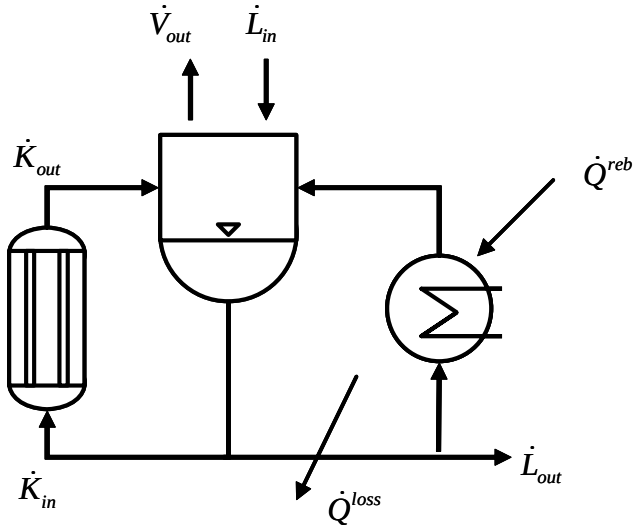

Fig. 3.13 „Twin“-LP-column bottom (left: coupling-heat exchanger, right: additional reboiler).

There are two ways of energy input. One input from outside with an external electric heater and one from the coupled heat exchanger (HP-column, Fig. 3.13). Both „reboilers“ can be used together or independent.

The following balances are used:

Overall mass balance:
$$\frac{d(HU^L + HU^V)}{dt} = \dot{L}_{in} - \dot{V}_{out} + \dot{K}_{in} - \dot{L}_{out} - \dot{K}_{out} \quad . \qquad \text{(eq. 3.67)}$$

Component balance:
$$\frac{d(HU^L \cdot x_i + HU^V \cdot y_i)}{dt} \quad ,$$

$$= \dot{L}_{in} \cdot x_{i,\,in} - \dot{V}_{out} \cdot y_{i,\,out} + \dot{K}_{in} \cdot x_{i,\,in} - \dot{K}_{out} \cdot y_{i,\,out} - \dot{L}_{out} \cdot x_{i,\,out}$$

with i = 1...NC. (eq. 3.68)

Energy balance:
$$\frac{d(HU^L \cdot u^L + HU^V \cdot u^V)}{dt} \quad . \qquad \text{(eq. 3.69)}$$

$$= \dot{L}_{in} \cdot h_{in}^L - \dot{V}_{out} \cdot h_{out}^V - \dot{L}_{out} \cdot h_{out}^L + \dot{K}_{in} \cdot h_{in}^K - \dot{K}_{out} \cdot h_{out}^K + \dot{Q}^{reb} - \dot{Q}^{loss}$$

The bottom is model as an ideal equilibrium stage, so the equations (eq. 3.36) & (eq. 3.37) will be used for the phase equilibrium and also the summation (eq. 3.34) is used.

Now the coupled heat exchanger will be described in detail.

3.2.2.2 Coupled heat exchanger

The model of the coupled heat exchanger is based on the model of the condenser shown above. It is a combination of the condenser for the vapor stream of the HP column and the reboiler of

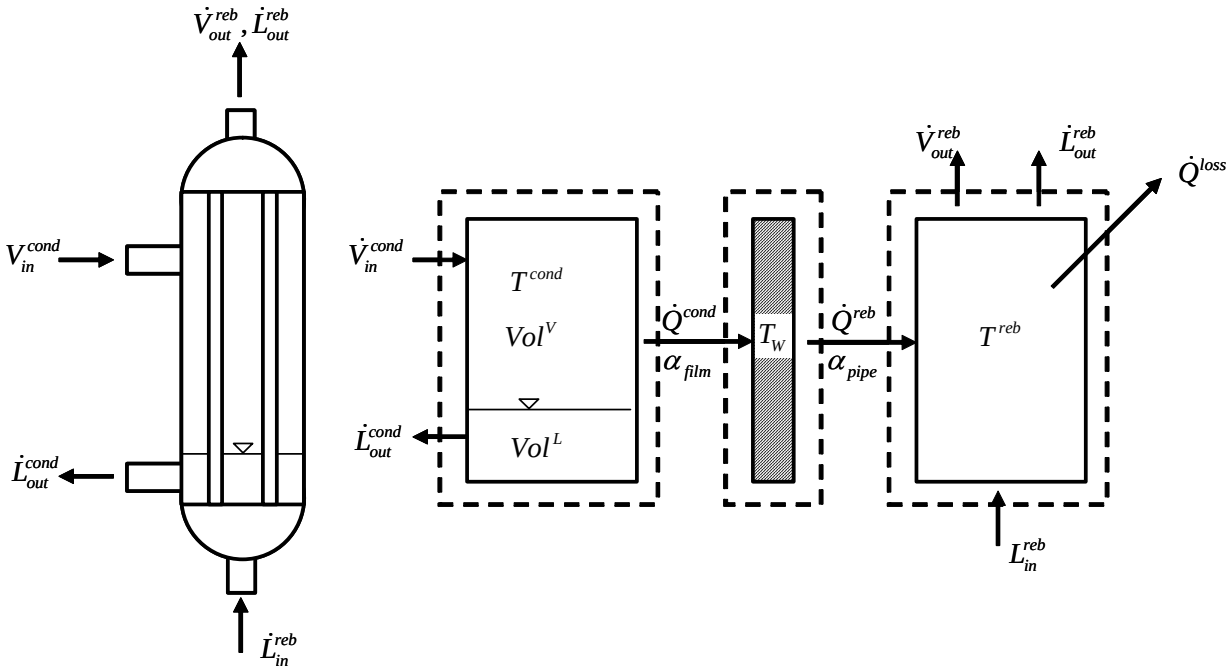

Fig. 3.14 Balance regions for the coupled heat exchanger.

the LP column. The HP side is modeled as a condenser and the LP side as a complete dynamic reboiler, which is a „cooling stream“ for the HP column. The LP reboiler runs in a forced mode, therefore a circulation pump is used, to pump the liquid through the bottom of the column and the coupled heat exchanger tank and the electric heater tank (see Fig. 3.6). We have three balance regions in this model, the condenser side (shell side), the wall and the reboiler side (Fig. 3.14).

Shell side . The model of the shell side is analog to the common condenser model (chapter 3.2.1.2). The following balance equation are used:

Overall mass balance:
$$\frac{d(HU^{L,\,cond} + HU^{V,\,cond})}{dt} = \dot{V}_{in}^{cond} - \dot{L}_{out}^{cond} \quad . \qquad \text{(eq. 3.70)}$$

Component balance:
$$\frac{d(HU^{L,\,cond} \cdot x_i + HU^{V,\,cond} \cdot y_i)}{dt} = \dot{V}_{in}^{cond} \cdot y_{i,\,in} - \dot{L}_{out}^{cond} \cdot x_{i,\,out} \quad ,$$
with i = 1...NC. (eq. 3.71)

Energy balance:
$$\frac{d(HU^{L,\,cond} \cdot u^{L} + HU^{V,\,cond} \cdot u^{V})}{dt} = \dot{V}_{in}^{cond} \cdot h_{in}^{V} - \dot{L}_{out}^{cond} \cdot h_{out}^{L} - \dot{Q}^{cond} \quad . \qquad \text{(eq. 3.72)}$$

To calculate the phase equilibrium the equations similar to the tray model are used (eq. 3.36) & (eq. 3.37), with the summation (eq. 3.34). The heat stream of the distillate stream is calculated with the film theory by Nusselt (chapter A.3):

$$\dot{Q}^{cond} = \frac{Vol^{V}}{Vol_{tot}} \cdot \alpha_{film} \cdot A_{inside}(T^{L} - T^{W}). \qquad \text{(eq. 3.73)}$$

The pressure drop is calculated with help of the vapor velocity w^{v} in a nozzle:

$$\Delta p = \zeta^{V} \cdot \frac{\rho^{V}}{2} \cdot (w^{v})^{2}. \qquad \text{(eq. 3.74)}$$

Wall. A balance around the wall is used to calculate the wall temperature:

$$M^{W} \cdot c_{p}^{W} \cdot \frac{dT^{W}}{dt} = \dot{Q}^{cond} - \dot{Q}^{reb} \quad . \qquad \text{(eq. 3.75)}$$

Reboiler side. The dynamic balance of the reboiler side leads to an index problem which has to be solved [Rix 1998]. To reduce the index only stationary balances are used. This brings only a very small error because of the negligible liquid hold up in the reboiler pipes compared to the bottom of the LP column and the very small influence on the dynamic. The condenser side has to be modeled dynamically because the liquid hold up of the shell side brings the heat into the system.

These are the balances for the reboiler side:

Overall mass balance: $0 = L_{in}^{reb} - V_{out}^{reb} - L_{out}^{reb}.$ (eq. 3.76)

Component balance: $0 = L_{in}^{reb} \cdot x_{i,\,in} - V_{out}^{reb} \cdot y_{i,\,out} - L_{out}^{reb} \cdot x_{i,\,out}$,
with i = 1...NC. (eq. 3.77)

Energy balance: $0 = L_{in}^{reb} \cdot h_{in}^{L} - V_{out}^{reb} \cdot h_{out}^{V} - L_{out}^{reb} \cdot h_{out}^{L} + \dot{Q}^{reb} - \dot{Q}^{loss}.$ (eq. 3.78)

To calculate the phase equilibrium the equations similar to the tray model are used (eq. 3.36) & (eq. 3.37), with the summation (eq. 3.34).

On the reboiler side we have a two-phase flow, so the calculation of the pressure drop is much more complicated. The following pressure drop equation is used, consisting of a hydraulic, a two phase and an acceleration pressure drop:

$$\Delta p \equiv \Delta p_{h} + \Delta p_{2ph} + \Delta p_{a}. \qquad \text{(eq. 3.79)}$$

The detailed calculation of the different pressure drops is done in the appendix (chapter A.2).

Also the heat transfer is calculated for a two phase flow:

$$\dot{Q}^{reb} = \frac{Vol^{V}}{Vol_{tot}} \cdot \alpha_{pipe}^{2ph} \cdot A_{inside}(T^{W} - T^{reb}). \qquad \text{(eq. 3.80)}$$

The heat transfer coefficient α_{pipe}^{2ph} consists of a convective term α_C and a term for still bubble boiling α_B. The calculation of the heat coefficients is done in detail in the appendix (chapter A.3).

3.2.3 Specifics of the batch-model

The rigorous dynamic discontinuous process model consists of only one column which is operated at different pressures. The model uses only the base units described in chapter 3.2.1.

The only modifications are additional tanks on the top or the bottom of the column to build the different setups for the inverted and the regular cases (Fig. 3.15). The inverted process has one or two tanks at the top, the regular process has one big reboiler at the bottom or an external feed tank beside the reboiler. Furthermore there are product tanks included at the top (regular process) or at the bottom (inverted process). For the unit connections see Fig. 3.15. There are no special models developed only for the batch process.

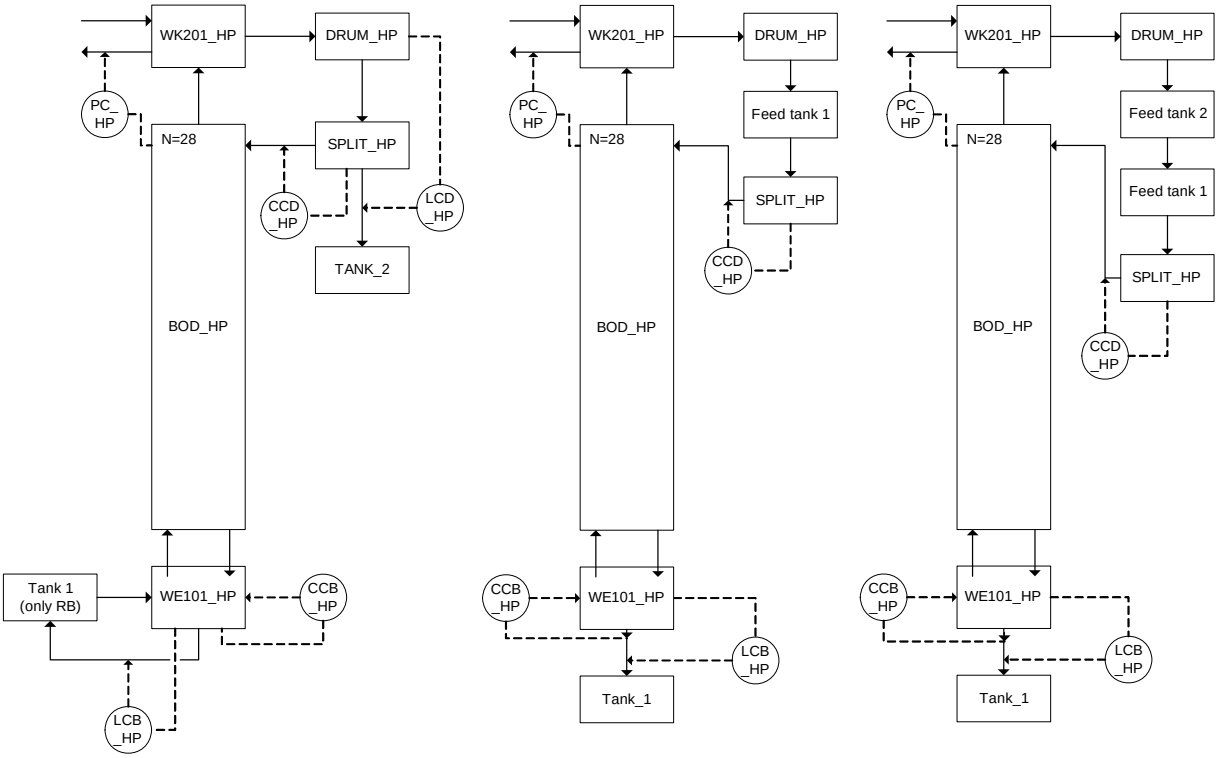

Fig. 3.15 Unit connection in gProms™ (left: regular batch; middle: inverted batch; right: advanced inverted batch).

3.3 The dynamic start-up model

In this chapter the dynamic start-up model starting from cold and empty for the batch and the continuous processes will be introduced. This is motivated due to the fact that for the comparison of the discontinuous processes consistent initial conditions are needed to get reliable

results. For the continuous process the coupling of the two columns are the main challenge. This part can also only be modelled with a start-up model.

The start-up model for the continuous (two column) and the discontinuous (one column) process bases on the work of Reepmeyer and Forner and has been modified for the given applications [Reepmeyer 2004a, Forner et al. 2006].

There is a switching of the model equations in the reboiler, the tray and the condenser units necessary to model the start-up from cold and empty. The three switching conditions are described now:

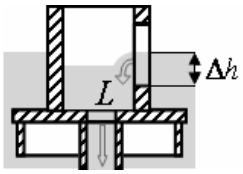

$$IF \quad level \geq h_w \quad THEN$$

$$\dot{L}_{out} = \frac{\rho_n^L l_w}{\tilde{M}^L}\left(\frac{h_{ow}}{750}\right)^{1.5}$$

$$ELSE$$

$$\dot{L}_{out} = 0$$

Step1: If the level on the tray is higher then the weir (Francis-Weir-function), liquid is leaving the tray. A leaking through the bubble caps on the tray is neglected in this case[1]. If the level is lower than the weir, the liquid outflow is zero (compare with (eq. 3.41)).

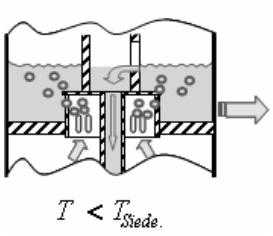

$$IF \quad p_n \geq p_{n-1} \quad THEN$$

$$\dot{V}_{in,n} = \frac{A_{active}}{\tilde{M}_n} \cdot \sqrt{\frac{2 \cdot \Delta p_{d,n} \cdot \rho_n^V}{\zeta^V}}$$

$$ELSE$$

$$\dot{V}_{in,n} = 0$$

Step2: Vapor reaches the tray or the condenser from the unit below, if the pressure in the unit below is higher than hydrostatic pressure inside the unit (tray or condenser). Otherwise the vapor stream is set to zero (compare with (eq. A.12) and (eq. 3.39)).

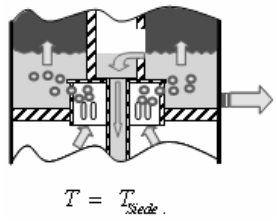

$$IF \quad T_{out,n} \geq T_{boil} \quad THEN$$

$$y_{i,n} p_n = x_{i,n} \gamma_{i,n} p_i^{vap}$$

$$T_{boil} = T_{out,n}$$

$$ELSE$$

$$y_{i,n} = x_{i,n}$$

$$P_{V_{out},n} = P_{initial}$$

Step3: Phase equilibrium is reached inside the unit if the VLE-boiling temperature is lower or equal the vapor outlet temperature of the same unit. If not alternative equations are used for pressure and vapor concentration to fulfil the overall equation number (compare with (eq. 3.36)).

The overall number of equations are always the same. Only the necessary equation depending on the current status of the start-up operation is used.

As initial conditions for the equation system an empty column under ambient temperature (25°C) is set. The start concentrations in every unit will be set equal to the feed concentration and the pressure is set to ambient condition (1,015 bar). The controllers are also in the start up status which means the controller is in inactive or in manual mode. Inactive mode means that the

1. leaking is neglected, because the error is very small due to very small leaking flows (only small droplets)

manipulated variable is set to zero and the controller is not working. A detailed description of the controller model will be given in the next section.

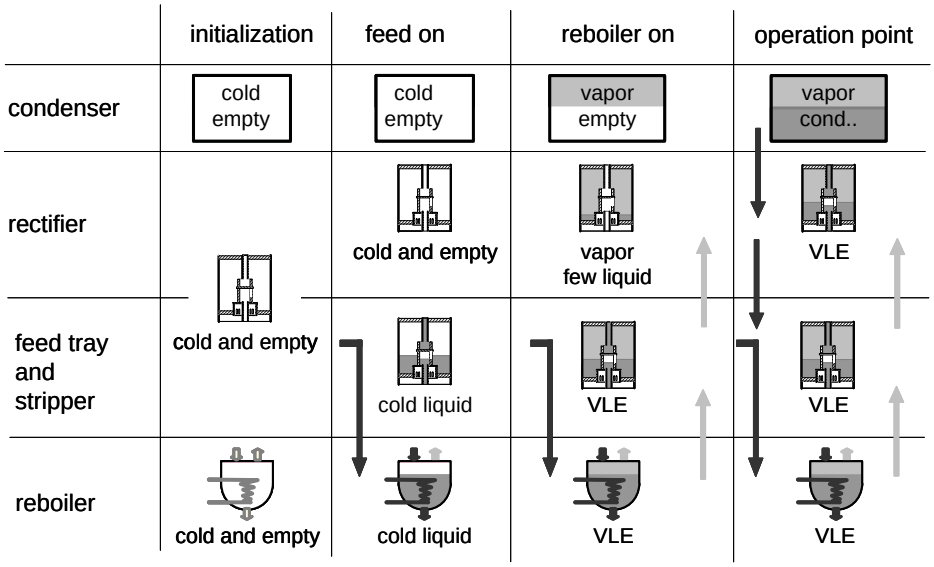

Fig. 3.16 Start-up sequence of a distillation column.

An overview about the different states is given in Fig. 3.16 during the start-up process in the case of a feed input in the middle of the column. For the regular and the inverted case, the feed input is at the bottom or at the top, but the states of the start-up process will be the same.

The different controllers in the system will be set to active only if they are needed. Also the coupling of the two columns for continuous operation takes place, if the corresponding conditions are reached. The coupling conditions have to be defined by the user in gProms™ and will be implemented in the schedule. The switching during the start-up of the batch columns is done by a trigger/threshold combination inside the controller model.

4. Experimental validation

This chapter introduces the pilot plant for the experimental validation. After that a detailed description of the experimental data reconciliation is given and than finally the model validation is presented for single columns (LP and HP), the continuous setup and of the discontinuous setups (regular and inverted batch).

4.1 The pilot plant

For the validation of the continuous and the discontinuous model of the pressure swing distillation system a pilot plant (Fig. 4.1, right) is used which can be modified for all cases (continuous, regular and inverted batch). The plant consist of two columns one with 20 bubble cap trays as a low pressure column (LP) and the other with 28 bubble cap trays as a high-pressure column (HP, Fig. 4.1, right). As trays bubble cap trays with one cap and a central down-comer are used (Fig. 4.1, left). The high-pressure column can be operated up to 5 bar. The pilot plant is fully automated by an industrial process control system (PCS) Freelance2000 by ABB. Both columns have a reboiler at the bottom and a condenser at the top, so they can operate separately. For the heat integration a coupled heat exchanger is implemented which works as a condenser at the high-pressure column and as a reboiler at the low pressure column. The main design parameters of the system can be found in table 4.1, all additional data of the plant can be found in the appendix (chapter A.4.2). For the batch processes the high pressure column is used, which can be operated due to additional tanks as a regular and as an inverted column.

Each column is equipped with temperature sensors on every tray, pressure sensors at the top and at the bottom, pressure difference sensors for each stripper and rectifier section, flow sensors for every stream and liquid sampling on selected trays at each column, at outlets on top and at the bottom and at the reflux pipes.

Each tank, reboiler, drum and coupled heat exchanger is equipped with level sensors.

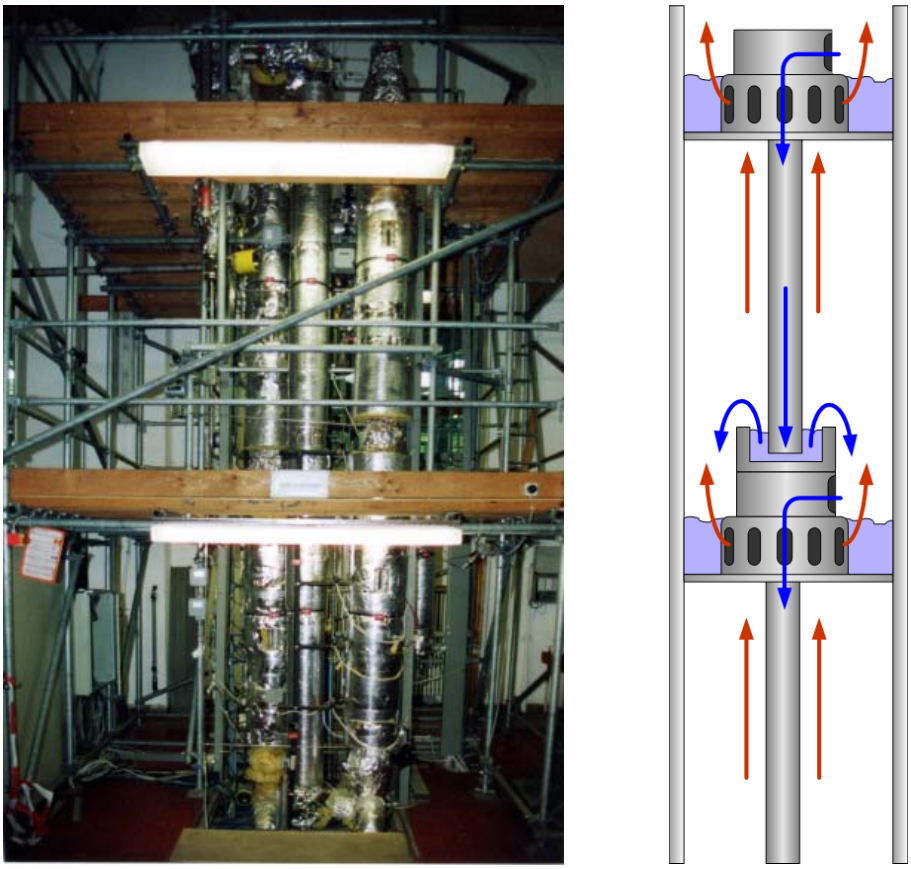

Fig. 4.1 Pressure swing column system (left), detailed draft of a tray (right).

All parts are made of stainless steel, the gaskets are mainly of teflon or viton. The reboiler, the feed preheater and the reflux heater work with an electric power supply. All control valves also have an electric power supply. To reduce heat losses the system has a thermal insulation, which reduces it, but a small value of heat losses will be left. With this equipment different process control strategies and process design are possible and also different column integrations can be implemented. With help of the PCS and the plant equipment different controller setups can be created. Especially for the pressure control at the top of the HP column two different concepts are implemented. The classic control of the pressure is the control with the cooling water flow rate Another possible control concept is the use of an additionaln inert gas stream to control the pressure at the top of the column to get another degree of freedom [Sloley 2001]. The pilot plant can be used for the steady state validation as well for the dynamic validation including start-up for continuous as well as for discontinuous operation, with or without mass and heat integration.

Table 4.1. Properties of the pressure swing column system

	LP-column	HP-column
number of trays	20	28
tray type	bubble cape trays with central down comer	
tray distance [mm]	210	150
feed/recycle input [tray]	2,4,6,8,10,12,14,16,18 (variable)	2,4,6,8,10,16,18,20,22,24 (variable)
column diameter [mm]	114	114
reboiler duty (electr.) [kW]	24,5	30,5
reboiler hold up [l]	26,5	25
type of reboiler	natural or forced circulation evaporator	natural circulation evaporator
condenser	total condenser	total condenser + coupled heat exchanger (reboiler of LP - column)
feed tanks [l]	500 or 300	300 or 500
feed preheater [kW]	10	10
product tanks [l]	2x 300	2x 300
temperature sensors (Pt100)	on every tray, all streams, cooling water	on every tray, all streams, cooling water
pressure	top, bottom, differential pressure stripping- and rectifying section	top, bottom, differential pressure stripping- and rectifying section, analog manometer at the top
concentration measurement (samples)	top, bottom, feed, reflux, tray 3, 9, 19	top, bottom, feed, reflux, tray 2, 7, 13, 23
flow measurement (mag. inductive)	top, bottom, feed, reflux, cooling water, forced circulation bottom	top, bottom, feed, reflux, cooling water
level measurement	tanks, bottom, drum, feed preheater	tanks, bottom, drum, feed preheater

All possible operation types can be found in the following list:

- LP- and HP-column independent and single:
  - *HP-column:* atmospheric pressure up to 5 bar.
  - *LP-column:* only atmospheric pressure.
- LP- and HP-column coupled:
  - *Feed split:* same feed for both columns (not used in this work).
  - *Individual feed:* each column gets an individual feed from different feed tanks; for pressure swing operation start-up not coupled: each feed has a concentration for the suitable distillation region (LP under the azeotropic point, HP above the azeotropic point), see Fig. 2.4.
  - *Heat integration:* condenser of the HP-column is used as a reboiler of the LP column, with or without an additional reboiler at the LP column.

    - *Mass integration*: the bottom product is send to the other column (not used in this work); each top product (distillate) is send to the other column (pressure swing, feedback as recycle streams), or in a row; that means only one distillate stream is send to the other column (no feedback).
- Products can be dumped in product tanks or can be put back into the feed tanks for longer experimental time and a reduced overall feed volume.
- Batch-operation (HP-column):
    - As a stripper column (inverted Batch): Feed input at the top of the column.
    - As a rectifier column (regular batch): Feed input at the bottom of the column with external feed tank.

The controllers which can be used are listed in table 4.2. This list includes all possible pairings but the right combination has to be set as defined in the control concept which needs to be analyzed.

Table 4.2. Possible controllers with their control- and manipulated variable pairing.

controller	**LP-column**		**HP-column**	
	control variable	**manipulated variable**	**control variable**	**manipulated variable**
feed stream	volume flow rate	control valve	volume flow rate	control valve
reboiler heat duty	1) temperature 2) concentration (external) 3) reboiler heat duty	electric heater	1) temperature 2) concentration (external) 3) reboiler heat duty	electric heater
reboiler level	level	drain stream (bottom)	level	drain stream (bottom)
condenser level	not available		level	1) reflux stream 2) distillate stream
reflux	1) volume stream 2) concentration (external)	1) reflux stream or distillate stream 2) reflux stream	1) volume stream 2) concentration (external)	1) reflux stream or distillate stream 2) reflux stream
distillate volume stream	volume stream	control valve	volume stream	control valve
drum level	level	1) reflux stream 2) distillate stream 3) feed stream to HP-column	not available	
pressure	column is open to atmosphere		pressure	1) inert gas input 2) condenser cooling water 3) condenser level
feed temperature	temperature	electric heater	temperature	electric heater
reflux temperature	temperature	electric heater	temperature	electric heater

The sketch of the P&ID is displayed in (Fig. 4.2).

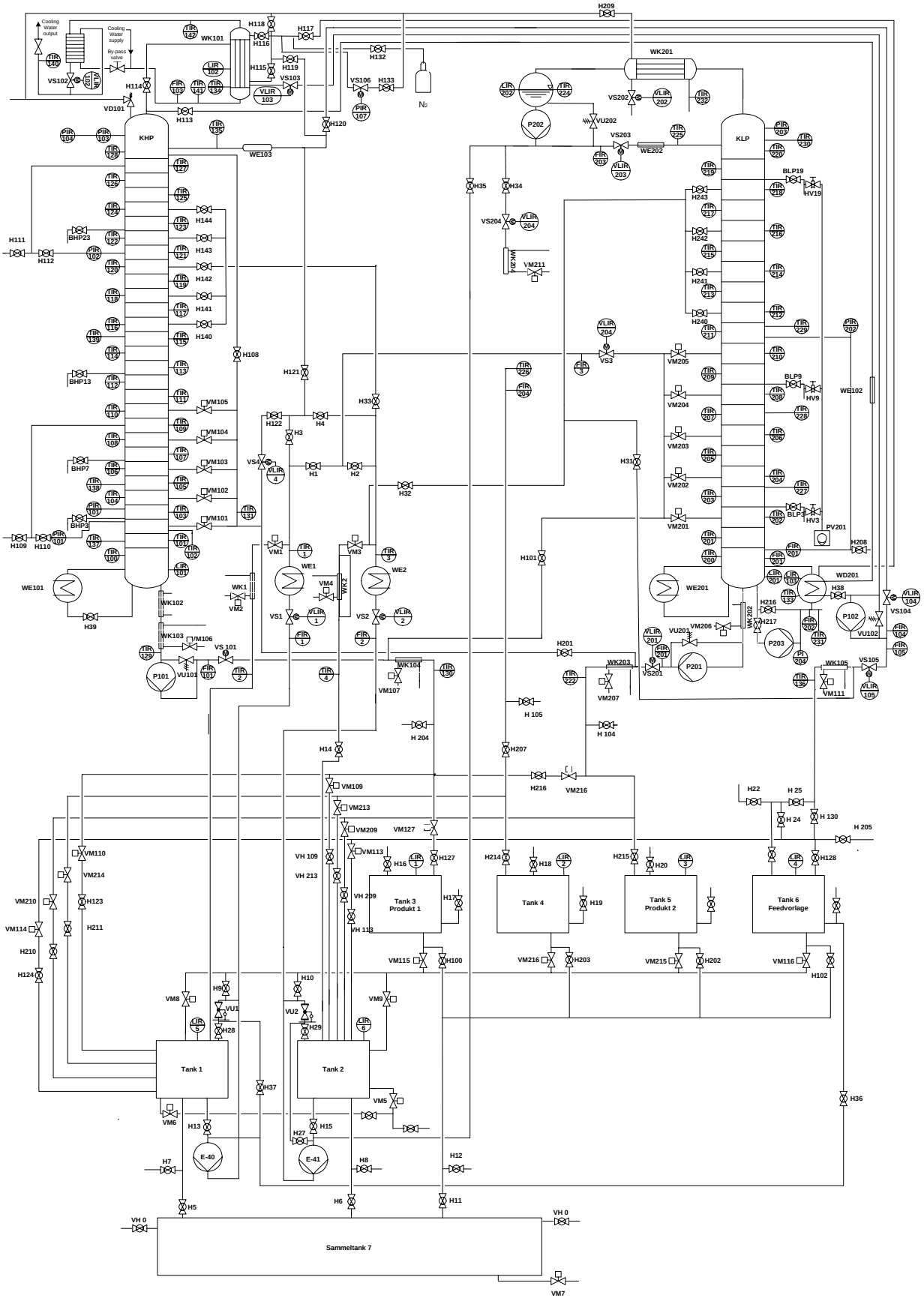

Fig. 4.2 P&ID-figure of the pressure swing column system.

4.2 Experimental data reconciliation

The main part of a comparison between simulation and experimental results is the analysis and interpretation of the experimental data. This section describes the method of the recalculation of the experimental data, used for all experimental data in all model validation chapters.

The measurement errors are very important for an interpretation of the experimental data. If the mass balance and the component balance is calculated with the experimental data there is an error because of the measurement errors. To reduce the influence of these measurement errors a simple process data reconciliation method is used for a better interpretation of the data. This method is described in detail by [Braun et al. 1993, Repke 2002] and is called the method of the Lagrangian multiplier. This methode uses the „spill-over“ of measured values, which is the fact if all input and output streams are measured, to get more consitent and reliable data records.

Mass balance. Therefore the mass balance around the process is used with a minimization of the summation of the weighted square errors:

$$\sum_{i=1}^{n_{in}} \dot{m}_i^{in,val} - \sum_{j=1}^{n_{out}} \dot{m}_j^{out,val} = 0\,, \qquad \text{(eq. 4.1)}$$

with i, j = number of input and output streams.

$$\sum_{k=1}^{n_{out}+n_{in}} \left(\frac{\Delta \dot{m}_k}{\delta_k}\right)^2 = \sum_{i=1}^{n_{in}} \left(\frac{\dot{m}_i^{in} - \dot{m}_i^{in,val}}{\delta_i}\right)^2 + \sum_{j=1}^{n_{aus}} \left(\frac{\dot{m}_j^{out} - \dot{m}_j^{out,val}}{\delta_j}\right)^2 \rightarrow \min \quad . \qquad \text{(eq. 4.2)}$$

Here (eq. 4.2) is the function which has to be minimized and (eq. 4.1) is the side condition which also has to be fulfilled. The method of the Lagrangian multiplier associate both equation:

$$G(\dot{m}_i^{in,val}, \dot{m}_j^{out,val}, \lambda) = S(\dot{m}_i^{in,val}, \dot{m}_j^{out,val}) + \lambda f(\dot{m}_i^{in,val}, \dot{m}_j^{out,val}), \qquad \text{(eq. 4.3)}$$

with S corresponding to (eq. 4.2) and f corresponding to (eq. 4.1), the side condition. Now this new function (eq. 4.3) has to be minimized. With differentiating for each variable the following equation system (eq. 4.4) to (eq. 4.6) can be calculated:

$$\frac{\partial G}{\delta \dot{m}_i^{in,val}} = -\frac{2}{\delta_i^2}(\dot{m}_i^{in} - \dot{m}_j^{in,val}) + \lambda = 0\,, \qquad \text{(eq. 4.4)}$$

$$\frac{\partial G}{\delta \dot{m}_i^{out,val}} = -\frac{2}{\delta_i^2}(\dot{m}_i^{out} - \dot{m}_j^{out,val}) + \lambda = 0\,, \qquad \text{(eq. 4.5)}$$

$$\frac{\partial G}{\delta \lambda} = f = \sum_{i=1}^{n_{in}} \dot{m}_i^{in,val} - \sum_{j=1}^{n_{out}} \dot{m}_j^{out,val} = 0\,. \qquad \text{(eq. 4.6)}$$

Combining (eq. 4.6) with (eq. 4.5) and (eq. 4.4) we get:

$$\sum_{i=1}^{n_{in}} \left(\dot{m}_i^{in,\,val} + \frac{\lambda}{2}\delta_i^2 \right) - \sum_{j=1}^{n_{out}} \left(\dot{m}_j^{out,\,val} + \frac{\lambda}{2}\delta_i^2 \right) = 0 . \qquad \text{(eq. 4.7)}$$

Now the multiplicand λ can be calculated to:

$$\frac{\lambda}{2} = \frac{\sum_{j=1}^{n_{out}} \dot{m}_j^{out} - \sum_{i=1}^{n_{in}} \dot{m}_i^{in}}{\sum_{k=1}^{n_{out}+n_{in}} \delta_{m,k}^2} . \qquad \text{(eq. 4.8)}$$

After that the validated mass flows follows:

$$\dot{m}_i^{in,\,val} = \dot{m}_i^{in} + \frac{\delta_{m,i}^2 \left(\sum_{j=1}^{n_{out}} \dot{m}_j^{out} - \sum_{i=1}^{n_{in}} \dot{m}_i^{in} \right)}{\sum_{k=1}^{n_{out}+n_{in}} \delta_{m,k}^2} \quad \text{and} \qquad \text{(eq. 4.9)}$$

$$\dot{m}_i^{out,\,val} = \dot{m}_i^{out} - \frac{\delta_{m,i}^2 \left(\sum_{j=1}^{n_{out}} \dot{m}_j^{out} - \sum_{i=1}^{n_{in}} \dot{m}_i^{in} \right)}{\sum_{k=1}^{n_{out}+n_{in}} \delta_{m,k}^2} . \qquad \text{(eq. 4.10)}$$

The validated standard deviation is calculated due to:

$$\delta_{m,k}^{val} = \delta_{m,k} \frac{\sqrt{\left[\left(\sum_{i=1}^{n_{out}+n_{in}} \delta_{m,i}^2 \right) - \delta_{m,k}^2 \right] \sum_{i=1}^{n_{out}+n_{in}} \delta_{m,i}^2}}{\sum_{i=1}^{n_{out}+n_{in}} \delta_{m,i}^2} . \qquad \text{(eq. 4.11)}$$

The complete derivation is done by [Braun et al. 1993, see also Repke 2002]. Similar to the mass balance this derivation can be done for the component balance.

Component balance. Also the component balance around the process can be used with a minimization of the summation of the weighted square errors. For the component balance the equation (eq. 4.9) and (eq. 4.10) will be changed to:

$$\dot{m}_{i,c}^{in,\,val} = \dot{m}_{i,c}^{in} + \frac{\delta_{m,i}^2 \left(\sum_{j=1}^{n_{out}} \dot{m}_{j,c}^{out} - \sum_{l=1}^{n_{in}} \dot{m}_{l,c}^{in} \right)}{\sum_{k=1}^{n_{out}+n_{in}} \delta_{m,k,c}^2} \quad \text{and} \qquad \text{(eq. 4.12)}$$

$$\dot{m}_{i,c}^{out,val} = \dot{m}_{i,c}^{out} - \frac{\delta_{m,i}^2 \left(\sum_{j=1}^{n_{out}} \dot{m}_j^{out} - \sum_{l=1}^{n_{in}} \dot{m}_l^{in} \right)}{\sum_{k=1}^{n_{out}+n_{in}} \delta_{m,k,c}^2}, \qquad \text{(eq. 4.13)}$$

$$\text{with } \dot{m}_{i,c} = \dot{m}_i^{val} \cdot w_{i,c}. \qquad \text{(eq. 4.14)}$$

In these equations the Index i stands for the stream, Index c for the component and w is the weight fraction. The standard deviation $\delta_{m,k,c}$ is calculated with help of the Gauss' error reproduction law (eq. 4.15) with (eq. 4.14) and the assumption that all mass flows are existing:

$$\delta_c = \sqrt{\left(\frac{\partial f}{\partial x_1}\right)\delta_1^2 + \left(\frac{\partial f}{\partial x_2}\right)\delta_2^2 + \ldots} \text{ and} \qquad \text{(eq. 4.15)}$$

$$\delta_{m,k,c} = \dot{m}_i^{val} \cdot \delta_c. \qquad \text{(eq. 4.16)}$$

The concentrations will now be calculated with this validated component streams:

$$w_{i,c}^{val} = \frac{\dot{m}_i^{val}}{\dot{m}_{i,c}^{val}} \text{ and} \qquad \text{(eq. 4.17)}$$

$$x_{i,c}^{val} = \frac{\dot{n}_i^{val}}{\dot{n}_{i,c}^{val}} = w_{i,c}^{val} \cdot \frac{\tilde{M}_i^{val}}{\tilde{M}_c}. \qquad \text{(eq. 4.18)}$$

The goal of this method is a coherent mass and/or component balance. Measurement errors, which are used to calculate the standard deviation δ_m for each measurement equipment were identified (table 4.3). The measurement error consists of the measurement uncertainty, the measurement equipment error, confidence factor and the conversion error, a detailed description can be found in [DIN-1319 1995]. The standard deviation δ_m for the mass flow is between 0,2 and 1,0 depending on the flow measurement equipment and the position of the equipment, respective the concentration measurement. For details see the work of Briki [Briki 2004].

Table 4.3. Overview about the main measurement errors of the used sensors in the experimental setup.

sensor	measurement errors [%]
flow sensors	2 - 4%
level sensors	4 - 8%
temperature sensors	2%
pressure sensors	2%
concentration measurement	4% - 6%

4.3 Experimental validation of the continuous process

The model validation starts with a steady-state validation of the single columns at different pressures. After that the validation of the continuous mass and heat integrated system without start-up from cold and empty will be presented for a steady-state operation point. Finally the start-up from cold and empty results will be discussed.

To fit the data between model and experiment the tray efficiency and the heat losses will be adapted. Each column has a different tray efficiency because of the tray design which is also a little bit different. The distance between the trays is different for each column (same column height, different number of trays, see table 4.1). Therefore tray efficiency is set to $\eta \approx 0{,}7$ for the LP column (20 trays) and to $\eta \approx 0{,}6$ for the HP column (28 trays). All experimental data are recalculated with the method described in chapter 4.2.

4.3.1 Single columns (steady state)

The validation starts with the steady states for the single columns; Fig. 4.3 left shows the steady state temperature profile of the LP column and Fig. 4.3 right the temperature profiles for the HP column at 2,2 bar. The simulation fits the experimental data quite well due to the error of measurement. The feed input is at tray 6 for the LP column and at tray 8 for the HP column. This point has the major error because of the positioning of the temperature sensor in the column. For an overview about all parameters see table 4.4. To get information about the concentrations as well, liquid sampling on selected trays were introduced and used for the steady state validation of the coupled system.

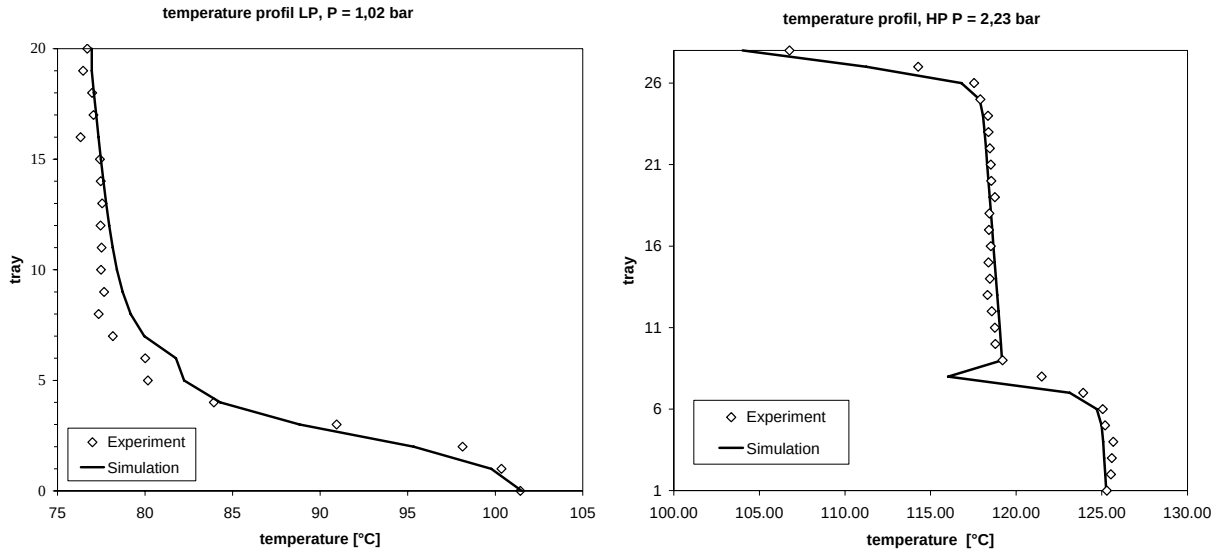

Fig. 4.3 Comparison of simulations and experiments for the single columns (temperature profile left: LP- column; right: HP-column).

Table 4.4. Setup of experiment and simulation for single column validation

	LP-column (single)		HP-column (single)	
	experiment	**simulation**	**experiment**	**simulation**
F [l/h]	25,01[a]	25[a]	19,5[a]	25[a]
$x_{F,ac}$ [mol/mol]	0,17	0,17	0,175	0,175
T_F [°C]	70	70	90	90
D [l/h]	13,61[a]	11,2[a]	16,33[a]	17,3[a]
R [l/h]	10,4	10,4	27,04	29,7
B [l/h]	15,20[a]	14,2[a]	9,33[a]	7,46[a]
P_D [bar]	1,02	1,02	2,23	2,23
$\dot{Q}_{HP}$ [kW]	5,65	5,7	13,57	13,57
$\dot{Q}_{loss}$ [W p. tray]	-[b]	14	-[b]	14

a. the deviation is due to measurement errors and volumetric values

b. not measured

4.3.2 Coupled column system (steady state)

In this step the steady-state validation of the coupled system is introduced. The experimental and the simulation data for the temperature and concentration profiles for both columns at the operating point shows Fig. 4.4 (see also table 4.5 for the data). The feed input is on tray 8 at the LP column.

Table 4.5. Setup of experiment and simulation for coupled column system validation.

	HP-column		LP-column	
	experiment	**simulation**	**experiment**	**simulation**
F [l/h]	0	0	10,06[a]	10[a]
$x_{F,ac}$ [mol/mol]	-	-	0,28	0,28
T_F [°C]	-	-	70	70
D [l/h]	19.38	17,2	25.04	20,3
R [l/h]	20,2	20.8	10,0	10
B [l/h]	5,6[a]	6,00[a]	4,27[a]	4,61[a]
P_D [bar]	3,08	3,18	1,013	1,013
$\dot{Q}_{HP}$ [kW]	8,43	8,43	0	0
$\dot{Q}_{loss}$ [W per tray]	-[b]	14	-[b]	14

a. the deviation is due to measurement errors and volumetric values

b. not measured

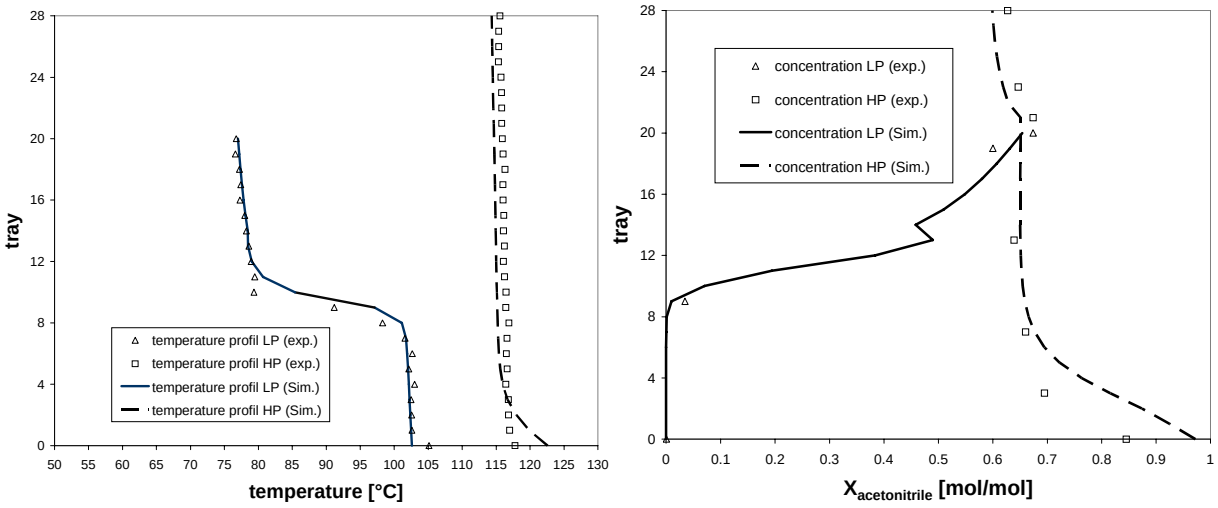

Fig. 4.4 Comparison of simulations and experiments for the coupled column system (left: temperature profile; right: concentration profile).

The liquid sample for the analysis of the concentration profile are taken from different positions along the column (table 4.1, concentration measurement). They are analyzed using a gas chromatography (GC). The method is described in detail in the standard operation procedure (SOP) of the two pressure column system. The measurement error of this analytical method (GC-Analysis) is around 4%.

There is a good agreement between the experimental results and the simulation especially for the new introduced concentration measurement on selected trays. The model is now validated for steady states.

4.3.3 Start-up validation (dynamic) of the coupled column system

The dynamic model of the coupled column system will now be validated including the start-up process from cold and empty. For the simulation and the experiment a feed input into the LP column with a concentration of 0,27 mol/mol. The main data of the experiment are listed in table 4.6.

Because of the heat integration and the feed input into the LP column which does not have a reboiler, for the start-up an auxiliary feed with a concentration higher than the azeotropic point is used for the HP column ($x_{ACN} > x^{HP}_{ACN,\,az}$). The auxiliary feed is used only until flow becomes available from the LP column condenser. The complete start-up procedure is sketched in Fig. 4.5. The operation schedule is illustrated in Fig. 4.6. The specifications used for the product streams require at most 0,05 mol% impurities. Both columns start from atmospheric pressure and from cold and empty. The pressure in the HP column will be increased gradually. The main feed flow rate into the LP column is 10 l/h.

Table 4.6. Setup of experiment and simulation for coupled column start-up validation (steady state).

	HP-column		LP-column	
	experiment	**simulation**	**experiment**	**simulation**
F [l/h]	0	0	10	10
$x_{F,ac}$ [mol/mol]	-	-	0,27	0,27
T_F [°C]	-	-	70	70
R [l/h]	20	20	10	10
P_D [bar]	3,3[a]	3,3[a]	1,013	1,013
$\dot{Q}_{HP}$ [kW]	12	12	0	0
$\dot{Q}_{loss}$ [W per tray]	-	14	-	14

a. Start condition P = 1,0 bar and an auxiliary feed for the HP column with a respective concentration higher than the azeotropic point. This feed stream will be switch of when the start-up process is finished

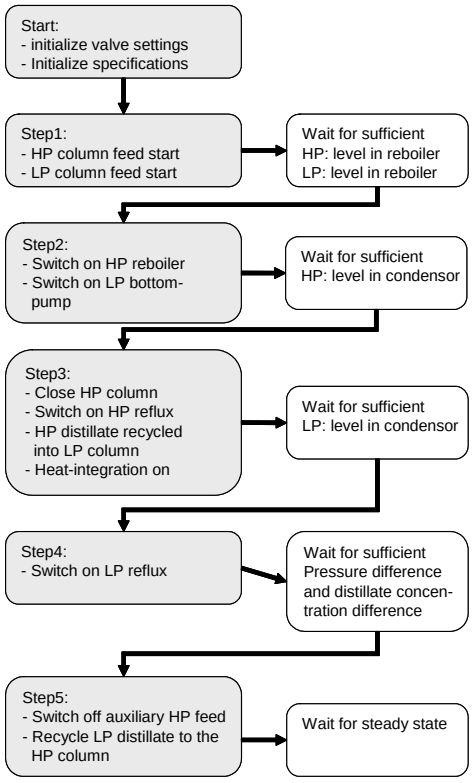

Fig. 4.5 Start-up procedure description.

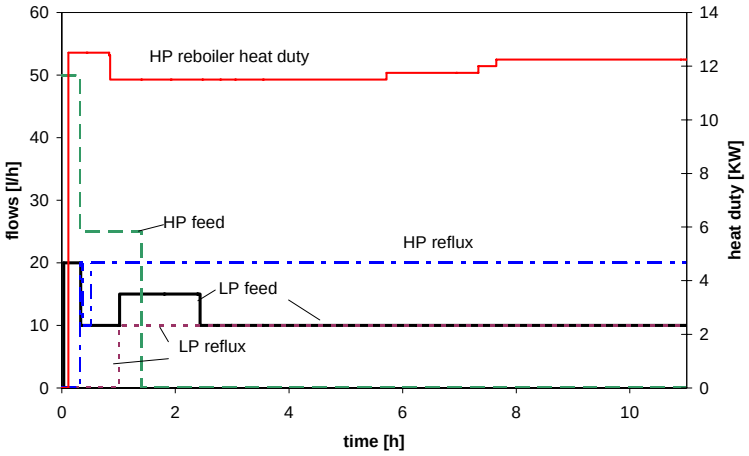

Fig. 4.6 Operation schedule for experiment and simulation.

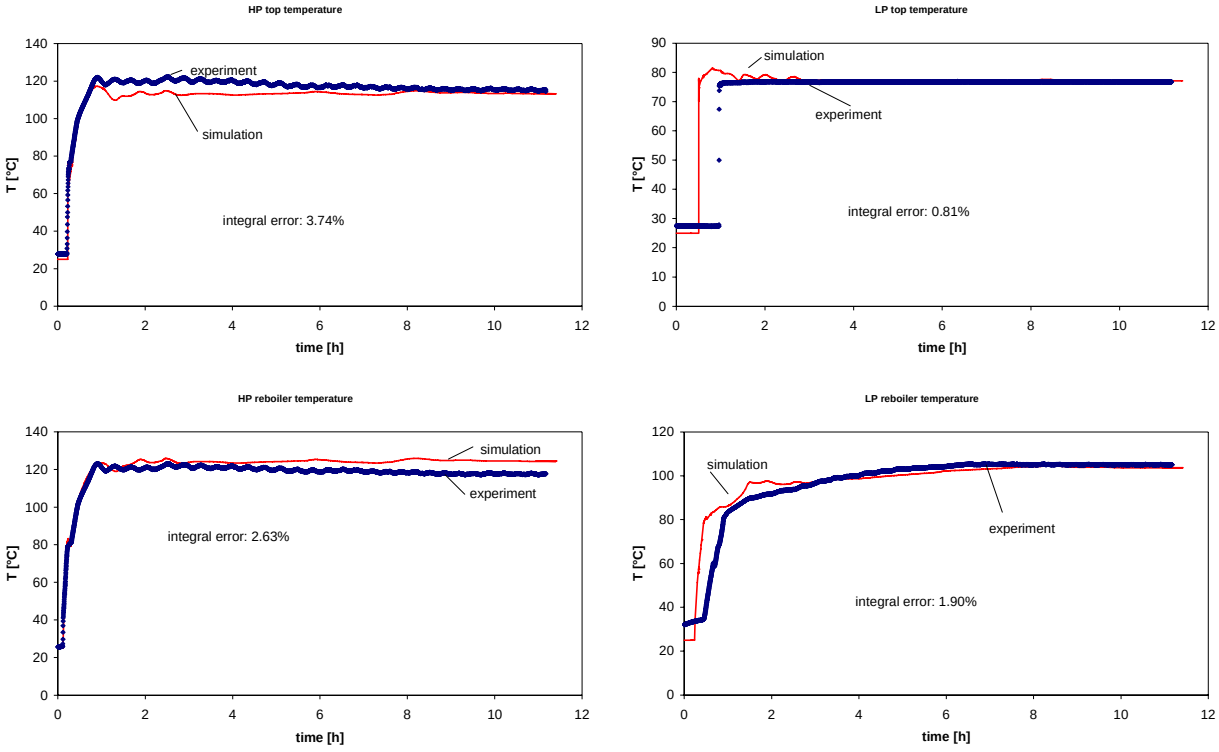

Fig. 4.7 Model validation using temperature profiles.

In Fig. 4.7 the temperature profiles for both columns at the top and at the bottom are presented including the integral error between the simulation and the experiment. The graphs show a good agreement between experiment and simulation. (see also integral error in the figure between experimental and simulation data). Only in Fig. 4.7 (up right) the LP top temperature profile shows a small gap between simulation and experiment during start-up. The heating up of the

column in the experiment is slower because the vapor pipe which connects the top of the HP column with the coupled heat exchanger has to be heated up. This pipe including the vapor flow is not described in the simulation model. But this fact has only a small influence as shown in the diagram.

4.4 Experimental validation of the batch process

The model validation of the discontinuous processes is done including the start-up operation from cold and empty, because the start-up operation is a main part of the whole batch process. All data for experiment and simulation are given in table 4.7.

Table 4.7. Setup of experiment and simulation for batch column validation.

	regular batch		**inverted batch**	
	LP	**HP**	**LP**	**HP**
feed tank column [l]	190	120	180	150
product tank volume [l]	40	27	30	29
pressure [bar]	1,013	4,4	0,998	3,7
feed conc. (ACN) [mol/mol]	0,37	0,65	0,38	0,67
forced stream bottom [l/h]	60	70	-	-
reflux/ feed stream [l/h]	controlled	controlled	40	55

In Fig. 4.8 the schedule of the processes are described. This is done for both processes (inverted and regular) for LP as well as the HP case.

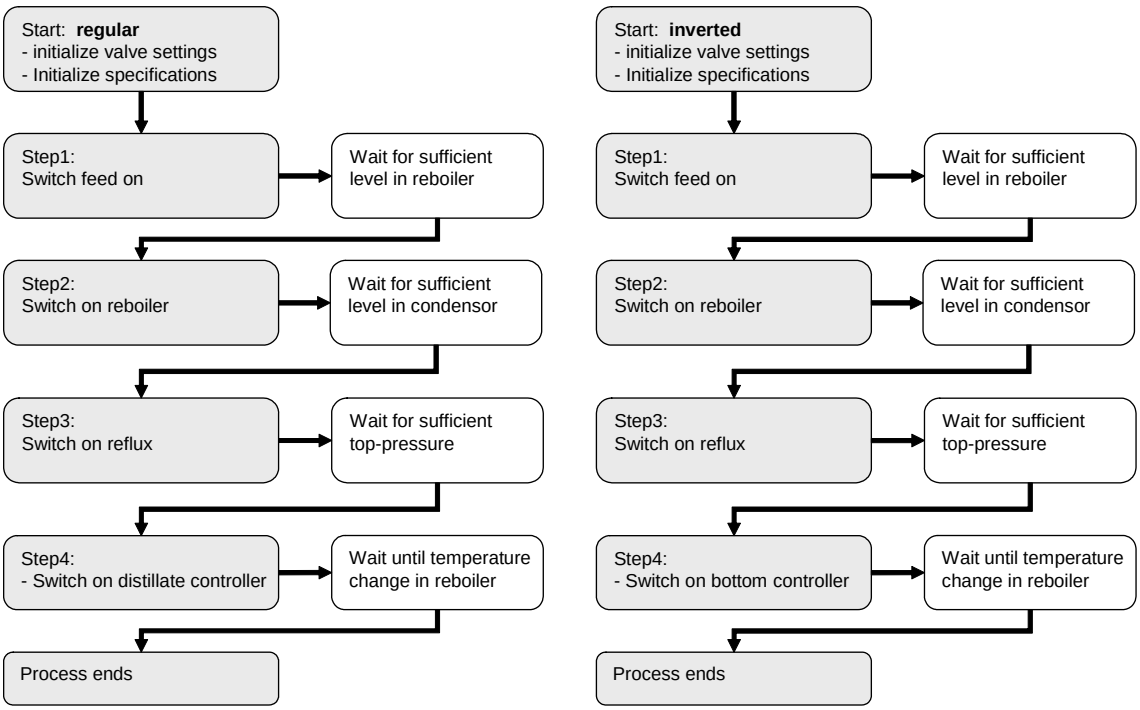

Fig. 4.8 Left: regular batch process schedule (LP/HP)
Right: inverted batch process schedule (LP/HP).

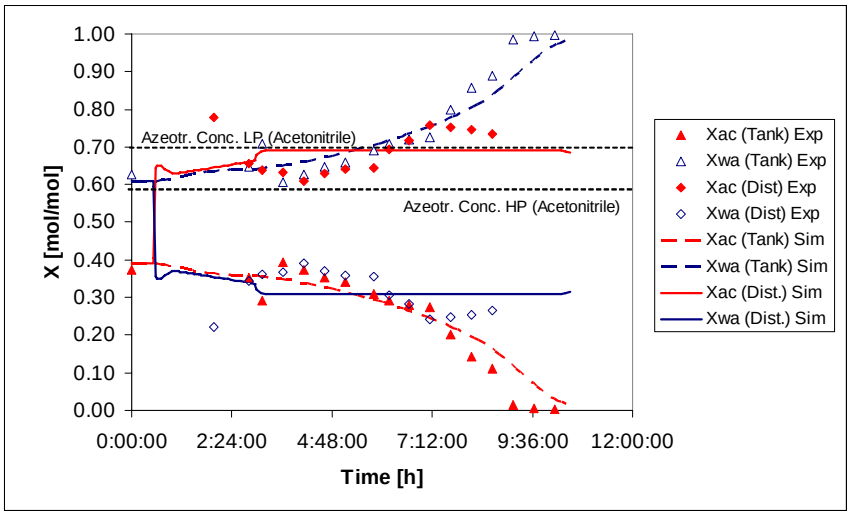

Fig. 4.9 Comparison of experiment and simulation: regular batch, LP, concentration profile.

The dynamic temperature and concentration trend for the regular low pressure case (Fig. 4.9 and Fig. 4.10) shows a very good agreement between experiment and simulation. The main errors in the concentration trends are due to measurement errors of the GC-analysis (approximately 2%). The start-up procedure fits very well.

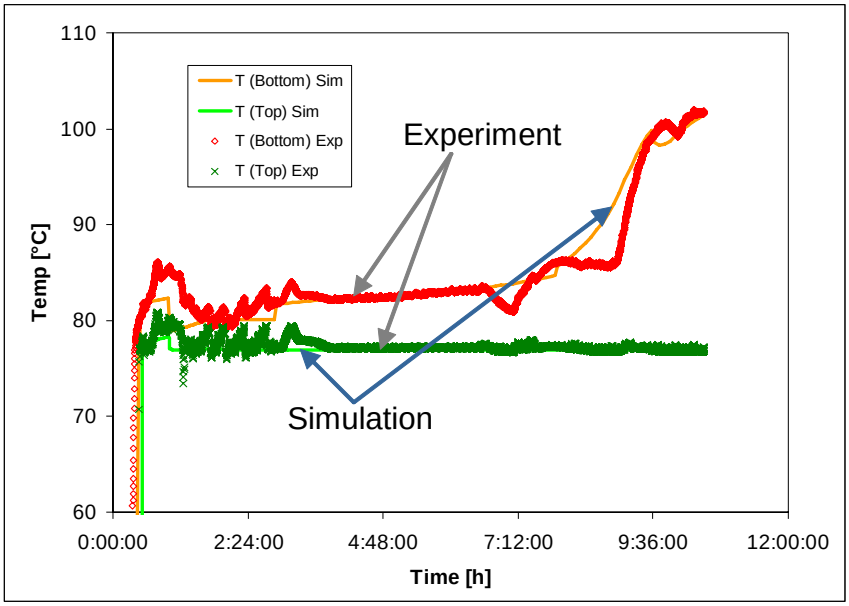

Fig. 4.10 Comparison of experiment and simulation: regular batch, LP, temperature profile.

In Fig. 4.11 and Fig. 4.12 the concentration and temperature trends for the regular high pressure batch are given. Also in this case the dynamic behavior in the simulations matches the experimental observations in a satisfactory manner.

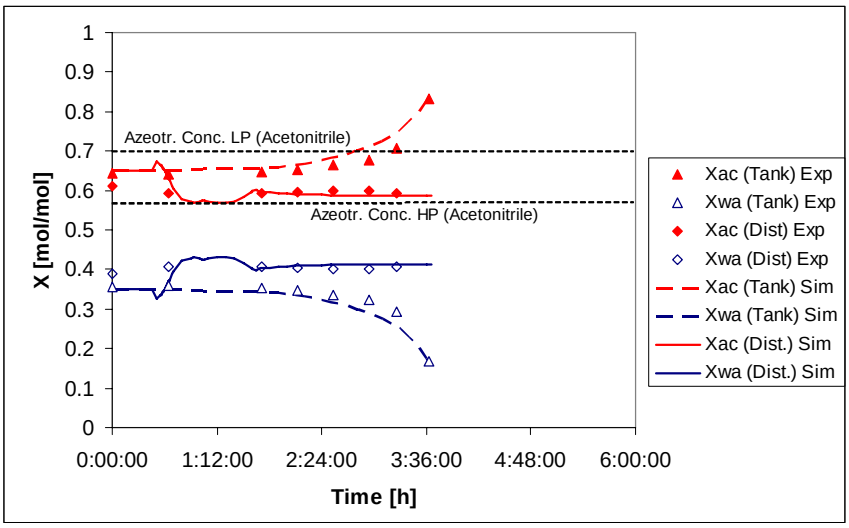

Fig. 4.11 Comparison of experiment and simulation: regular batch, HP, concentration profile.

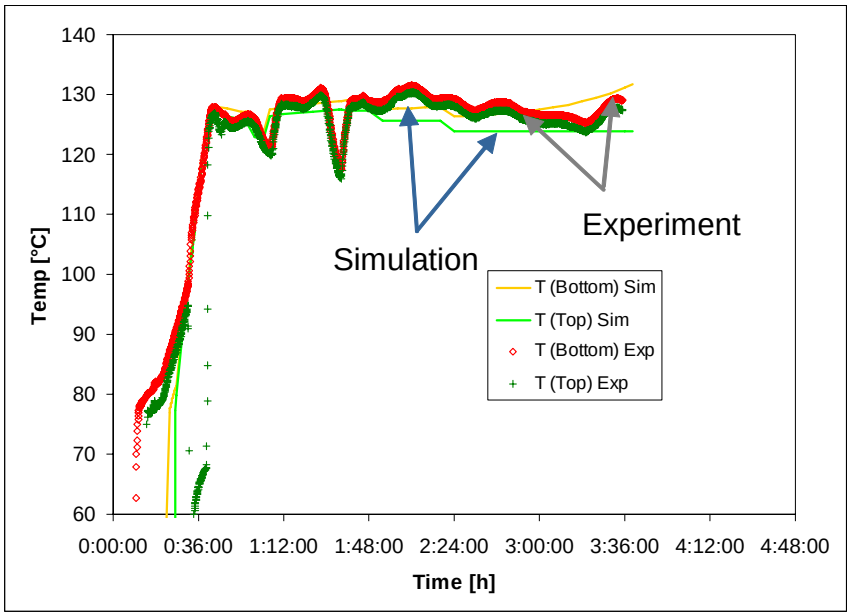

Fig. 4.12 Comparison of experiment and simulation: regular batch, HP, temperature profile.

The next diagrams show the validation for the inverted batch also for low (Fig. 4.13 and Fig. 4.14) and high pressure cases (Fig. 4.15 and Fig. 4.16). Experimental data and simulation results are also in a good agreement. The start-up procedure is reproduced very well so the model for the discontinuous processes is also validated dynamically.

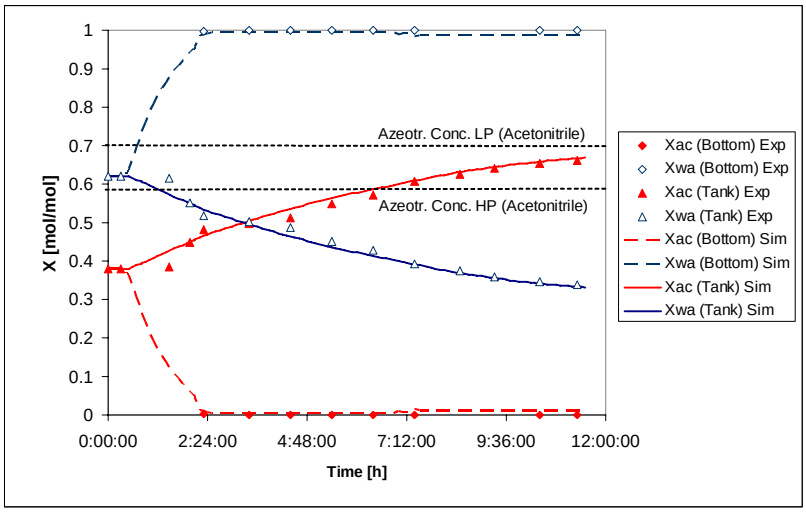

Fig. 4.13 Comparison of experiment and simulation: inverted batch, LP, concentration profile.

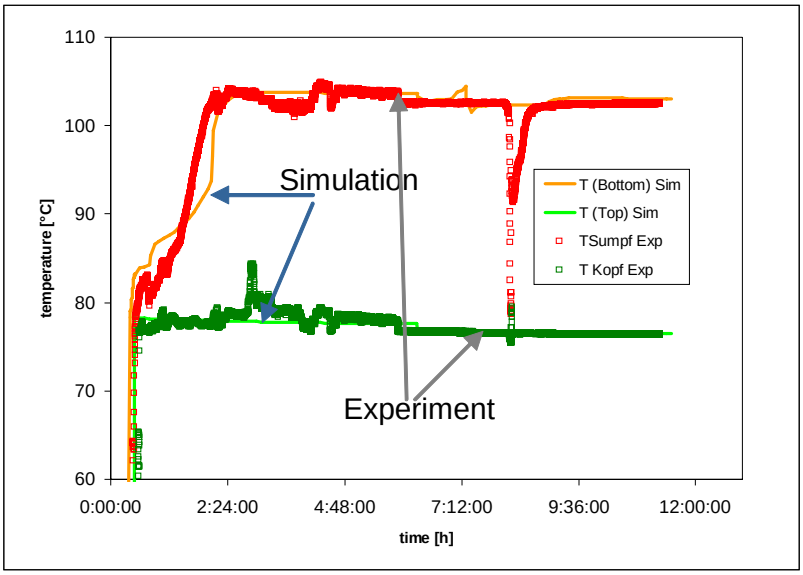

Fig. 4.14 Comparison of experiment and simulation: inverted batch, LP, temperature profile.

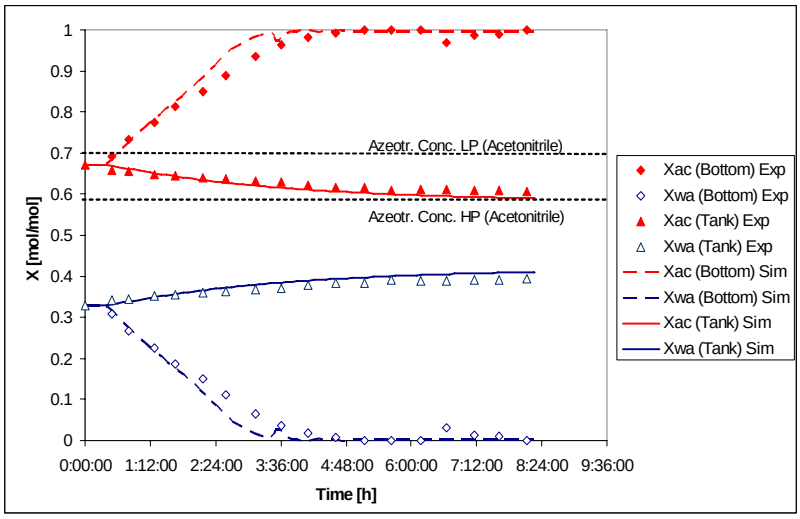

Fig. 4.15 Comparison of experiment and simulation: inverted batch, HP, concentration profile.

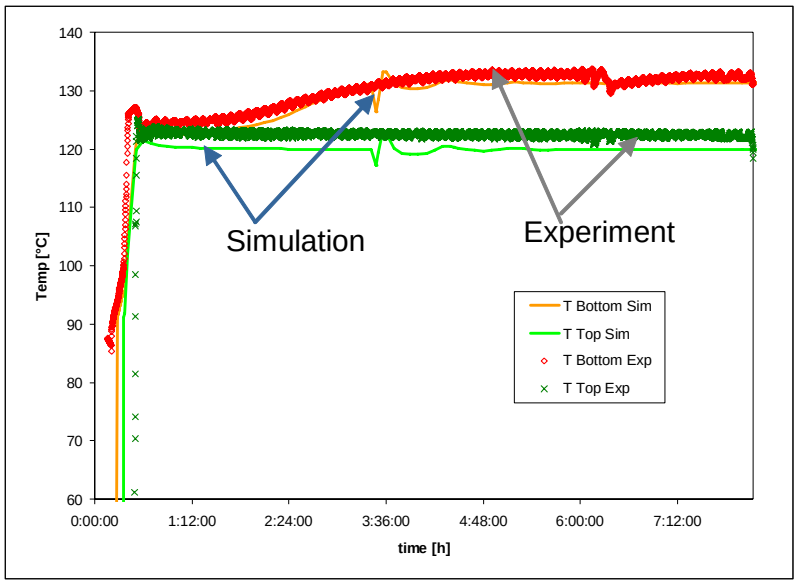

Fig. 4.16 Comparison of experiment and simulation: inverted batch, HP, temperature profile.

5. *The continuous pressure swing distillation*

This chapter contains a detailed analysis of the continuous pressure swing process. Different process control concepts and process design concepts will be discussed and a start-up strategy from cold and empty state for the coupled process will be introduced. The chapter ends with the evaluation of the process control concepts.

5.1 Process control concepts and designs for the continuous process

Under the assumption that more complex processes need a more complex automation the two column system normally had a great automation expense to control the heat- and mass- integrated two column system. Especially because of the pressure difference of the columns and to guarantee a difference between the azeotropic points, which are depending on the pressure, the complexity could increase. Furthermore the mass integration (recycle streams) which causes feed backs into the other column is also difficult to handle. Useful process control strategies are needed to control such a process. This section will start with the introduction of different design concepts and then useful process control concepts will be discussed.

5.1.1 Process design of the continuous operation

The thermodynamical behavior of the mixture leads to a general process flow sheet for the pressure swing operation (Fig. 5.1) for a low boiling mixture as the example acetonitrile - water.

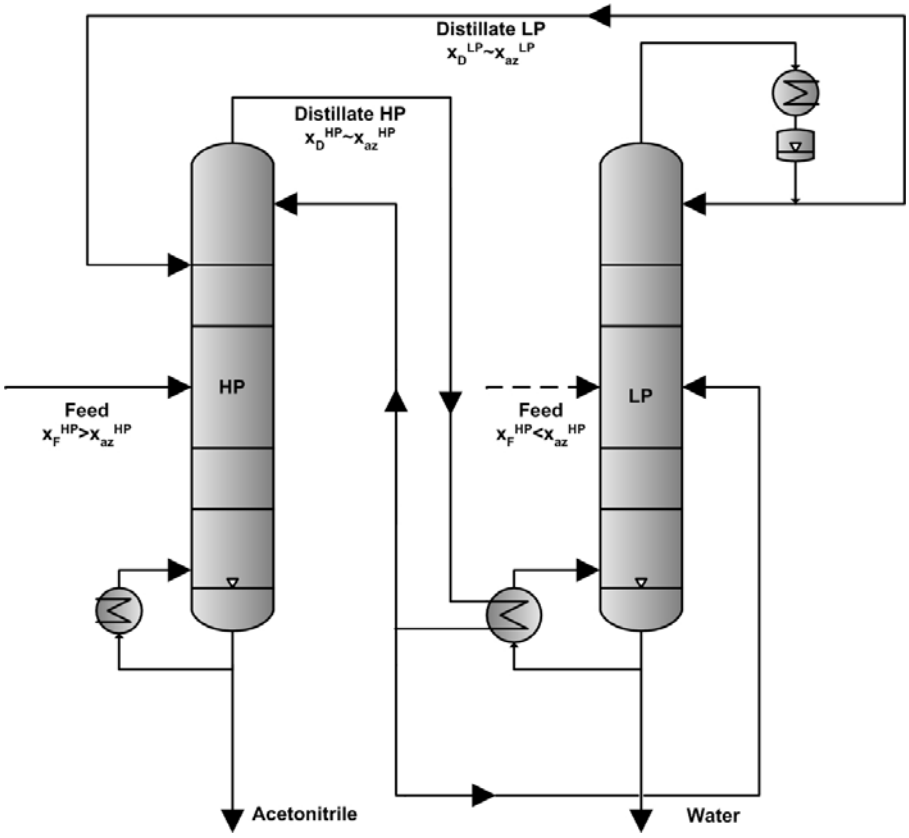

Fig. 5.1 Process flow sheet - continuous pressure swing distillation.

Depending on the initial feed concentration the feed concentration is in the distillation region below or above the azeotropic point. Two different inputs for the feed are possible. For a feed concentration below the azeotropic point it is useful to feed into the low pressure column (LP); for a feed concentration above the azeotropic point, it is useful to feed into the high pressure column (HP). In both cases we get pure acetonitrile at the bottom of the high pressure column and pure water at the bottom of the low pressure column. The concentration of both distillate (near the azeotropic point) are depending on the respective pressures. Each distillate stream is put into the other column, which causes a feed back situation, which means a mass integrated column system (Fig. 5.3). For a high-boiling homogeneous azeotropic mixture, the bottom streams have to feed back respectively to the other column and the pure products will be at the top. But the high boiling concept will not be discussed in the context of this work.

Now we will have a short look at other possible process designs. One design element is the use of an additional reboiler at the bottom of the LP column. This increases the degree of freedom by one but adds additional cost (investment and operation costs) because of additional equipment and energy (see chapter 5.1.2.1).

There are some natural restrictions in the design. The pressure swing distillation system for a binary homogenous azeotropic separation must consist of two columns, which are mass integrated because of the azeotropic mixture at the top of each column (low boiling azeotrope). The feed is fed into the LP or the HP column depending on the feed concentration and the location in the distillation region (Fig. 5.3). The columns need an energy input at the bottom which can be done with a reboiler or an energy integration like the coupled heat exchanger (LP bottom) and a condenser at the top or also the coupled heat exchanger (HP top).

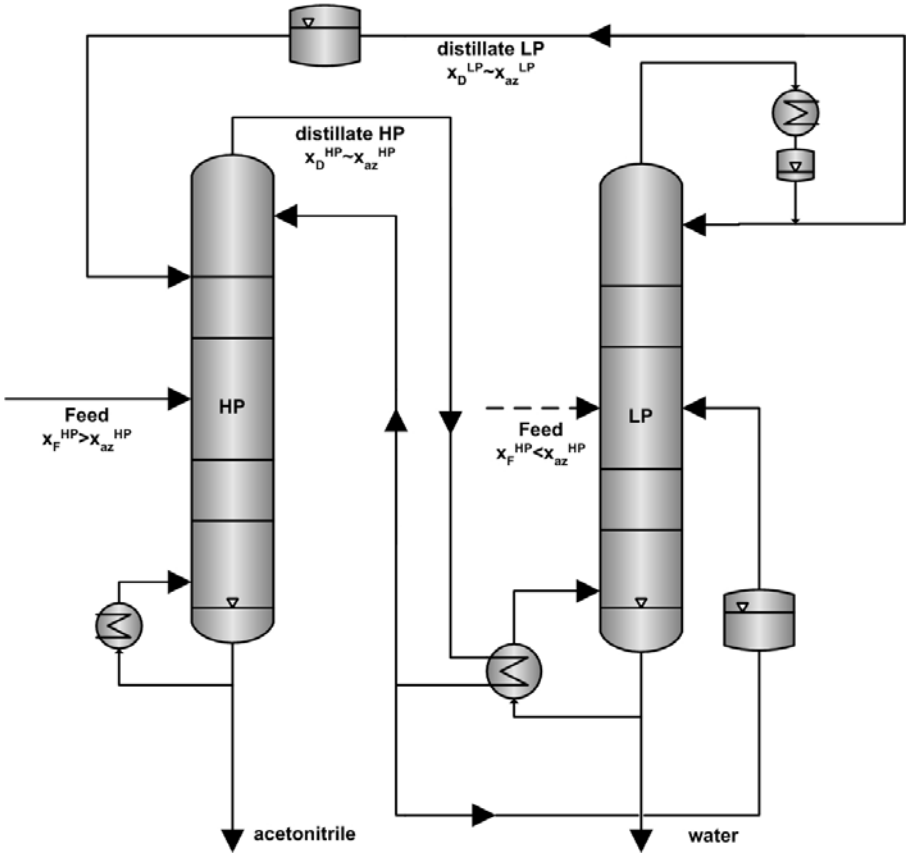

Fig. 5.2 Process flow chart with additional buffer tanks in the distillate pipes.

One possible change in the main design concept can be an introduction of buffer tanks in the distillate pipes to de couple the two columns (Fig. 5.2). Changes of the concentration have a smaller influence on the other column. As the open loop study in the chapter before shows, the influence of the distillate concentration on the process is very small (chapter 5.1.2.1). The influence of the buffer tanks seems to be also very small and will not be analyzed in this work.

5.1.2 Process control concepts for the continuous operation

After a short discussion about different design concepts for the continuous system, the different control concepts will be introduced. Since pressure swing distillation is based on operating the two columns at different sides of the azeotrope, it seems to be necessary to always keep the distillate concentrations at their set points to guarantee the transition between the two pressure stages. In addition it is expected that the process is very sensitive to disturbances in the feed

concentration and that a robust operation of the two columns in their corresponding distillation regions is only possible for a very limited range of feed concentrations.

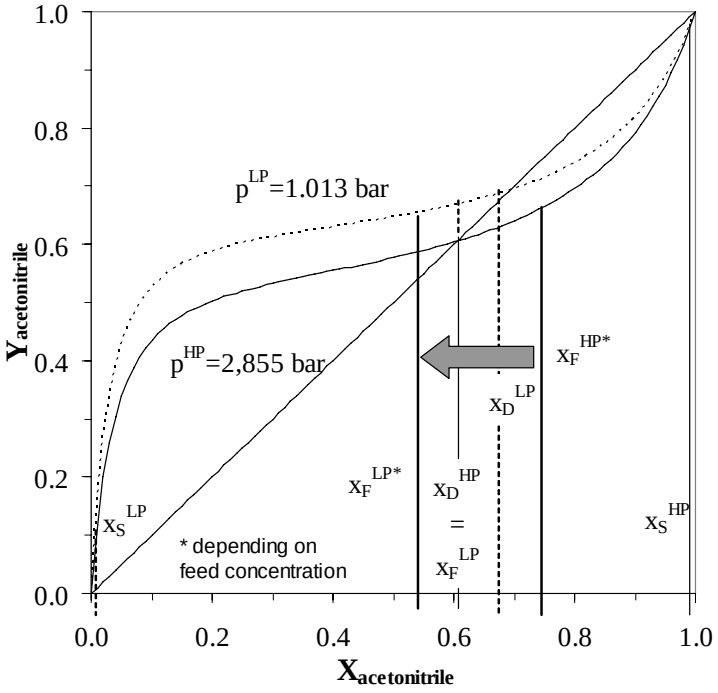

Fig. 5.3 Feed input into the appropriate distillation region.

In the following it will be shown that feed disturbances can be counteracted even with a rather simple control structure and that the process can be operated robustly in a very large feed concentration range.

On the base of the validated rigorous model of the continuous system the different control structures will be introduced and compared. At first, a choice for control variables concerning the secure operation has to be done (controlling pressure and level) and then for the compliance of the product specifications (mostly purities and mass flows). The first concept includes the following control variables:

1. Bottom concentration x_B^{LP} and x_B^{HP} (required purities).
2. Bottom level, $level_B^{LP}$ and $level_B^{HP}$, for an sufficient liquid level in the reboiler.
3. Level in the distillate drums $level_D^{LP}$ and shell side level in the coupled heat exchanger $level_{CHE}$, for a constant reflux stream.
4. Distillate concentration x_D^{LP} and x_D^{HP}, because it seems that these concentration has to be in an optimal point for the operation of the hole process, to operate each column in the right distillation region.

The pressure of the high pressure column is setting up on its own depending on other parameters like heat duty. Because of the missing additional degree of freedom. The pressure of the LP column is atmospheric and will not be controlled. In the model the pressure is controlled with the cooling water stream of the condenser. This avoids an index problem in the model, too.

As manipulated variables, the bottom, distillate, and reflux streams are used as well as the heat duty of the HP reboiler (heat integration) or the reboilers of both columns (without heat integration). The following table shows the pairing in the different control concepts (table 5.1). For all controllers proportional-integral (PI) controllers are used with out dead time (chapter 3.2.1.5). The description and analysis follows in the next section.

Table 5.1. Pairing in the different control concepts.

Controller concept	Pairing							
	x_D^{LP}	x_D^{HP}	x_B^{LP}	x_B^{HP}	$level_D^{LP}$	$level_{KWT}$	$level_B^{LP}$	$level_B^{HP}$
With additional LP reboiler	R^{LP}	R^{HP}	$\dot{Q}^{LP}$	$\dot{Q}^{HP}$	D^{LP}	D^{HP}	B^{LP}	B^{HP}
Bottom-concentration-reflux-controller[a,b]	-	-	R^{LP}	$\dot{Q}^{HP}$	D^{LP}	D^{HP}	B^{LP}	B^{HP}
Alignment of the LP-bottom concentration[a,c]	R^{LP}	R^{HP}	-	$\dot{Q}^{HP}$	D^{LP}	D^{HP}	B^{LP}	B^{HP}
Bottom concentration cascade controller[a,d]	-	-	$level_{KWT}$	$\dot{Q}^{HP}$	D^{LP}	D^{HP}	B^{LP}	B^{HP}

a. without an additional reboiler at the LP column, fully heat integrated

b. reflux stream HP with constant flow rate (flow controller)

c. bottom concentration HP is not controlled

d. reflux streams LP and HP with constant flow rate (flow controller)

5.1.2.1 Control structure with addition reboiler

To find the optimal pairings the following different heuristics are used. The most important characteristics are the sensitivities and the time constants of the controller. The influence of the manipulated variable on the control variable is very important. The influence must be big enough to reduce the range of the control intervention. To reduce the time constants it is necessary to connect manipulated variables and control variables not from different columns or units. These have to be nearby if possible. Buckley says, to get the right pairing it is necessary to connect levels and pressures with external streams, which goes to other units of the plant, to have smooth changes [Buckley 1964]. If there is a fixed feed stream, the flow out of the units has to be coupled with levels inside their unit [Luyben 1990].

Table 5.2. Overview: Pairing of the control and manipulated variables.

x_D^{LP}	x_D^{HP}	x_B^{LP}	x_B^{HP}	$level_D^{LP}$	$level_{KWT}$	$level_B^{LP}$	$level_B^{HP}$
↕	↕	↕	↕	↕	↕	↕	↕
R^{LP}	R^{HP}	$\dot{Q}^{LP}$	$\dot{Q}^{HP}$	D^{LP}	D^{HP}	B^{LP}	B^{HP}

Because of the connection of the distillate streams into the other columns, they will be connected to the nearby levels, the drum levels, which means for the LP column the drum level and for the HP column the coupled heat exchanger shell side level. Corresponding to the distillate stream the bottom streams are coupled to the reboiler levels (table 5.2). The concentrations are connected to the reflux streams (distillate concentrations) and to the heat duty (bottom concentration).

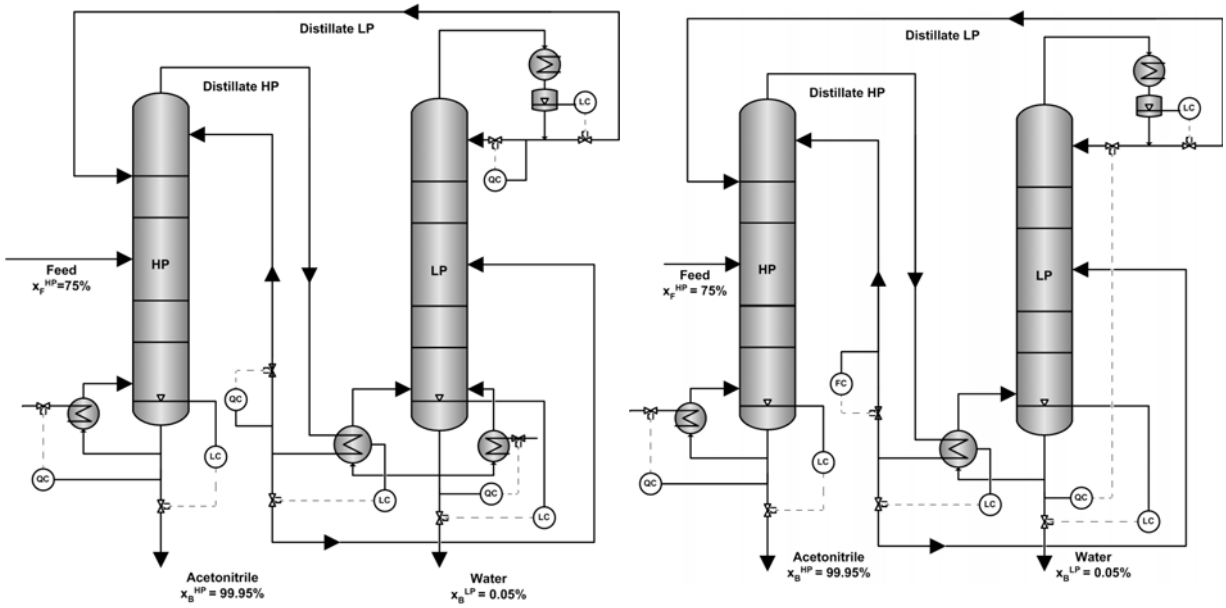

Fig. 5.4 Control concepts. Left: Structure A with additional reboiler at the LP- column; right: Structure B without an additional reboiler (example: bottom concentration control with reflux stream at the top of the LP- column).

The first structure (A) uses an additional reboiler at the LP-column. To operate the system without an additional reboiler at the LP-column the structure must be changed (B). The two different control structures are presented in Fig. 5.4.

Structure A conflicts with the heat integration concept and has therefore higher investment and operating costs.

In the first step the sensitivity of the distillate concentrations on a disturbance of the feed concentration (step from 75 mol% to 55 mol%) for an open loop will be analyzed. The results show us that the distillate concentration stays in the right region and the sensitivity on the feed concentration change is very low. A control of the distillate concentrations are not necessary (Fig. 5.5).

This is due to the fact that the distillate concentration does not have to be controlled on a fixed value, only the following conditions has to be warranted to be in the right distillation region (for the low boiling component acetonitrile).

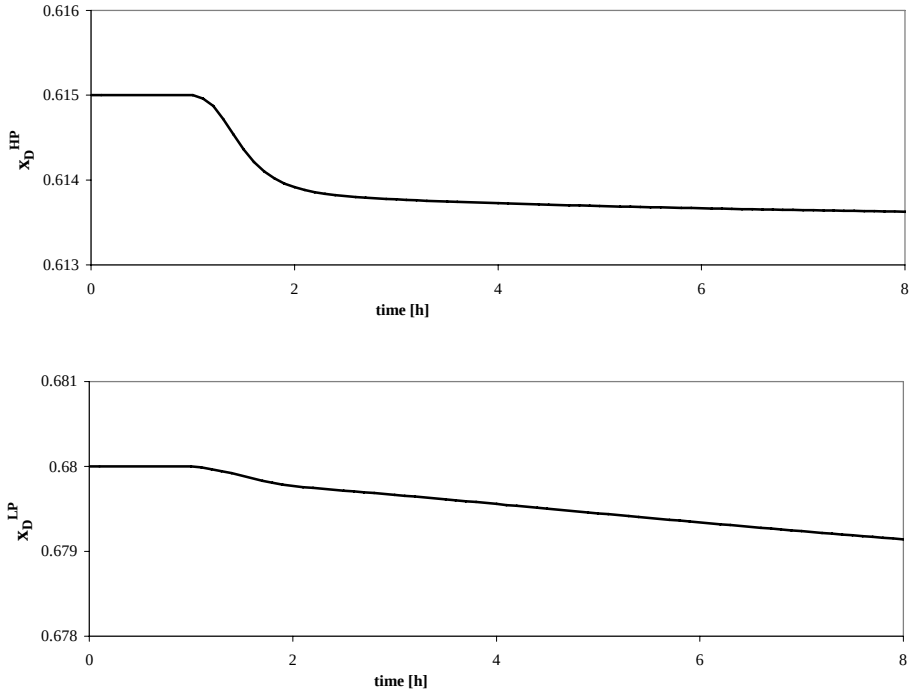

Fig. 5.5 Step response of the uncontrolled columns for a step of the feed concentration from 75 mol% to 55 mol% Acetonitrile (top: distillate concentration HP, below: distillate conc. LP).

Conditions - feed LP:

$$x_D^{LP} > x_{az}^{HP} : \text{and} \qquad \text{(eq. 5.1)}$$

$$\left(\frac{D^{HP} \cdot x_D^{HP} + F^{LP} \cdot x_F^{LP}}{D^{HP} + F^{LP}} \right) < x_{az}^{LP} . \qquad \text{(eq. 5.2)}$$

Conditions - feed HP:

$$x_D^{HP} < x_{az}^{LP} : \text{and} \qquad \text{(eq. 5.3)}$$

$$\left(\frac{D^{LP} \cdot x_D^{LP} + F^{HP} \cdot x_F^{HP}}{D^{LP} + F^{HP}} \right) > x_{az}^{HP} . \qquad \text{(eq. 5.4)}$$

It must be pointed out that for the column with the feed input the mixture of the feed and the distillate is important (eq. 5.2) and (eq. 5.4). If the concentration of the mixture is in the right distillations region a correct operation is possible. The mixture of the feed and the distillate is responsible for an optimal operation and not the distillate stream on its own.

With this abdication of the control of the distillate concentrations a lot of other control concepts are now possible and will be described in the next section.

In the next step for close loop studies the controllers have to be parameterized. This is done by identifying the transfer function of the simulated step responses and approximating them with

first order plus dead time function. The high non-linearity of the system yields difficulties due to the existing asymmetric dynamic, which causes problems in calculating the average of the steps in positive and negative directions. Thus, only the step direction that leads to the response, which can better approximated, is used. The controller parameters found using the IMC rule are implemented in the model and further tuned with simulations studies using the non-linear model [Repke et al. 2005a, Repke et al. 2005b].

This structure is a classical LV structure. The bottom levels, the drum level at the LP column, the shell side level of the coupled heat exchanger (HP), the bottom concentrations and the distillate concentrations are controlled. The purity of the LP bottom is controlled with help of the additional reboiler (Fig. 5.6).

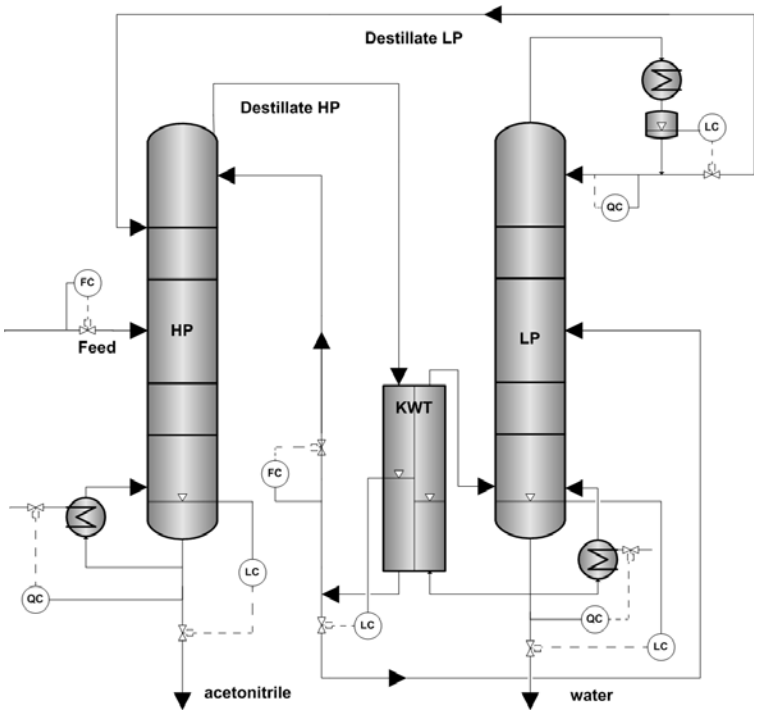

Fig. 5.6 Control structure with additional reboiler at the LP- column.

Beside the additional reboiler also the heat integration is done. This means that the main part of the energy consumption of the LP column is done by the condensing vapor of the HP column using the coupled heat exchanger. The LP reboiler is exclusively used to control the bottom concentration of the LP column and it will also be used if the energy of the coupled heat exchanger is not enough, which is not the case, if the HP column works properly. We can refer to this concept as a partially heat integrated process.

In the normal analysis of a controller concept the disturbance is only 10% of the operating point value. But to come up with the possible stability problem of the system because of the different distillation region, the step must be greater to reach the other distillation region. If this works properly, a small disturbance does not make any problem.

So for the analysis of the first process control concept with additional reboiler the feed concentration will be changed from 75 mol% into the other distillation region to 55 mol% (Fig. 5.7).

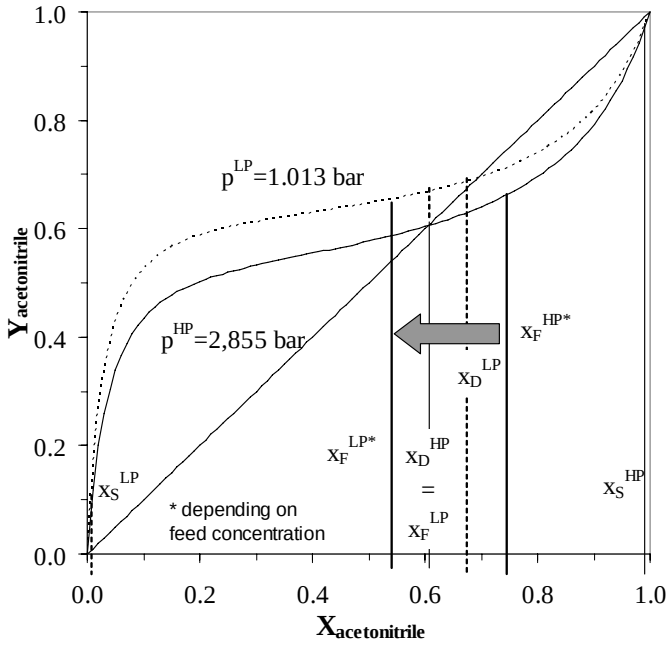

Fig. 5.7 Demonstration of a feed step from the HP- distillation region (75 mol%) into the LP- distillation region (55 mol%).

The steady state conditions are summarized in table 5.3.

Table 5.3. Steady state conditions in the simulation.

	HP column	LP column
x_F [mol%]	75	-
F [l/h]	10	-
P_F [bar]	3,0	-
T_F [°C]	70	-
P_{top} [bar]	2,855	1,013
x_S [mol%] ACN	99,95	0,05
x_{az} [mol%] ACN	60,6	69,4

The analysis of the disturbance behavior shows a system which is stable against these disturbances, because the distillate concentration changes are very small and also the bottom concentrations can be brought back to the operating point in an acceptable time (Fig. 5.8 and Fig. 5.9). This behavior can be explained with the fact that only the mixture of the feed and the distillate has to be in the right distillation region and not only the feed itself. Here only the concentration changes are discussed. In chapter 5.1.3 also the flow rates and the heat duties will be discussed.

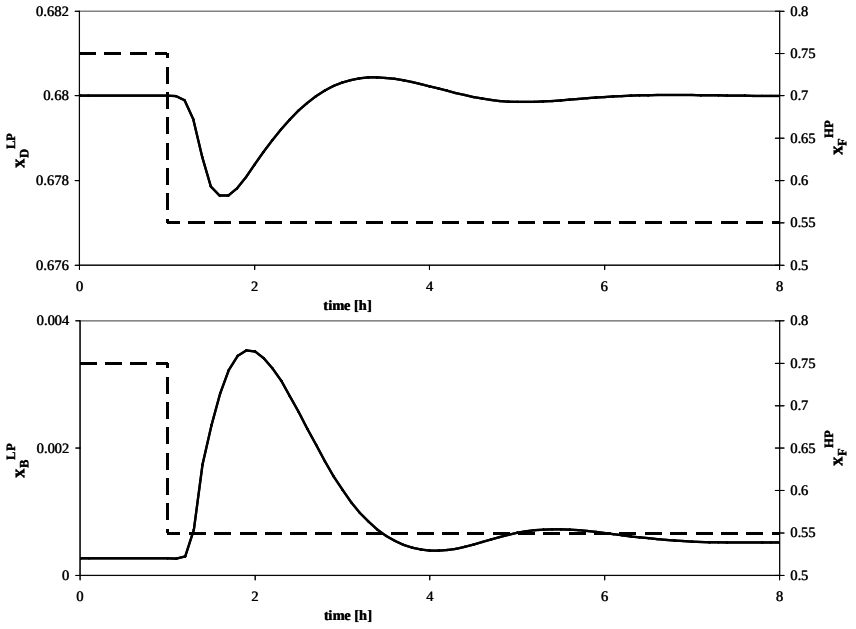

Fig. 5.8 Bottom and top concentration disturbance behavior (LP) for a feed concentration step (HP) from 75 mol% to 55 mol% ACN.

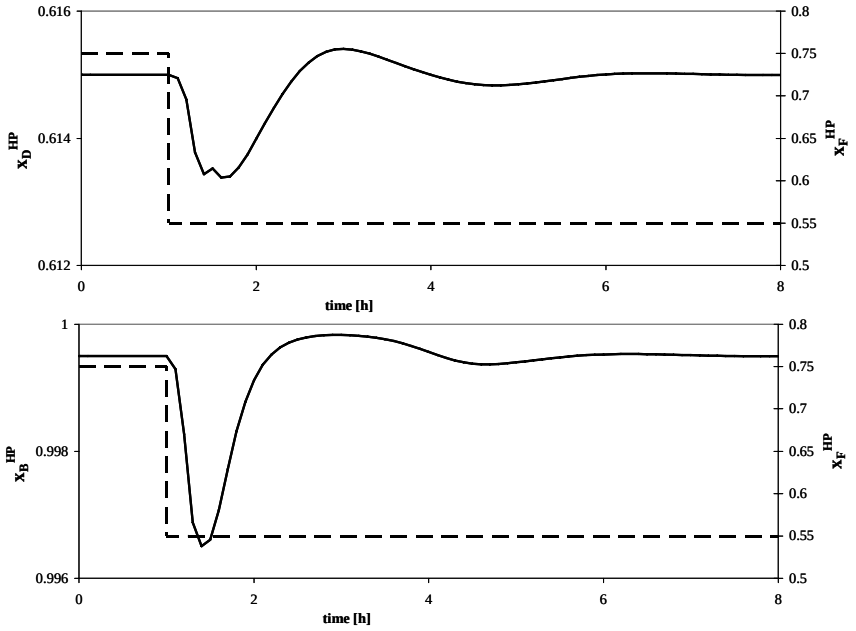

Fig. 5.9 Bottom and top concentration disturbance behavior (HP) for a feed concentration step (HP) from 75 mol% to 55 mol% ACN.

5.1.2.2 Control structure without additional reboiler

Without an additional reboiler at the LP column the system has a full-heat integration but a reduction of the degree of freedom of one. Therefore new control concepts are necessary and

possible. Mostly the control structure changes are for the LP column, having in mind the rules by Buckley [Buckley 1964]. Most of the process control concepts in this section are based on the abdication of controlling the distillate concentrations at the top of the column.

The basic control concept of the HP column will be the same for the different control concepts which will be introduced now. This basic concept for the HP column consists of a pairing of the bottom concentration with the heat duty of the HP reboiler, the bottom level with the HP bottom outlet stream and the reflux stream are changed by a flow controller or by a distillation concentration controller. The presented concepts in the next section mainly concentrates on the LP column.

Bottom-concentration-reflux-controller. In this concept the reflux flow rate at the top of the LP column is paired with the bottom concentration. The reflux stream of the HP column is changed by a flow controller. Both distillate concentration (LP and HP column) will not be controlled. The structure is sketched in Fig. 5.10. The control and the manipulated variable are not very close to each other which can be difficult concerning a big time constant in the practical operation.

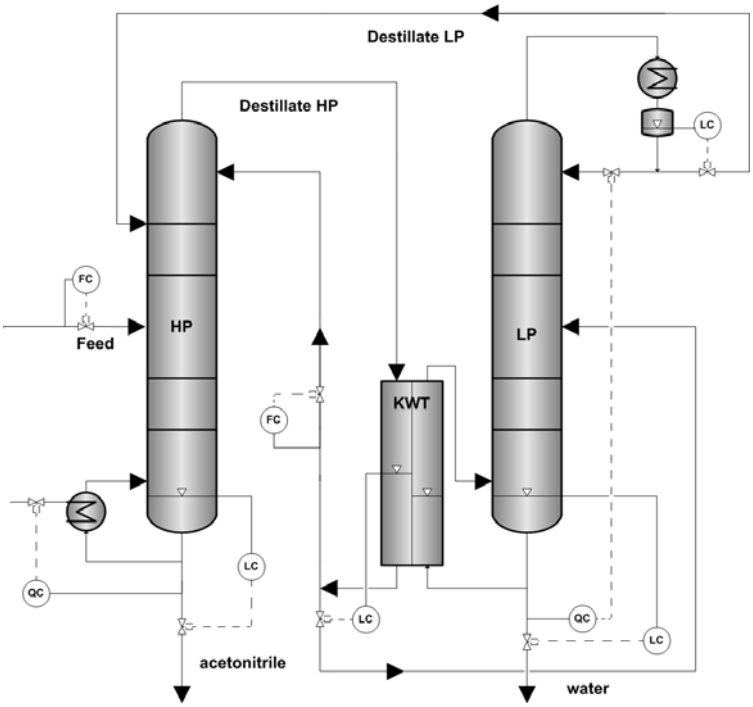

Fig. 5.10 Bottom-concentration-controller with reflux stream LP.

As in the previous example the feed disturbance into the other distillation region will be analyzed. The disturbance behaviors of the distillate concentration at the top columns and the bottom concentrations are sketched in Fig. 5.11 and Fig. 5.12.

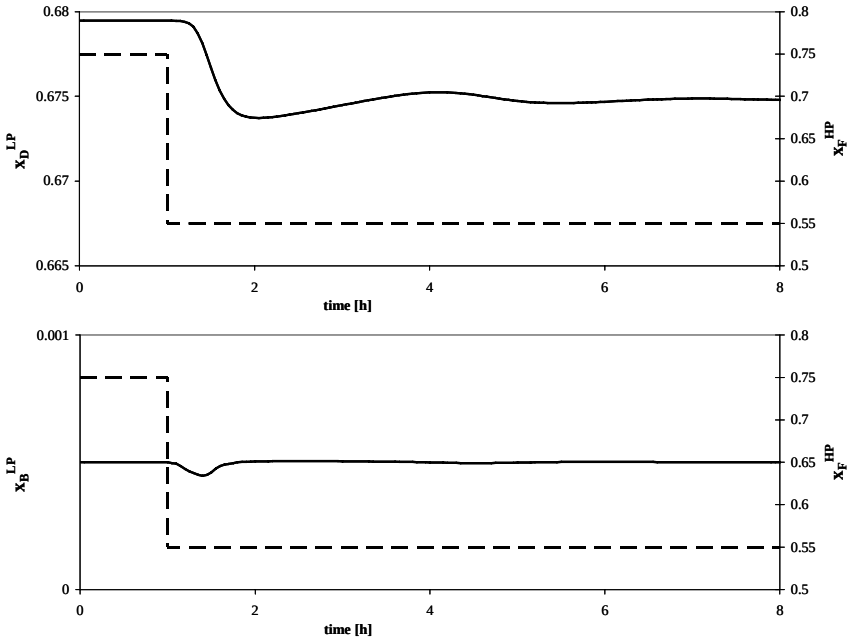

Fig. 5.11 Bottom and top concentration disturbance behavior (LP) for a feed concentration step (HP) from 75 mol% to 55 mol%, for the bottom concentration reflux controller.

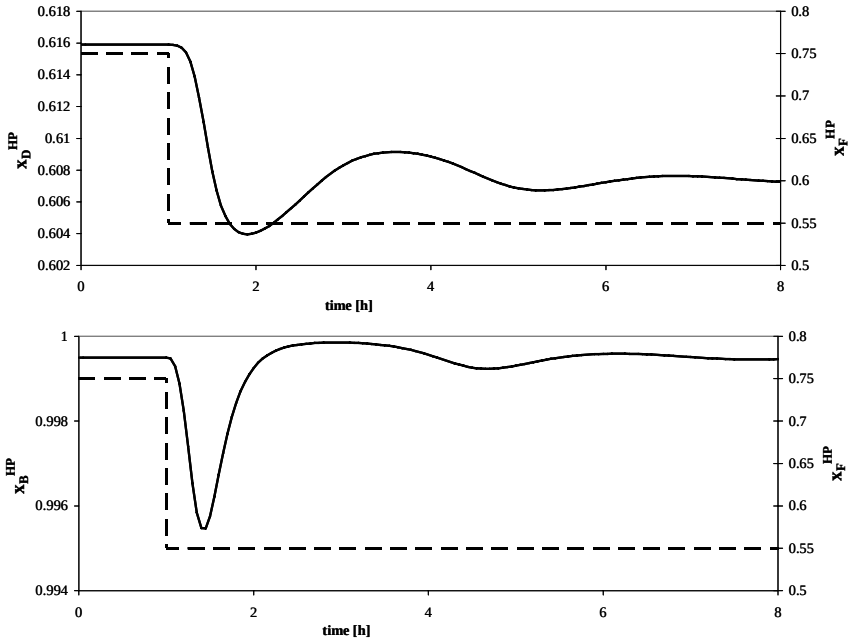

Fig. 5.12 Bottom and top concentration disturbance behavior (HP) for a feed concentration step (HP) from 75 mol% to 55 mol%, for the bottom concentration reflux controller.

There is a change in the distillate concentration which is a must, because they are not controlled. But in the high pressure case the distillate concentration decreases and gets nearer to the azeotropic point and which is better for the process. In the LP case the gap between the

azeotropic point and the distillate concentrations increases, but this has no consequence on the process operation. The bottom concentrations are controlled very well, concerning time constant and purity. The disturbance behavior of the bottom controller of the LP column has no difference concerning time against the others. With these results, this control concept is a suitable solution for the control of this heat- and mass- integrated system.

Alignment of the LP-bottom concentration with help of the distillation concentration controller. In this setup the concentration at the top of the LP and the HP column are controlled this way, that the bottom concentration of the LP column is lower than the set point. This is not a direct control concept for the bottom concentration. The open loop experiment shows a very low sensitivity of the LP column bottom concentration on disturbances of the feed concentration, so this concept might be a possible solution. The Fig. 5.13 shows the control structure.

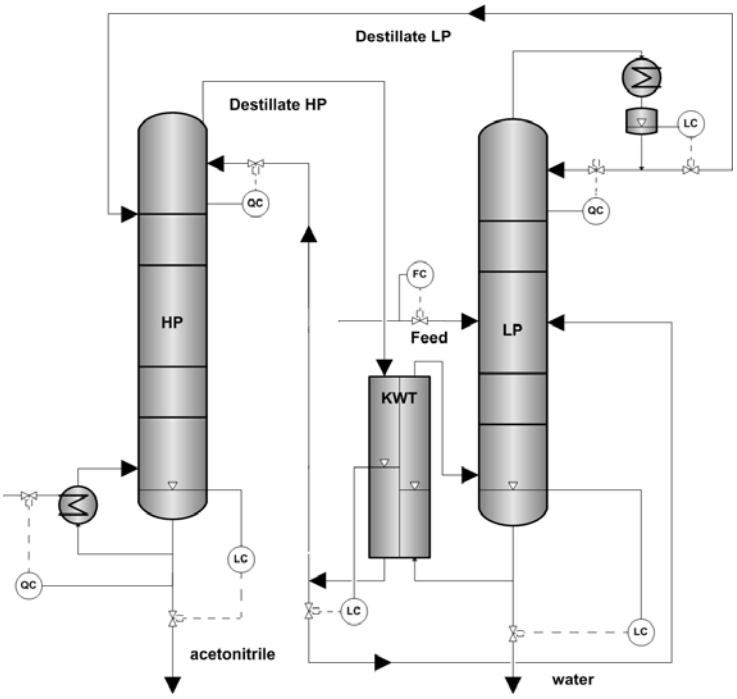

Fig. 5.13 Bottom LP concentration alignment with help of the distillation controllers.

As the results in Fig. 5.15 indicates, it is possible to influence or better set a bottom concentration of the LP column with the set points of the distillate concentrations. To be safe against disturbances, the bottom concentration must be set to a value as low as suitable for the highest expected disturbance, because it is not possible to bring the bottom concentration back to the operating point. After the disturbance the concentration is on a different level as shown in the next picture Fig. 5.16.

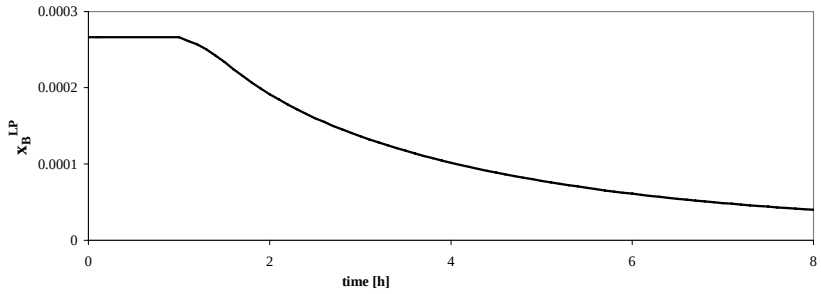

Fig. 5.14 Step response of the uncontrolled columns for a step of the feed concentration from 75 mol% to 55 mol% Acetonitrile for the bottom LP concentration.

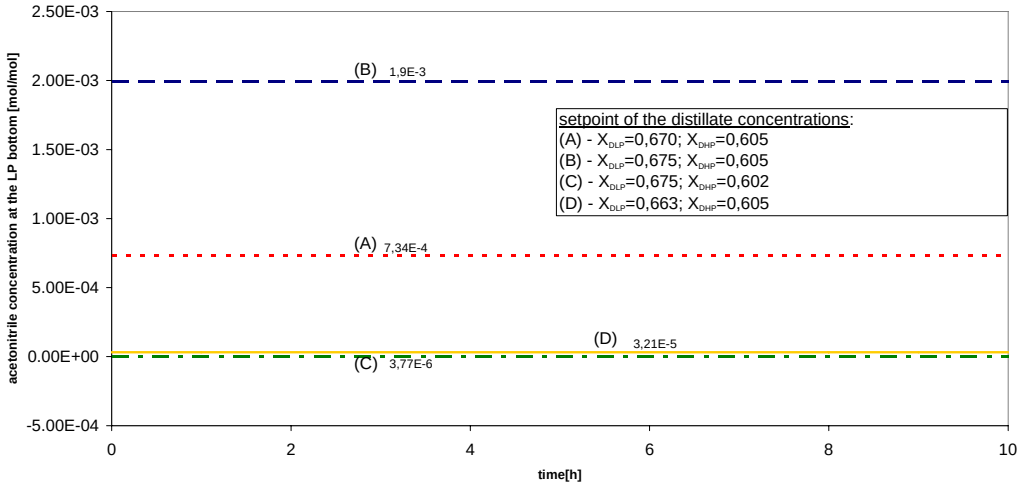

Fig. 5.15 LP-bottom concentrations for different set points of the controlled distillate concentrations.

The picture shows the concentration trends of the bottom concentration of the LP column for a very big feed concentration disturbance from 75 mol% to 40 mol%. The bottom concentration changes are manageable and not as big as expected (Fig. 5.16).

But this concept seems not to be a very practical solution concerning an industrial use because of the in the end not controllable bottom LP concentration and also the necessary operation under over specified conditions, which means that in the normal operation the purities of the LP bottom are higher than needed. This operation needs a lot of energy and therefore costs. It is more an academic example.

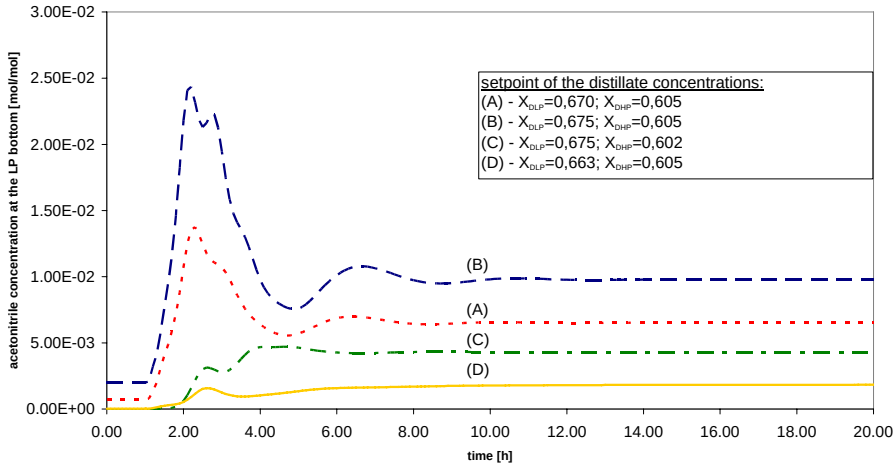

Fig. 5.16 Bottom concentration step response for different set point parings of distillate concentrations; feed concentration step from 75 mol% to 40 mol%.

Bottom concentration cascade controller. In this concept the shell side level controller of the coupled heat exchanger is paired with the bottom concentration of the LP column. This is a cascade control system where the level controller influences the heat entry into the LP column system and therefore the bottom concentration. In this concept the distillate concentrations in both columns are also controlled (Fig. 5.17).

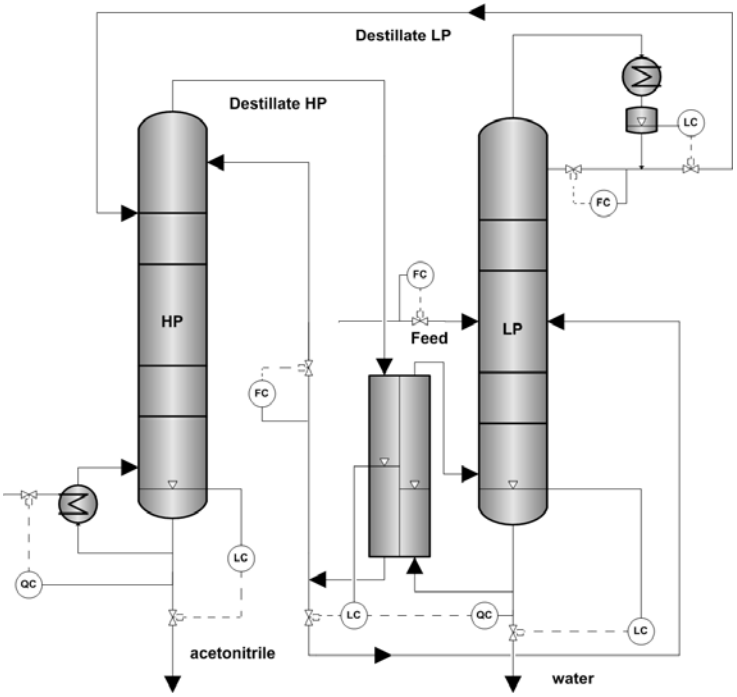

Fig. 5.17 Cascade controller.

The controller scheme is sketched in Fig. 5.18.

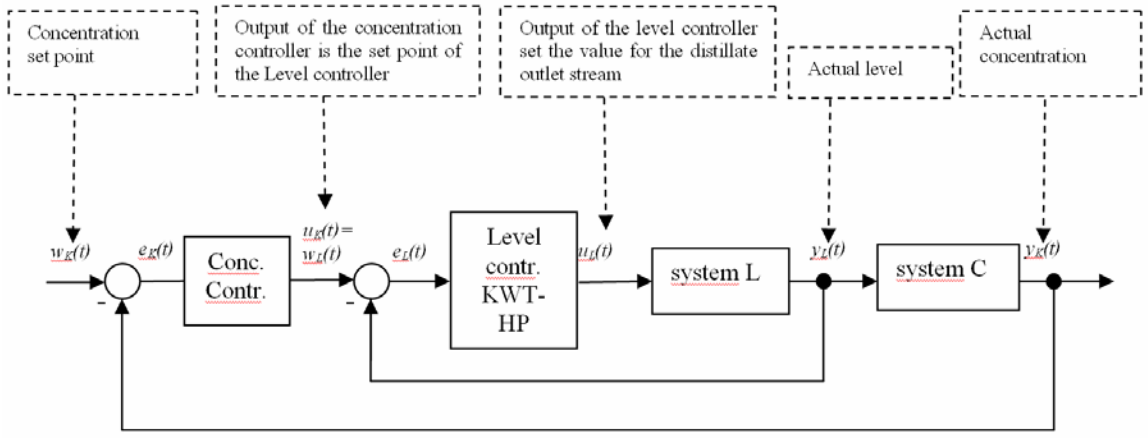

Fig. 5.18 Control scheme for the cascade controller.

To analyze the system a feed concentration-change from 50 mol% to 47,5 mol% (-5,6%) is done. For the open-loop analysis the level of the coupled heat exchanger is set to constant. The feed change has a positive influence on the bottom concentration, because more water (high boiling component) is entering the system. In the next step the analysis is done for the closed loop system, this means that the level is controlled to influence with help of the cascade the concentration in the bottom. But the opposite as expected happens. The bottom concentration becomes high concentrated. Normally an increasing of the bottom concentration will case an increase of the coupled heat exchanger level, to reduce the heat input. But this also cause a smaller recycle stream and this means less acetonitrile (part of the azeotropic low boiling mixture). So more water and less overall volume is in the system and the controller does not work in the way expected (Fig. 5.19).

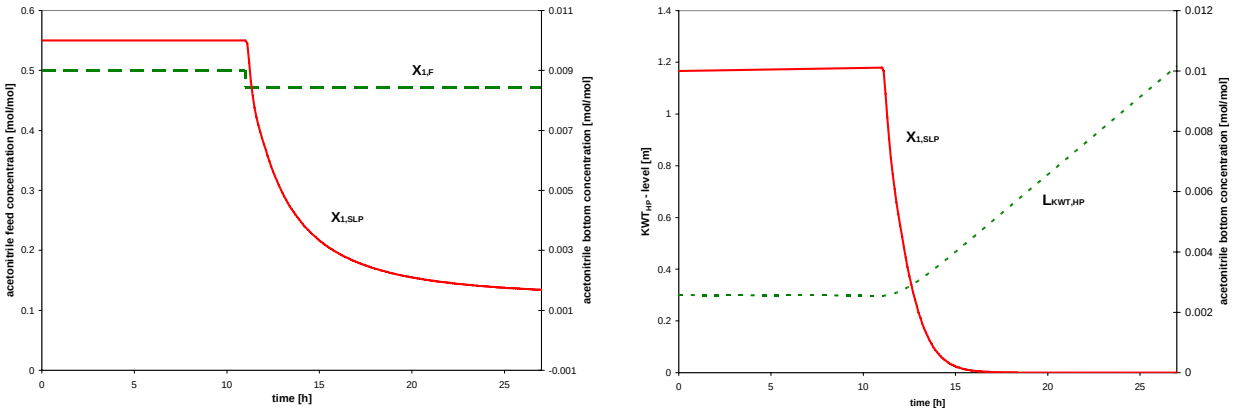

Fig. 5.19 Cascade controller analysis: left open loop, LP bottom concentration reaction an a feed concentration disturbance; right close loop, LP bottom concentration reaction with cascade controller.

This concept is not a feasible solution, because the influence of the level on the concentration is extremely small. The influence of the changes of the recycle stream, which also change if the

level of the coupled heat exchanger changes, has much more influence on the bottom concentration than the level change and therefore the change of the heat input into the LP reboiler. So the controller does not make any sense here.

5.1.3 Summary of the control concepts

Overall there are two feasible and practical process control structures for the operation of the PSD system both heat integrated. First the structure with an additional reboiler at the bottom of the LP column (see chapter 5.1.2, structure A) and second the structure with out an additional reboiler and the LP-bottom concentration control, with help of the LP reflux (see chapter 5.1.2, Fig. 5.10, structure B). The main difference is the higher investment costs of the structure A because of the reboiler, but as the reboiler is only used for controlling the investment cost are lower than for a non heat integrated concept. To give an impression which one will be the more suitable solution, the energy consumption at the operation point and the energy demand which is needed for controlling of feed concentration disturbances are compared (table 5.4 and table 5.5).

Table 5.4. Comparison of the heat duties (structure A).

x_F	**0.85**	**0.80**	**0.75**	**0.70**	**0.65**
$\dot{Q}^{HP}$ [kW]	6.51	7.50	8.66	9.89	11.15
$\dot{Q}^{LP}$ [kW]	0.00	0.00	0.00	0.44	1.15
$\dot{Q}^{\Sigma}$ [kW]	6.51	7.50	8.66	10.33	12.30
D^{LP} [l/h]	12.84	17.30	22.50	28.15	34.29
R^{LP} [l/h]	6.79	6.59	6.81	8.95	12.00
B^{LP} [l/h]	0.56	0.77	1.01	1.26	1.53
D^{HP} [l/h]	13.67	18.98	24.74	31.02	37.90
R^{HP} [l/h]	11.51	10.52	9.90	9.02	7.68
B^{HP} [l/h]	10.27	10.06	9.84	9.60	9.34

The tables show the operation point (grey marked) and the feed disturbances (new concentration) started from the operation point. At the operation point (grey marked) the energy demand is nearly equal for both structures because at this point the additional LP reboiler (only for control) is not in use. For high deviation of the feed concentration from the operation point the differences increases to smaller energy demands of the structure B (without an additional reboiler).

Table 5.5. Comparison of the heat duties (structure B).

x_F	**0.85**	**0.80**	**0.75**	**0.70**	**0.65**
$\dot{Q}^{HP}$ [kW]	6.06	7.31	8.65	10.06	11.51
$\dot{Q}^{LP}$ [kW]	0.00	0.00	0.00	0.00	0.00
$\dot{Q}^{\Sigma}$ [kW]	6.06	7.31	8.65	10.06	11.51
D^{LP} [l/h]	12.62	17.67	23.03	28.59	34.26
R^{LP} [l/h]	4.62	5.39	6.23	7.16	8.18
B^{LP} [l/h]	0.56	0.77	1.01	1.26	1.53
D^{HP} [l/h]	13.80	19.36	25.29	31.49	37.87
R^{HP} [l/h]	9.30	9.30	9.30	9.30	9.30
B^{HP} [l/h]	10.25	10.05	9.84	9.60	9.35

If the heat-integrated PSD is compared with no heat-integrated PSD, which means that each column has its own condenser at the top and its own reboiler at the bottom, which are used for heating the respective column and for control of the bottom concentration, the energy saving is up to 45% (see table 5.6).

Table 5.6. Comparison of the energy consumption to identify the possible energy savings.

$\mathbf{x_F}$	**0,85**	**0,8**	**0,75**	**0,7**	**0,65**
P^{HP} [bar]	2,63	2,73	2,84	2,98	3,12
x_S^{LP} [mol% water]	99,95	99,95	99,95	99,95	99,95
x_S^{HP} [mol% acetonitrile]	99,95	99,95	99,95	99,95	99,95
Q^{HP} [kW][a]	6,06	7,31	8,65	10,06	11,51
Q^{LP} [kW][b]	4,82	5,96	7,17	8,43	9,71
Q^{LP+HP} [kW][c]	10,88	13,28	15,83	18,49	21,23
Saving [%]	44%	45%	45%	45%	45%

a. overall energy demand with heat-integration

b. energy demand of the LP column without heat-integration

c. overall energy demand of the PSD system without heat-integration

5.2 Analysis of the start-up processes

In this chapter the start-up processes for the continuous operation will be analyzed. In the first section the start-up of the coupled continuous column system will be analyzed with a consideration on a heuristic basis. In the second section the structure of the start-up schedule for the simulation will be given.

5.2.1 Start-up of the continuous process

In the case of the continuous process the start-up concept is very complex. It bases on the start-up description including model equation changes as described in the modeling section (chapter 3.3), but the interesting part is the coupling (heat and mass) of the two columns. Therefore a preliminary analysis of the start-up process has to be done. Afterwards the start-up of the continuous system will be introduced.

5.2.1.1 Pre-consideration on a heuristic basis

The start-up from cold and empty of the pressure swing system can be separated into two different cases depending on the feed concentration. If the feed concentration is lower than the azeotropic point, the feed stream has to be added to the low-pressure column. This means that the feed is added to a column without a reboiler, so in addition an auxiliary feed for the high-pressure column with the reboiler has to be introduced, which has a concentration above the azeotropic point. The second case is a feed concentration above the azeotropic point. In this case the start-up can start with the high pressure column without an additional start-up feed. The two cases will now be described separately.

Low feed concentration - feed LP. In this case the start-up of the column system starts with the filling of the high and the low pressure columns with the respective feed. After a certain level the reboiler of the HP column will be switched on and the column is started up as in the general model description (chapter 3.3). If the coupled heat exchanger (mainly the condenser) is working, the columns will be heat integrated to heat up the LP column. The temperature difference between the shell side and the reboiler side of the coupled heat exchanger is enough because the LP column is still cold. During the next time the pressure in the HP column increases, which also means an increase of the temperature at the top of the column, so the temperature difference will be always positive. The more complex part is the mass integration, because the mass integration is practically possible only if the distillate concentrations are in the feasible distillation region. As mentioned in chapter 5.1.2.1 only the concentration of the mixture of feed and distillate stream has to be in the feasible region (eq. 5.5) and (eq. 5.6), but this can cause very high distillate streams. This can cause streams, which are higher than the acceptable values of the column system. So it is possible that these streams cannot be handle in the column, because the system works beyond its limits. The Fig. 5.20 shows such a situation in a practical experiment, were the distillate streams reach their limits and which causes a shut down of the process.

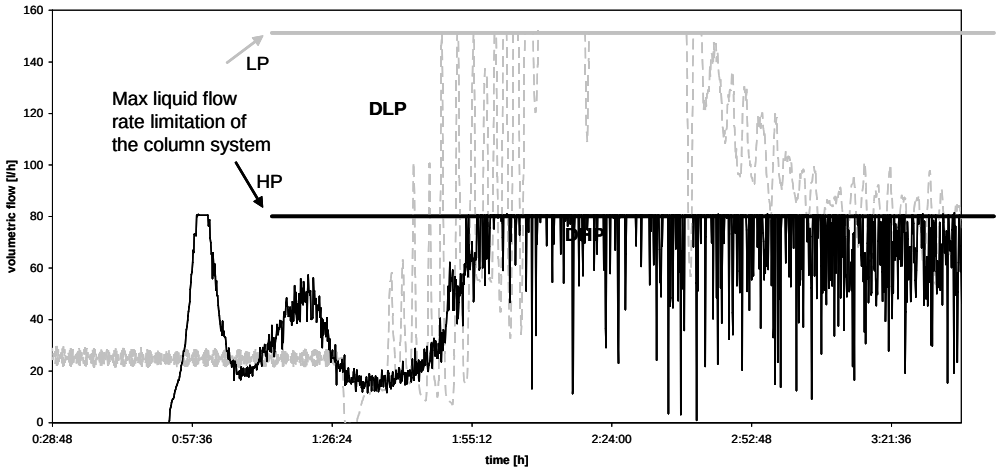

Fig. 5.20 Distillate volumetric flows at the top of the LP (light grey) and of the HP (black) column over limit (experimental data, with liquid flow rate limitations, overload at the top of the columns).

Conditions - feed LP:

$$x_D^{LP} > x_{az}^{HP} : \text{and} \qquad \text{(eq. 5.5)}$$

$$\left(\frac{D^{HP} \cdot x_D^{HP} + F^{LP} \cdot x_F^{LP}}{D^{HP} + F^{LP}} \right) < x_{az}^{LP} . \qquad \text{(eq. 5.6)}$$

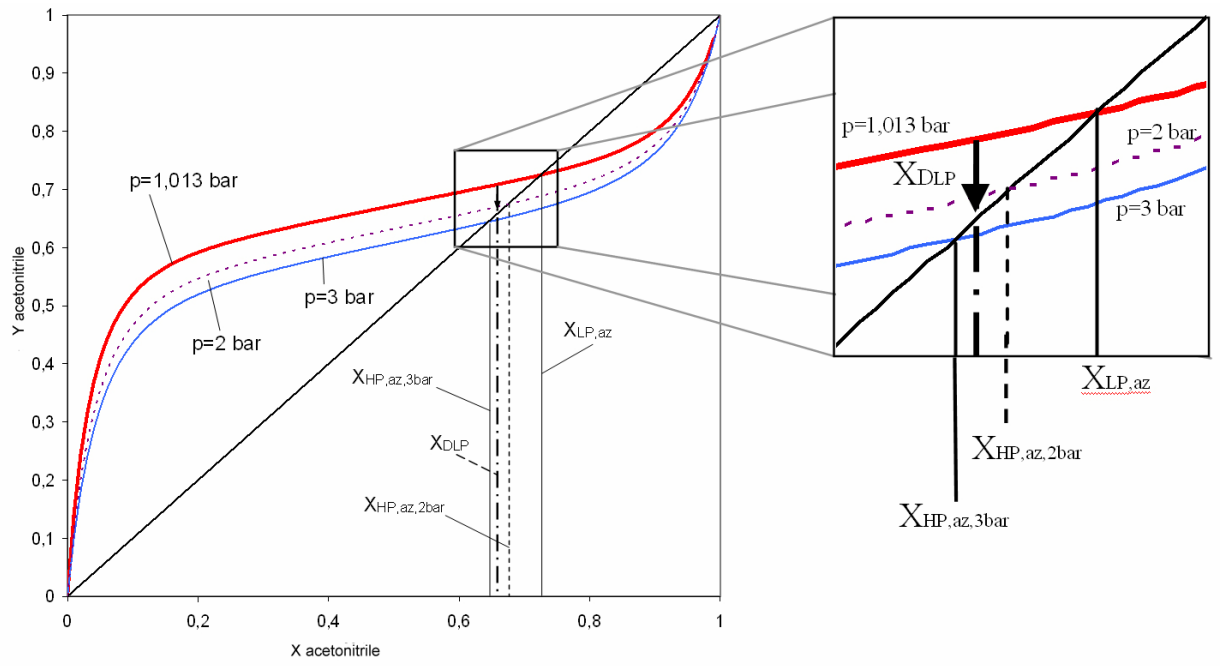

Fig. 5.21 Recycle stream (Distillate stream LP) in a not feasible distillation region.

To illustrate the problem, in Fig. 5.21 three equilibrium curves are sketched. If the pressure is not high enough, which means that the azeotropic point difference is too small, the distillate concentration of the LP column could be too low to be added into the HP column. If so, the column operates in the wrong distillation region and the theoretical bottom product switches from acetonitrile to water and following from (eq. 5.5) and (eq. 5.6) the distillate streams have to increase significantly.

This leads to the following start-up heuristic for a coupled pressure swing distillation system:

- Heat integration:
  - Vapor must exist at the top of the HP-column.
  - Temperature difference between HP top and LP bottom must be greater than zero for the energy coupling of both columns.
- Mass integration:
  - Top distillate concentrations must be high enough of each column to reach the feasible distillation region of the other column under the respective operation pressure.
  - Pressure in the HP-column must be high enough for a suitable azeotropic concentration difference between the columns.

In table 5.7 the main task of the start-up schedule are summarized.

Table 5.7. General schedule for starting up the column system (feed LP).

step	task
1	HP column feed starts (if the feed has a feed concentrations higher than the azeotropic point, or as an auxiliary feed only for start-up reasons).
2	LP column feed starts (if feed concentration is lower than the azeotropic point, or as an auxiliary feed only for start-up reasons).
3	If HP-reboiler is filled, reboiler starts.
4	If LP reboiler is filled, circulation pump switched on for forced bottom - reboiler stream.
5	If condensate is in the HP condenser, HP - reflux switched on.
6	Column now will be closed to increase pressure and also an heat integration is possible.
7	Wait for suitable level in the coupled heat exchanger and switch on the level control.
8	If condensate is in LP drum, switch on LP drum level control, and LP - reflux.
9	Depending on the start-up concept distillate streams goes back into the feed tank („higher set point values start-up“) or distillate streams are set to zero („infinite reflux start-up“).
10	If distillate concentrations are overlapping, which means suitable temperatures at the top of the column and a maximal pressure difference between the columns, distillate streams are switched to recycle streams.
11	If „higher set point values start-up“, set values to set point values.
12	Wait until all profiles are stable and constant, steady state is reached.

High feed concentration - feed HP. In this case the feed input is the HP column. The start-up follows the general description in chapter 3.3 only for the HP column. If no additional feed is used, the HP column has to be start-up including pressure increase, to produce feed (distillate

stream of the HP) for the LP column which lies in the feasible distillation region. As for the LP-feed case in the HP-feed case the following conditions are necessary:

$$x_D^{HP} < x_{az}^{LP} : \text{and} \qquad \text{(eq. 5.7)}$$

$$\left(\frac{D^{LP} \cdot x_D^{LP} + F^{HP} \cdot x_F^{HP}}{D^{LP} + F^{HP}} \right) > x_{az}^{HP} . \qquad \text{(eq. 5.8)}$$

After starting up the HP column and adding the recycle stream as feed into the LP column the heat integration follows, if the level in the LP reboiler is suitable. The complete mass integration is reached, if also the distillate concentration of the LP column is at its set point and the pressure difference is high enough. In table 5.7 the main task of the start-up schedule are summarized.

In both cases the start-up procedure ends if the steady state conditions are reached.

The developed start-up strategies are the basis for the simulation of the start-up of the continuous system in gProms™ which will be described in the next section.

Distillate concentration observer. In practical operation of the two column system during the start-up operation the main difficulty is to recognize at which time the distillate concentrations at the top of the columns are in the right distillation region. One possible solution is to take online samples, but this needs an expensive measurement equipment and also the time of the analysis can be to long.

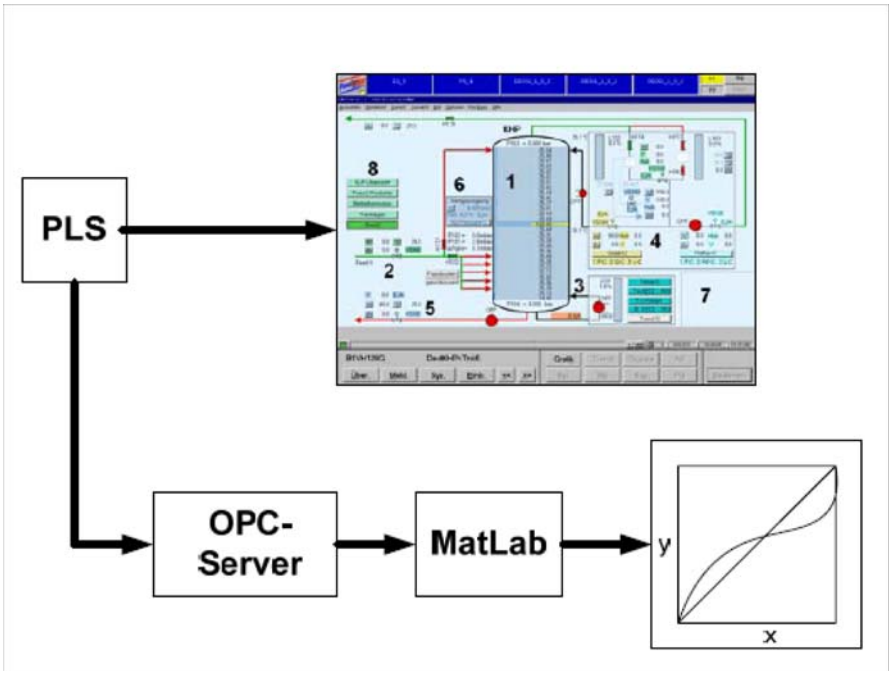

Fig. 5.22 Communication structure of the observer.

To avoid a non suitable connection in the experiment an observer was programmed in Matlab[1], which calculates out of the measured parameters (temperature and pressure at the top of the

1. Matlab: commercial mathematical software package by Mathworks INC, http://www.mathworks.com

column) concentrations in real time during the experiment using the equilibrium data. These calculated concentrations were then plotted for the operator (Fig. 5.22 and Fig. 5.23). A possible connection point is reached, if the plotted distillation regions (left: LP-column, right: HP-column) are overlapping (Fig. 5.23). The connection of Matlab to the PCS is done via OPC[1] (Fig. 5.22).

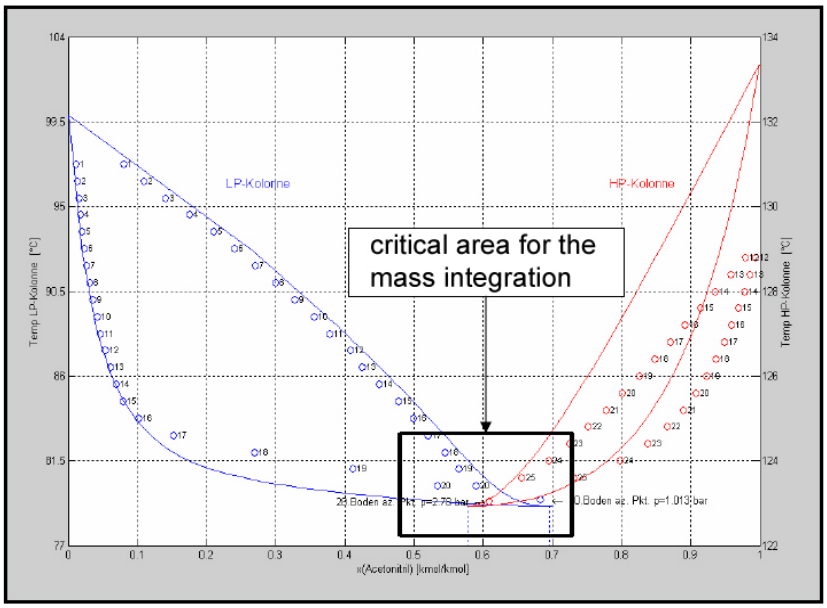

Fig. 5.23 Graphic generated by the observer in real time.

This new developed external program will help to find the right point for the mass integration of the two columns in practical operation. The complete system is described in [v. Ahnen 2006].

5.2.1.2 Simulation of start-up of the coupled system

The introduced start-up strategy is based on the more complex case of feed concentrations lower than the azeotropic point which means a feed input into the LP column and the use of an additional start-up feed for the HP column. The continuous process uses the following controllers (table 5.8) and the following states of these controllers (table 5.9):

Table 5.8. Controller with manipulated and control variable (continuous process).

controller	manipulated variable	control variable
top reflux flow rate controller (HP)	reflux flow rate (valve)	reflux flow rate
coupled heat exchanger level (HP) = distillate drum (HP)	recycle flow rate to LP column (valve)	coupled heat exchanger HP level
distillate drum level (LP)	recycle flow rate to HP column (valve)	distillate drum level
bottom conc.controller (LP)	reflux flow rate at column top (valve)	bottom product conc.
bottom conc. controller (HP)	reboiler heat duty (HP)	bottom concentration (HP)
bottom level controller (HP)	outlet flow rate HP (valve)	bottom level (HP)
bottom level controller (LP)	outlet flow rate LP (valve)	bottom level (LP)

1. OPC: OLE for process control [OPC]

Table 5.9. Dynamic start-up model: states of the controller (continuous process).

step	action	controller	state	trigger	threshold
0	cold and empty		all controller *inactive*	-	-
1	feed in HP	feed flow rate controller	*manual*	-	-
2	feed in LP	feed flow rate controller	*manual*	feed in HP	-
3	switch on HP reboiler	bottom concentration controller	manual (30%)	reboiler level	*50%*
4	switch on circulation pump LP	-	-	-	-
5	close HP column	-	-	-	-
6	heat integration on	-	-	condensed vapor in the CHE	-
7	switch on HP reflux	reflux flow rate controller	manual	level in coupled heat exchanger (CHE)	50%
8	HP distillate recycled into LP column	distillate drum (CHE) level controller	automatic	pressure	>3 bar
9	switch on reflux LP	reflux flow rate controller	manual	level in the drum (condensed vapor)	20%
10	switch off auxiliary feed HP	feed flow rate controller	inactive	level in the drum (stable reflux flow rate)	-
11	recycle LP distillate to HP column	distillate drum level controller	automatic	-	-
12	switch on outlet stream HP	bottom level controller	automatic	reboiler level HP	80%
13	switch on outlet stream LP	bottom level controller	automatic	reboiler level LP	80%
14	waiting for steady state (LP + HP)	bottom concentration controller	automatic	working level controller	-

In some cases especially the coupling of the columns the schedule instead of the trigger threshold concept is used. For the start-up schedule see chapter 4.3.3.

In an additional work [Varbanov 2007, Varbanov 2007b] the optimization of the start-up procedure of a continuous PSD system was tried using an stochastic search algorithm. A significant problem with these stochastic search algorithms is the very long computing time, which needs to be spent in order to arrive at a reasonable time an optimal solution. This can take such a very long time, which is definitely not suitable for solving problems of optimal process

operation. Therefore on the basis of the start-up approach shown above and the validated start-up model from cold and empty (chapter 4.3.3) a more conceptional optimization approach was developed. This approaches bases on inequations concerning system throughput, hold ups of the column reboilers, internal flow rates, and concentrations. With help of the inequations upper and lower bounds were indicated for the reflux flow rate the feed flow rate, and the boil up rate /heat duty. Keeping this boundaries in mind, the start-up schedule can be design, which is leading to a faster start-up operation (up to 80% of start-up time reduction compared to the heuristic schedule, see chapter 4.3.3).

The main measures allowing this significant reduction in the start-up duration are:

- Increase in the boil-up rates through raising the HP reboiler heat duty. This allows increasing the throughput of the system. This is based on the fact that larger heat input provides more scope for increasing the combined liquid flow rates inside the columns.
- Larger reflux flow rates result in faster approach of the distillate compositions to the respective azeotropic points. This, however, also reduces the scope for increasing the flow rates of the other liquid column inputs and, consequently, the column throughput.
- Adjustment, as much as possible, of the distillate flow rates recycled between the columns. These also depend on the capacities of the distillate drums and the chosen values of the reflux flow rates.

For the detailed conceptional optimization approach see [Varbanov 2007, Varbanov 2007b]. To make this approach more general, further studies will be necessary, but the important thing is the high potential of time saving during start-up also for this high complex integrated column system with help of simple inequations.

6. Batch pressure swing distillation

This chapter consists of a detailed analysis of the discontinuous pressure swing processes (the regular and the inverted batch process). Different process design concepts and process control concepts for each process will be discussed and a start-up strategy from cold and empty state and its motivation to do so, will be introduced. The chapter ends with the evaluation and comparison of the different batch processes against batch time and energy consumption, using the analytical model and the rigorous dynamic start-up model.

6.1 Process design and process control concepts

For the discontinuous process the possible designs have much more influence on the process than for the continuous operation. This section starts with the introduction and analysis of the different designs followed by the analysis of the influences on the batch time and ends with the discussion of the process control concepts.

6.1.1 Process design

In general there are four different process designs in the batch operation possible, the regular batch, the inverted batch, the batch with middle vessel, and the batch with multi vessel. The last two designs do not make sense for the separation of binary azeotropic mixtures, so both concepts will not be analyzed in the context of this work [Furlonge et al. 1999]. Under one general design variations are possible.

The regular and the inverted processes (see also chapter 2.2.2) differ in the position of the feed tank and therefore in the column

configuration (Fig. 6.1). For the regular column the feed mixture is in the bottom of the column. The column works as a rectifier column. The top product is the azeotropic mixture. The process come to an end, if the bottom product purity (high boiling component) is reached. After that the azeotropic mixture is drained back into the bottom of the column and the pressure is changed. The batch is finished, if the bottom concentration reaches the desired purity of the other product.

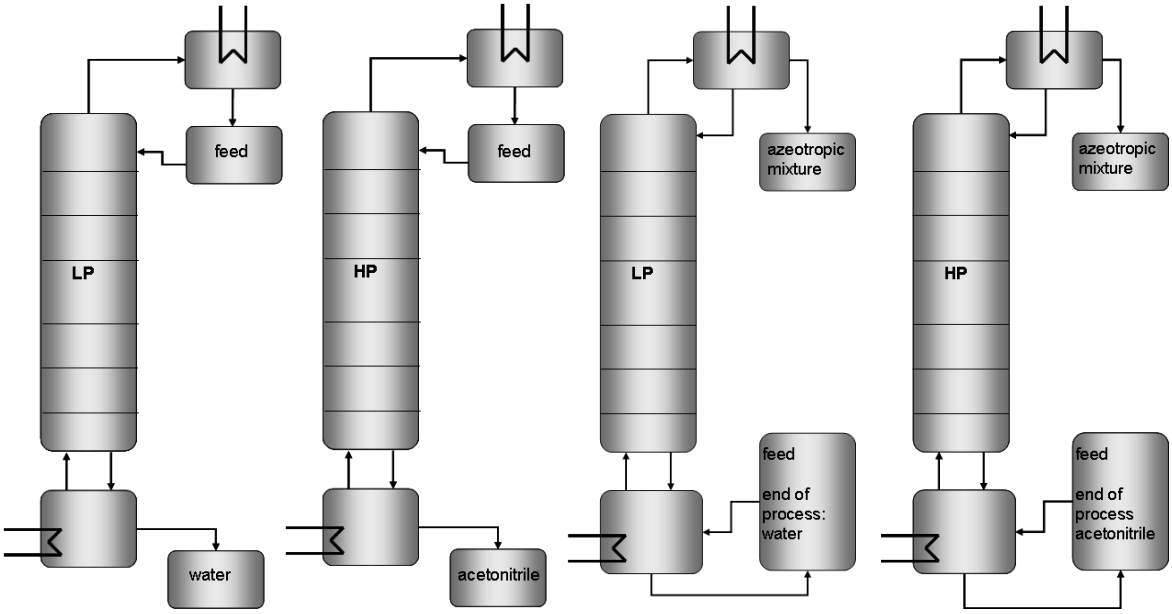

Fig. 6.1 Discontinuous pressure swing distillation - inverted batch process (left), regular process (right).

The inverted column works like a stripper column, which means that the feed is in a tank at the top of the column and pure product is drained from the bottom (concentration controller). The process ends if the desired top azeotrope concentration (low boiling azeotrope) is reached. In the next step the pressure can be increased immediately because there is no pumping of feed into another tank necessary. The feed for the next step is already in the right tank at the top. Pure product (second component) is drained from the bottom of the column. The batch is finished, if the desired azeotropic concentration at the respective pressure is reached in the feed tank.

The inverted batch mentioned above is not the exact opposite of the regular batch process. If so it is called the true inverted batch. As Sørensen describes in her work, the true inverted batch would need a vaporized feed and also the distillate drum or tank has to be vaporized [Sørensen & Skogestad 1996]. This true inverted process is an academic example and not feasible for industrial applications. An analysis of the true inverted batch as done in [Sørensen & Skogestad 1996] will not be done in this work.

The main concepts of regular and inverted batch structure can be divided into other sub-structures. The different process designs, the inverted and the regular structure and its variations, will now be introduced and analyzed in detail. After that the influences on the batchtime will be discussed.

6.1.1.1 Regular batch

In the regular case there are two variations possible. The first is a structure with a big reboiler tank at the bottom (RB-bB, Fig. 6.2 left) and the second is a structure with an additional feed tank besides the reboiler (RB, Fig. 6.2 right, experimental plant structure).

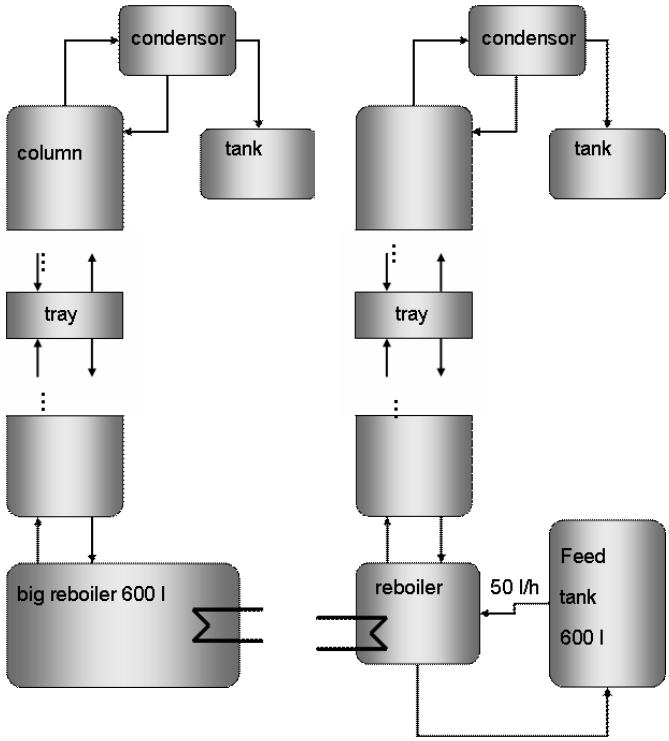

Fig. 6.2 Process structure: left - regular batch with a big reboiler tank (RB-bB); right - regular batch with an additional tank besides the reboiler (RB).

The additional tank structure has the main advantage that the residence time in the hot reboiler is much less than in the structure with the big reboiler. This structure is mainly interesting for temperature sensitive mixtures. Furthermore the connection of a small reboiler and a scalable tank is much more flexible. The potential application does not depend on the feed volume, because the reboiler can be operate at a suitable level and the feed tank can be as big as necessary. The disadvantage is the circulation pump between the reboiler and the tank and the feed-back mixing between tank and reboiler. In the simulation study the feed flow rate (circulation flow rate) is set to 50 l/h equal to the feed flow rate at the top of the inverted column and equal to possible flow rates at the pilot plant. The main advantage of the regular batch with a big reboiler is the fact, that the complete feed volume is already in the column, so there is no back mixing as with an additional tank in the bottom. The main disadvantage is the long residence time of the mixture in the reboiler with high temperatures, which can be a problem for temperature sensitive mixtures. The feed hold-up is for all experiments 600 l also similar to the real plant.

The regular batch process time could mainly be influenced by the pressure, the heat duty at the top of the column and the distillate concentration at the top.

6.1.1.2 Inverted batch

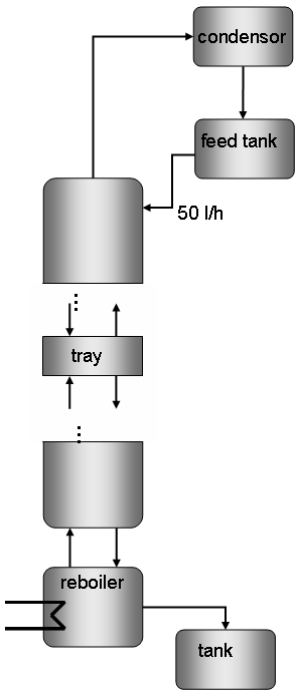

Fig. 6.3 Structure of the normal inverted batch (NIB).

The inverted batch has the feed input at the top of the column. The feed is stored in an external tank (600 l) and is added similar to a reflux stream to the column (Fig. 6.3). The feed flow rate is fixed (50 l/h, similar to the bottom flow rate in the RB case) and directly influences the f-factor which means the hydrodynamic load of the column and finally the process time. The pure product is drained from the bottom. The process ends when the azeotropic concentration is reached in the feed tank. The influence of the top concentration which means the concentration at the end of the process at the feed tank will also be analyzed (see chapter 6.1.2).

The process time of the inverted process could mainly be influenced by the feed stream, the pressure, the top end concentration, and the feed back mixing in the feed tank. The feed- back mixing will be discussed first because this leads to an additional structure.

6.1.1.3 Advanced inverted batch (AIB)

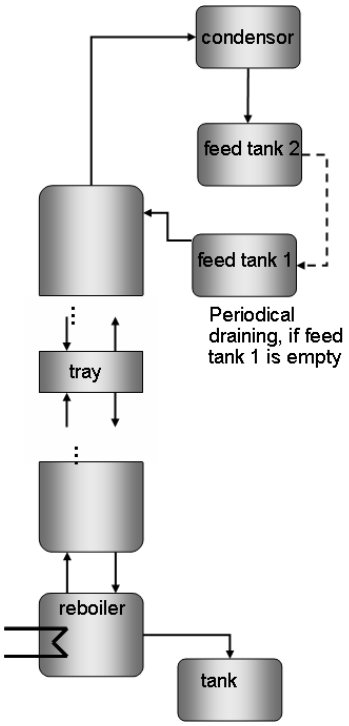

Fig. 6.4 Process structure of the advanced inverted batch process (AIB).

The back mixing at the top of the inverted column occur because higher concentrated condensed distillate is drained back to a lower concentrated feed tank. To reduce the back mixing in the feed tank an additional tank will be introduced at the top of the column. This tank (feed tank 2, 600 l) is used to store the distillate during the feed is added from an additional tank (feed tank 1, 600 l) to the column. If the feed tank runs out of liquid the distillate is drained into the feed tank and the loop continuous (Fig. 6.4). The loop runs until the desired azeotropic concentration is reached in feed tank 1. The conclusion of this concept is that the back mixing of high concentrated distillate and low concentrated feed is reduced. This new process design is called advanced inverted batch (AIB). The advanced inverted batch can also be used for zeotropic mixtures, but will only be analyzed in the context of the pressure swing distillation. The setup is the same for both

processes except the tanks at the top (table 6.1). The important fact is the dumping of distillate in an additional tank and the concentration in that tank.

Table 6.1. setup of the simulation case study.

x_F	0.3 mol/mol
x_B^{set}	0.99 mol/mol
x_D^{set}	0.687 mol/mol
V_F	600 l
P	1,015 bar
R	50.5 l/h

As fast as the proper top concentration set point is reached in this tank as fast is the process. Because of the reduced back mixing, the set point can be reached much faster than for the NIB process. The comparison under the same conditions of the NIB and the AIB pointed out a significant acceleration of the AIB process of up to 40 % (Fig. 6.5).

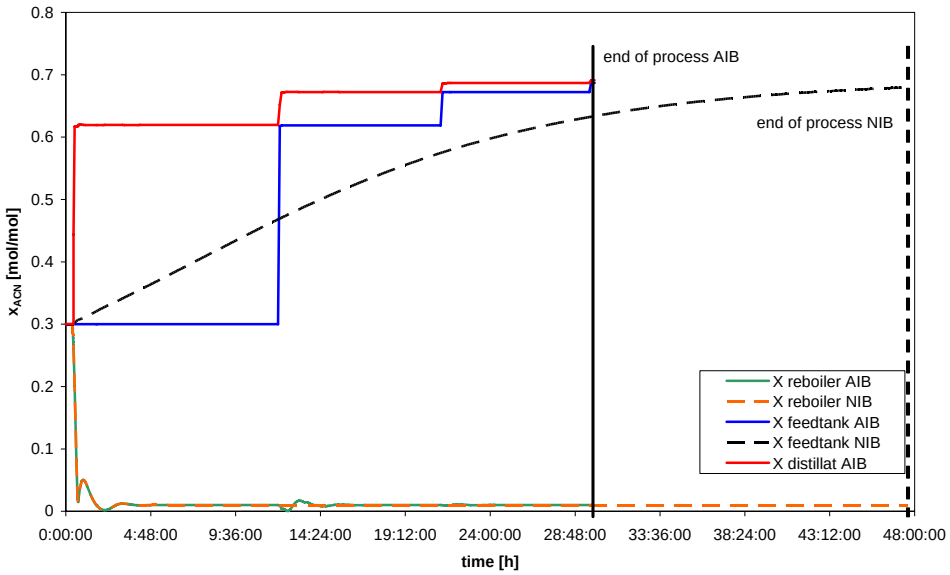

Fig. 6.5 Comparison of normal inverted batch (NIB) with advanced inverted batch (AIB): top- and bottom concentration against time, for a feed of 30 mol%.

6.1.1.4 Batch design structures - an overview

Besides the introduced structures above with or without additional feed tanks and feed volume rates for the comparison with help of the dynamic rigorous model an equivolumetric design is needed. In the analysis of the batch structures volumetric streams instead of molar streams are always used because volumetric streams are more practical. Molar streams cannot be controlled in a real plant; so they are more for academic discussions.

The goal of the analytical approach is to use it as a practical short-cut method for the comparison of an inverted and a regular batch column. This approach is based on molar magnitudes to keep it simple. To get nearly equal conditions in the analytical approach and the rigorous simulation an equivolumetric design is needed. An equivolumetric design means that the volumetric hold up of the feed tank is equal to the feed volume stream added to the column for the inverted case. For the comparison the constraints of the regular batch process (constant f-factor equal to one, column design) will be equal to those of the inverted batch. The idea is that under these conditions the back mixture of the inverted case is similar to the regular case without an additional feed tank.

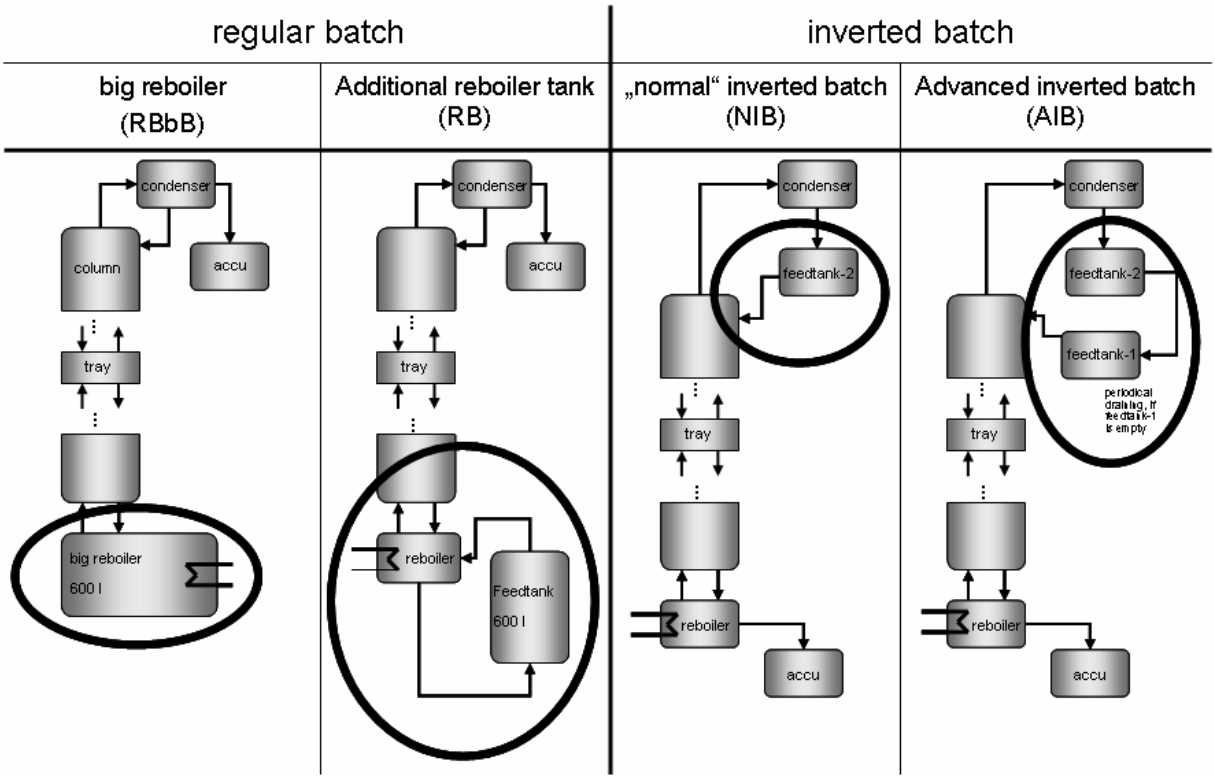

Fig. 6.6 Different process structures in the simulation study (base cases).

In the batch studies the following different structures will be used (Fig. 6.6):

- Regular batch structures:
  - *RB:* regular batch with additional feed tank at the reboiler (setup of the pilot plant).
  - *RB-bB*: regular batch with a big reboiler tank, without an additional tank at the bottom.
  - *RB-bB4x:* structure as RB-bB with quad capacity. Is used for the comparison with the inverted structures with a larger feed stream on top of the column (see later on), quad column cross area.
  - *RB-bBeq:* regular batch with a big reboiler tank, were the feed tank column is equal to the feed stream (e.g. 100 l feed tank column, 100 l/h feed stream into the column).
- Inverted batch structures:

- *NIB:* normal inverted batch, with one feed tank at the top.
- *AIB:* advanced inverted batch, with two feed tanks at the top, one for the feed and one to dump the distillate. If the feed tank is empty the distillate is drained to the feed tank and the process is going on.
- *NIB2x:* normal inverted batch with twice higher feed volume stream at the top, doubled column cross area.
- *NIB4x und AIB4x:* structures as above, but with quad feed volume stream and quad column cross area.
- *NIBeq:* normal inverted batch, were the feed tank volume is equal to the feed stream (e.g. 100 l feed tank volume, 100 l/h feed stream into the column).

6.1.2 Analysis of influences on the batch time

To get a realistic comparison of the regular and the inverted batch structures other influences on process time and energy consumption has to be identified and than set to comparable values that all process are operated under the same conditions. The analysis of the influences will be done for both general batch structures, the inverted and the regular batch under the following conditions:

- Constant hydrodynamic conditions in the column (constant F-factor).
- Same number of trays (28 trays).
- Comparable process control concept.

6.1.2.1 Volumetric feed flow rate

A change of the volumetric feed-flow rate has a significant influence on the batch time of the inverted batch process, but also on the hydrodynamics of the plant. An increase of the feed-flow rate causes an increase of the internal column load and therefore an increasing F-factor (eq. 3.43).

Table 6.2. Conditions (influence of the feed stream).

x_F	0,1 mol/mol
D	114,0 mm, (50 l/h, NIB) 151,32 mm, (100 l/h, NIB2x) 214,0 mm, (200 l/h, NIB4x)
x_D^{set}	0,687 mol/mol
V_F	600 l
P	1,015 bar
F-factor	constant 1 $\sqrt{Pa}$

This is because the reboiler heat duty has to be increased also to get proper specifications. For a constant F-factor the column diameter has to be increased also, to increase the cross column area, which leads to a new column design, depending on the feed stream. Also the dimension of the reboiler and the condenser has to be adjusted. The influence on the performance of the inverted batch column for an increasing feed stream is illustrated in Fig. 6.7 and the data can be

found in table 6.2. The study is done under the assumption of constant hydrodynamic conditions which directly influences the column diameter when the f-factor is still constant and set to one.

The figure shows a significant time reduction with an increasing feed volume stream for a constant F-factor. The doubling of the feed stream leads to a cut in half of the batch time. The energy consumption also decreases significantly (table 6.3).

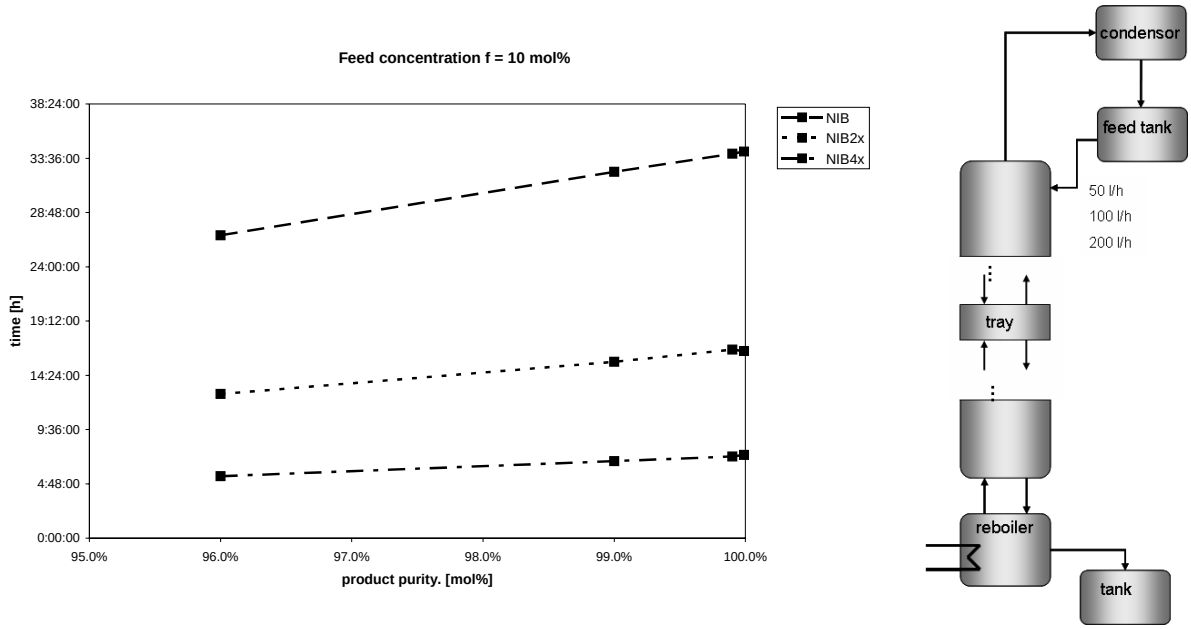

Fig. 6.7 Comparison of the batch time for a variation of the volume of the feed flow rate for different product concentrations for the inverted batch structure (NIB, right).

In the regular case the reduction of the batch time is not so big as for the inverted case, also the energy consumption reduction is much small than in the inverted case (table 6.3).

Table 6.3. Comparison of batch time and energy demand for a variation of the volumetric feed stream (feed concentration. = 10 mol%) and the reduction of the 200 l/h case compared to the base case (50 l/h).

product purity	feed stream	inverted batch (NIB)		regular batch (RB-bB)	
		batch time	energy demand	batch time	energy demand
96 mol%	50 l/h	26:47 h	230.01 kW	6:46 h	81.14 kW
	100 l/h	12:45 h	213.10 kW	-	-
	200 l/h	5:29 h	153.25 kW	1:54 h	76.19 kW
50 to 200 l/h reduction [%]		*80%*	*33%*	*72%*	*6%*
99 mol%	50 l/h	32:23 h	306.97 kW	9:39 h	115.89 kW
	100 l/h	15:35 h	290.94 kW	-	-
	200 l/h	6:48 h	230.76 kW	2:41 h	107.32 kW
50 to 200 l/h reduction [%]		*79%*	*25%*	*72%*	*7%*
99.9 mol%	50 l/h	34:00 h	329.94 kW	12:51 h	154.13 kW
	100 l/h	16:40 h	322.30 kW	-	-
	200 l/h	7:13 h	255.24 kW	3:33 h	142.36 kW

Table 6.3. Comparison of batch time and energy demand for a variation of the volumetric feed stream (feed concentration. = 10 mol%) and the reduction of the 200 l/h case compared to the base case (50 l/h).

product purity	feed stream	inverted batch (NIB)		regular batch (RB-bB)	
		batch time	energy demand	batch time	energy demand
50 to 200 l/h reduction [%]		*79%*	*23%*	*72%*	*8%*
99.99 mol%	50 l/h	34:12 h	332.92 kW	15:40 h	187.97 kW
	100 l/h	16:32 h	318.09 kW	-	-
	200 l/h	7:22 h	264.69 kW	4:22 h	174.69 kW
50 to 200 l/h reduction [%]		*78%*	*20%*	*72%*	*7%*

The influence of the feed volumetric flow rate on the performance of the inverted batch is much bigger than on the regular case (RB-bB). The main reasons for this fact is that in the inverted case the feed must first be pumped into the column (in the case of 50 l/h this means 12h pumping time) and then can be separated in the column. In the regular case the feed is already in the column (reboiler), so there is no need of pumping the feed around.

$$\text{ratio} = \frac{\text{feed hold up } (t_0)}{\text{feed volume flow rate}} \qquad \text{(eq. 6.1)}$$

In general the ratio of the feed hold up to the feed volume flow rate gives an information of the performance of the inverted batch process. The smaller this ratio the better is the performance of the inverted batch compared to the regular one. Sørensen uses in her study a ratio of one which means a very good performance of the inverted batch [Sørensen 1996]. In our study we have ratios between 12 (50 l/h) to 3 (200 l/h). The inverted process with a ratio of 3 has the best performance of all inverted batch examples (see table 6.3).

6.1.2.2 Pressure influence

The pressure in the pressure swing distillation process directly influences the concentration of the azeotropic mixture. For the operation at two different pressures the difference between the azeotropic points of the low and the high-pressure column has to be big enough for a suitable operation. The pressure can be freely chosen under the above mentioned constraints (potential optimization variable). It depends only on the construction of the column.

The influence of the pressure is not so significant on the batch time. The batch time differ a little bit because of the longer start-up time for higher pressures (Fig. 6.8), but the influence is nearly the same on both batch processes.

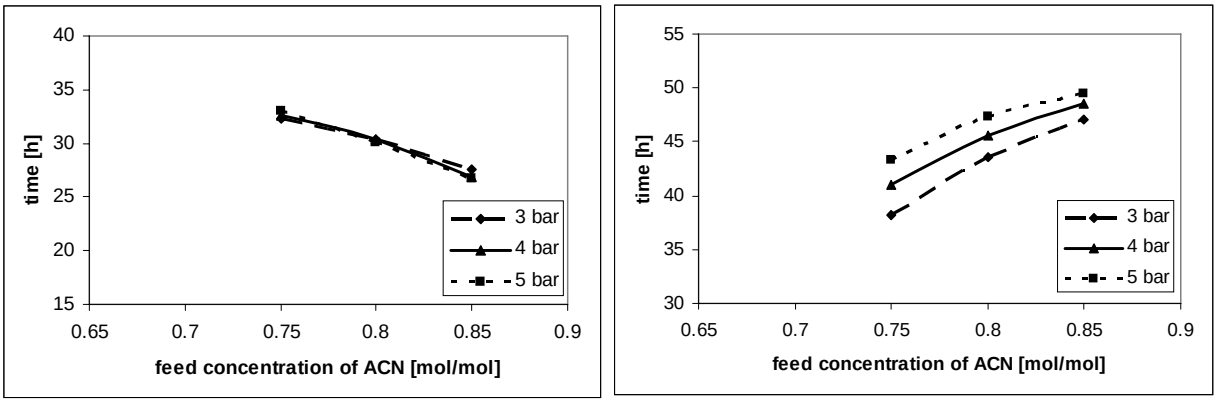

Fig. 6.8 Comparison of different pressures for the high pressure distillation region (left: inverted batch; right: regular batch).

6.1.2.3 Distillate concentration

The maximal possible distillate concentrations are depending on the pressure in the column, but the top concentration depends on the process time (inverted case) or the amount of reflux (regular case). These real distillate concentrations can be chosen freely under the following constrains:

- *Compliance of an adequate distillate concentration between the distillate concentration of the low and high pressure column.* The bigger the gap the bigger the amount of product in the second step of the discontinuous pressure swing operation.
- *Minimizing the process time.* The smaller the difference between the distillate concentrations and the azeotropic point the longer the process time will be because of a higher reflux stream (regular case) or a purer „feed tank concentration“ in the inverted case.

The maximal possible amounts can be calculated with the equations listed in table 6.4 with the assumption of an ideal separation and pure products in the bottom.

Table 6.4. Calculation of the maximal possible distillate to bottom amount ratios depending on the feed concentration and the azeotropic point difference (pressure sensitive).

	LP-Feed $z^{LP} = 0 \ldots x_{az}(P^{LP})$	**HP-Feed** $z^{LP} = 0 \ldots x_{az}(P^{LP})$
1. step	$\frac{D^{LP}}{B^{LP}} = \frac{z^{LP}}{(x_D^{LP} - z^{LP})}$	$\frac{D^{HP}}{B^{HP}} = \frac{1 - z^{HP}}{(z^{HP} - x_D^{HP})}$
2. step	$\frac{D^{HP}}{B^{HP}} = \frac{1 - x_D^{LP}}{(x_D^{LP} - x_D^{HP})}$	$\frac{D^{LP}}{B^{LP}} = \frac{x_D^{HP}}{(x_D^{LP} - x_D^{HP})}$

The maximal ratio of top to bottom product is calculated in the first process step with help of the feed concentration and the azeotropic point concentration at the respective pressure. In the second step the ratio depends only on the difference between the two azeotropic points at the

respective pressures. This analytical calculation is only for an ideal separation. To look at a real separation problem, with lower distillate concentration than the maximal possible, a small simulation study is done. Three different distillate concentration at the top of the column (x_D = 0,66; 0,68 ;0,69), which means 4,5%; 1,5% and 0,5% deviation from the azeotropic point in the low pressure case (table 6.5) are simulated. For the high pressure case see table 6.5.

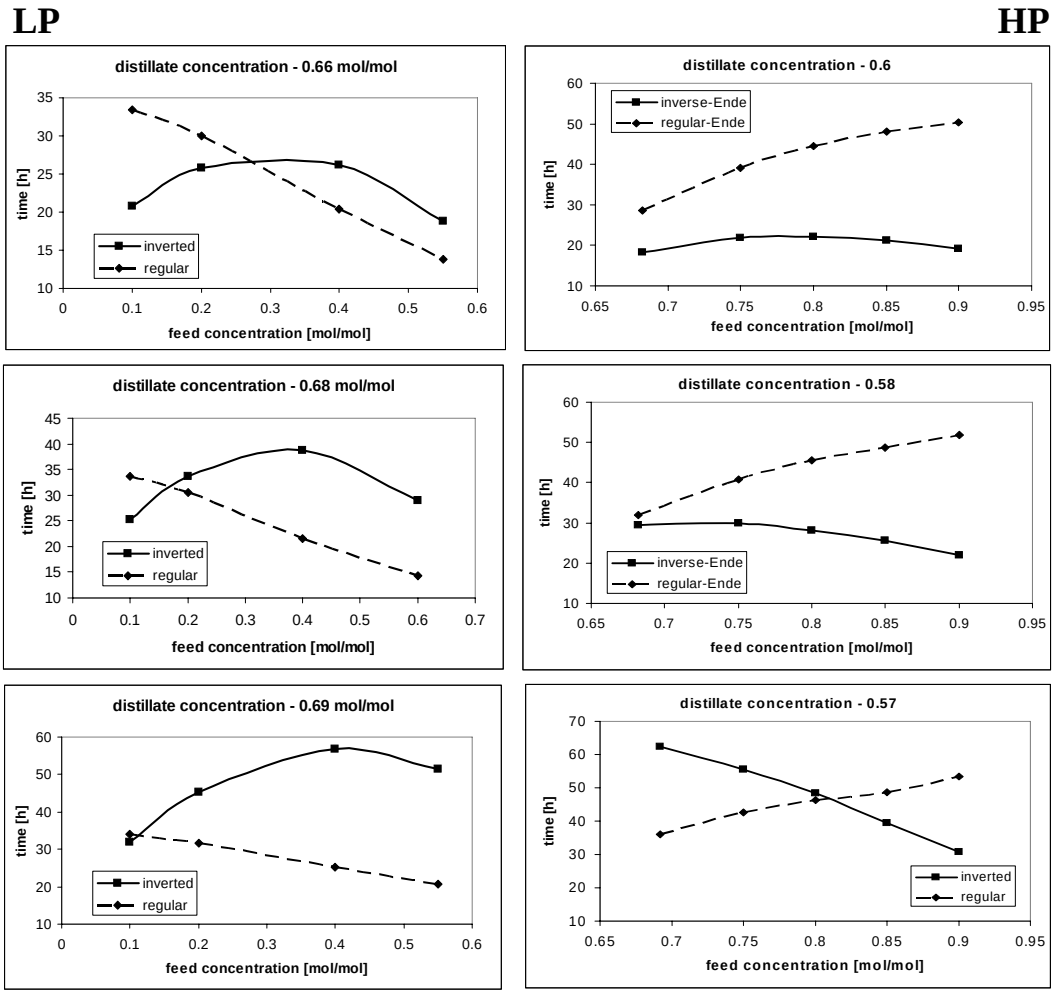

Fig. 6.9 Comparison of different distillate end concentrations and their influence on the batch time (left column: LP, right column: HP; from top to bottom: increasing deviation between distillate and azeotropic concentration).

Table 6.5. Conditions for the distillate concentration study.

Case	x_D	Deviation form the azeotropic point
LP - 1 (1,013 bar)	0,66	5%
LP - 2 (1,013 bar)	0,68	1,9%
LP - 3 (1,013 bar)	0,69	0,4%
LP azeotropic point	0,693	0%
HP - 1 (4 bar)	0,6	5%

Table 6.5. Conditions for the distillate concentration study.

Case	x_D	Deviation form the azeotropic point
HP - 2 (4 bar)	0,58	1,9%
HP - 3 (4 bar)	0,57	0,5%
HP azeotropic point	0,573	0%

all cases: feed flow rate 70 l/h, variation of the feed start concentration,
bottom product purity of 99.9 mol%, feed start volume 600 l

As shown in Fig. 6.9 there is a significant influence of the distillate concentration on the batch time. For distillate concentrations near the azeotropic point, the inverted batch gets slower compared to the regular one and vice versa. Furthermore the batch time, as well as the energy consumption (not shown in Fig. 6.9) increases significantly with a decrease of the distillate azeotropic concentration gap.

For the comparison of the two processes it is necessary to have comparable conditions. This means, that the distillate concentration at the top have to be fixed for both batch structures in the same way. The first thing will be the definition of the same deviation from the azeotropic point for both structures (regular and inverted). To give an example: If the distillate concentration of the regular process have a deviation of 5% from the azeotropic point at the respective pressure, the inverted process must have the same. To decide which deviation has to be chosen, the effectiveness of the processes for different distillate concentrations will be analyzed. Effectiveness means in this case the ratio of product amount to batch time.

$$\text{ratio} = \frac{\text{product amount}}{\text{batch time}} \qquad \text{(eq. 6.2)}$$

The conditions for the comparison study can be found in table 6.6.

Table 6.6. Conditions (influence of the feed stream).

x_F	variable
column diameter	114,0 mm
x_D^{set}	0,4 %, 1,9 %, 5 % of the azeotropic point
V_F	600 l
P	1,015 bar (LP) and 4 bar (HP)
F-factor	constant 1 $\sqrt{Pa}$
feed flow rate	70 l/h
x_B^{set}	99,9 mol%

In Fig. 6.10 the ratios for different distillate concentrations are shown, depending on the feed start concentration for the first step of the pressure swing process. The main result is, that the ratio increases with an increase of the gap between the azeotropic point and the set point of the distillate concentration. In other words as much as the distillate concentration is far from the respective azeotropic point, as shorter the process is and as effective in relation to the product amount the process is.

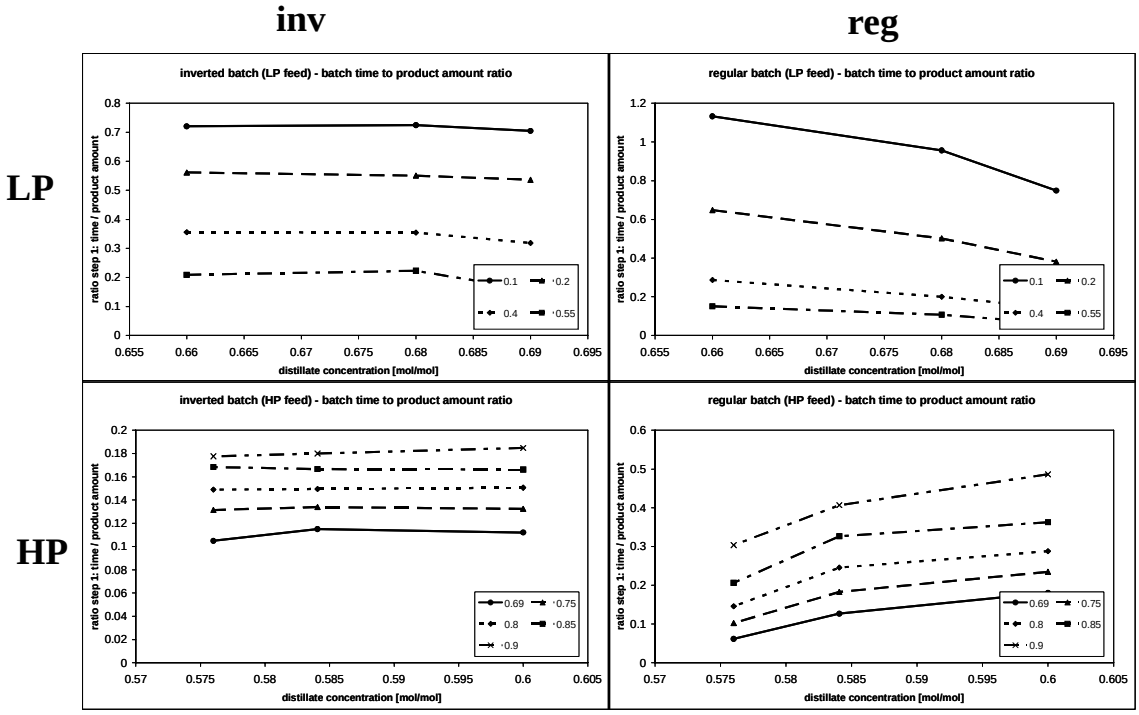

Fig. 6.10 batch time to product amount ratio for different distillate conc. for different feed start concentrations for the inverted and the regular batch process (top: LP feed, left: inverted, right: regular; down: HP feed, left: inverted, right: regular)

But second it is necessary to have a „pure“ as possible distillate product for the second step of the pressure swing distillation processes, to have a big gap between the distillate concentration, which is now the new feed start concentration, and the new azeotropic concentration of the new pressure. If this gap increases also the product amount in this second process step increases. In conclusion to respect both competing influences, a distillate concentrations which is in the middle will be chosen for the comparison study. In our case this will be 2% of the respective azeotropic point. The distillate concentration will be a good optimization variable, but this will not be discussed in this work.

6.1.3 Process control concepts

The operation of the discontinuous columns differs from the continuous operation in the missing of a steady state point, which means the batch operation does not have a real operation point as the continuous process. The controller concept is different from the continuous one. Only the pressure and the level control are similar to the continuous operation. Also, for the batch operation the manipulated variable and the control variable must be near to each other. The level (distillate drum and reboiler) is mostly controlled by the nearest outlet stream, the pressure with the cooling water stream of the condenser, or with help of an inert gas stream. In general there are different control concepts. Stichlmair lists three different concepts: the operation with constant reflux, with constant distillate composition, and an operation with minimal energy

input [Stichlmair & Fair 1998]. Mutjaba lists four different concepts: operation with constant vapor boiling rate, with constant condenser vapor load, with constant distillate rate, which is similar to constant reflux and with constant reboiler duty [Mutjaba 2004]. In this study, I concentrate on the concept with constant distillate composition (regular process) respectively a constant bottom concentration (inverted process) which is also similar to the control concept by [Sørensen & Skogestad 1996] were optimal reboil and reflux ratios are used, to get the specified product purities.

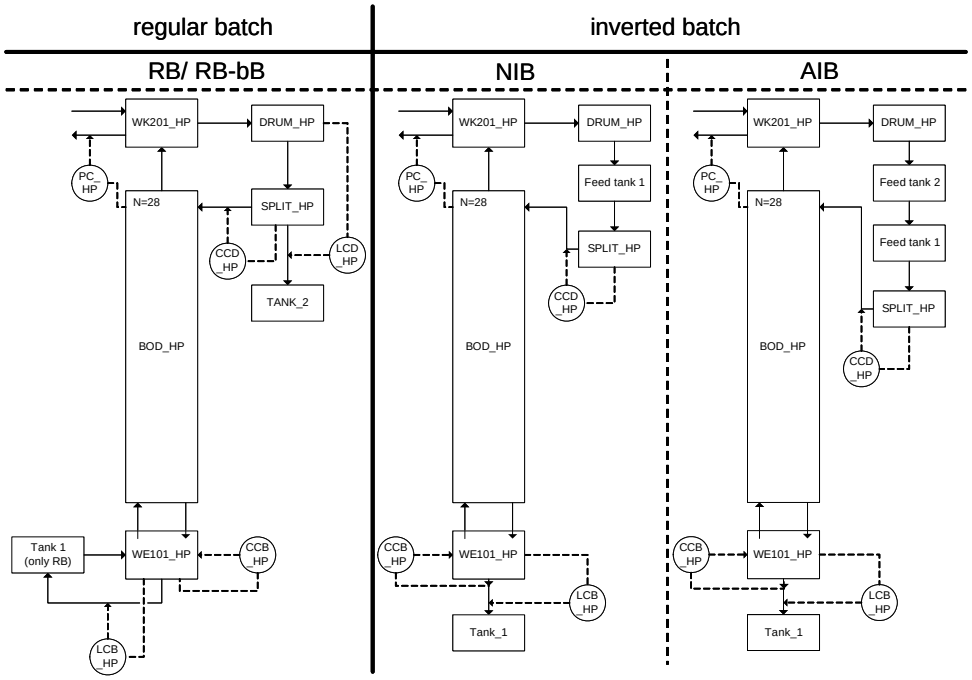

Fig. 6.11 Process control concepts for the different batch structures (RB, RB-bB, AIB, NIB; see appendix for explanation of the Abbreviations).

Regular batch. In the regular case, the feed tank is at the bottom and therefore the azeotropic mixture is withdrawn from the top, in our case it is the azeotropic mixture. This concentration must be constant. There will be two possibilities to do this. First, the plant is operated under constant reflux. This means that the distillate stream decreases during the operation. Second, having a constant distillate stream, which means a changing reflux. The process ends if the given bottom concentration in the feed tank is reached.

In this work the distillate concentrations, which are the concentrations of the outlet stream at the top, are controlled with help of the reflux. The heat duty is set to constant, so the plant operates with a nearly constant F-factor (Fig. 6.11) and (eq. 6.3).

$$F - Faktor = u_G \sqrt{\rho_G} \qquad \text{(eq. 6.3)}$$

Inverted batch. In the inverted case the product is withdrawn from the bottom because the feed tank is at the top of the column. This means that the bottom concentration has to be set to constant. As in the regular case two different control structures are possible. First, the control with a variation of the outlet stream, which means a decrease of outlet stream during the

operation. Second, which is also the more feasible solution, is the control of the bottom concentration with help of the heat duty. The process ends when the given azeotropic distillate concentration set point is reached.

In this work, the bottom concentration control with help of the heat duty is used. This is more practical because the reboiler level can be set to constant (Fig. 6.11). This control structure is similar to the regular case which is also the reason in the regular case to do so, because in the regular case the reflux stream is used. This is also a back stream into the system as well as the vapor stream which changes, if the heat duty is changed. In table 6.7 an overview of both control concepts are given.

Table 6.7. Control concepts for the discontinuous process.

controller	**regular batch**		**inverted batch**	
	control variable	**manipulated variable**	**control variable**	**manipulated variable**
bottom level	1) level (reb., if external feed tank) 2) feed tank = reboiler	1) flow rate 2) no controller	level	flow rate
bottom product concentration	abort criterion		concentration	heat duty
top product concentration	concentration	reflux	abort criterion	
pressure	pressure	cooling water	pressure	cooling water stream
distillate drum level	level	distillate outlet stream	no controller	

6.2 Analysis of the start-up processes

In this chapter the start-up processes for the discontinuous operation will be analyzed. In the first section a motivation for the analysis of the start-up of the batch distillation processes is given and in the second section the start-up schedules and the controller switching for the different process designs are given.

6.2.1 Start-up of the batch processes

Why is the start-up simulation of the batch processes necessary? To motivate the start-up modeling and answer this question an example is given. The start-up time between the regular and the inverted batch differs very much (Fig. 6.12).

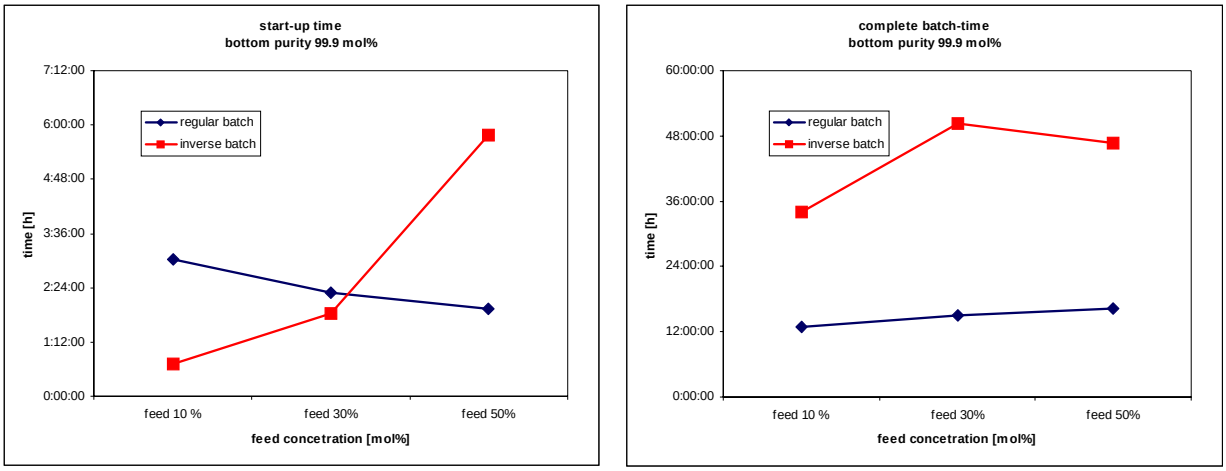

Fig. 6.12 Comparison of start-up time and batch time for the inverted and the regular process. (Calculation is done with the dynamic model described in chapter 3.2).

As shown in the Fig. 6.12 left, the start-up time for the inverted batch is faster for small feed start concentrations and higher for high feed start concentrations, but for the overall batch time (Fig. 6.12 right), the inverted batch process is always slower than the regular one. In conclusion, to get consistent initial conditions, comparable setups and reliable results in the simulations study, the including of start-up simulation from cold and empty is necessary.

6.2.2 Start-up schedule and controller switching

The start-up of the single batch column basis on the equation switches described in general in the modeling chapter (chapter 3.3). To describe the whole process start-up well, there is also a need in changing the controller states. In the inverted case the following controllers (table 6.8) are used and the following state changes of these controllers are implemented (table 6.9) using the threshold/trigger concept included in the controller model (chapter 3.3). The pairing of the control and manipulated variables are listed in table 6.8, including the stop criterion for the inverted batch process. The schedule is given in table 6.9.

Table 6.8. Controller with manipulated and control variable (inverted column).

controller	manipulated variable	control variable
top concentration controller	feed stream (inverted) is fixed	- (abort criterion is distillate concentration)
bottom concentration controller	reboiler heat duty	bottom concentration
bottom level controller	valve	level

Table 6.9. Dynamic start-up model: states of the controller (inverted column).

step	action	controller	state	trigger	threshold
0	cold and empty		all controller *inactive*	-	-
1	feed in	top concentration controller	*manual*	-	-
2	filling of the column	bottom concentration controller	*inactive* (0)	reboiler level	> 65% *manual (30%)*
3	bottom concentration	bottom concentration controller	*manual (30%)*	bottom concentration	> set point *automatic*
4	product stream	bottom level controller	*manual (0)*	bottom concentration	> set point *automatic*

In the regular case the following controllers are used and the following controller state changes are implemented. The pairing is listed in table 6.10 and the schedule in table 6.11.

Table 6.10. Controller with manipulated and control variable (regular column).

controller	manipulated variable	control variable
top concentration controller	reflux	top concentration
bottom concentration controller	reboiler heat duty is fixed	- (abort criterion is bottom concentration)
distillate drum level controller	distillate stream	level

Table 6.11. Dynamic start-up model: states of the controller (regular column).

step	action	controller	state	trigger	threshold
0	cold and empty		all controller *inactive*	-	-
2	filling of the column	bottom concentration controller	*manual* (30%)	-	-
3	filling of the drum	distillate drum level controller	*inactive*	level	> set point *direct channel*

Table 6.11. Dynamic start-up model: states of the controller (regular column).

step	action	controller	state	trigger	threshold
4	distillate stream	distillate drum level controller	*direct channel*	distillate concentration	> set point *automatic*
5	top concentration	top concentration controller	*inactive*	distillate concentration	> set point *automatic*

After the last step the start-up operation has finished, and the batch is running until the end.

6.3 Evaluation and comparison of the batch processes

The comparison and evaluation of batch processes is subdivided into two parts. The first part is the comparison of the batch structures concerning the analytical method described in chapter 3.1 and the second part compares different batch structures (see chapter 6.1.1) concerning batch time and energy consumption on the basis of the rigorous dynamic model (see chapter 3.2).

6.3.1 Analytical method: Comparison and evaluation of different batch processes

With help from the analytical approach introduced in chapter 3.1 for the calculation of the minimal energy demand of a simplified regular and inverted batch process, the performance will be evaluated. The study starts with a comparison of both processes for a theoretical zeotropic mixture. After that azeotropic mixture will be analyzed and the influence of the simplifications of the separation factor on the results will be explained. In the end the results will be validated against the rigorous dynamic model. For this validation the equivolumetric structures will be used (chapter 6.1.1.4). The following simplifications will be used in the analytical model:

- Steady state (without start-up).
- Infinite number of stages and therefore a minimal energy demand.
- A minimal reflux ratio / reboil ratio.
- Different separation factor equations approximating the equilibrium curve.

6.3.1.1 Zeotropic mixtures

The analytic approach is based on the derivation of general mass and component balances for general binary mixtures; so the evaluation of this approach for a zeotropic mixture will be the first step.

A comparison of the product to feed amount ratio for different feed start concentrations for the respective process $\frac{D}{F}$ (regular) and $\frac{B}{F}$ (inverted) shows an intersection of both graphs at 0.5 mol/mol which is a must because there is no difference between the models of both processes except the different products. Left of this intersection the product to feed amount is higher for the inverted case and right from the intersection for the regular case (Fig. 6.13). But this conclusion is only for infinite energy requirements (see chapter 3.1, Fig. 3.3 and´Fig. 3.5), which is interesting only in theory but not for real operation.

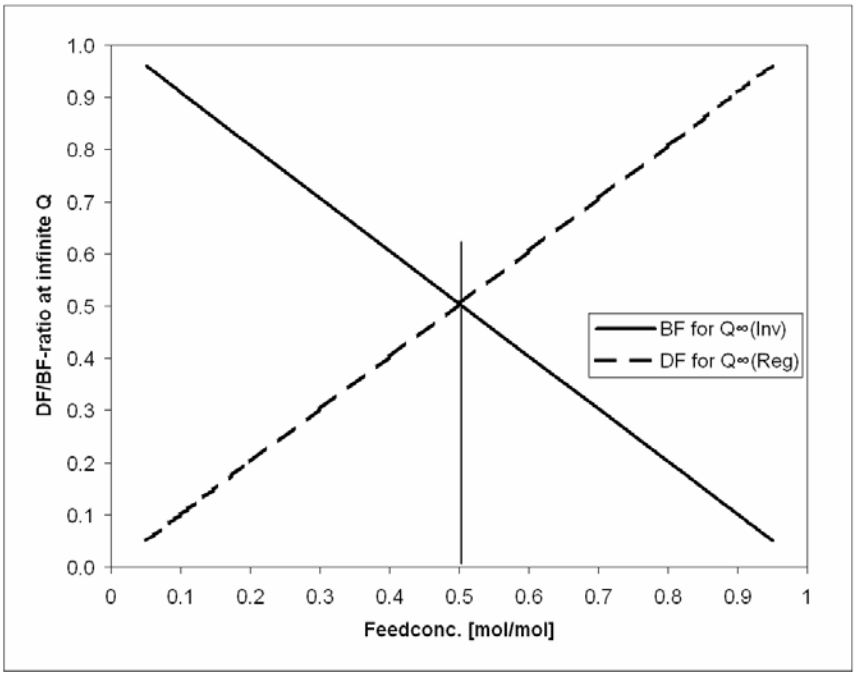

Fig. 6.13 Comparison of the product to feed amount ratio for the regular and the inverted process (zeotropic mixture) for an infinite energy consumption.

To analyzes the energy amount which is necessary for the comparison the $\frac{B}{F}$ and the $\frac{D}{F}$ value for the product purity, set points have to be calculated. In the regular case $\frac{D}{F}$ is calculated with:

$$\left.\frac{D}{F}\right|_{set} = \frac{x_F - x_{B,\,set}}{x_{D,\,set} - x_{B,\,set}} \quad , \qquad \text{(eq. 6.4)}$$

in the inverted case $\frac{B}{F}$ is calculated with:

$$\left.\frac{B}{F}\right|_{set} = \frac{x_F - x_{D,\,set}}{x_{B,\,set} - x_{D,\,set}} \quad . \qquad \text{(eq. 6.5)}$$

With these equations the respective minimal energy $\left.\frac{Q_{min}^{reg}}{r \cdot F}\left(\frac{D}{F}\right)\right|_{set}$ and $\left.\frac{Q_{min}^{inv}}{r \cdot F}\left(\frac{B}{F}\right)\right|_{set}$ for the respective product purity can be calculated for each feed concentrations. The results are shown in the next Fig. 6.14. The y-axis shows the energy demands in respect to the ratio (D/F for regular and B/F for inverted) for a more realistic comparison. The top product purity is set to 0.99 mol/mol and the bottom product purity to 0.01 mol/mol. The separation factor is constant by 1.3.

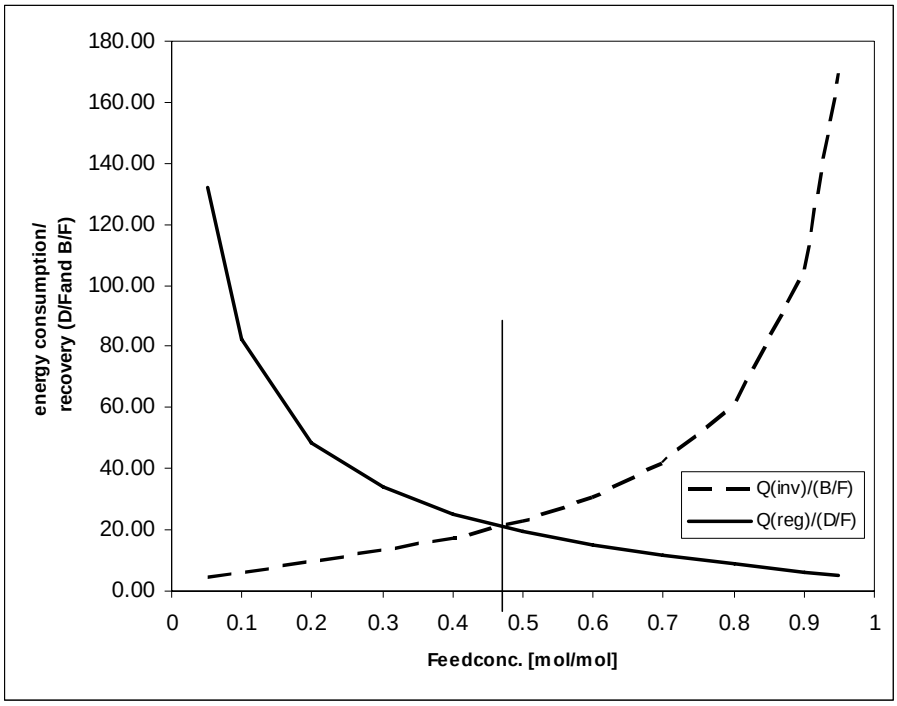

Fig. 6.14 Comparison of the energy consumption related to the product amount for the regular and the inverted process (zeotropic mixture).

Now the graphs cross at a feed concentration of 0,47 mol/mol. The regular batch is for a wider range of feed concentrations attractive. Hasebe et al. explained that the difference between regular and inverted batch with the fact, that the equilibrium curve (x,y - diagram) is not symmetrical around the vertical line at x = 0,5, for a constant separation factor [Hasebe et al. 1992]. But Sørensen and Skogestad explained this phenomenon with the fact, that the regular batch is only compared to the inverted and not to the real inverted batch, were the feed flow rate and the feed tank has to be in vapor phase [see Sørensen & Skogestad 1996]. In the inverted case a little bit more energy for the evaporation of the mixture has to be used than in the respective regular case. Both explanations justifies the deviation of the cross section and the symmetric line.

6.3.1.2 Azeotropic mixtures

The zeotropic results can easily be transferred to the azeotropic example. The azeotropic point is set to 0.7 mol/mol. The zeotropic results will be changed to the azeotropic case at ambient pressure with a coordinate transformation:

$$x_{new,\,az} = x_{old,\,zeo} \cdot x_{az}\,. \qquad \text{(eq. 6.6)}$$

(Fig. 6.15 shows the results). The separation factor of $\alpha = 1{,}3$ corresponds to the average separation factor of the mixture acetonitrile - water at atmospheric pressure. The intersection is left from the middle of the diagram as expected.

But a constant separation factor $\alpha = 1{,}3$ is not a good approximation for real mixtures as the following results will show. To consider the influence of the separation factor, the α-function is approximated with a linear and an optimal the equilibrium curve (Wilson-model) [Gmehling et al. 1981] fitting function. The respective α-function depends on the concentration which is changing in the process ($\alpha(x_B)$ regular and $\alpha(x_D)$ inverted).

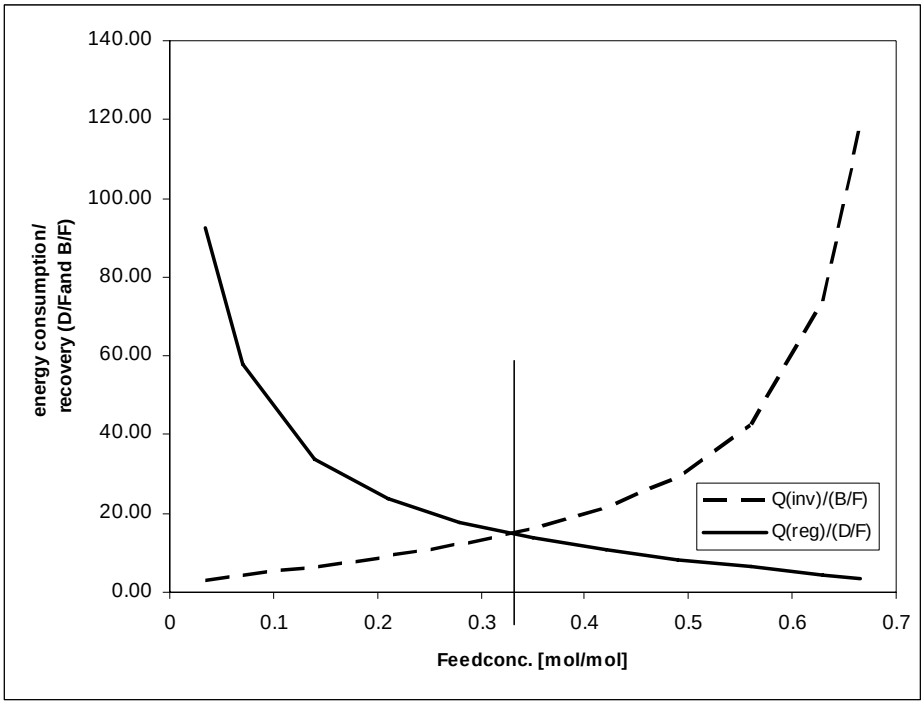

Fig. 6.15 Comparison of the product to feed amount ratio for the regular and the inverted process for the azeotropic mixture acetonitrile - water.

In the linear case the separation factor is approximated between $x = 0$ and $x = x_{az}^{LP}$ for atmospheric pressure with:

$$\alpha_{reg;linear} = -5{,}821 \cdot x_B + 5 \text{ and} \qquad \text{(eq. 6.7)}$$

$$\alpha_{inv;linear} = -5{,}821 \cdot x_D + 5\,. \qquad \text{(eq. 6.8)}$$

In the optimal case (fitting the curve best) the separation factor is approximated with:

$$\alpha_{reg;optimal} = \frac{1}{0{,}0488 - 0{,}3750 \cdot x_B + 1{,}2699 \cdot x_B^2} \text{ and} \qquad \text{(eq. 6.9)}$$

$$\alpha_{inv;optimal} = \frac{1}{0{,}0488 - 0{,}3750 \cdot x_D + 1{,}2699 \cdot x_D^2}\,. \qquad \text{(eq. 6.10)}$$

Optimal approximation means a function which has the same characteristics as the equilibrium curve calculated with the Wilson-approach. For the approximation the equilibrium data are used and approximated with help of the program *curve expert 1.3* [CurveExp 2005].

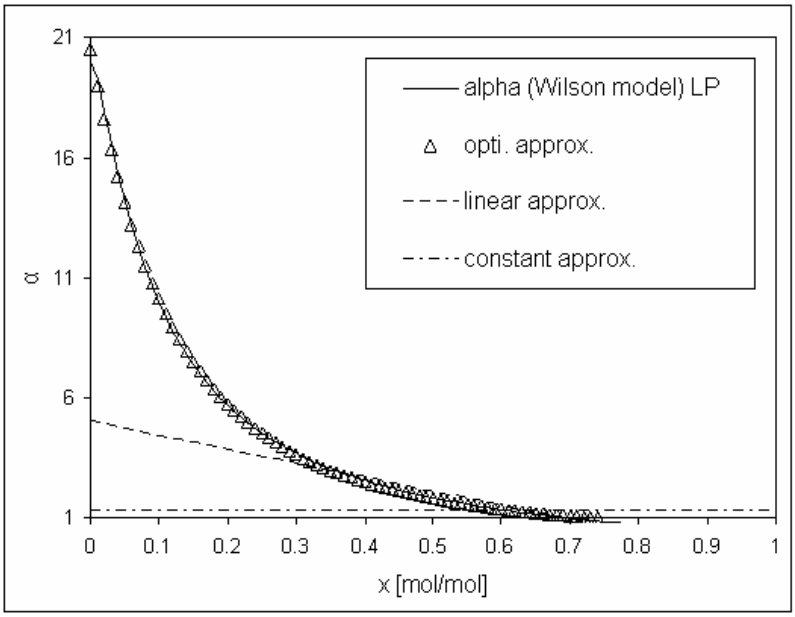

Fig. 6.16 Comparison of different approximations of the equilibrium function for acetonitrile at P = 1,015 bar.

In Fig. 6.16 the comparison of the α-function calculated with the Wilson approach for the mixture acetonitrile - water and the approximations are shown. The approximations are given only for the low pressure case, which means concentrations between x = 0…0,69 (azeotropic point for P = 1,015 bar). A similar approximation can be done for the high-pressure case (Fig. 6.19). The standard deviations for the different approximations are:

- Constant α: 0,330.
- Linear α-function: 0,297.
- Optimal α-function: 0,022.

The results for the comparison of the inverted and the regular batch processes are given in Fig. 6.17. The results are calculated for a bottom product purity of 0,01 mol/mol and a distillate concentration of 0,68 mol/mol with help of the linear and the optimal approximation of the α-function. The Diagrams shows the energy consumption to product yield ratio in respect to the feed concentration (acetonitrile) for the LP case. The intersection of the graphs move with a better approximation of α to smaller feed concentrations, that means a smaller more energy efficient region for the inverted process and a wider range for the regular process.

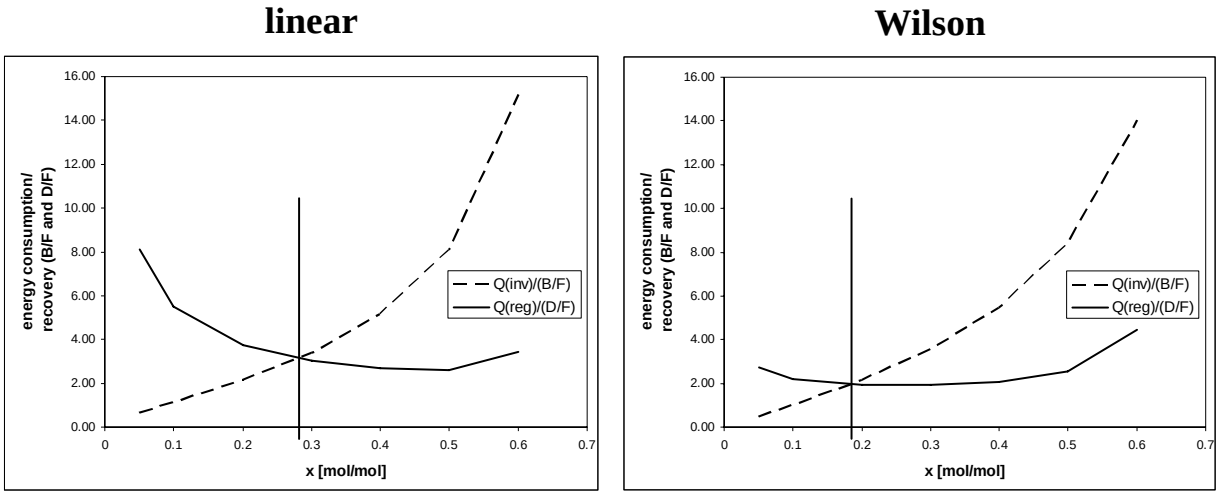

Fig. 6.17 Comparison of regular and inverted batch process (LP) for product concentrations of $x_{D_e} = 0{,}68$ and $x_{B_e} = 0{,}01$ (azeotropic case; left: linear α-function; right: optimal α-function); feed concentration scale for acetonitrile.

For the high pressure case here are the following diagrams (Fig. 6.19).

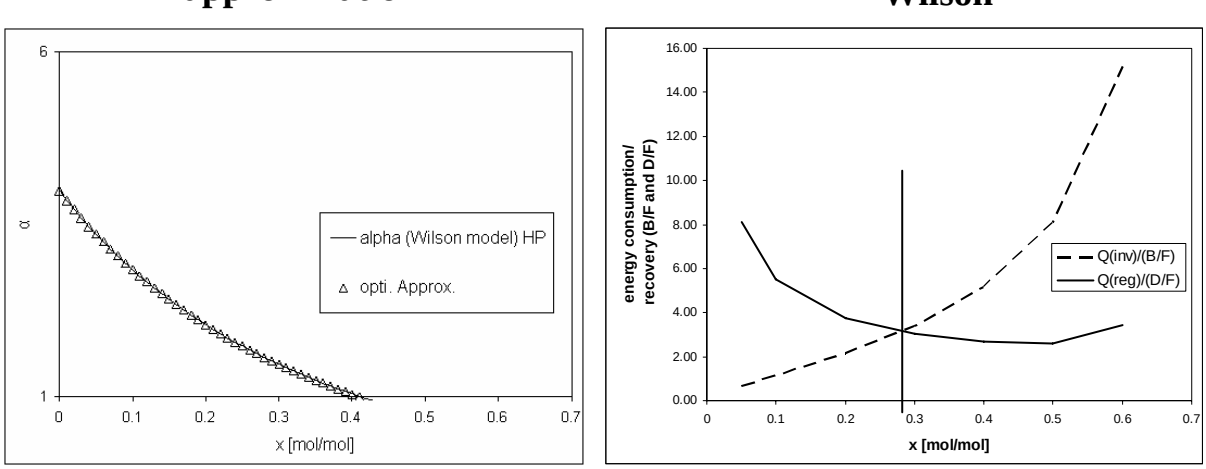

Fig. 6.19 Comparison of regular and inverted batch process (HP) for product concentrations of $x_{D_e} = 0{,}41$ and $x_{B_e} = 0{,}01$ (azeotropic case; left: approximations of the equilibrium function for acetonitrile at P = 3,5 bar. right: optimal α-function and equilibrium); feed concentration scale for water.

The Diagrams show the optimal approximation of the HP equilibrium data curve for feed concentrations above the azeotropic point from the view point of acetonitrile, which results in a concentration range of water from 0...0,4 mol/mol. The Equilibrium curve is approximate with the following optimal α-function:

$$\alpha_{reg;optimal} = \frac{-0{,}133 + 1{,}06 \cdot x_B}{1 - 0{,}99 \cdot x_B + 0{,}2235 \cdot x_B^2} \text{ and with} \qquad \text{(eq. 6.11)}$$

$$\alpha_{inv;optimal} = \frac{-0{,}133 + 1{,}06 \cdot x_D}{1 - 0{,}99 \cdot x_D + 0{,}2235 \cdot x_D^2}, \text{ with a standard deviation of 0,001.} \quad \text{(eq. 6.12)}$$

A combination of the low-pressure (Fig. 6.17) and the high pressure (Fig. 6.19) results leads to a decision table for the pressure swing process depending on the feed start concentration and the product purity for the lowest energy consumption (table 6.12).

Table 6.12. optimal combination of inverted and/or regular batch process depending on the feed start concentration and the product purity.

product purity	**feed** $< x_{az}^{LP}$		**feed** $> x_{az}^{HP}$	
	1. step (LP; product: water)	**2. step (HP; product: ACN)**	**1. step (HP; product: ACN)**	**2. step (LP; product: water)**
96 mol%	$x_F^{LP} < 0{,}21$ Inv. $x_F^{LP} > 0{,}21$ Reg.	regular batch	$x_F^{HP} > 0{,}78$ Inv. $x_F^{HP} < 0{,}78$ Reg.	regular batch
99 mol%	$x_F^{LP} < 0{,}19$ Inv. $x_F^{LP} > 0{,}19$ Reg.	regular batch	$x_F^{HP} > 0{,}8$ Inv. $x_F^{HP} < 0{,}8$ Reg.	regular batch
99.9 mol%	$x_F^{LP} < 0{,}2$ Inv. $x_F^{LP} > 0{,}2$ Reg.	regular batch	$x_F^{HP} > 0{,}78$ Inv. $x_F^{HP} < 0{,}78$ Reg.	regular batch
99.99 mol%	$x_F^{LP} < 0{,}23$ Inv. $x_F^{LP} > 0{,}23$ Reg.	regular batch	$x_F^{HP} > 0{,}76$ Inv. $x_F^{HP} < 0{,}76$ Reg.	regular batch

Because the start concentration is very near to the azeotropic point in the second step, the regular batch is always the better process. With help from the analytical method, it is possible to find a combination with the smallest energy demand for a given mixture.

6.3.1.3 Validation of the results

The analytical approach has to be validated. For this the rigorous dynamic model is used with the following boundary conditions for the simulation:

- Constant F-factor of 1 $\sqrt{\text{Pa}}$.
- Feed flow rate value is set equal to the feed tank volume value („equivolumetric“: 50 l/h feed flow rate and 50 l feed tank start volume).
- Variation of the product purities (x_B^{Wa} = 0,04... 0,0001) and the feed. concentrations (x_F^{ACN} = 0,1; 0,3; 0,5).
- P = 1,015 bar.

- Azeotropic point at $x_{D,\,az}^{ACN} = 0{,}6914$, distillate purity: $x_{D}^{ACN} = 0{,}67$.
- Equilibrium data calculated with Wilson approach [Gmehling 1981].

In the simulation the equivolumetric processes (chapter 6.1.1.4) will be used.

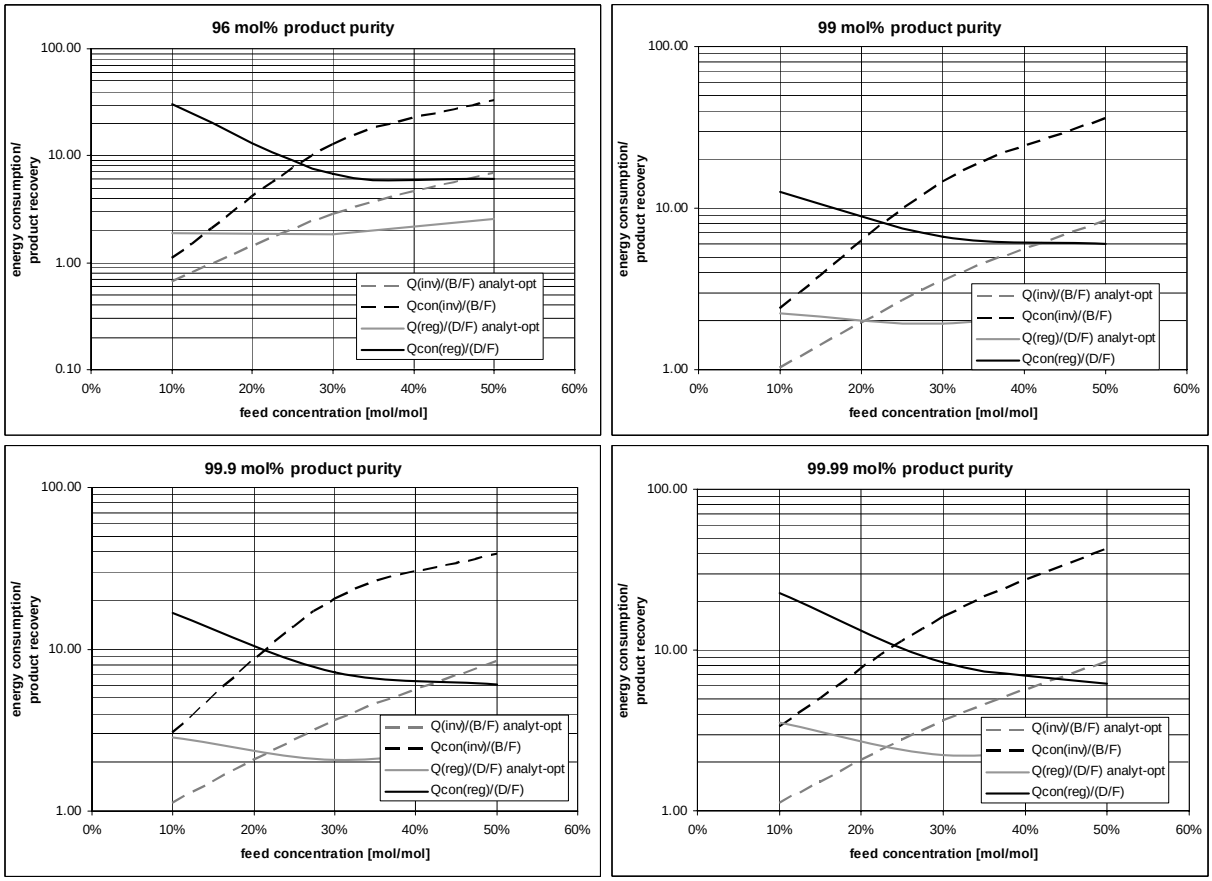

Fig. 6.20 Comparison of the analytical method with the simulation (LP), feed concentration (acetonitrile), for different product purities.

The diagrams (Fig. 6.20) show the comparison of the results of the analytical method with the simulation results for different product purities. The energy demand in the simulation is calculated with the heat duty of the reboiler reduced less the start-up energy which is used to heat up the mixture from ambient temperature to boiling temperature because the simulation includes the start-up and the analytical method do not.

As the diagrams show, the intersection point of the analytical solution is in the same range of the simulation but there is a big gap between the energy demands. To calculate the quantitative energy demands in advance the analytical method cannot be used. In case of replacing the regular batch with an inverted batch, which will be the most interesting question, the analytical method is a suitable approach.

The reason for the difference in the energy demands can be explained with the calculation on a molar basis with infinite number of trays in the analytical case. In the simulation the calculation

is done with realistic volumetric flow rates, which means no constant molar flow rate in the dynamic simulation and a limited number of trays (28).

6.3.2 Simulations study: Comparison and evaluation of different batch processes

After the discussion of the analytical method for an equivolumetric regular and inverted process we will discuss both processes with help of the rigorous dynamic model (chapter 3) for the following different structures (Condition of all simulations see table 6.13):

- Regular batch structures:
  - *RB:* regular batch with additional feed tanks at the reboiler (setup of the pilot plant).
  - *RB-bB*: regular batch with a big reboiler tank, without an additional tank at the bottom.
  - *RB-bB4x:* structure as RB-bB with quad capacity. Is used for the comparison with the inverted structures with a larger feed stream on top of the column see later on), quad column cross area.
- Inverted batch structures:
  - *NIB:* normal inverted batch, with one feed tank at the top.
  - *AIB:* advanced inverted batch, with two feed tanks at the top, one for the feed and one to dump the distillate. If the feed tank is empty the distillate is drained to the feed tank and the process is going on.
  - *NIB4x and AIB4x:* structures as above, but with quad feed volume stream and quad column cross area.

Table 6.13. Simulation conditions.

	NIB, AIB, RB-bB, RB	**NIB4x, AIB4x, RB-bB4x**
F-factor	1 $\sqrt{\text{Pa}}$	1 $\sqrt{\text{Pa}}$
feed volumetric stream (external tank)	50 l/h	200 l/h
column type	28 bubble cap trays	
diameter	114 mm	214 mm
pressure	constant LP: 1 bar; HP: 3,5 bar	
feed volume	600 l	600 l
feed start concentration x_F	variable (10, 30, 50, 70, 80, 90 mol%)	
top distillate concentration	68 mol% (LP) and 58 mol% (HP): - regular batch: controlled reflux - inverted batch: stop condition	
azeotropic point	LP: 69,3 mol%; HP: 57,3 mol%	
bottom concentration	96 - 99,99 mol% (LP: water; HP: acetonitrile): - regular batch: stop condition - inverted batch: controlled	
product withdraw	if the desired purity is reached (Top product withdraw in the regular case and bottom product with draw in the inverted case)	

Due to a better clarity the results for only the highest and lowest product purity will be presented. For the complete results see the appendix (chapter A.5) with all diagrams and tables for all considered cases. All diagrams are for acetonitrile (feed concentration). The top distillate concentrations are set to 1,9% of the respective azeotropic point to get comparable conditions for the LP as well as for the HP cases.

6.3.2.1 Simulations at low pressure (LP)

The comparison will be first done for the LP side which means under atmospheric pressure.

Comparison of NIB and RB. The comparison of the normal inverted batch (NIB) and the regular batch with additional tank (RB) are displayed for the batch time in Fig. 6.21 and Fig. 6.22. It starts with this comparison because the regular batch with additional tank (RB) is in the context of the plant structure directly comparable to the inverted batch because each structure has an additional tank and therefore related back mixing.

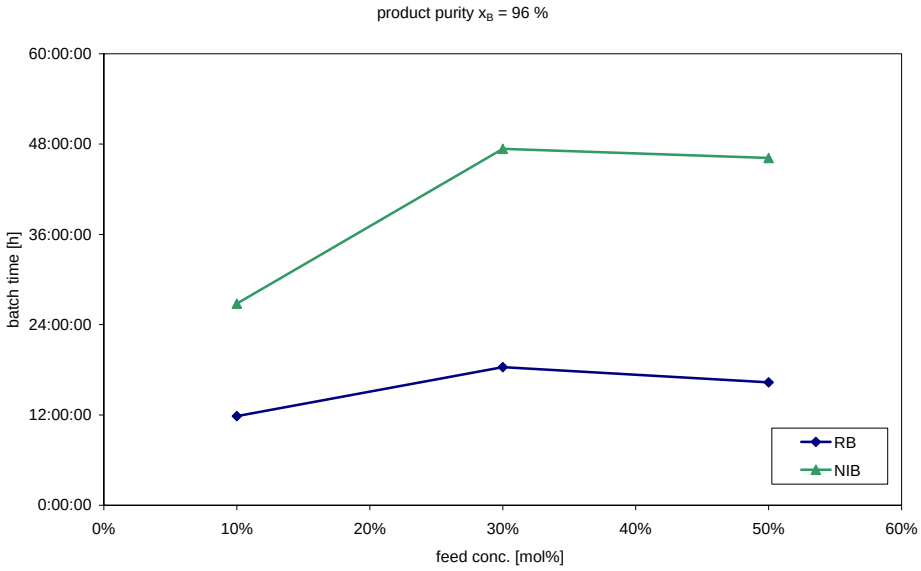

Fig. 6.21 Comparison of the normal inverted batch (NIB) with the regular batch with additional bottom tank (RB) concerning the batch time, for a product purity of 96 mol% water at ambient pressure.

In the study the feed start concentration varies (10 mol%, 30 mol% and 50 mol%) inside the LP-distillation region. In both cases the feed input stream is 50 l/h.

For low-product purities, the regular batch is always faster than the inverted batch. For high product purities there is an intersection between the graphs at a feed concentration of 28 mol%. Left from this intersection the inverted batch is faster and right from the intersection the regular batch.

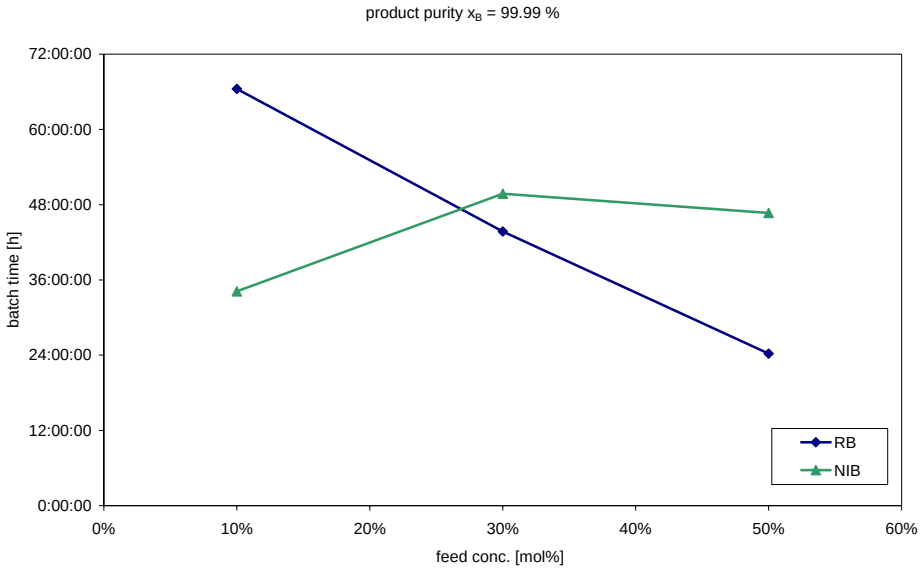

Fig. 6.22 Comparison of the normal inverted batch (NIB) with the regular batch with additional bottom tank (RB) concerning the batch time, for a product purity of 99,99 mol% water at ambient pressure.

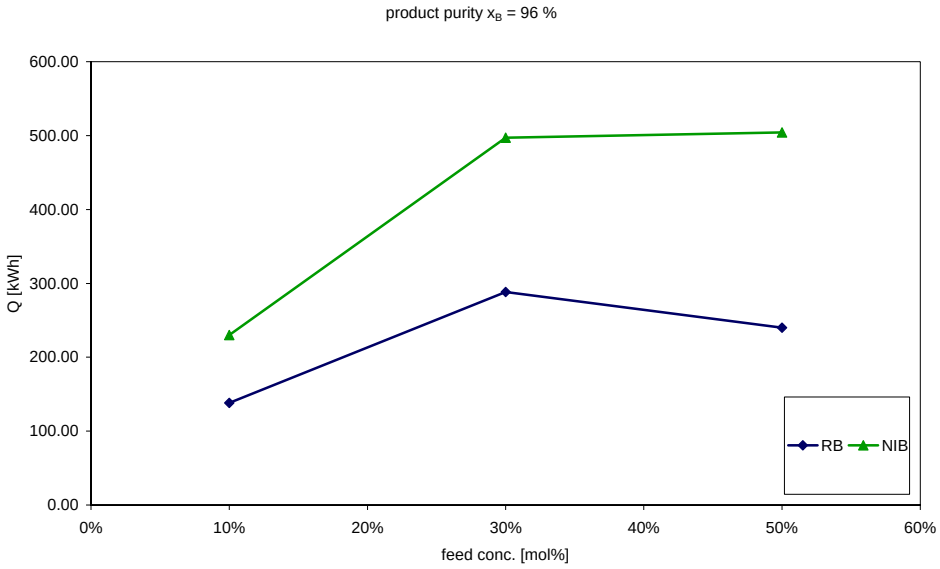

Fig. 6.23 Comparison of the normal inverted batch (NIB) with the regular batch with additional bottom tank (RB) concerning the energy consumption, for a product purity of 96 mol% water at ambient pressure.

The next figures show the energy demands of both processes for high and low product purity (Fig. 6.23 and Fig. 6.24). Like the batch time, the regular batch is always faster than the inverted batch for low-product purities and there is an intersection for high purities. The intersection is located at 40 mol% feed start concentration. Compared to the batch time the intersection is

shifted to higher feed concentrations, this means a bigger range of less energy consumption of the inverted batch compared to the regular batch concerning the energy consumption.

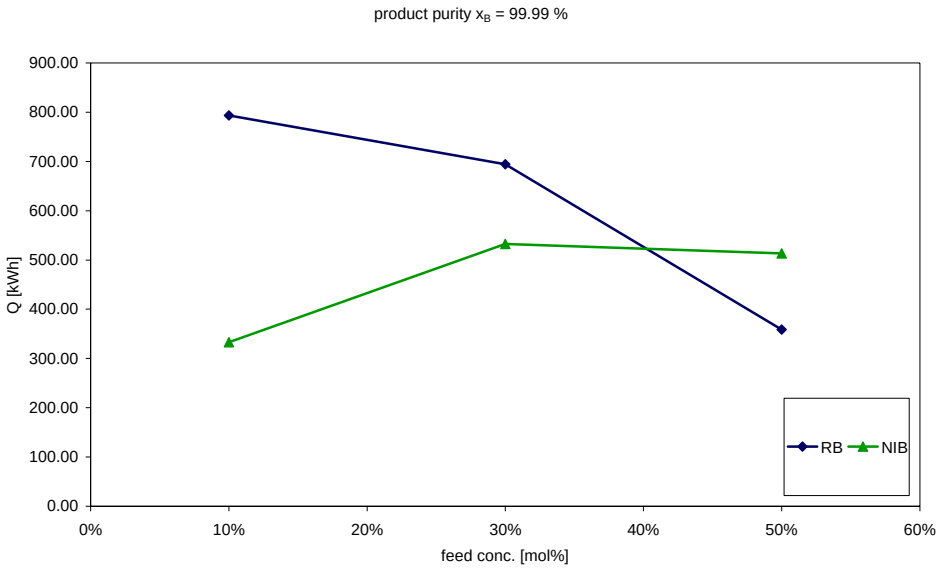

Fig. 6.24 Comparison of the normal inverted batch (NIB) with the regular batch with additional bottom tank (RB) concerning the energy consumption, for a product purity of 99,99 mol% water at ambient pressure.

If we look at the high pressure process the results are a little bit different than the low-pressure case concerning the batch time and the energy consumption. For low product purities the regular batch is always faster than the inverted batch but for high product purities the inverted batch is always better than the regular batch. For the energy consumption there is already an intersection for low product purities at 72 mol% acetonitrile. So for feed start concentration bigger than 72 mol% the inverted batch is better. Also concerning the energy consumption the inverted batch is always the best for high product purities compared to the regular process RB (see Fig. A.5 to Fig. A.8, Fig. A.13 to Fig. A.16). The remarkable difference between the high pressure and the low pressure case will be discussed later (chapter 6.3.2.4).

Comparison of RB, RB-bB, NIB and AIB. If the comparison of the NIB and the RB is expanded with the regular batch with a big reboiler at the bottom (RB-bB) and the new developed advanced inverted batch (AIB) we get the following diagrams concerning the batch time Fig. 6.25 and Fig. 6.26 for low and high product purities at ambient pressure.

The figures show that for low and high product purities always the RB-bB process will be the fastest. The AIB process will always be faster than the NIB process. If the AIB is compared with the RB, we see that for low product purities the AIB is slower than the RB but the gap is much smaller than for the NIB/RB comparison. For high product purities the intersection between the AIB/RB curves is at higher feed concentrations (38 mol%).

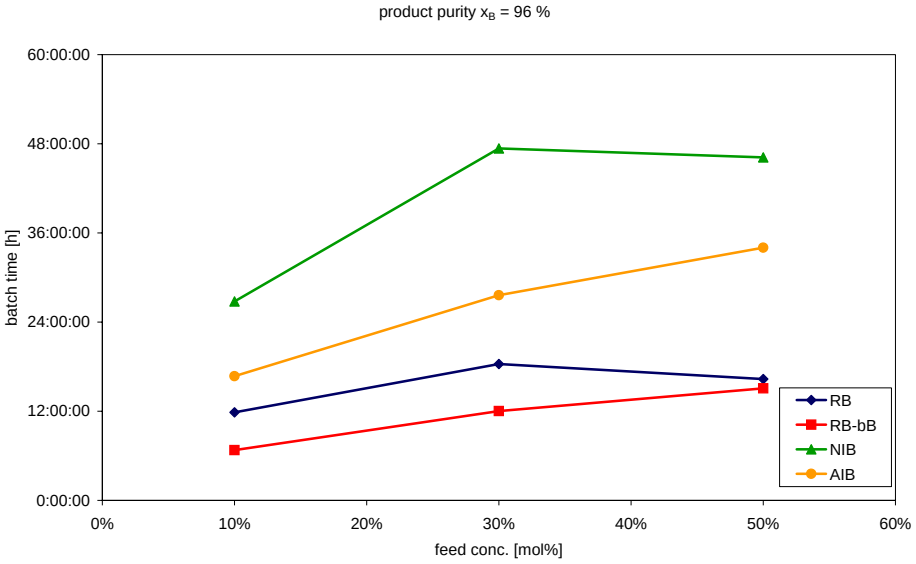

Fig. 6.25 Comparison concerning the batch time for different structures (RB, RB-bB, NIB, AIB): ambient pressure, product purity 96 mol% water, feed conc. 10 mol%, 30 mol%, 50 mol% ACN.

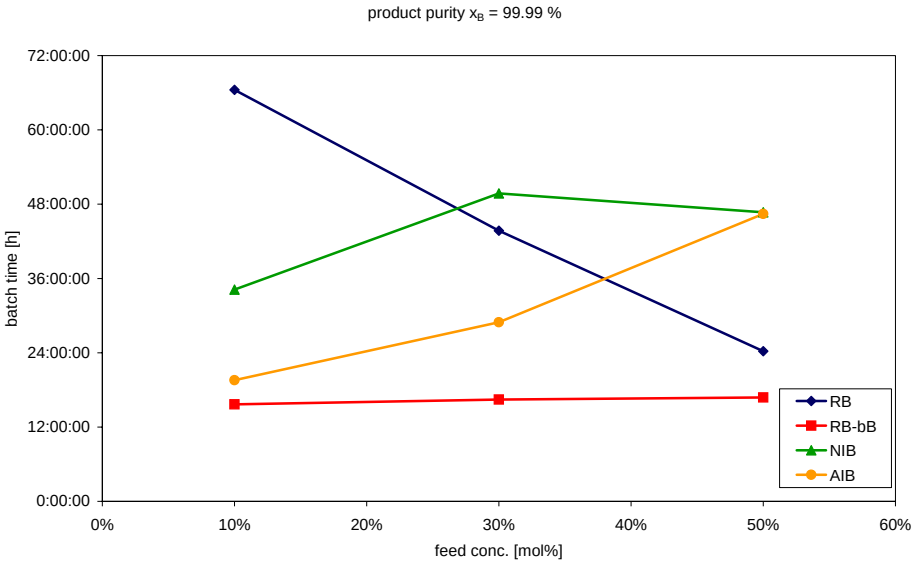

Fig. 6.26 Comparison concerning the batch time for different structures (RB, RB-bB, NIB, AIB): ambient pressure, product purity 99,99 mol% water, feed conc. 10 mol%, 30 mol%, 50 mol% ACN.

An overview about all results can be found in table 6.14.

Table 6.14. Overview - batch structures (LP) - batch time.

batch time	Comparison: RB, RB-bB, AIB, NIB	Comparison: RB, NIB, AIB	Comparison: RB, NIB
96 mol%	RB-bB	RB	RB
99 mol%	RB-bB	> 22 mol%: RB < 22 mol%: AIB	RB
99,9 mol%	RB-bB	> 33 mol%: RB < 33 mol%: AIB	> 19 mol%: RB < 19 mol%: NIB
99,99 mol%	RB-bB	> 38 mol%: RB < 38 mol%: AIB	> 27 mol%: RB < 27 mol%: NIB

For the comparison concerning the energy consumption the results differ. The RB-bB is also always the best process for low product purities. For high product purities there is an intersection between the RB-bB and the AIB at 11 mol%. Comparing the AIB with the RB there is an intersection for low product purities at 30 mol%. But both process are nearly equal concerning the energy consumption for feed concentration lower than 30 mol%.

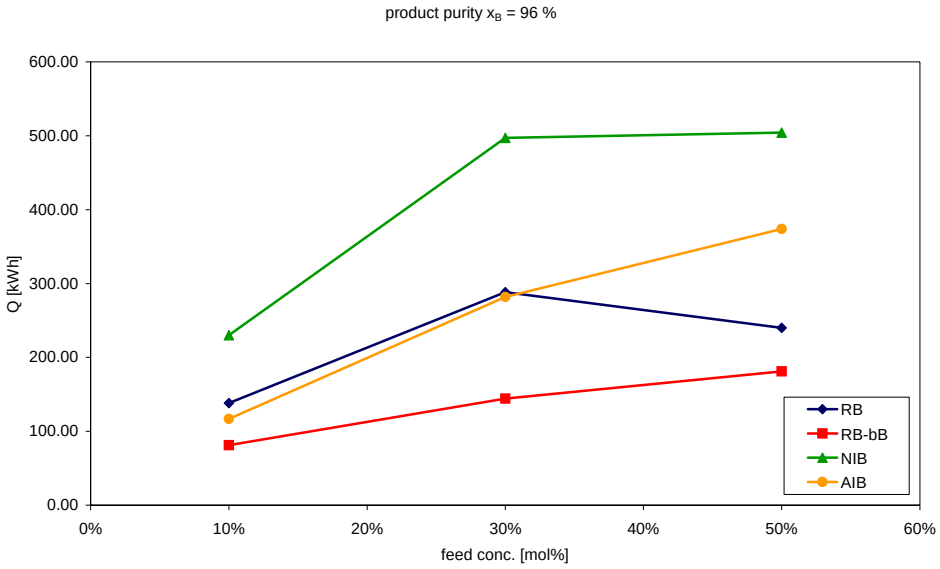

Fig. 6.27 Comparison concerning the energy consumption for different structures (RB, RB-bB, NIB, AIB): ambient pressure, product purity 96 mol% water, feed conc. 10 mol%, 30 mol%, 50 mol% ACN.

The intersection between AIB and RB for the high product purities are at higher feed concentrations than for the batch time. An overview about all results can be found in table 6.15.

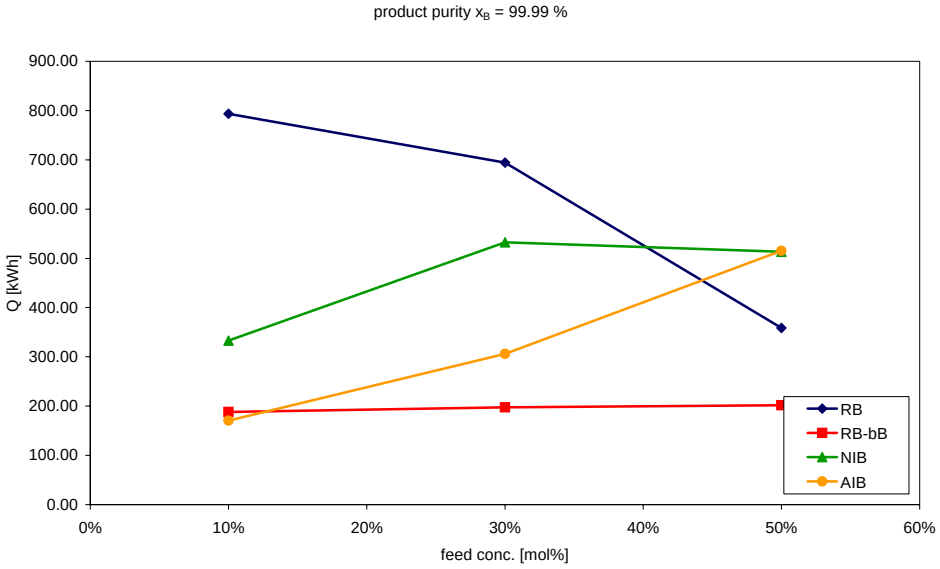

Fig. 6.28 Comparison concerning the energy consumption for different structures (RB, RB-bB, NIB, AIB): ambient pressure, product purity 99,99 mol% water, feed conc. 10 mol%, 30 mol%, 50 mol% ACN.

Table 6.15. Overview - batch structures (LP) - energy consumption.

energy consumption	**comparison: RB, RB-bB, AIB, NIB**	**comparison: RB, NIB, AIB**	**comparison: RB, NIB**
96 mol%	RB-bB	> 30 mol%: RB < 30 mol%: AIB	RB
99 mol%	RB-bB	> 38 mol%: RB < 38 mol%: AIB	RB
99,9 mol%	RB-bB	> 40 mol%: RB < 40 mol%: AIB	> 30 mol%: RB < 30 mol%: NIB
99,99 mol%	> 12 mol%: RB-bB < 12 mol%: AIB	> 45 mol%: RB < 45 mol%: AIB	> 40 mol%: RB < 40 mol%: NIB

Summarizing the ambient pressure case, it can be noticed that the AIB is always the better solution compared to the NIB because of a shorter batch time and a less energy consumption. If there is only the RB process because of properties of the mixture or design reasons in most cases the inverted batch will be a good alternative to the regular one, except for feed concentration near the azeotropic point and very low product purities.

Comparison RB-bB4x, NIB4x and AIB4x. The analysis for a quad feed volumetric stream is done for the same F-factor (1 $\sqrt{\text{Pa}}$) as in the study before (Fig. 6.29). This has as a consequence a bigger diameter and a higher reboiler heat duty. The results are better concerning the inverted process, because the different intersections move to higher feed start concentrations.

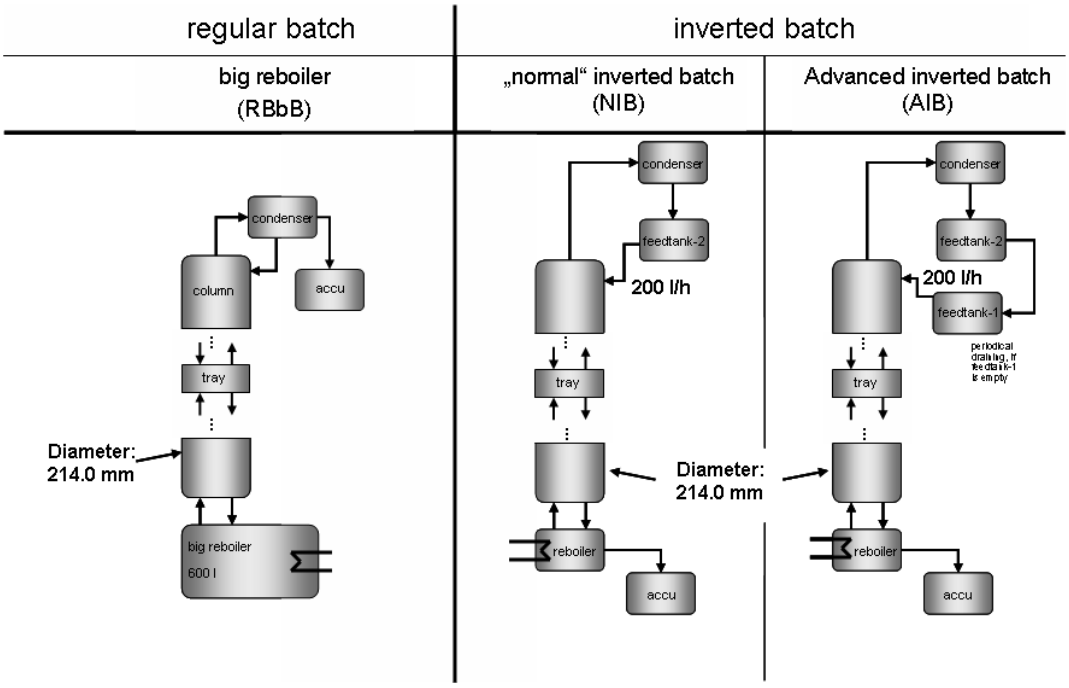

Fig. 6.29 Comparison of RB-bB4x, NIB4x and AIB4x: quad diameter, quad feed flow rate (inverted batch), same f-factor = 1 $\sqrt{\text{Pa}}$.

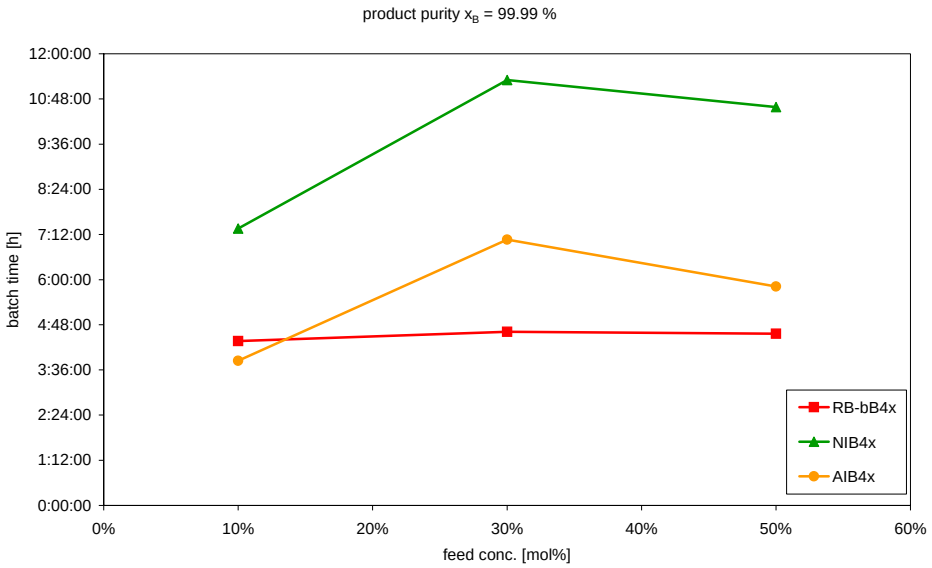

Fig. 6.30 Comparison concerning the batch time for different structures (RB-bB4x, NIB4x, AIB4x): ambient pressure, product purity 99,99 mol% water, feed conc. 10 mol%, 30 mol%, 50 mol% ACN.

Overall the processes are much faster than in the study before, because of the higher throughput. The RB-bB is for low product purities the fastest solution, but not so significant as in the study with smaller diameter. In the case of high product purities the AIB is faster than the RB-bB for feed concentrations lower than 14 mol% (Fig. 6.30).

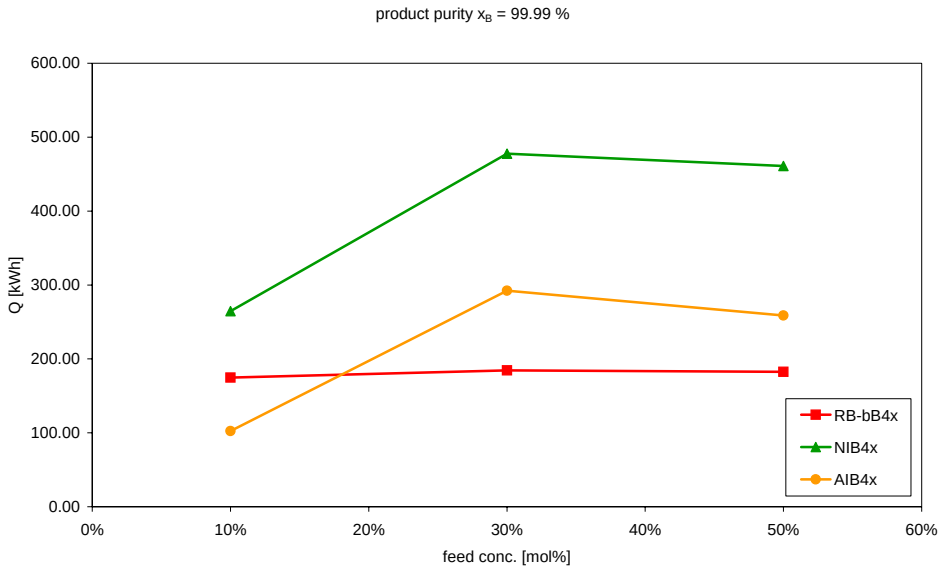

Fig. 6.31 Comparison concerning the energy consumption for different structures (RB-bB4x, NIB4x, AIB4x): ambient pressure, product purity 99,99 mol% water, feed conc. 10 mol%, 30 mol%, 50 mol% ACN.

For the energy consumption, all processes are at a lower level as in the study with smaller diameter, but the energy saving is much bigger than in the regular cases. For lower product purities there is already an intersection of the AIB and the RB-bB as well as for the high product purities (Fig. 6.31). All results can be found in table 6.16 for the batch time study and in table 6.17 for the energy consumption study.

Table 6.16. Overview - batch structures (LP) - batch time (quad throughput).

batch time	**comparison: RB-bB4x, AIB4x, NIB4x**	**comparison: RB-bB4x, NIB4x,**
96 mol%	RB-bB4x	RB-bB4x
99 mol%	RB-bB4x	RB-bB4x
99,9 mol%	RB-bB4x	RB-bB4x
99,99 mol%	> 14 mol%: RB-bB4x < 14 mol%: AIB4x	RB-bB4x

Table 6.17. Overview - batch structures (LP) - energy consumption (quad throughput)

energy consumption	comparison: RB-bB4x, AIB4x, NIB4x	comparison: RB-bB4x, NIB4x,
96 mol%	> 12 mol%: RB-bB4x < 12 mol%: AIB4x	RB-bB4x
99 mol%	> 13 mol%: RB-bB4x < 13 mol%: AIB4x	RB-bB4x
99,9 mol%	> 15 mol%: RB-bB4x < 15 mol%: AIB4x	RB-bB4x
99,99 mol%	> 18 mol%: RB-bB4x < 18 mol%: AIB4x	RB-bB4x

The main conclusion of the study so far is that for an advantageous operation and the right decision of the process design the dimension of the plant is very important. An increasing diameter for a constant F-factor which also leads to a higher flow in the column can save energy and time and also influences the choice which process will be the best solution. The inverted batch is for a wider range of feed concentrations and a bigger column diameter better than the regular batch. In general the ratio of the feed hold up to the feed volume flow rate gives an information of the performance of the inverted batch process. The smaller this ratio is the better is the performance of the inverted batch compared to the regular one. The ratio for the analyzed process are 12 (50 l/h, first study) and 3 (200 l/h, second study).

6.3.2.2 Simulation at high pressure (3,5 bar)

The following is a presentation of the high pressure simulation study results. The possible feed concentrations are between an azeotropic concentration at 3.5 bar of 58 mol% and pure acetonitrile.

Comparison RB, RB-bB, NIB and AIB. In the high-pressure case the RB-bB is not always either the fastest or the process with the less energy consumption. For high product purities the AIB is always the fastest process (Fig. 6.33) and the process with the less energy consumption (Fig. 6.35). Compared to the other process the regular batch process is near the azeotropic point the fastest and best solution, for acetonitrile rich feed the inverted batch (table 6.18 and table 6.19).

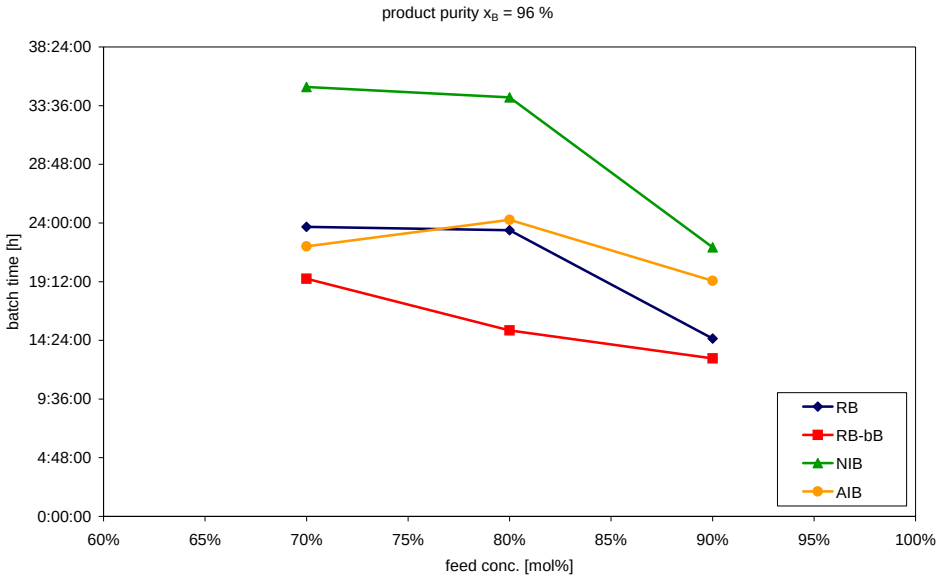

Fig. 6.32 Comparison concerning the batch time for different structures (RB-bB4x, NIB4x, AIB4x): high pressure, product purity 96 mol% water, feed conc. 70 mol%, 80 mol%, 90 mol% ACN.

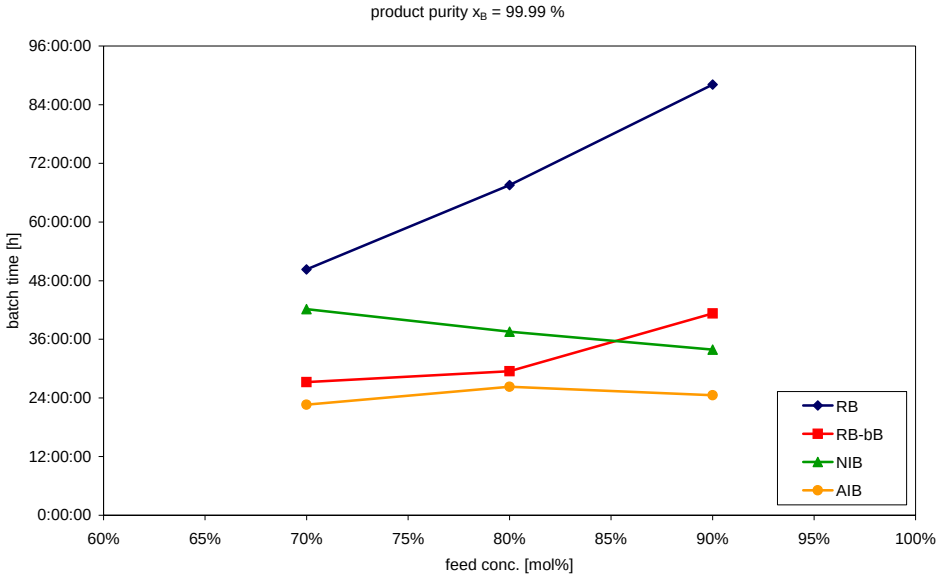

Fig. 6.33 Comparison concerning the batch time for different structures (RB-bB4x, NIB4x, AIB4x): high pressure, product purity 99,99 mol% water, feed conc. 70 mol%, 80 mol%, 90 mol% ACN.

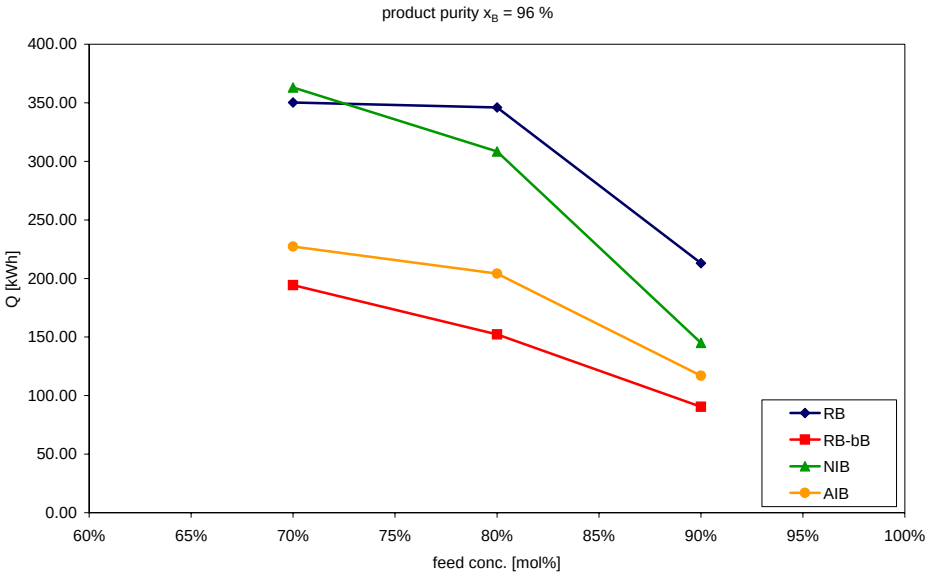

Fig. 6.34 Comparison concerning the energy consumption for different structures (RB-bB4x, NIB4x, AIB4x): high pressure, product purity 96 mol% water, feed conc. 70 mol%, 80 mol%, 90 mol% ACN.

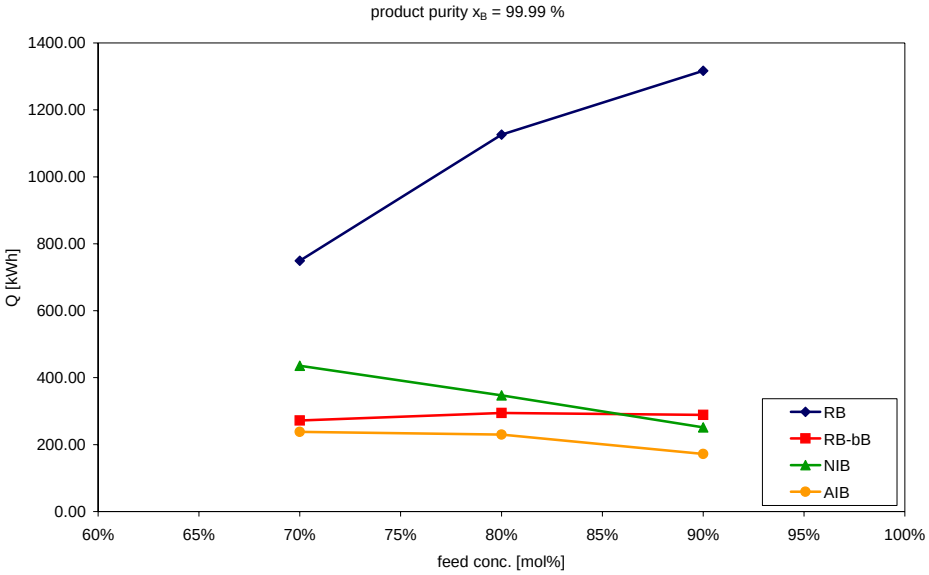

Fig. 6.35 Comparison concerning the energy consumption for different structures (RB-bB4x, NIB4x, AIB4x): high pressure, product purity 99,99 mol% water, feed conc. 70 mol%, 80 mol%, 90 mol% ACN.

Table 6.18. Overview - batch structures (HP) - batch time.

batch time	comparison: RB, RB-bB, AIB, NIB	comparison: RB, NIB, AIB	comparison: RB, NIB
96 mol%	RB-bB	> 76 mol%: RB < 76 mol%: AIB	RB
99 mol%	RB-bB	AIB	> 80 mol%: NIB < 80 mol%: RB
99,9 mol%	AIB	AIB	NIB
99,99 mol%	AIB	AIB	NIB

Table 6.19. Overview - batch structures (HP) - energy consumption.

energy consumption	comparison: RB, RB-bB, AIB, NIB	comparison: RB, NIB, AIB	comparison: RB, NIB
96 mol%	RB-bB	AIB	> 73 mol%: NB < 73 mol%: RB
99 mol%	RB-bB	AIB	NIB
99,9 mol%	AIB	AIB	NIB
99,99 mol%	AIB	AIB	NIB

The RB with its additional tank at the bottom is not a suitable solution for the high pressure case because of the very high energy consumption. As already remarked in the discussion of the NIB/ RB process the difference between the results of the low pressure and the high pressure study will be discussed in the next chapter (chapter 6.3.2.4).

Comparison RB-bB4x, NIB4x and AIB4x. For the high-pressure case with a bigger column diameter and a quad feed throughput the results are similar to the study before with a little better results for the inverted processes. See all results in table 6.20 and table 6.21 (Diagrams see chapter A.5).

Table 6.20. Overview - batch structures (HP) - batch time (quad throughput).

batch time	comparison: RB-bB4x, AIB4x, NIB4x	comparison: RB-bB4x, NIB4x,
96 mol%	RB-bB4x	RB-bB4x
99 mol%	RB-bB4x	RB-bB4x
99,9 mol%	RB-bB4x	RB-bB4x
99,99 mol%	AIB4x	RB-bB4x

Table 6.21. Overview - batch structures (HP) -energy consumption (quad throughput).

energy consumption	comparison: RB-bB4x, AIB4x, NIB4x	comparison: RB-bB4x, NIB4x,
96 mol%	RB-bB4x	RB-bB4x
99 mol%	> 88 mol% AIB4x < 88 mol% RB-bB4x	RB-bB4x
99,9 mol%	> 74 mol% AIB4x < 74 mol% RB-bB4x	> 89 mol% NIB4x < 89 mol% RB-bB4x
99,99 mol%	AIB4x	> 86 mol% NIB4x < 86 mol% RB-bB4x

6.3.2.3 Summary and evaluation of the results

Summarizing the complete study we get the following results. The AIB process is always faster and less energy consuming compared to the NIB process. For high product purities and water rich feed start concentrations mostly the inverted batch structures (NIB and AIB) are faster and less energy consuming than the regular structures (RB-bB and RB). The regular cases are better near the azeotropic points. The RB-bB has in the most cases a better performance than the other structures (NIB, AIB, RB), because the feed is at the start already in the column and does not have to be pumped around which causes a lot of back mixing problems. The RB is the regular structure with a similar behavior than the NIB because the plant design is comparable. Therefore, the disadvantages (back mixing) are also very similar. The reduced back mixing problem is on the other hand the reason for the AIB to be a competitor to the RB-bB where as well the back mixing problem is reduced or is lacking.

6.3.2.4 Differences between the LP and the HP study

If the results of the low-pressure study are compared with the results of the high pressure study there is a remarkable difference between the results concerning especially the intersection between the inverted and the regular batch curves. In the HP study in general the inverted case is better for a bigger range of feed concentrations than in the low pressure study. There are some possible reasons for this. If the separation factors are compared, it is obvious that the separation is more complicated for the high-pressure case than for the low-pressure case, because the α-function is lower (Fig. 6.36). It might be a possible hypothesis that with a decreasing of the separation factor which means with more complex separation problem, the inverted batch process gets the better solution against the regular batch. To validate this another mixture has to be analyzed. To do so the mixture acetone-methanol is chosen. This mixture has also a low boiling azeotropic point, but has a much lower separation factor curve than the mixture acetonitrile-water (Fig. 6.37).

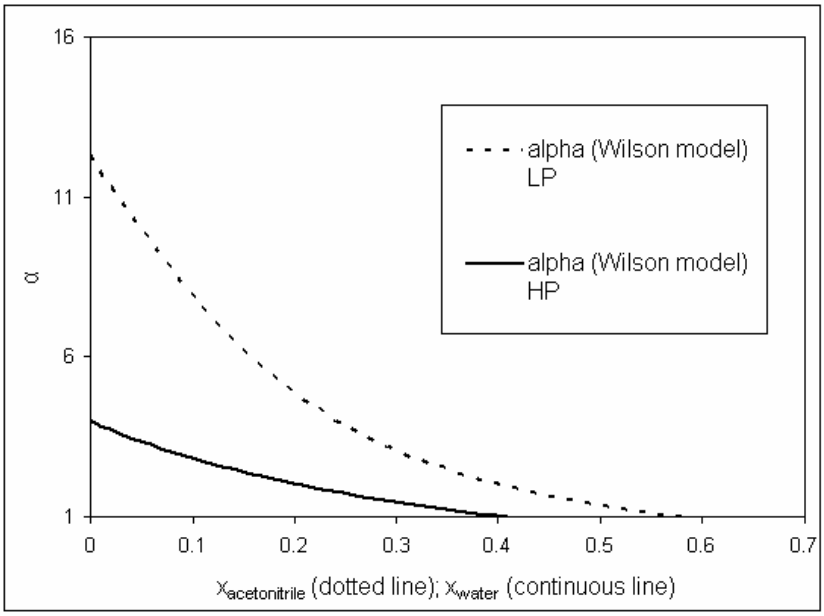

Fig. 6.36 Comparison of the α-functions for LP and HP equilibrium curves.

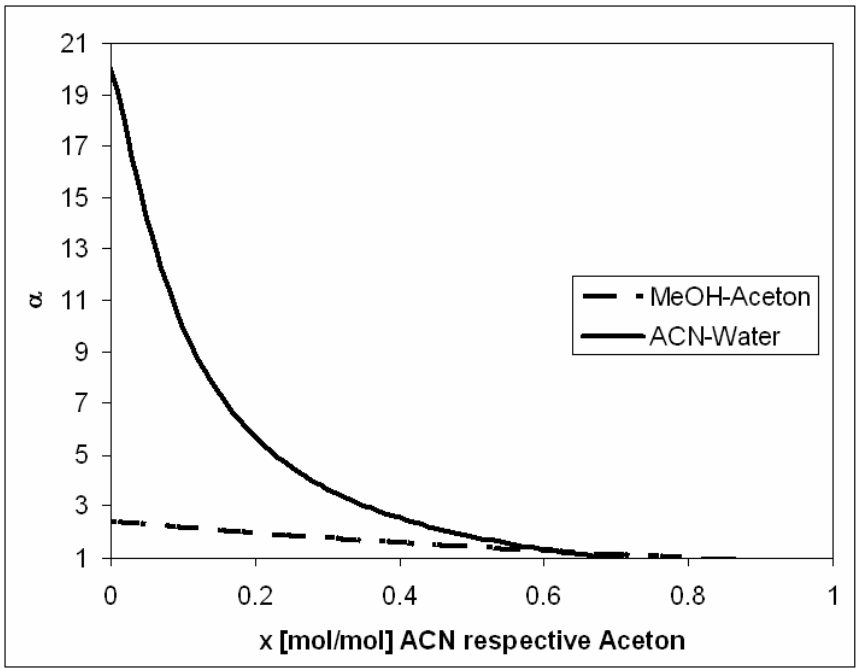

Fig. 6.37 Comparison of the separation factor for the mixtures acetone-methanol and acetonitrile (ACN) - water [Chem 2000] (for component data see appendix chapter A.1).

In the next step the ratio of the energy consumption to the product yield of the inverted and the regular batch against the feed concentration will be calculated for a product purity of 99,9 mol%

with help of the analytical approach as done in chapter 3.1. This mixture has an intersection at a feed concentration of 0,3 mol/mol. Compared to the mixture acetonitrile - water under the same conditions (intersection by 0,2 mol/mol) the intersection is at higher feed concentrations (Fig. 6.38). This fact reconfirmed the hypothesis done before that mixture with a lower gradient of the α-function (which means a smaller separation factor) has a bigger suitable range of feed concentrations where the inverted case is better than the regular one than mixtures with a big separation factor.

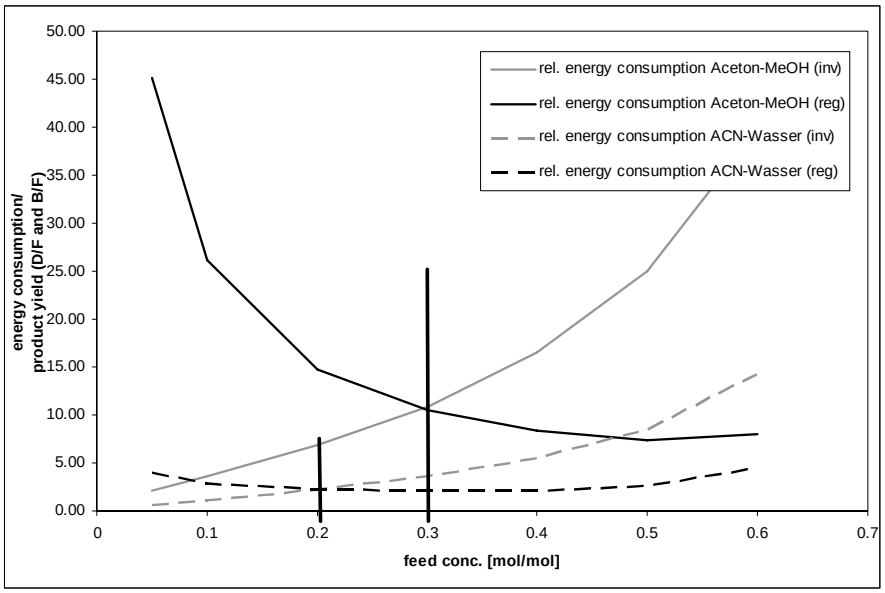

Fig. 6.38 Comparison of acetonitrile-water and methanol-water mixture for a product purity of 99,9 mol% concerning energy consumption related to the product amount for the regular and the inverted process (feed concentration correspond to the respective low boiling component acetonitrile (ACN) and acetone).

So this fact can be the reason why the results of the LP and the HP study differ.

6.3.2.5 Pressure swing process

Summarizing and analyzing all results presented above, it is possible to define the optimal combination concerning batch time or energy consumption for a respective feed concentration and product purity for the complete looped pressure swing distillation process. An overview of the best choices are presented in table 6.22 (batch time) and table 6.23 (energy demands) for a feed flow of 50 l/h and table 6.24 (batch time) and table 6.25 (energy demands) for a feed flow of 200 l/h.

Table 6.22. Optimal combination (50 l/h feed flow rate, batch time).

batch time (50 l/h feed flow)	feed concentration lower than the HP-azeotropic point		feed concentration higher than the HP-azeotropic point	
	1. step: LP	2. step: HP	1. step: HP	2. step: LP
96 mol%	RB-bB	RB-bB	RB-bB	RB-bB
99 mol%	RB-bB	RB-bB	RB-bB	RB-bB
99.9 mol%	RB-bB	RB-bB or AIB	> 82 mol% AIB < 82 mol% RB-bB	RB-bB
99.99 mol%	RB-bB	AIB	AIB	RB-bB

Table 6.23. Optimal combination (50 l/h feed flow rate, energy demand).

energy demand (50 l/h feed flow)	feed concentration lower than the HP-azeotropic point		feed concentration higher than the HP-azeotropic point	
	1. step: LP	2. step: HP	1. step: HP	2. step: LP
96 mol%	RB-bB	RB-bB	RB-bB	RB-bB
99 mol%	RB-bB	RB-bB or AIB	RB-bB or AIB	RB-bB
99.9 mol%	< 10 mol% RB-bB or AIB > 10 mol% RB-bB	AIB or RB-bB	AIB or RB-bB	RB-bB
99.99 mol%	< 13 mol% AIB > 13 mol% RB-bB	AIB	AIB	RB-bB

Table 6.24. Optimal combination (200 l/h feed flow rate, batch time).

batch time (50 l/h feed flow)	feed concentration lower than the HP-azeotropic point		feed concentration higher than the HP-azeotropic point	
	1. step: LP	2. step: HP	1. step: HP	2. step: LP
96 mol%	RB-bB4x	RB-bB4x	RB-bB4x	RB-bB4x
99 mol%	RB-bB4x	RB-bB4x	RB-bB4x	RB-bB4x
99.9 mol%	< 10 mol% RB-bB4x or AIB4x > 10 mol% RB-bB4x	RB-bB4x	RB-bB4x	RB-bB4x
99.99 mol%	< 13 mol% AIB4x > 13 mol% RB-bB4x	AIB	AIB	RB-bB4x

Table 6.25. Optimal combination (200 l/h feed flow rate, energy demand).

energy demand (50 l/h feed flow)	feed concentration lower than the HP-azeotropic point		feed concentration higher than the HP-azeotropic point	
	1. step: LP	2. step: HP	1. step: HP	2. step: LP
96 mol%	< 12 mol% AIB4x > 12 mol% RB-bB4x	RB-bB4x	RB-bB4x	RB-bB4x
99 mol%	< 12 mol% AIB4x > 12 mol% RB-bB4x	RB-bB4x	< 88 mol% RB-bB4x > 88 mol% AIB4x	RB-bB4x

Table 6.25. Optimal combination (200 l/h feed flow rate, energy demand).

energy demand (50 l/h feed flow)	feed concentration lower than the HP-azeotropic point		feed concentration higher than the HP-azeotropic point	
	1. step: LP	**2. step: HP**	**1. step: HP**	**2. step: LP**
99.9 mol%	< 16 mol% AIB4x > 16 mol% RB-bB4x	AIB4x	< 73 mol% RB-bB4x > 73 mol% AIB4x	RB-bB4x
99.99 mol%	< 18 mol% AIB4x > 18 mol% RB-bB4x	AIB4x	AIB4x	RB-bB4x

For high product purities and low feed concentrations (LP case) and mostly always in the HP case (HP case) the advanced inverted batch (AIB) is the more fast and energy efficient solution for the first operation step in pressure swing distillation. The second step, the operation between the two azeotropic points, mostly the regular batch (RB-bB) is the better one, except for high feed flow rates and purities. For low purities and small feed flow rates the regular batch (RB-bB) is the best solution. In conclusion this means that pure regular (RB-bB) as well as pure advanced inverted batch (AIB) combinations are suitable as well as mixed combinations depending on the product purity and the feed flow rate and concentration.

7. Comparison of the PSD-concepts

In the prior chapters both concepts, the discontinuous and the continuous pressure swing distillation, were analyzed and evaluated on their own. In this chapter a comparison of both concepts will be attempted.

First the PSD process itself has same main advantages compared to other unit operations for the separation of homogenous azeotropic mixtures. The main advantages are:

- Smaller costs of investment because of a smaller number of distillation columns (compared to concepts with entrainer).
- High energy savings in the case of the continuous PSD operation.
- No additional substances are needed for the separation.

The main disadvantages are:

- Available and reliable azeotropic data.
- More complex control structure and automation concept.
- Pressure sensitive azeotropic mixture.
- In the case of a low temperature azeotrop, the products are in the column bottom, which could be mean that there are also all contaminations (high boiling by-products).

If the two PSD concepts will be compared, the continuous and the discontinuous, there are in general same main differences listed in table 7.1.

Table 7.1. Comparison of the continuous and the discontinuous PSD process.

continuous	**discontinuous**
advantages:	*advantages*:
smaller operation costs	complexity of the plant is very small
energy saving up to 45%	lower investment costs
continuous, no cyclic start-up needed	much more flexible
disadvantages:	*disadvantages*:
more complex automation	non productive time between steps
larger investment costs	needs more energy because there is no heat integration possible
difficult start-up	

Overall it is very difficult to compare the continuous and the discontinuous processes, because they have both their eligibility, but for different use cases. If there is a need in producing only small volumes of a mixture and there are a lot of changes of the mixtures during the year, a continuous process makes no sense. If there is a need of the separation of only one mixture with high overall volumes a year, the continuous process is the more efficient and the more reasonable process, because of less unproductive times (start-up, pressure change, dumping in case of the discontinuous process) during the process.

The main result of this study is that both processes can be run in pressure swing distillation mode, save, robust and stable. So both process are good alternative for the separation of homogeneous azeotropic mixtures.

8. Hybrid process

Beside the continuous and the discontinuous processes a combination of two unit operations can be used for the separation of azeotropic mixtures - the hybrid process - consisting of a pervaporation unit and a distillation unit. In the context of this work this modern and until now not extensively studied process will be introduced with the focus on heat integration, to give a motivation of using advanced heat integration techniques also for other processes. To use the effective and successful heat integration approach for other unit operations a new heat integrated hybrid process concept has been developed. In this concept a high pressure distillation column is combined with a pervaporation unit including a heat integration system.

Under the topic of hybrid-processes has a wide range of process combinations are addressed, but they will not be discussed here in detail. The following is only a small description of the combination of pervaporation and distillation, which is the new topic of the ongoing work on azeotropic separation at the department. In this work only the basic ideas of the newly developed heat integrated process will be introduced, a feasibility study will be presented, and future plans will be described.

8.1 The hybrid process

The word *Hybrid-process* means a combination of two different thermal unit operations, like a combination of distillation and reaction (reactive distillation), distillation and adsorption or distillation, and a membrane process. A definition of the word *Hybrid-process* is given by [Strube et al. 2004]:

„...Hybrid-process means the connection of at least two different, device-independent unit operations“.

The main advantage is to use the positive effects of each unit operation to balance the negative effects. Here the combination of distillation and pervaporation (Fig. 8.1) will be discussed. The

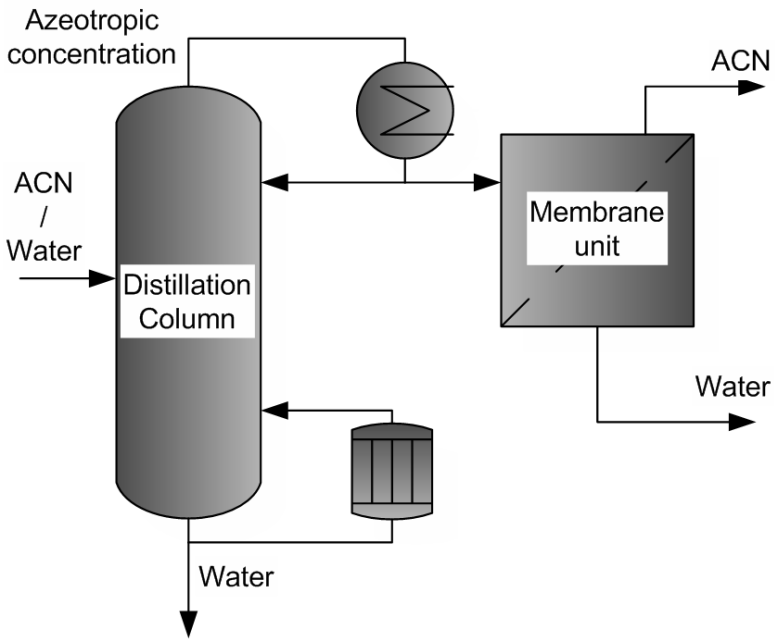

Fig. 8.1 Example hybrid-process for the separation of acetonitrile - water (feed rich of water).

negative effect of the distillation, only distillating to the azeotropic point, will be compensated by the pervaporation process. One example of a combination of distillation and pervaporation is given in Fig. 8.1. Other examples can be found in [Pressly & Ng 1998].

In our example, the feed is put into the distillation column. At the bottom the product (pure water) can be withdrawn and at the top of the column we get an azeotropic mixture at the respective pressure. The top of the column is coupled with the pervaporation module for the separation above the azeotropic point, to get the other pure product (acetonitrile). Depending on the membrane properties the product is on the retentat or the permeate side. The main disadvantage of the process is that membranes are very expensive up to now [Kreis & Gorak 2006]. The combination of distillation, which is a very cheap process compared to the membrane process leads to a much smaller membrane area, if the membrane would by used alone. Another possibility to reduce the membrane area and the costs is to make the membrane module more effective. This can be done by heat integration, the newly developed concept which will be introduced in the next section.

This Hybrid process can be used for dewatering of solvents, water purification as well as the application range of distillation [Kreis & Gorak 2006].

8.2 Heat integration concept

For the continuous pressure swing distillation, a great saving potential of energy was found with help of the heat integration. This concept has to be transferred to the hybrid process.

First the pervaporation process will be introduced and after that different heat integration possibilities will be pointed out.

Pervaporation. The pervaporation process is characterized by a liquid feed which is put into the module under a higher pressure than the permeate and a vaporized permeate operated under vacuum. Liquid retentat leaves the membrane module at the outlet (Fig. 8.2). The separation mechanism of the membrane based on the selective solubility and the diffusion of one component into the membrane. For the vaporization of the diffused component, energy is needed. This energy is taken from the processes as vaporization enthalpy which normally leads to a temperature decrease over the length of the module. The main influences on the process are:

- *Pressure difference* between retentat- and permeate side: The bigger the pressure difference the bigger is the permeate flux through the membrane.
- *Temperature* of the feed-/retentat stream: The bigger or better more constant the temperature, the bigger is the flux through the membrane.
- *Membrane properties*: Membrane area, separation performance, membrane type.
- *Velocity*: The permeate flux is mostly better for a turbulent flow than for a laminar flow.

One possible approach for modelling such a module is the one by Wijmans and Baker (Fig. 8.2). An overview about different modelling approach is given by [Liepnizki 2001].

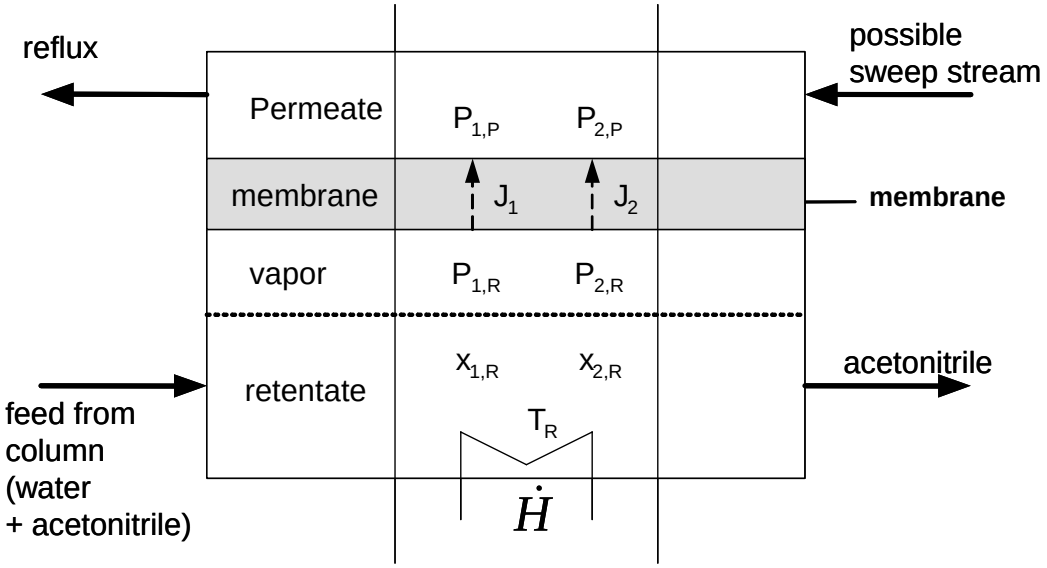

Fig. 8.2 Membrane model by Wijmans and Baker [Wijmans & Baker 1993].

The retentat side is modeled as two phases, one as liquid and one as vapor. The permeate goes vaporized through the membrane. The transfer from liquid to vapor is modelled with the vapor liquid equilibrium. The vaporization enthalpy needs as much additional energy as the flow

through the membrane needs. The conventional case uses external heaters to heat up the liquid flow between the membrane stages and reduce the heat loss (Fig. 8.3) [Lipnizki et al. 1999].

The sweep stream shown in Fig. 8.2 is used to reduce the partial pressure of the permeate by introducing a different component, mostly retentat. The reduction of the partial pressure leads to an increasing of the total pressure difference between retentat and permeate side [Wijmans & Baker 1993]. The sweep stream is not essentially, but can influence the process performance in a positive way.

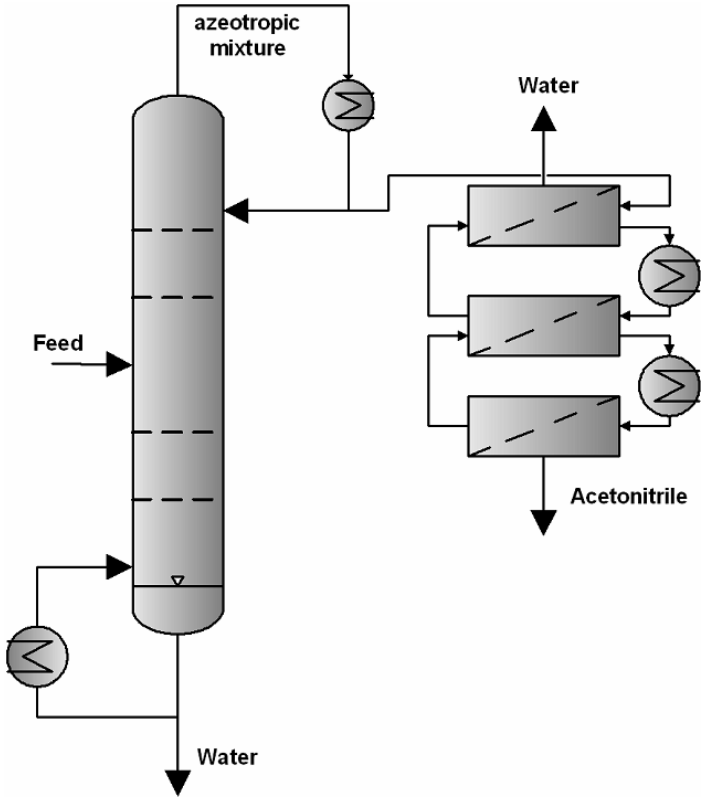

Fig. 8.3 Conventional hybrid process with external heat exchanger.

Heat integration concept. At the top of the distillation column the vapor has to be condensed to put back the liquid stream as reflux into the column and also to have a liquid stream for the pervaporation module. This energy from the condensation process can be used to heat up the pervaporation modules (Fig. 8.4). Moreover, it is a fact that the energy of the vapor stream is enough for heating up the modules because not the whole distillate stream has to be vaporized. Only the component stream through the membrane needs additional vaporization energy. So the condensing distillate stream always has more energy than needed, because of the reflux and the partial vaporization also the temperature difference of the heat exchangers and the heat losses can be compensated.

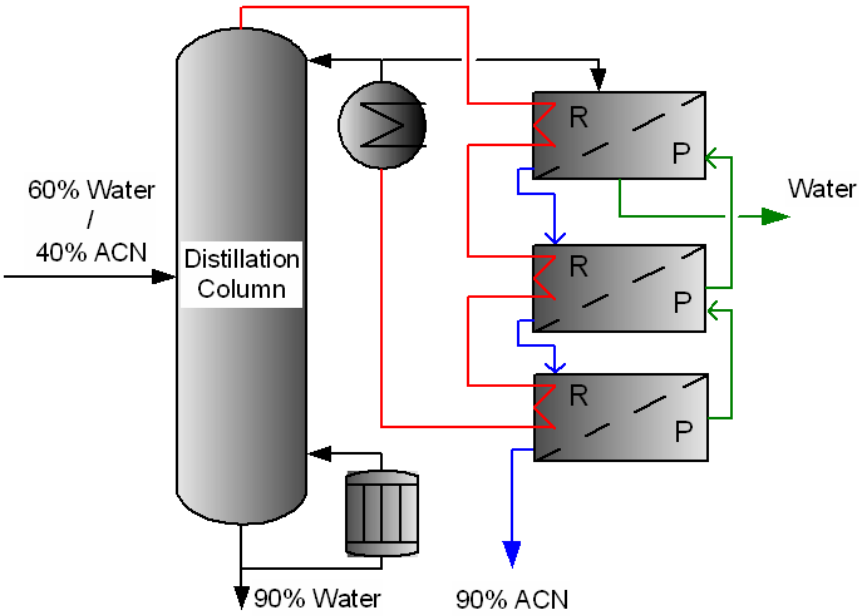

Fig. 8.4 Heat integration concept.

A possible integration of a heat pipe in a membrane is shown in Fig. 8.5. It shows a combination of a pipe membrane module with a ripped pipe. These are the main expected advantages:

- The turbulence increases because of the ripped pipes which leads to an increasing permeate flux (radial).
- The temperature along the membrane (in axial direction) can be set to constant because of the heat exchanger pipe.
- The velocity in axial direction increases because of the reduced cross section, which also leads to a better flux through the membrane.

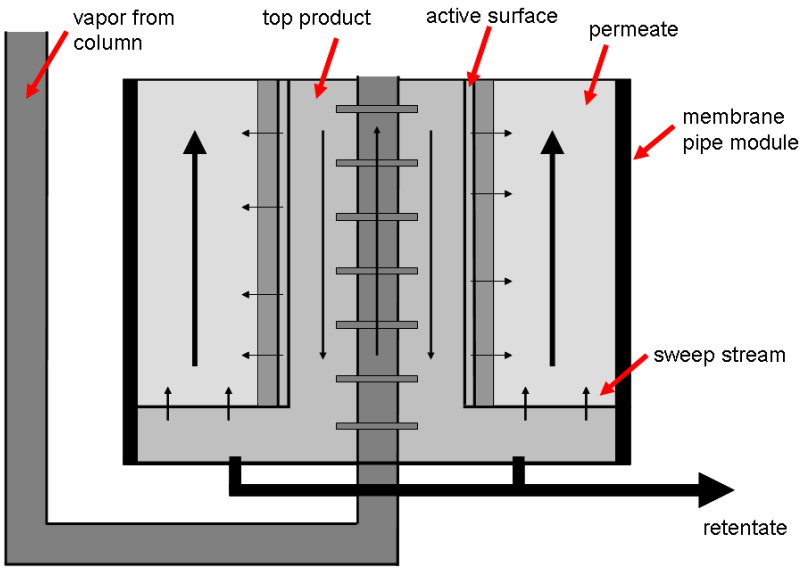

Fig. 8.5 Membrane pipe module with a ripped heat exchanger pipe.

The main expected disadvantage of this construction could be the pressure loss through the heat exchanger pipes because of the very small diameter which is needed for the integration into the membrane module. The main problem is that vapor must go through this pipe.

This theoretical concept must be proved in practice. To solve the pressure drop problem there could be two possible solutions. The first one is to introduce an additional heat exchanger for transferring the vapor energy to a heating fluid which goes through the heat exchanger membrane pipe. The main disadvantage is the temperature difference over the heat exchanger which could lead to a higher column pressure and the much more complex system. The second one is to use the condensation energy in the heat exchanger between the pervaporation modules and not in the inside. This concept can also be easily introduced into existing process setups without buying new membrane modules. All this approaches must be discussed and evaluated in the future.

Feasibility study . A first simulation study will demonstrate the significant enhancement of the separation performance respectively the great reduction of the membrane area with constant permeate amount and concentration with help of the heat integration concept [Zerry et al. 2005, Klein et al. 2006].

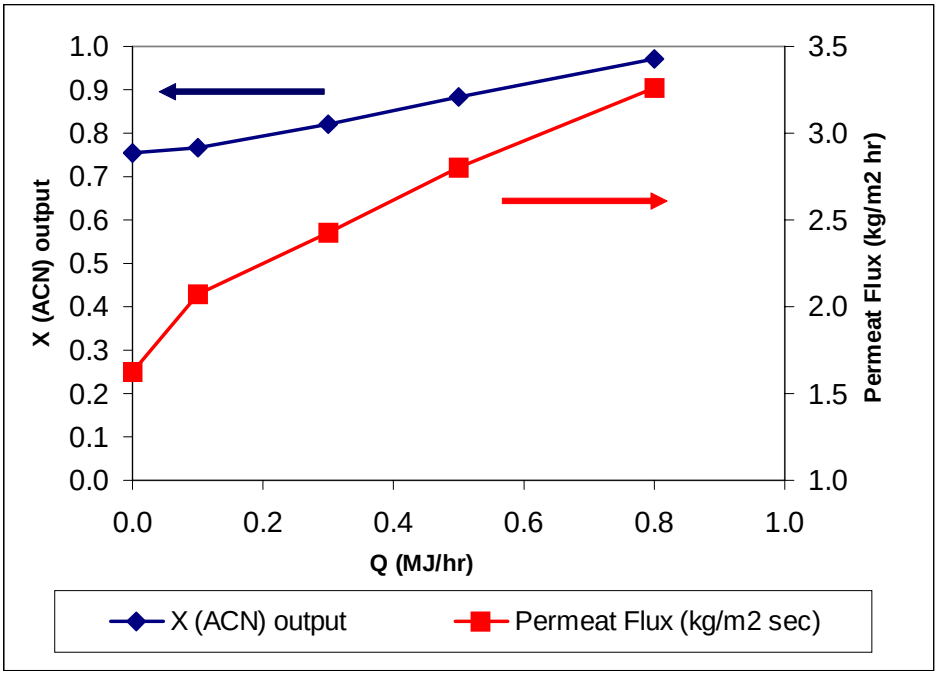

Fig. 8.6 Influence of the energy support to the performance of the pervaporation module.

For this study the high pressure column model (see chapter 3.2) is combined with a simple membrane model [Zerry et al. 2005 and Wusterhausen 2005]:

- Feed: 30 mol% ACN, 10 l/h.
- Product purity: 99 mol% (water, bottom of the column).
- 28 trays, D = 114 mm.

- Membrane feed: 7,7 l/h (distillate stream).
- Membrane has a diameter of D = 7,0 mm and a area of 0,44 m².
- The membrane in the model consists of 20 discrete elements.

For a constant membrane area the permeate concentration can be increased due to the heat integration concept from 0,75 mol/mol to 0,98 mol/mol (Fig. 8.6). 29 % of the possible condensation energy is used to reach a permeate concentration of 0,98 mol/mol (table 8.1). Vice versa this means a high potential for a reduction of the membrane area for a constant permeate concentration because of the heat integration concept.

Table 8.1. Influence of the energy support to the performance of the pervaporation module.

Case	Q [MJ/h]	% Q_{Kon}	X_{ACN}	J_P [kg/m²h]
1	0	0	0,74	1,6
2	0.3	3,5	0,76	2,0
3	0.9	10,6	0,82	2,4
4	1,5	17,7	0,88	2,8
5	2,4	28,3	0,98	3,3

8.3 Outlook

In the context of additional continuative studies the feasibility of this concept has to be experimentally and also theoretically evaluated. Furthermore the membrane design has to be optimized or new concepts have to be developed to get an optimal performance with the heat integration. The simple model used in the feasibility study has to be developed to a full dynamic model with all needed aspects to get a reliable validated dynamic model. The heat integration is not only a possible alternative for the homogeneous azeotropic separation in a hybrid process. Also other mixtures can be separated in such a system or in another combination of a membrane and a distillation column with heat integration.

9. Conclusion and outlook

The objectives of this work are the analysis, evaluation and comparison of the continuous and the discontinuous (batch) pressure swing distillation processes. With help of a new developed rigorous dynamic model with start-up from cold and empty for both process types, different design concepts and different process control structures have been compared and evaluated. The new own experimental data are used for the validation of the different models and helps to close the lack of missing experimental data in the literature, especially for the inverted pressure swing process. The focus in this works is the analysis of the process concepts attending practical and industrial realistic conditions which leads to a process comparison on a new volumetric basis and not as usual on a molar bases. This more practical approach helps to make the pressure swing distillation process more attractive for industrial use.

The works is divided into five main parts. It starts with the state of the arts and an illustration of the different pressure swing processes. After that the simple model for an analytical view on the batch process was introduced and than the dynamic model including start-up from cold and empty is explained to model the continuous and the batch process. The second parts ends with the steady state as well the dynamic experimental validation of the different process models. The third part of the work deals with the analysis and evaluation of the continuous pressure swing process. Different process control structure with total and partial heat integrations as well as with out heat integration are evaluated. The main result of this part is the fact that the total heat and mass integrated continuous pressure swing column system can be operated very stable and robust with a relatively simple process control structure for small feed

concentration changes and even for large feed concentration changes into the other distillation region. Energy savings of up to 45% are possible with this concept. The limiting factor for this process structure is mainly the distillate flow rates (recycle streams) at the top of the column system, which gets very huge for big concentration changes. In the end of the chapter the start-up of the heat and mass integrated column system was analyzed on a heuristic basis. To get such a highly coupled system running, the overlapping of the distillate concentration at the respective pressure of the different columns are mandatory. Therefore an online visualizations tool coupled to the process control system were introduced to help the operator starting up such kind of coupled systems.

The chapter is followed by the analysis and evaluation of the batch processes. The main focus in this chapter were not the comparison of different process control systems, but the comparison of different process structures, called the regular and the inverted process. To do so, a new analytical approach is presented, which helps to find easy the most feasible batch structure (regular or inverted) in respect to the feed start concentration and product purity and distillation region (Low or high pressure). With these information the most feasible process structure combination for the pressure swing distillation loop can be designed. A quantitative evaluation of the process concerning energy, batchtime, column detailed structure (diameter, additional tanks, tray number, ...) is not possible with this new analytical approach. Therefore the rigorous dynamic model including start-up is used. The comparison study starts with the analysis of the different influences on the batch time, where especially for the inverted process structure, the feed flow rate into the column the limiting factor is. For both processes the distillate concentration, which means the „purity“ of the azeotropic concentration at the column top, has also an influence on the batch time and energy consumption. With this information the comparison study is done, introducing a new advanced inverted batch process, which reduces the back mixing at the feed tank at the top of the column. The main results of this study are, that the regular batch process has its advantages especially for feed concentration near the azeotropic point and the inverted batch process is better for feed concentrations near the pure components and also for close boiling mixtures. Especially the advanced inverted batch can compete very well with the established regular batch process and is a real improvement of the inverted process.

The work ends with a comparison of the opposed pressure swing concepts and introduces another possible application of the heat integration concept used successfully for the continuous pressure swing distillation. The main ideas of the use of heat integration in a hybrid-process consisting of a distillation column and a pervaporation membrane were presented in the last chapter.

Finally I will give an outlook on ongoing and possible future work. Distillation is one of the oldest unit operation in chemical engineering and up to know quite well research, but there are always gaps and new ideas which have to be examined. Especially with the growing of high speed computing and modern multi processor computer, optimization of real process structures and systems with high complex and more detailed models becomes more and more a challenging topic in chemical engineering. An interesting future research topic would be the optimization of the in this work evaluated processes concerning not only theoretical aspects but

much more practical details, such as controller boundaries, volumetric flow rates, start-up procedure and non ideal behavior. Furthermore the topic of heat integration has a high potential also for other processes, especially for hybrid processes and will be in my opinion in the context of growing energy prices a main task in the future.

A. Appendix

In the appendix the detailed description of the Wilson approach, the pressure drop calculations and the heat transfer coefficient calculations are explained. After that there is an overview about the gProms™ models, the properties of the used mixtures and properties, diagrams and tables of the complete batch simulations study. The appendix ends with a table of all student theses which I attended during this work.

A.1 Phase equilibrium calculation

The activity coefficients of the phase equilibrium for the mixture acetonitrile -water are calculated with help of the Wilson approach and the vapor pressure with the Antione equation. In the case of the mixture acetone - methanol the NRTL approach and a corresponding vapor pressure equation is used.

Wilson approach. The Wilson approach consists the following equations:

$$\ln\gamma_1 = -\ln(x_1 + \Lambda_{12}x_2) + x_2\left(\frac{\Lambda_{12}}{x_1 + \Lambda_{12}x_2} - \frac{\Lambda_{21}}{x_2 + \Lambda_{21}x_1}\right), \qquad \text{(eq. A.1)}$$

$$\ln\gamma_2 = -\ln(x_2 + \Lambda_{21}x_1) + x_1\left(\frac{\Lambda_{12}}{x_1 + \Lambda_{12}x_2} - \frac{\Lambda_{21}}{x_2 + \Lambda_{21}x_1}\right), \qquad \text{(eq. A.2)}$$

$$\text{with } \Lambda_{12} = \frac{v_2^L}{v_1^L}\exp\left(-\frac{\lambda_{12}-\lambda_{11}}{RT}\right) \text{ and} \qquad \text{(eq. A.3)}$$

$$\Lambda_{21} = \frac{v_1^L}{v_2^L}\exp\left(-\frac{\lambda_{21}-\lambda_{22}}{RT}\right). \qquad \text{(eq. A.4)}$$

The common gas constant is R = 1,98721 cal/(molK). The temperature is given in Kelvin. The Antione equation looks like:

$$\log(p_{oi}^{LV}) = A_i - \frac{B_i}{C_i + \vartheta}, \qquad \text{(eq. A.5)}$$

with pressure in mmHG and temperature in °C.

The following table A.1 shows parameters of the Wilson model and the corresponding Antoine parameters for the calculation of the vapor pressures for the mixture acetonitrile - water.

Table A.1. Parameter for phase equilibrium calculation for the mixture acetonitrile - water [Gmehling et al. 1981].

	acetonitrile	**water**
Wilson-approach		
$\lambda_{12}-\lambda_{11}$ **[cal/mol]**	643,9541	
$\lambda_{21}-\lambda_{22}$ **[cal/mol]**	1388.0606	
v_i^L **[ml/mol]**	52,86	18,07
Antione-equation (temperature in °C, pressure in mmHG)		
A_i	7,33986	8,07131
B_i	1482,290	1730,630
C_i	250,523	233,426

NRTL approach. The NRTL approach consists the following equations:

$$\ln\gamma_1 = x_2^2 \cdot \left[\tau_{21}\cdot\left(\frac{G_{21}}{x_1 + x_2\cdot G_{21}}\right)^2 + \frac{\tau_{12}\cdot G_{12}}{(x_2 + x_1\cdot G_{12})^2}\right], \qquad \text{(eq. A.6)}$$

$$\ln\gamma_2 = x_1^2 \cdot \left[\tau_{12}\cdot\left(\frac{G_{12}}{x_2 + x_1\cdot G_{12}}\right)^2 + \frac{\tau_{21}\cdot G_{21}}{(x_1 + x_2\cdot G_{21})^2}\right], \qquad \text{(eq. A.7)}$$

$$\text{with } \tau_{ij} = \Delta g_{ij}/T,\ \tau_{ii} = 0 \qquad \text{(eq. A.8)}$$

$$\text{and } G_{ij} = \exp(-\alpha_{ij}\cdot\tau_{ij}). \qquad \text{(eq. A.9)}$$

The vapor pressure is calculated with the following equation:

$$p_{oi}^{LV} = \exp\left(A_i + \frac{B_i}{T} + C_i \cdot \ln T + D_i \cdot T^{E_i}\right) . \qquad \text{(eq. A.10)}$$

Table A.2. Parameter for phase equilibrium calculation for the mixture acetone - methanol [Chem 2000].

	acetone	methanol
NRTL-approach		
Δg_{21}	123,661	
Δg_{21}	87,8485	
α_{ij}	0,3008	
Equation parameters (eq. A.10) (temperature in T, pressure in Pa)		
A_i	70,72	81,768
B_i	-5684	-6876
C_i	-7,351	-8,7078
D_i	6,3e-6	7,1926e-6
E_i	2	2

A.2 Pressure drop calculation

This chapter introduces all pressure drop equations used in the dynamic gProms™ model.

A.2.1 Column tray

The pressure drop of the column tray is calculated with the following equation:

$$\Delta p_n \equiv \Delta p_{d,n} + \Delta p_{h,n} + \Delta p_{r,n} . \qquad \text{(eq. A.11)}$$

The pressure drop Δp_n consists of the dry pressure drop $\Delta p_{d,n}$, the hydrostatic pressure drop $\Delta p_{h,n}$ and the rest pressure drop $\Delta p_{r,n}$. The rest pressure drop is normally negligible, because it is much smaller than the other pressure drops [Stichlmair 1998].

The dry pressure drop describes the pressure drop of the through flowing vapor through the trays in a dry column. For bubble cap trays the following equation is used [Stichlmair & Fair 1998]:

$$\Delta p_{d,n} = \zeta^V \cdot \frac{\rho_n^V}{2}(w_n^V)^2 . \qquad \text{(eq. A.12)}$$

The hydrostatic pressure drop is calculated with the mass of the froth region, which imposes pressure upon the tray and the height of the liquid part [Stichlmair & Fair 1998]:

$$\Delta p_{h,n} = h_{cl,n}\rho_n^L g . \qquad \text{(eq. A.13)}$$

A.2.2 Coupled heat exchanger

The calculation of the pressure drop of reboiler side of the coupled heat exchanger includes the following parts:

$$\Delta p \equiv \Delta p_h + \Delta p_{2ph} + \Delta p_a \,. \qquad \text{(eq. A.14)}$$

The pressure drop of the two phase flow consists of the hydrostatic pressure drop Δp_h, the friction pressure drop Δp_{2ph} and the acceleration pressure drop Δp_a.

The hydrostatic pressure drop is defined for an upright pipe bundled heat exchanger with the average vapor-liquid-mixture density and the pipe length:

$$\Delta p_h = g\rho^{2ph}H \,. \qquad \text{(eq. A.15)}$$

The friction pressure drop of the two phase flow is calculated with the approach by Lockhardt and Martinelli against one phase (vapor phase). The influence of the other phase is included in a correction factor Ψ_{2ph}^V [Lockhardt & Martinelli 1949]:

$$\Delta p_{2ph} = \Psi_{2ph}^V \Delta p_{1ph}^V = \Psi_{2ph}^V \zeta^V \frac{\dot{m}^{V^2}}{2\rho^V} \frac{H}{d_{inside}}, \qquad \text{(eq. A.16)}$$

were the resistance coefficient ζ^V for a one-phase pressure drop Δp_{1ph}^V is calculated with the modified Blasius law:

$$\zeta^V = 0{,}184 Re^{V^{-0,2}} \,. \qquad \text{(eq. A.17)}$$

The correction factor Ψ_{2ph}^V can be calculated with the approach by Rohsenow and Harnett out of the Martinelli parameter, which is a relation between the one phase pressure drop to both phase [Rohsenow & Hartnett 1973]:

$$\Psi_{2ph}^V = 1 + 20X_m + X_m^2, \qquad \text{(eq. A.18)}$$

$$\text{with } X_m = \sqrt{\frac{\left(\frac{dp}{dz}\right)^V}{\left(\frac{dp}{dz}\right)^L}} = \left(\frac{\rho^V}{\rho^L}\right)^{0,5} \left(\frac{\eta^V}{\eta^L}\right) \left(\frac{1 - x^*}{x^*}\right)^{0,9} \qquad \text{(eq. A.19)}$$

$$\text{and } x^* = \frac{\dot{m}^V}{\dot{m}_{com}} \,. \qquad \text{(eq. A.20)}$$

The specific volume of the flow increases because of the increasing vapor part along the flow line, which causes an increasing velocity due to the continuity condition. The acceleration pressure drop is defined in dependency of the mass content of the flow $\dot{x}$ and the volumetric vapor content ε:

$$\Delta p_a = \dot{m}^2\left(\frac{(1-\dot{x})^2}{(1-\varepsilon)\rho^L} + \frac{\dot{x}^2}{\varepsilon\rho^V} - \frac{1}{\rho^L}\right), \qquad \text{(eq. A.21)}$$

$$\text{with } \varepsilon = \frac{Vol^V}{Vol_{com}}. \qquad \text{(eq. A.22)}$$

A.3 Identification of the heat transfer coefficient

The calculation of the heat transfers through the wall uses different approaches for the condenser and the coupled heat exchanger, which will be introduced now.

A.3.1 Nusselt-approach for film flow

The calculation of the heat transfer coefficient for the heat transfer inside the pipes (distillate) of the condenser is done with the Nusselt film theory [Nusselt 1918].

The Nusselt number is defined as follows:

$$Nu_{film} = \frac{\alpha_{film}}{\lambda_{film}}\left(\frac{\eta_{Film}^2}{(\rho^L)^2 \cdot g}\right)^{1/3}. \qquad \text{(eq. A.23)}$$

The Nusslet water skin theory calculates the Nusselt number: Nu_{film} with this equation:

$$Nu_{film} = 0{,}9245 \cdot Re_{film}^{-1/3}. \qquad \text{(eq. A.24)}$$

The Reynolds Re number is defined to:

$$Re_{film} = \frac{\dot{M}^{con}}{\eta_{film} \cdot \pi \cdot d_{outside}}. \qquad \text{(eq. A.25)}$$

A.3.2 Nusselt-approach for flow through pipes

The calculation of the heat transfer coefficient through a pipe the approach by Gnielinski [Gnielinski 1994] is used

$$Nu_{pipe} = \frac{\alpha_{pipe} \cdot d_{inside}}{\lambda^{CW}}, \qquad \text{(eq. A.26)}$$

$$Nu_{pipe} = 0{,}012(Re_{pipe}^{0,87} - 280)Pr^{0,4}\left(1 + \left(\frac{d_{inside}}{H}\right)^{\frac{2}{3}}\right), \qquad \text{(eq. A.27)}$$

$$\text{with } Re_{pipe} = \frac{\dot{m}^{CW} \cdot d_{inside}}{\eta^{KW}} \qquad \text{(eq. A.28)}$$

$$\text{and } Pr_{pipe} = \frac{\eta^{CW} \cdot c_p^{CW}}{\lambda^{CW}} . \qquad \text{(eq. A.29)}$$

A.3.3 Heat transfer for two phase pipe flow

The heat transfer calculation in the coupled heat exchanger makes use of a heat transfer for a two phase pipe to calculate the bottom/reboiler heating stream of the LP column (chapter 3.2.2). Starting from an equation for the calculation of the heating stream of the reboiler:

$$\dot{Q}^{reb} = \frac{Vol^V}{Vol_{tot}} \cdot \alpha_{pipe}^{2ph} \cdot A_{inside}(T^W - T^{reb}), \qquad \text{(eq. A.30)}$$

α_{pipe}^{2ph} consists of two parts:

$$\alpha_{pipe}^{2ph} = S\alpha_B + F\alpha_K . \qquad \text{(eq. A.31)}$$

The heat transfer coefficient α_B calculates the heat transfer of the still bubble boiling and α_K includes the convective transport in a one-phase flow. The enhancement factor F_e considers the concurrent formation of bubbles and the factor S considers the rejection of the bubble formation due to a forced flow by high temperature gradient [Rix 1998]. The convective transport is calculated with the Dittus-Boelter approach:

$$\alpha_K = 0{,}023 Re^{L\,0{,}8} Pr^{L\,0{,}4} \frac{\lambda^L}{d_{inside}}, \qquad \text{(eq. A.32)}$$

$$\text{with } Re^L = \frac{\dot{m}^L d_{inside}}{\eta^L} \text{ and } Pr^L = \frac{\eta^L c_P^L}{\lambda^L}. \qquad \text{(eq. A.33)}$$

The enhancement factor uses also the Martinelli-parameter:

$$F_e = \max\left(2{,}35\left(\frac{1}{X_m} + 0{,}213\right)^{0{,}736}, 1\right). \qquad \text{(eq. A.34)}$$

The part due to still bubble boiling is done with the approach by Forster and Zuber [Forster & Zuber 1955]:

$$\alpha_B = 0{,}00122 \frac{\lambda^{L\,0{,}79} c_p^{L\,0{,}45} \rho^{L\,0{,}49}}{\sigma^{L\,0{,}5} \eta^{L\,0{,}29} (\rho^V \Delta h^{LV})^{0{,}24}} \Delta T^{W\,0{,}24} \Delta p^{W\,0{,}75}, \qquad \text{(eq. A.35)}$$

$$\text{with } \Delta T^W = T^W - T^L \text{ and } \Delta p^W = p^{LV}(T^W) - p^{LV}(T^L). \qquad \text{(eq. A.36)}$$

Factor S is defined as:

$$S = (1 + 2{,}53 Re_{2ph}^{1{,}17})^{-1}, \qquad \text{(eq. A.37)}$$

with $Re_{2ph} = Re^{L} F_e^{1,25}$. (eq. A.38)

A.4 Properties

This section lists the properties of the mixture acetonitrile - water and the properties of the used pilot plant [Chem 2000].

A.4.1 Acetonitrile - water

The following table A.3 and table A.4 contains all properties and property calculation equations for water, used in the dynamic gProms™ model.

Table A.3. Water - part 1.

Properties	Unit	Equation	Values
heat of vaporization	[kJ/mol]	$h^{LV} = A \cdot T^2 + B \cdot T + C$	A = -0.0908; B = 18.679; C = 4.6376e4
isobar heat capacity of the saturated liquid	[J/kgK]	$c_P = A \cdot T^2 + B \cdot T + C$	A = 106.975; B = -0.1913; C = 2.8882e-4
thermal conductivity	[W/mK]	$\lambda = A \cdot T^3 + B \cdot T^2 + C \cdot T$	A = -0.0058; B = 4.7414; C = -290.9832
molar volume of the saturated vapor	[m³/kmol]	$v_G = A \cdot T^4 + B \cdot T^3 + C \cdot T^2 + D \cdot T$	A = -2.7248e-7; B = 4.12e-4; C = -0.2273; D = 51.9202
molar volume of the saturated liquid	[l/kmol]	$v_L = A \cdot T^2 + B \cdot T + C$	A = 6.4031e-5; B = -0.0336; C = 22.4037
viscosity	[Pas]	$\eta = \exp(A \cdot T^3 + B \cdot T^2 + C \cdot T)$	A = 1.3894e-7; B = 2.0303e-4; C = 0.1042; D = 23.4844
surface tension	[N/m]	$\sigma = A \cdot T^2 + B \cdot T + C$	A = -2.0038e-4; B = -0.042; C = 102.4311

Table A.4. Water - part 2.

Properties	Unit	Value
molecular weight	[kg/kmol]	18.015
critical temperature	[K]	647.35
critical pressure	[bar]	221.1823
critical volume	[m³/kmol]	0.063494
normal boiling point	[K]	373.15
melting point	[K]	273.15
heat of formation	[J/kmol]	-2.4182e8

The following table A.5 and table A.6 contains all properties and property calculation equations for acetonitrile, used in the dynamic gProms™ model.

Table A.5. Acetonitrile - part 1.

Properties	Unit	Equation	Values
heat of vaporization	[J/kmol]	$h^{LV} = A \cdot (1 - Tr)^{B}$ [a]	A = 4.31e7; B = 3.354e-1
isobar heat capacity of the saturated liquid	[J/kmolK]	$c_P = A + B \cdot T + C + T^2$	A = 9.7582e4; B = -122.2; C = 3.4085e-1
thermal conductivity	[W/mK]	$\lambda = A + B \cdot T + C + T^2$	A = 0.30703; B = -4.002e-4
molar volume of the saturated vapor	[m³/kmol]	$v_G = (1/(A \cdot T^4 + B \cdot T^3 + C \cdot T^2 + D \cdot T))/41,053$	A = -86.98; B = 0.8525; C = -2.816e-3; D = 3.144e-6
liquid density	[kmol/kg]	$\rho = \frac{A}{B^{1+\left(1-\frac{T}{C}\right)^{D}}}$	A = 1.3088; B = 0.22642; C = 5.455e2; D = 2.8128e-1
viscosity	[Pas]	$\eta = \exp\left(A + \frac{B}{T} + C \cdot \ln(T)\right)$	A = 14.486; B = -423.7; C = -3.926
surface tension	[N/m]	$\sigma = A \cdot (1 - Tr)^{B}$ [a]	A = 6.8249e-2; B = 1.097

a. Tr = T/(Tcritical)

Table A.6. Acetonitrile - part 2.

Properties	Unit	Value
molecular weight	[kg/kmol]	41.053
critical temperature	[K]	545.5
critical pressure	[bar]	48.332
critical volume	[m³/kmol]	0.173
normal boiling point	[K]	354.75
melting point	[K]	229.32
heat of formation	[J/kmol]	7.404e7

A.4.2 Pilot plant

In this section all relevant properties of the pilot plant are listed. In table A.7 all the HP column related data and in table A.8 all the LP column related data.

Table A.7. HP column.

Properties	Unit	Value
number of tray	[-]	28
tray diameter	[mm]	107
tray volume	[m³]	1.8042e-3
tray weir height	[m]	28e-3
tray weir length	[m]	25e-3
condenser[a] shell side volume	[m³]	4.85e-3
condenser number of tubes	[-]	15
condenser inner tube diameter	[m]	0.006
condenser outer tube diameter	[m]	0.01
condenser tube length	[m]	1
condenser weir level shell side	[m]	0.095
condenser overall heat capacity - tube wall	[MJ/K]	2.627e-3
condenser overall heat capacity - cooling water hold-up	[MJ/K]	1.78e-3
CHE[b] number of tubes	[-]	16
CHE free cross-section of the shell base	[m²]	7.312e-3
CHE cross-section shell inlet orifice	[m²]	0.004
CHE inner tube diameter	[m]	0.009
CHE outer tube diameter	[m]	0.012
CHE tube length	[m]	1,5
drum volume	[m³]	5e-3
drum cross sectional area	[m²]	3.14/(4*0.1²)
reboiler overall volume	[m³]	30e-3
reboiler cross sectional area	[m²]	8.99e-3

a. for single column use only

b. CHE: coupled heat exchanger (HP condenser side)

Table A.8. LP column.

Properties	Unit	Value
number of tray	[-]	20
tray diameter	[mm]	107
tray volume	[m³]	1.8042e-3
tray weir height	[m]	38e-3
tray weir length	[m]	18e-3

Table A.8. LP column.

Properties	Unit	Value
condenser shell side volume	[m³]	4.85e-3
condenser tube count	[-]	15
condenser inner tube diameter	[m]	0.006
condenser outer tube diameter	[m]	0.010
condenser tube length	[m]	1
condenser overall heat capacity - tube wall	[MJ/K]	2.627e-3
condenser overall heat capacity - cooling water hold-up	[MJ/K]	1.78e-3
drum volume	[m³]	10e-3
drum cross sectional area	[m²]	3.14/(4*0.1²)
reboiler overall volume	[m³]	40e-3
reboiler cross sectional area	[m²]	8.99e-3
pump pressure difference	[mbar]	570

A.5 Overview of the complete batch study

In this chapter all results of the batch simulation study (see chapter 6.3.4) will be shown. First the main conditions of the simulations study are collected in table A.9.

Table A.9. Simulation study conditions.

	NIB, AIB, RB-bB, RB	NIB4x, AIB4x, RB-bB4x
F-factor	1 $\sqrt{Pa}$	1 $\sqrt{Pa}$
feed volumetric stream (external tank)	50 l/h	200 l/h
column type	28 bubble cap trays	
diameter	114 mm	214 mm
pressure	constant LP: 1 bar; HP: 3.5 bar	
feed volume V_F	600 l	600 l
feed start concentration x_F	variable (10, 30, 50, 70, 80, 90 mol%)	
top distillate concentration	68 mol% (LP) and 58 mol% (HP): - regular batch: controlled reflux - inverted batch: stop condition	
azeotropic point x_D^{set}	LP: 69.3 mol%; HP: 57.3 mol%	
bottom concentration	96 - 99.99 mol% (LP: water; HP: acetonitrile): - regular batch: stop condition - inverted batch: controlled	
product withdraw	if the desired purity is reached (Top product withdraw in the regular case and bottom product with draw in the inverted case)	

A.5.1 Comparison of RB, RB-bB, NIB, AIB - batch time

Ambient pressure batch (P = 1,015 bar).

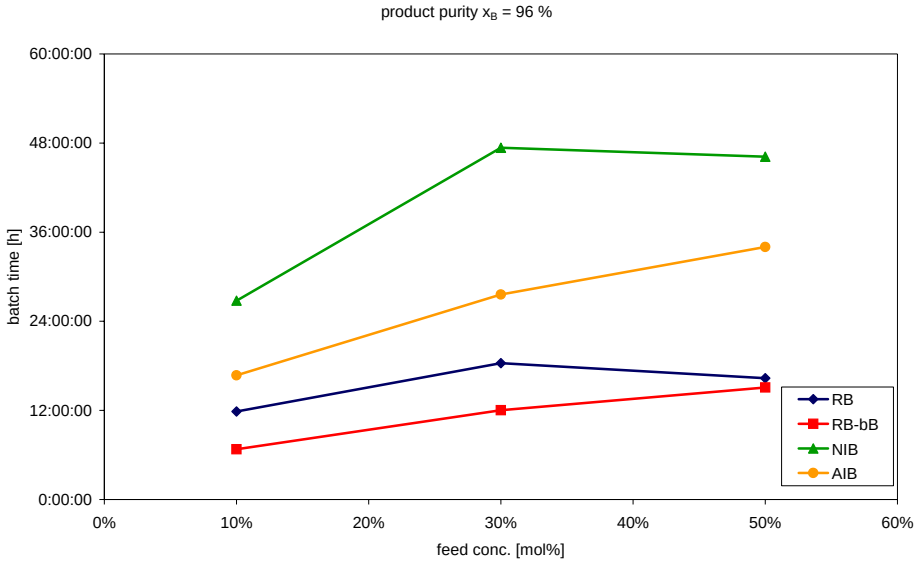

Fig. A.1 Comparison concerning the batch time for different structures (RB, RB-bB, NIB, AIB): ambient pressure, product purity 96 mol% water, feed conc. 10 mol%, 30 mol%, 50 mol% ACN.

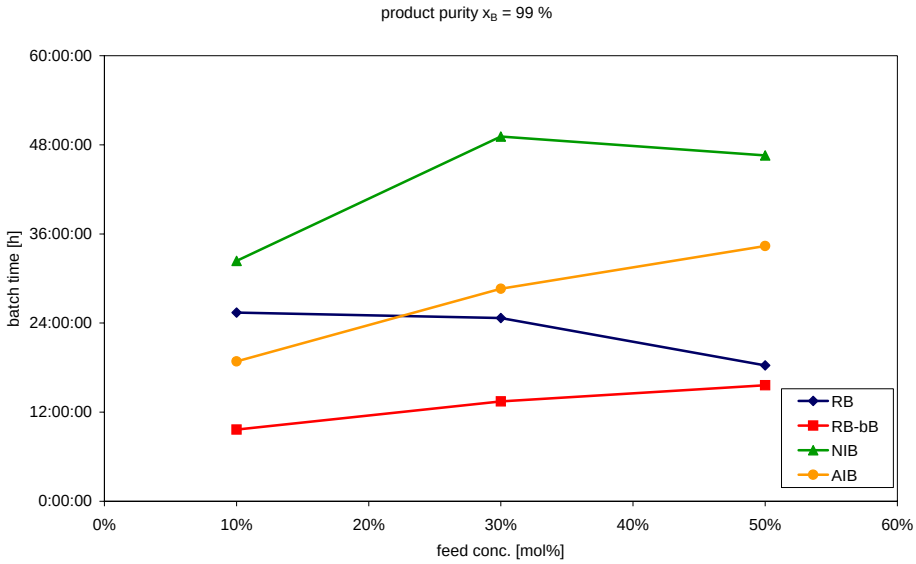

Fig. A.2 Comparison concerning the batch time for different structures (RB, RB-bB, NIB, AIB): ambient pressure, product purity 99 mol% water, feed conc. 10 mol%, 30 mol%, 50 mol% ACN.

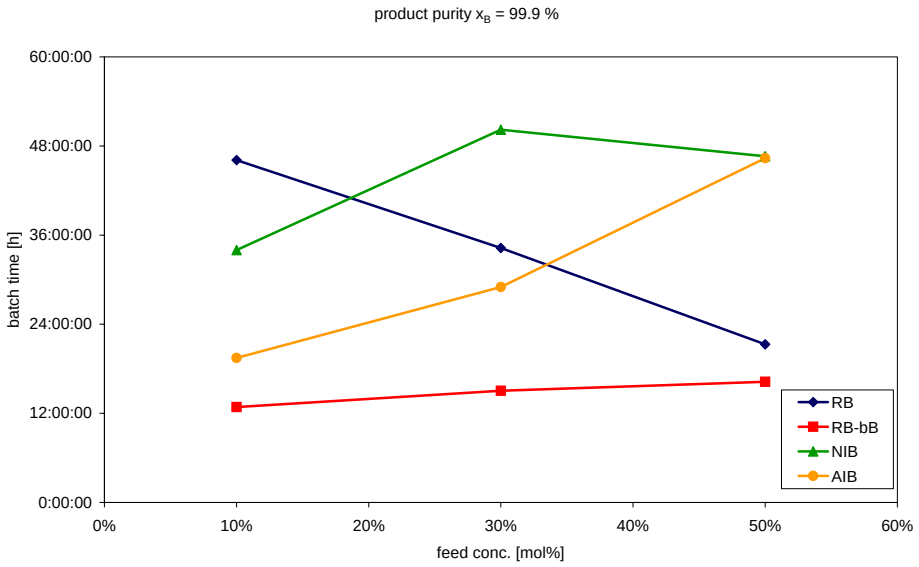

Fig. A.3 Comparison concerning the batch time for different structures (RB, RB-bB, NIB, AIB): ambient pressure, product purity 99,9 mol% water, feed conc. 10 mol%, 30 mol%, 50 mol% ACN.

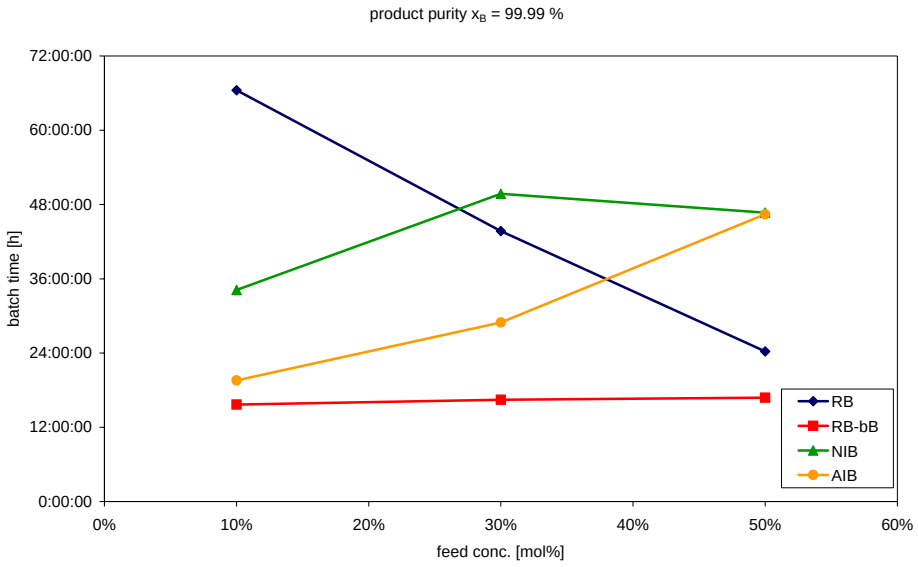

Fig. A.4 Comparison concerning the batch time for different structures (RB, RB-bB, NIB, AIB): ambient pressure, product purity 99,99 mol% water, feed conc. 10 mol%, 30 mol%, 50 mol% ACN.

High pressure batch (P = 3,5 bar).

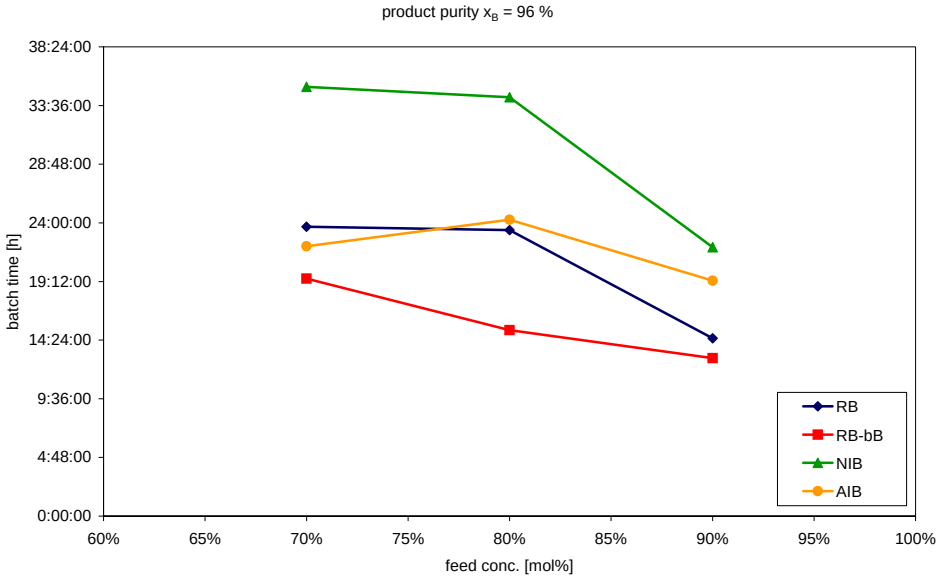

Fig. A.5 Comparison concerning the batch time for different structures (RB, RB-bB, NIB, AIB): high pressure, product purity 96 mol% water, feed conc. 70 mol%, 80 mol% ACN.

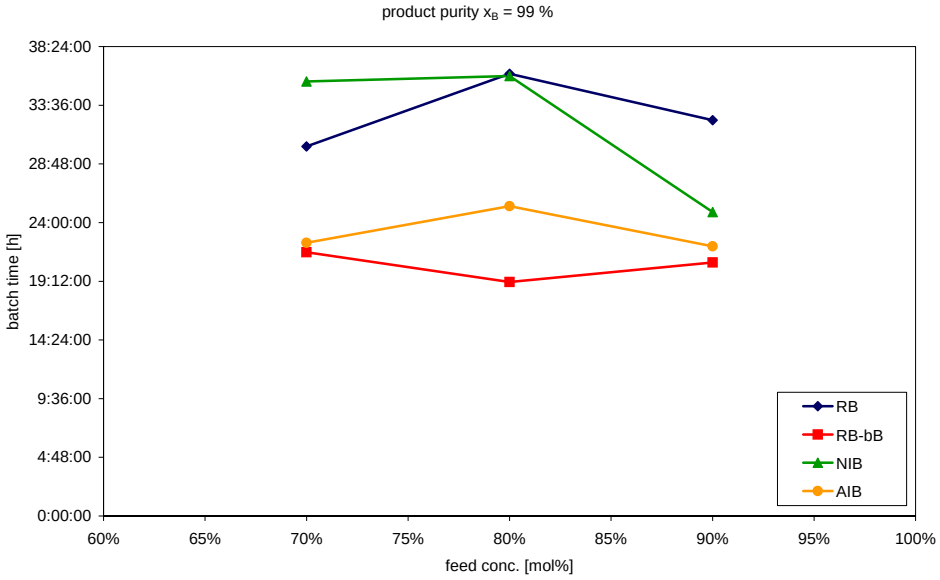

Fig. A.6 Comparison concerning the batch time for different structures (RB, RB-bB, NIB, AIB): high pressure, product purity 99 mol% water, feed conc. 70 mol%, 80 mol% ACN.

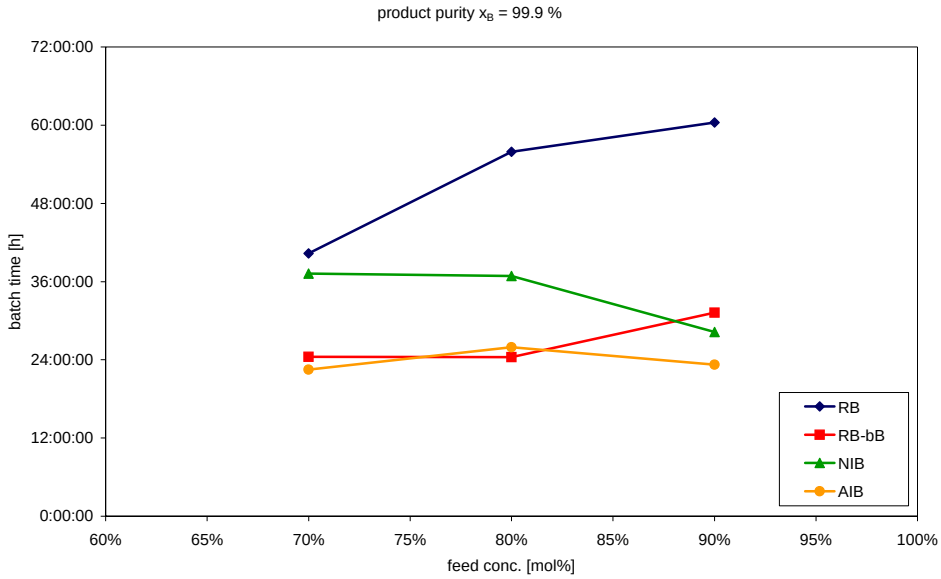

Fig. A.7 Comparison concerning the batch time for different structures (RB, RB-bB, NIB, AIB): high pressure, product purity 99,9 mol% water, feed conc. 70 mol%, 80 mol%, 90 mol% ACN.

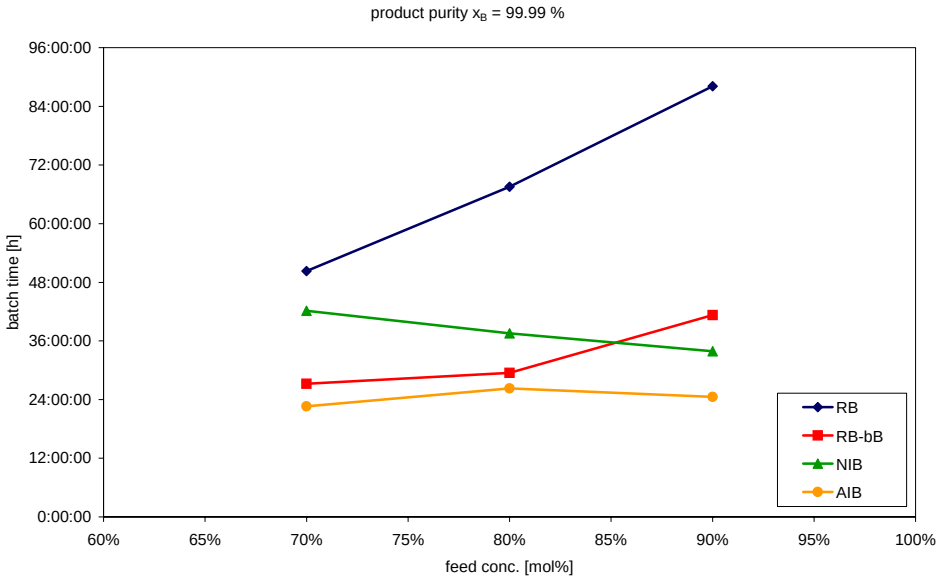

Fig. A.8 Comparison concerning the batch time for different structures (RB, RB-bB, NIB, AIB): high pressure, product purity 99,99 mol% water, feed conc. 70 mol%, 80 mol%, 90 mol% ACN.

A.5.2 Comparison of RB, RB-bB, NIB, AIB - energy consumption

Ambient pressure batch (P = 1,015 bar).

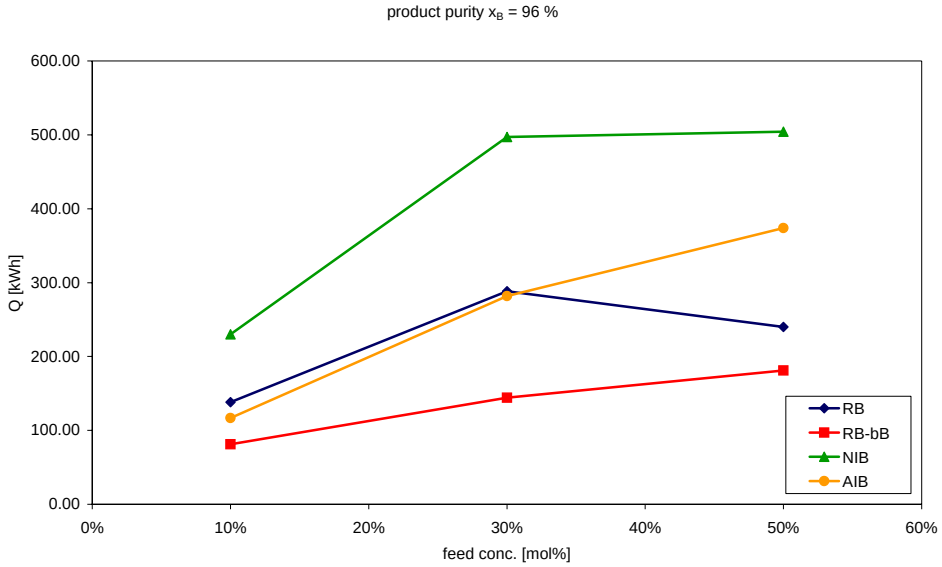

Fig. A.9 Comparison concerning the energy consumption for different structures (RB, RB-bB, NIB, AIB): ambient pressure, product purity 96 mol% water, feed conc. 10 mol%, 30 mol%, 50 mol% ACN.

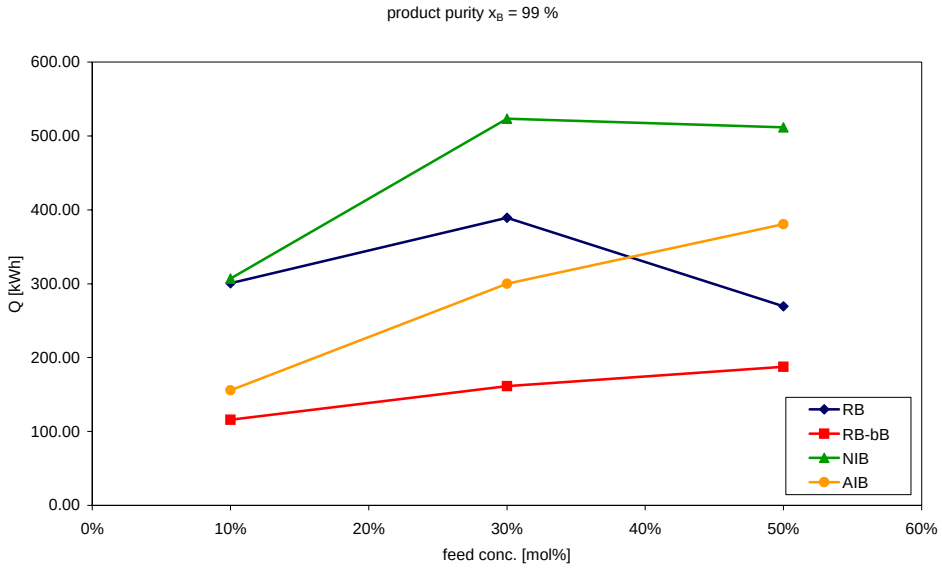

Fig. A.10 Comparison concerning the energy consumption for different structures (RB, RB-bB, NIB, AIB): ambient pressure, product purity 99 mol% water, feed conc. 10 mol%, 30 mol%, 50 mol% ACN.

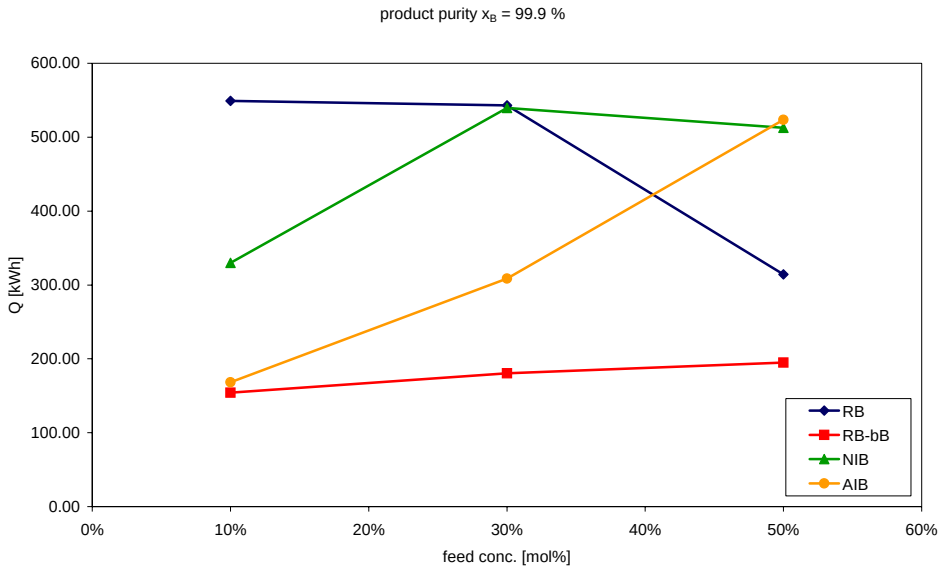

Fig. A.11 Comparison concerning the energy consumption for different structures (RB, RB-bB, NIB, AIB): ambient pressure, product purity 99,9 mol% water, feed conc. 10 mol%, 30 mol%, 50 mol% ACN.

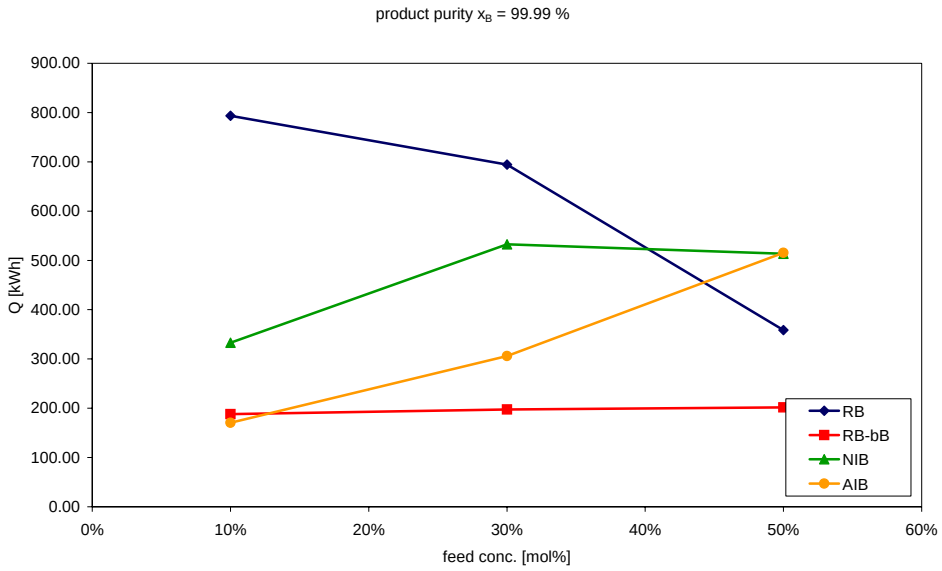

Fig. A.12 Comparison concerning the energy consumption for different structures (RB, RB-bB, NIB, AIB): ambient pressure, product purity 99,99 mol% water, feed conc. 10 mol%, 30 mol%, 50 mol% ACN.

High pressure batch (P = 3,5 bar).

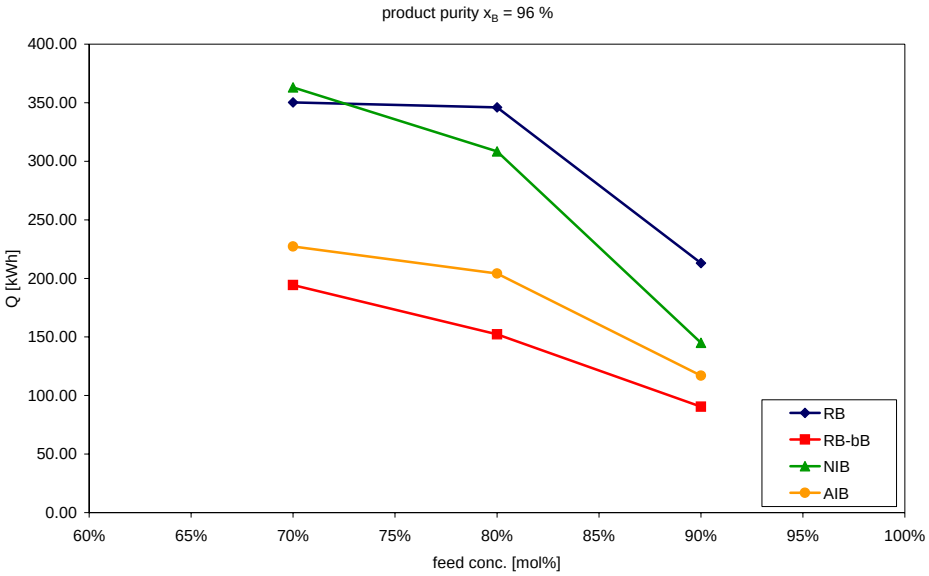

Fig. A.13 Comparison concerning the energy consumption for different structures (RB, RB-bB, NIB, AIB): high pressure, product purity 96 mol% water, feed conc. 70 mol%, 80 mol%, 90 mol% ACN.

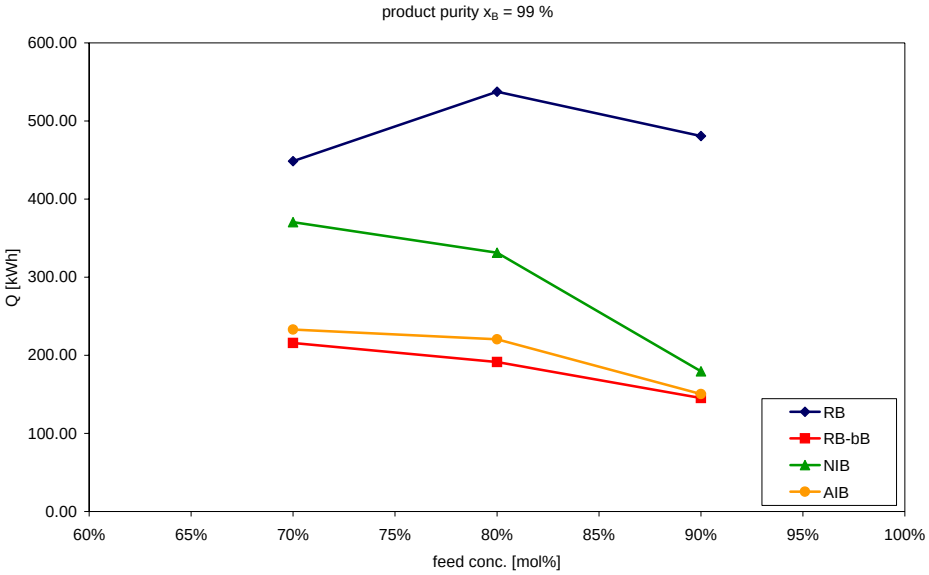

Fig. A.14 Comparison concerning the energy consumption for different structures (RB, RB-bB, NIB, AIB): high pressure, product purity 99 mol% water, feed conc. 70 mol%, 80 mol%, 90 mol% ACN.

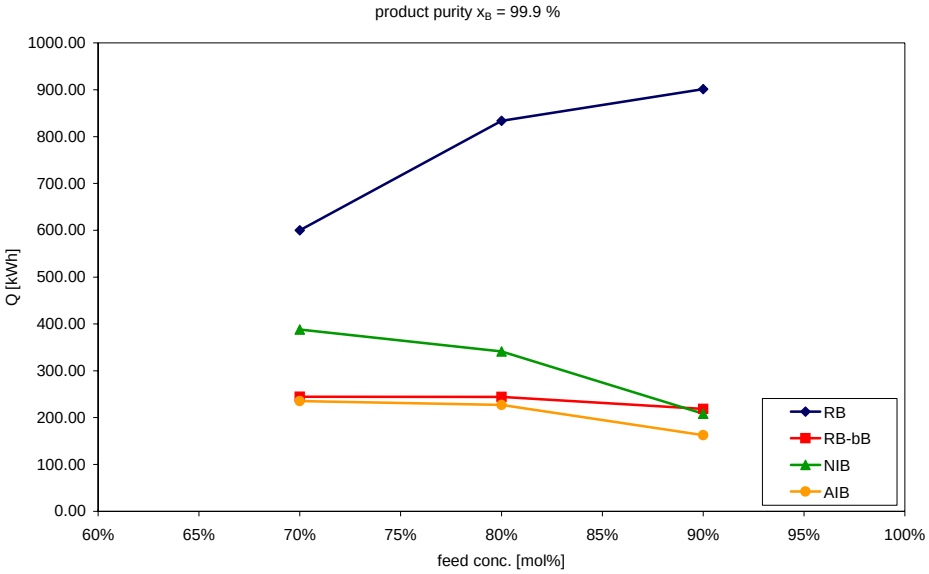

Fig. A.15 Comparison concerning the energy consumption for different structures (RB, RB-bB, NIB, AIB): high pressure, product purity 99,9 mol% water, feed conc. 70 mol%, 80 mol%, 90 mol% ACN.

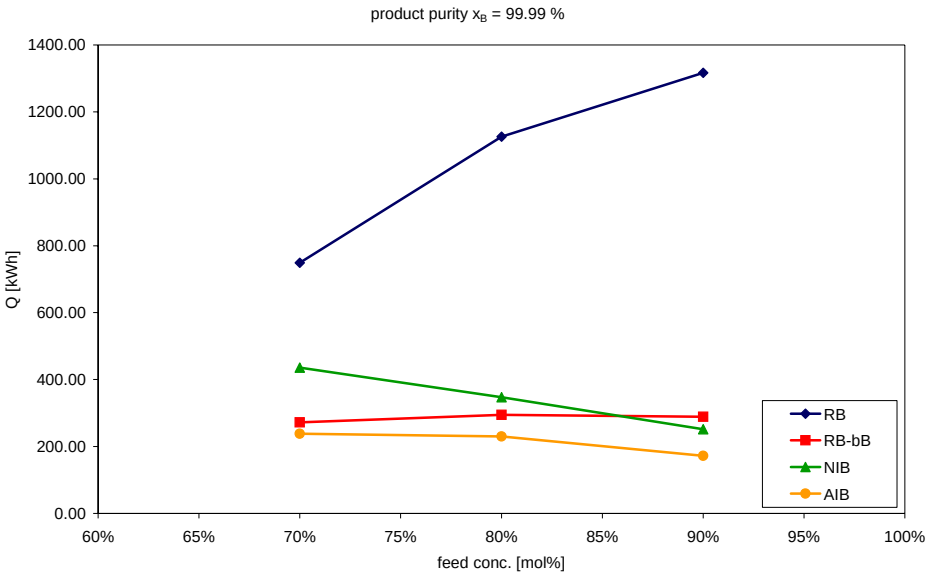

Fig. A.16 Comparison concerning the energy consumption for different structures (RB, RB-bB, NIB, AIB): high pressure, product purity 99,99 mol% water, feed conc. 70 mol%, 80 mol%, 90 mol% ACN.

Table A.10. Overview about the batch time and the energy consumption for different structures (RB, RB-bB, NIB, AIB), feed flow 50 l/h

Bottom conc. (water) →		time			Q [kwh]		
Feed Conc. (ACN) ↓		0.96	0.99	0.999	0.9999	0.96	0.99	0.999	0.9999
10 mol%	RB	11:50:52	25:23:53	46:06:09	66:28:07	138.14	300.74	549.20	793.59
	RB-bB	**6:45:42**	**9:39:26**	**12:50:40**	**15:39:51**	**81.14**	**115.89**	**154.13**	187.97
	NIB	26:46:52	32:23:17	33:59:49	34:11:42	230.01	306.97	329.94	332.92
	AIB	16:43:01	18:49:39	19:27:26	19:33:35	116.76	155.65	168.29	**170.55**
30 mol%	RB	18:21:24	24:40:11	34:16:50	43:43:46	288.33	389.34	543.12	694.30
	RB-bB	**12:00:56**	**13:26:41**	**15:02:01**	**16:26:46**	**144.19**	**161.34**	**180.40**	**197.35**
	NIB	47:22:35	49:07:34	50:11:51	49:44:52	497.12	523.25	539.66	532.60
	AIB	27:37:40	28:37:47	29:01:28	28:56:06	281.84	300.10	308.77	305.89
50 mol%	RB	16:20:11	18:17:55	21:17:25	24:14:16	240.01	269.44	314.32	358.53
	RB-bB	**15:05:28**	**15:37:38**	**16:14:32**	**16:46:41**	**181.09**	**187.53**	**194.91**	**201.61**
	NIB	46:09:29	46:35:04	46:37:40	46:41:08	504.34	511.59	512.78	513.63
	AIB	34:00:51	34:22:49	46:22:14	46:26:19	373.86	380.55	523.51	515.59
70 mol%	RB	23:41:08	30:14:05	40:20:08	50:17:31	350.25	448.48	600.00	749.34
	RB-bB	**19:26:47**	**21:34:31**	24:27:36	27:13:42	**194.46**	**215.75**	244.60	272.28
	NIB	35:07:17	35:32:40	37:13:54	42:08:51	363.16	370.57	387.81	435.82
	AIB	22:05:03	22:20:47	**22:28:53**	**22:37:23**	227.36	233.06	**235.40**	**238.08**
80 mol%	RB	23:24:21	36:10:07	55:55:07	67:33:00	346.05	537.49	833.74	1126.24
	RB-bB	**15:13:04**	**19:08:26**	**24:24:43**	29:28:05	**152.18**	**191.41**	244.12	294.68
	NIB	34:16:19	35:59:43	36:52:43	37:31:44	308.51	331.43	341.26	347.30
	AIB	24:15:19	25:21:06	25:55:31	**26:16:00**	204.21	220.42	**227.03**	**229.95**
90 mol%	RB	14:32:35	32:22:51	60:25:04	88:06:50	213.11	480.67	901.23	1316.67
	RB-bB	**12:55:04**	**20:44:27**	31:13:54	41:17:05	**90.42**	**145.19**	218.62	288.99
	NIB	22:00:41	24:51:53	28:14:42	33:51:44	144.88	179.56	208.39	251.53
	AIB	19:16:37	22:03:36	**23:15:18**	**24:33:31**	116.92	150.37	**162.60**	**171.90**

A.5.3 Comparison of RB-bB4x, NIB4x, AIB4x - batch time

Ambient pressure batch (P = 1,015 bar).

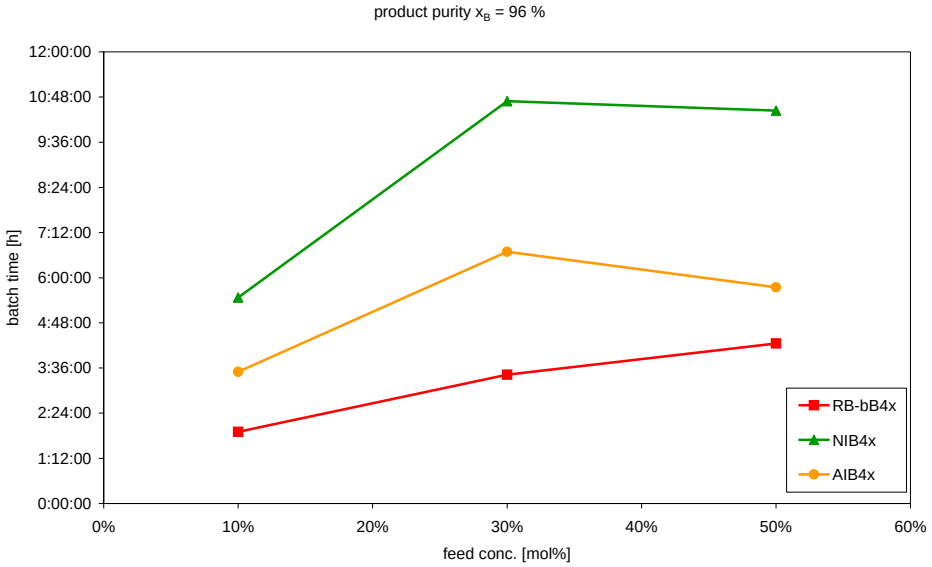

Fig. A.17 Comparison concerning the batch time for different structures (RB-bB4x, NIB4x, AIB4x): ambient pressure, product purity 96 mol% water, feed conc. 10 mol%, 30 mol%, 50 mol% ACN.

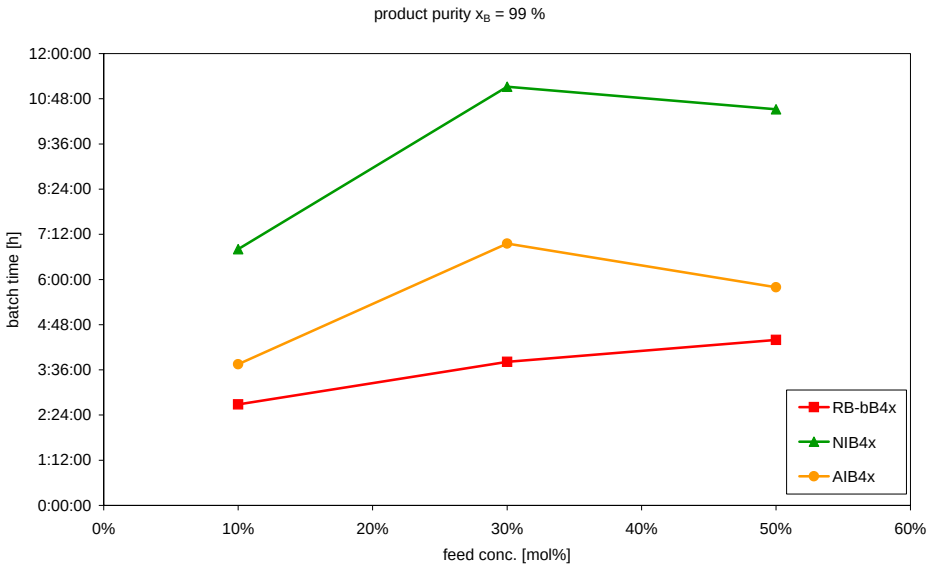

Fig. A.18 Comparison concerning the batch time for different structures (RB-bB4x, NIB4x, AIB4x): ambient pressure, product purity 99 mol% water, feed conc. 10 mol%, 30 mol%, 50 mol% ACN.

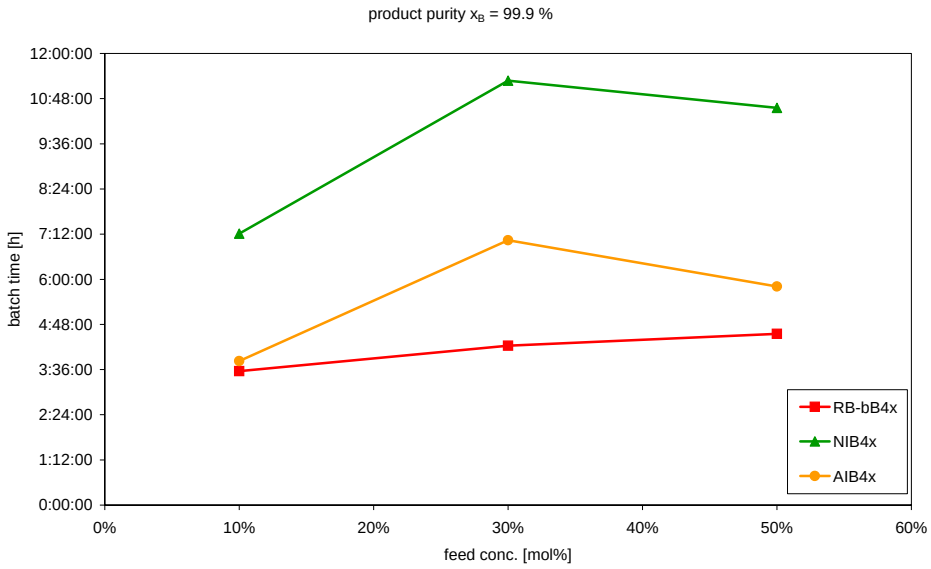

Fig. A.19 Comparison concerning the batch time for different structures (RB-bB4x, NIB4x, AIB4x): ambient pressure, product purity 99,9 mol% water, feed conc. 10 mol%, 30 mol%, 50 mol% ACN.

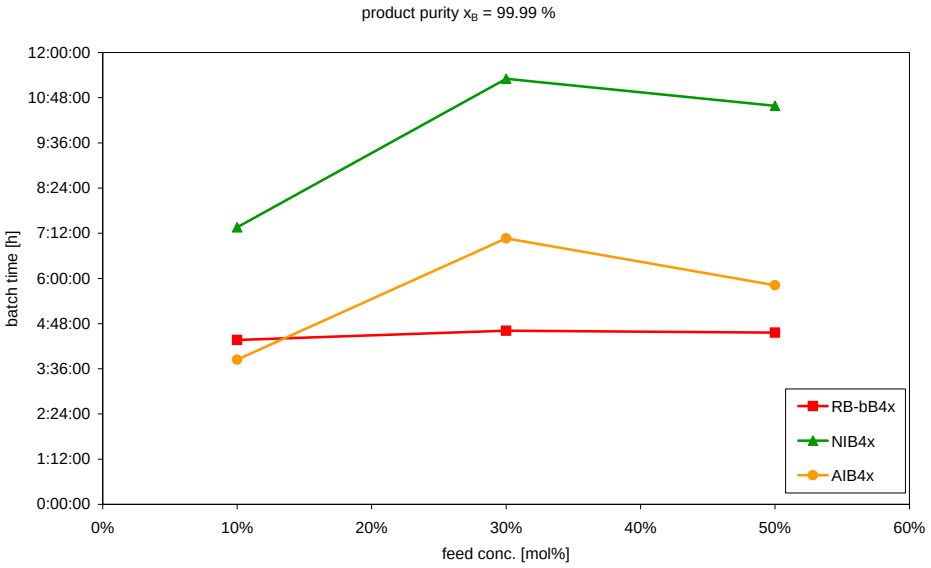

Fig. A.20 Comparison concerning the batch time for different structures (RB-bB4x, NIB4x, AIB4x): ambient pressure, product purity 99,99 mol% water, feed conc. 10 mol%, 30 mol%, 50 mol% ACN.

High pressure batch (P = 3,5 bar).

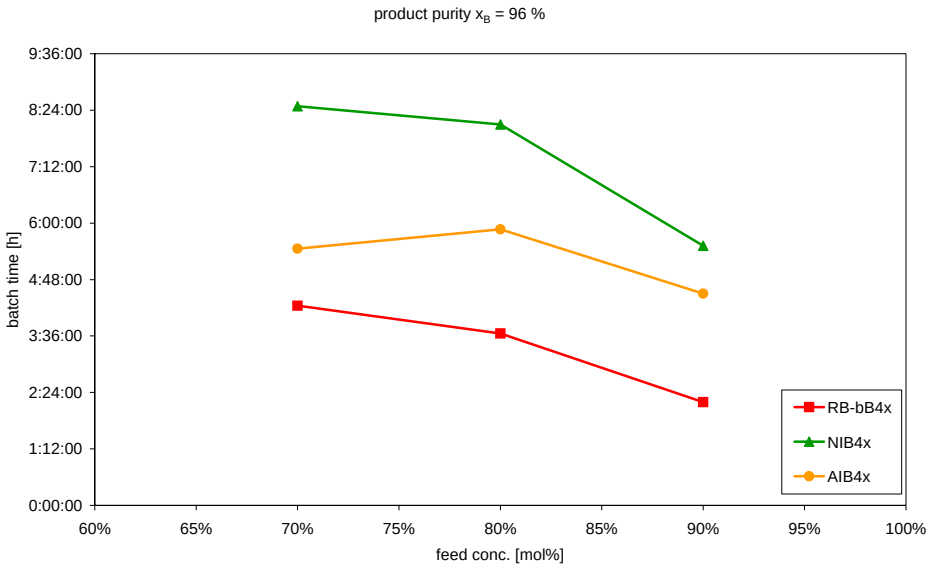

Fig. A.21 Comparison concerning the batch time for different structures (RB-bB4x, NIB4x, AIB4x): high pressure, product purity 96 mol% water, feed conc. 70 mol%, 80 mol%, 90 mol% ACN.

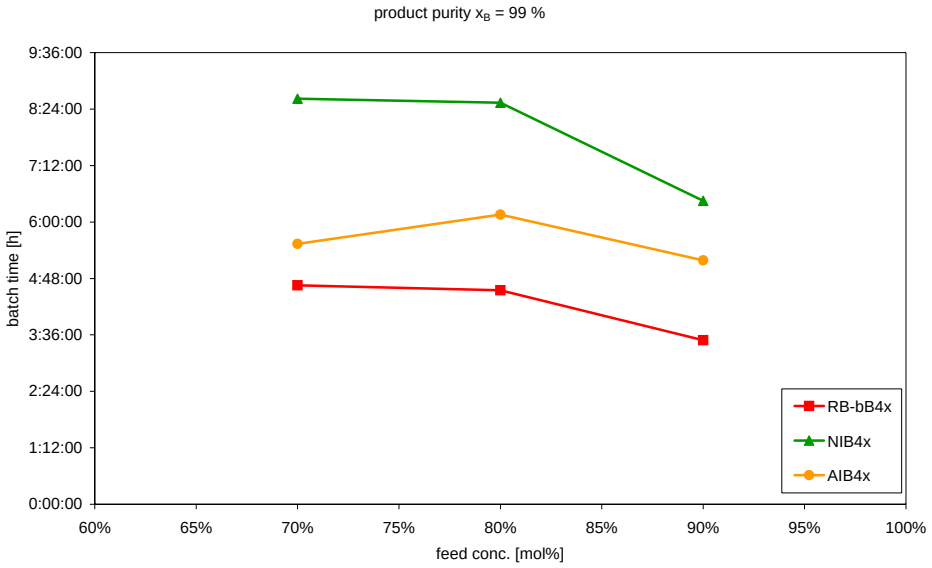

Fig. A.22 Comparison concerning the batch time for different structures (RB-bB4x, NIB4x, AIB4x): high pressure, product purity 99 mol% water, feed conc. 70 mol%, 80 mol%, 90 mol% ACN.

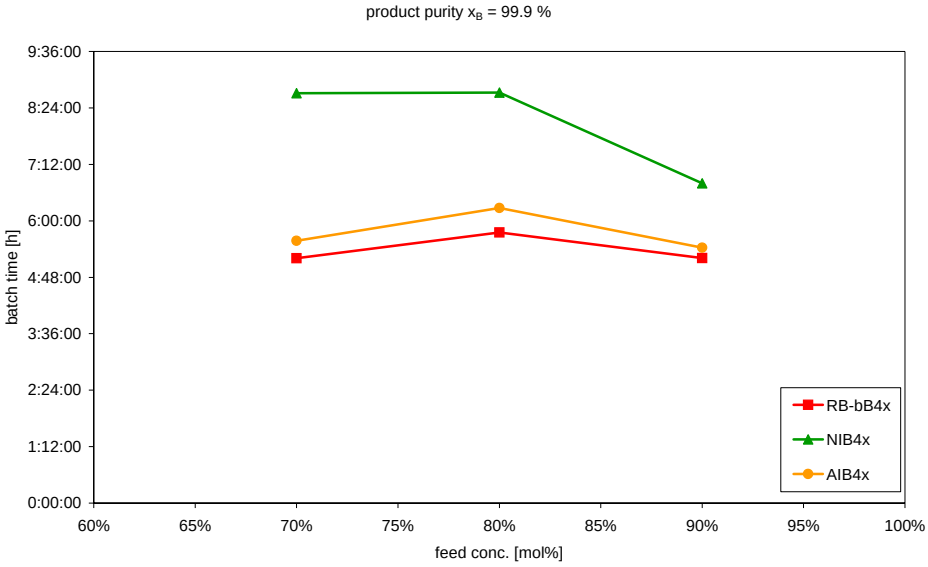

Fig. A.23 Comparison concerning the batch time for different structures (RB-bB4x, NIB4x, AIB4x): high pressure, product purity 99,9 mol% water, feed conc. 70 mol%, 80 mol%, 90 mol% ACN.

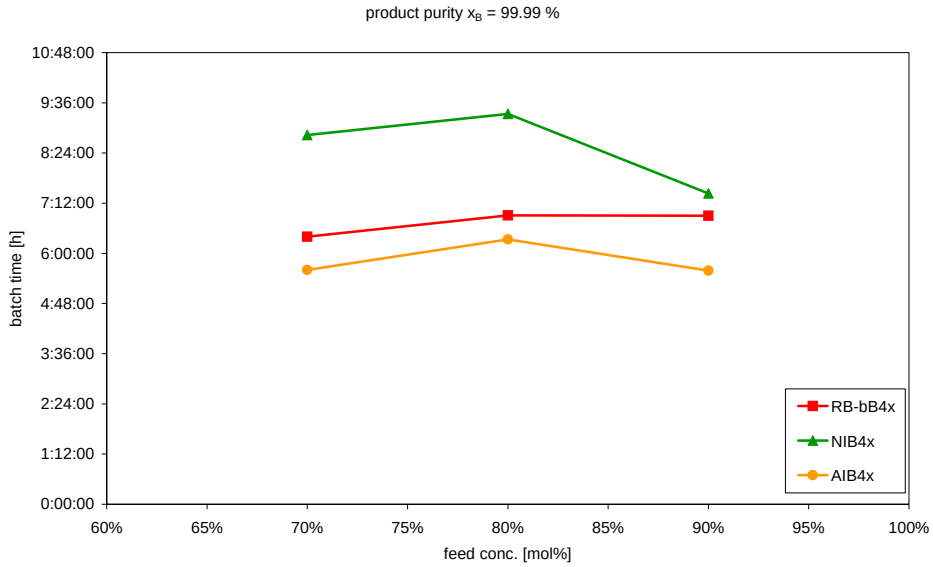

Fig. A.24 Comparison concerning the batch time for different structures (RB-bB4x, NIB4x, AIB4x): high pressure, product purity 99,99 mol% water, feed conc. 70 mol%, 80 mol%, 90 mol% ACN.

A.5.4 Comparison of RB-bB4x, NIB4x, AIB4x - energy consumption

Ambient pressure batch (P = 1,015 bar).

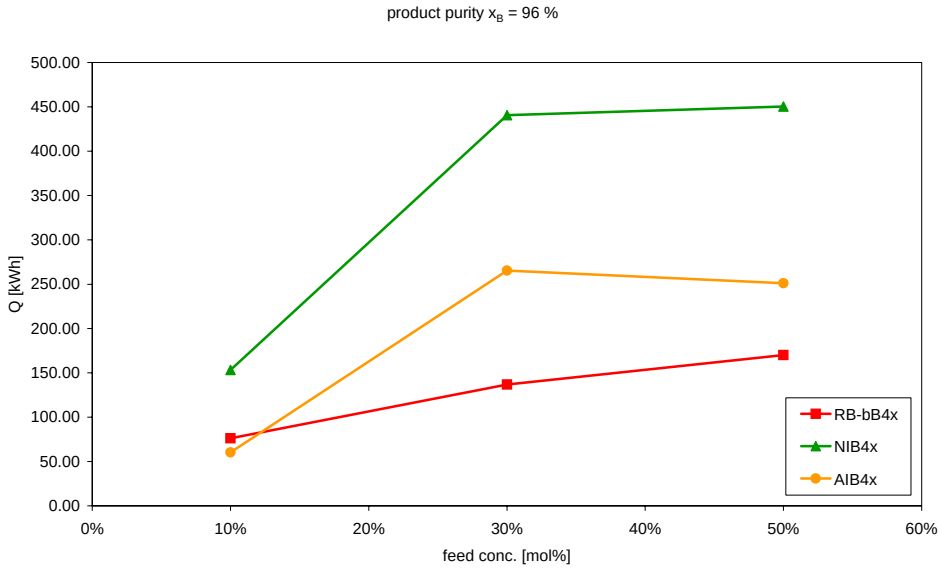

Fig. A.25 Comparison concerning the energy consumption for different structures (RB-bB4x, NIB4x, AIB4x): ambient pressure, product purity 96 mol% water, feed conc. 10 mol%, 30 mol%, 50 mol% ACN.

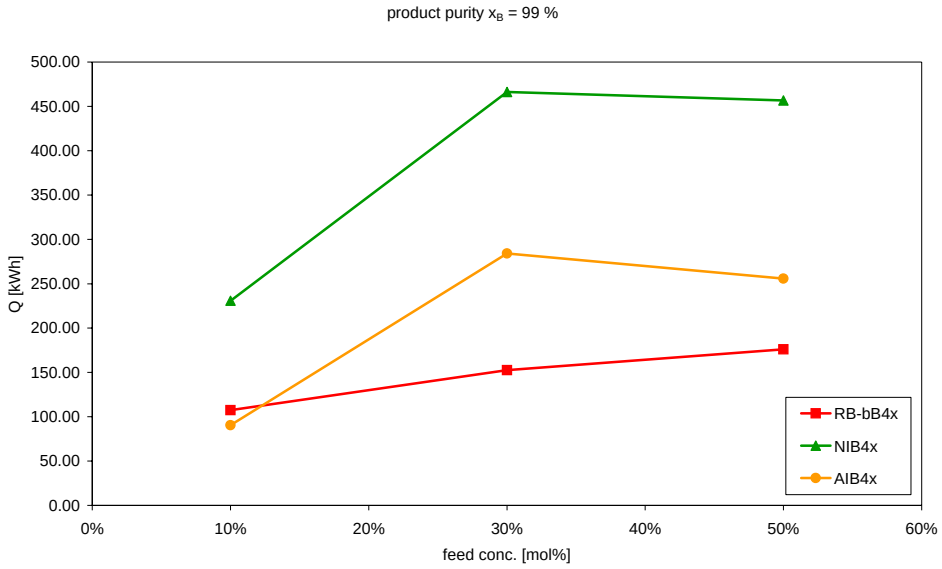

Fig. A.26 Comparison concerning the energy consumption for different structures (RB-bB4x, NIB4x, AIB4x): ambient pressure, product purity 99 mol% water, feed conc. 10 mol%, 30 mol%, 50 mol% ACN.

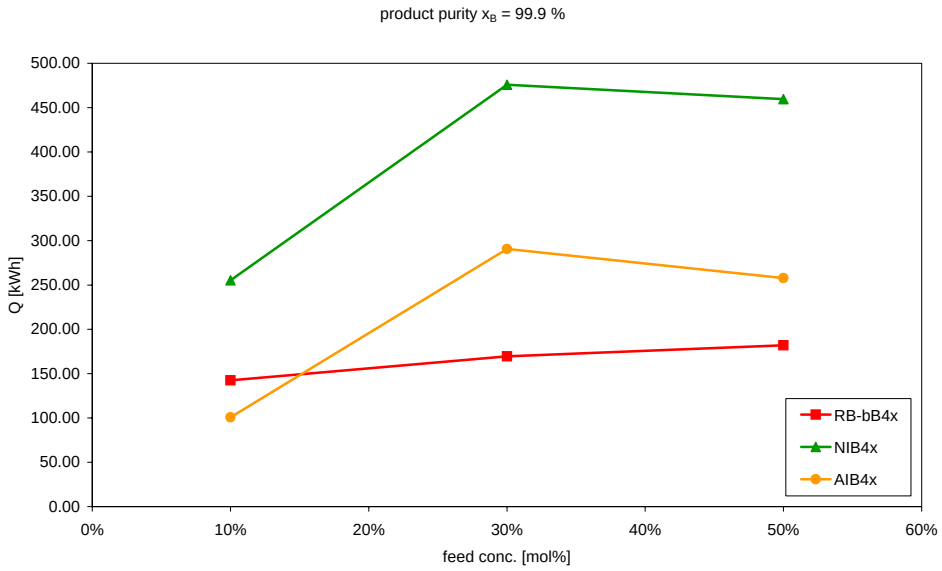

Fig. A.27 Comparison concerning the energy consumption for different structures (RB-bB4x, NIB4x, AIB4x): ambient pressure, product purity 99,9 mol% water, feed conc. 10 mol%, 30 mol%, 50 mol% ACN.

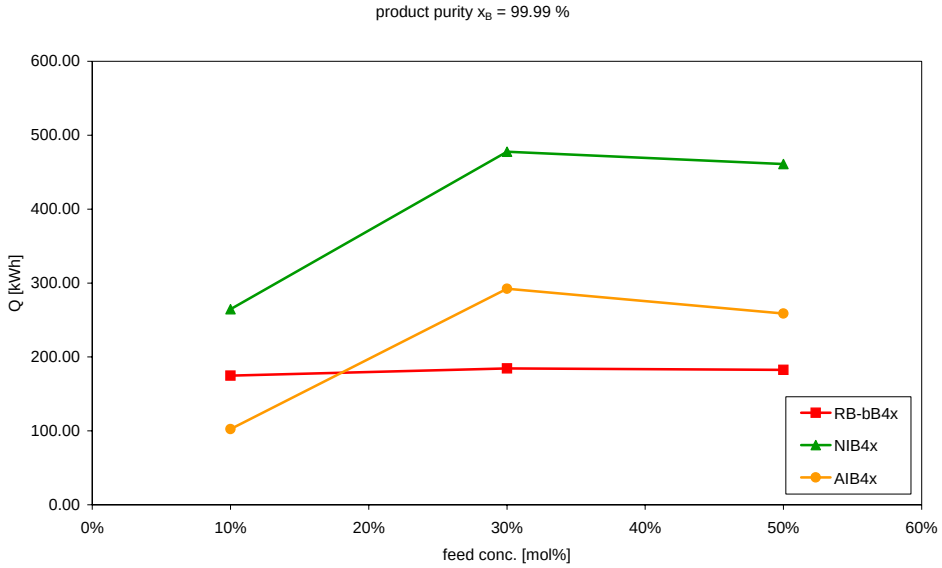

Fig. A.28 Comparison concerning the energy consumption for different structures (RB-bB4x, NIB4x, AIB4x): ambient pressure, product purity 99,99 mol% water, feed conc. 10 mol%, 30 mol%, 50 mol% ACN.

High pressure batch (P = 3,5 bar).

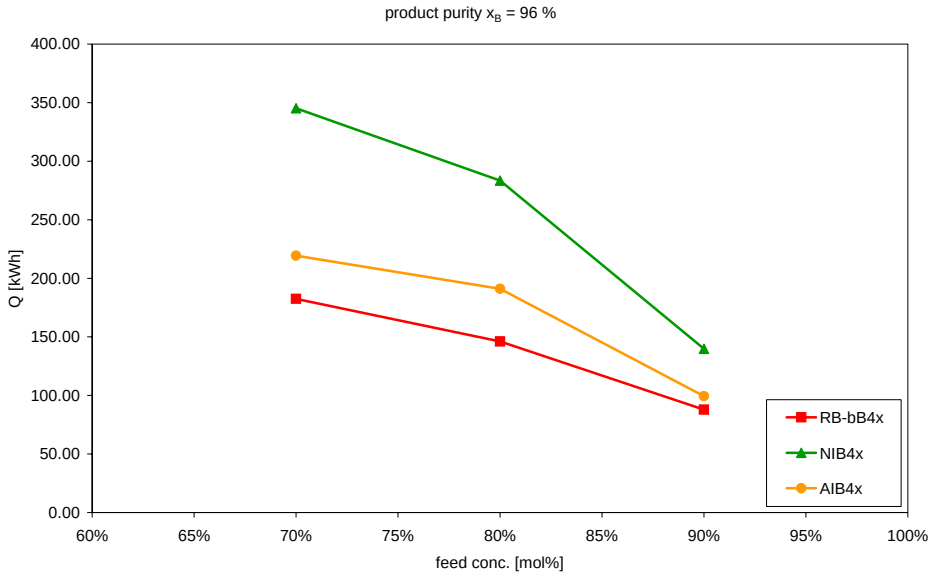

Fig. A.29 Comparison concerning the energy consumption for different structures (RB-bB4x, NIB4x, AIB4x): high pressure, product purity 96 mol% water, feed conc. 70 mol%, 80 mol%, 90 mol% ACN.

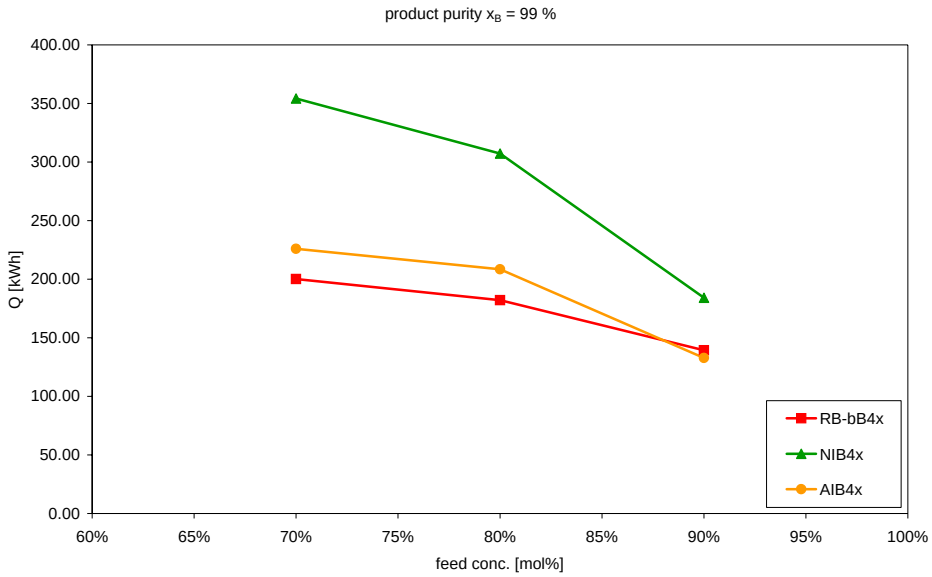

Fig. A.30 Comparison concerning the energy consumption for different structures (RB-bB4x, NIB4x, AIB4x): high pressure, product purity 99 mol% water, feed conc. 70 mol%, 80 mol%, 90 mol% ACN.

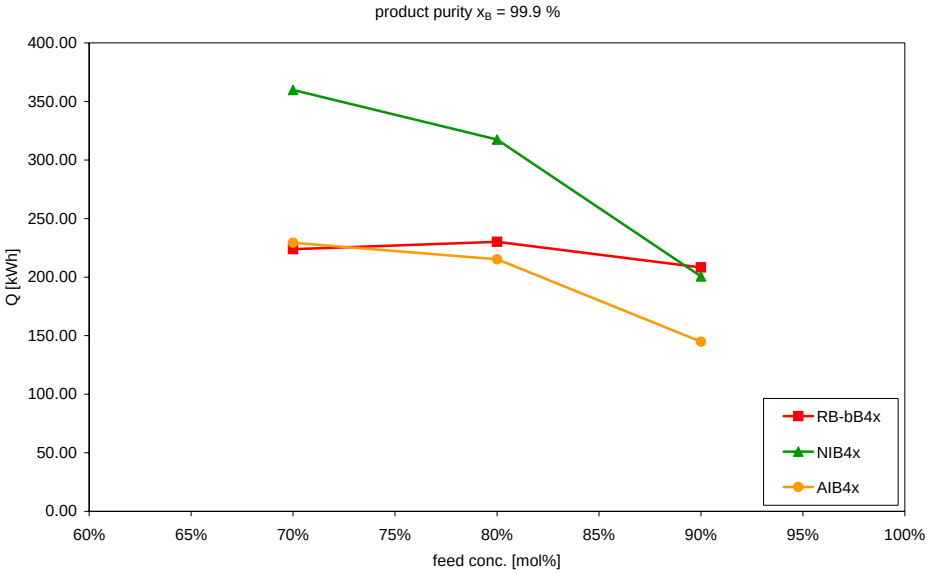

Fig. A.31 Comparison concerning the energy consumption for different structures (RB-bB4x, NIB4x, AIB4x): high pressure, product purity 99,9 mol% water, feed conc. 70 mol%, 80 mol%, 90 mol% ACN.

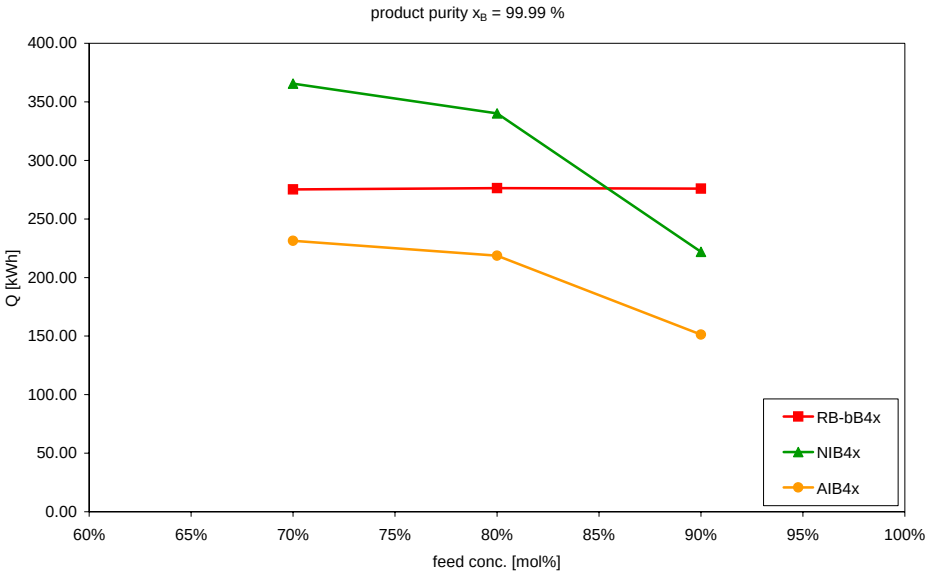

Fig. A.32 Comparison concerning the energy consumption for different structures (RB-bB4x, NIB4x, AIB4x): high pressure, product purity 99,99 mol% water, feed conc. 70 mol%, 80 mol%, 90 mol% ACN.

Table A.11. Overview about the batch times and energy consumption for different structures (RB-bB4x, NIB4x, AIB4x) with quad feed flow (feed flow 200 l/h)

Feed Conc. (ACN)	Bottom conc. (water)	time				Q [kwh]			
		0.96	0.99	0.999	0.9999	0.96	0.99	0.999	0.9999
10 mol%	RB-bB4x	**1:54:17**	**2:40:59**	**3:33:32**	4:22:02	76.19	107.32	142.36	174.69
	NIB4x	5:28:36	6:48:13	7:12:49	7:21:36	153.25	230.76	255.24	264.69
	AIB4x	3:29:47	3:44:50	3:49:38	**3:50:40**	**60.22**	**90.41**	**100.75**	**102.38**
30 mol%	RB-bB4x	**3:25:17**	**3:48:43**	**4:14:08**	**4:36:43**	**136.85**	**152.48**	**169.42**	**184.48**
	NIB4x	10:41:31	11:07:06	11:16:32	11:18:15	440.55	466.28	475.76	477.55
	AIB4x	6:41:30	6:57:11	7:02:27	7:03:57	265.38	284.13	290.67	292.39
50 mol%	RB-bB4x	**4:15:04**	**4:23:46**	**4:32:48**	**4:33:43**	**170.05**	**175.85**	**181.86**	**182.48**
	NIB4x	10:26:17	10:31:11	10:33:24	10:34:59	450.45	456.77	459.55	461.07
	AIB4x	5:44:57	5:47:35	5:48:42	5:49:17	251.12	255.89	257.92	258.74
70 mol%	RB-bB4x	**4:14:44**	**4:39:17**	**5:12:20**	6:24:01	**182.56**	**200.15**	**223.84**	275.21
	NIB4x	8:29:10	8:37:11	8:42:47	8:49:46	345.27	354.24	359.83	365.57
	AIB4x	5:27:31	5:32:06	5:34:41	**5:36:22**	219.36	225.93	229.33	**231.47**
80 mol%	RB-bB4x	**3:39:03**	**4:33:05**	**5:45:15**	6:54:38	**146.04**	**182.06**	230.17	276.42
	NIB4x	8:05:45	8:32:02	8:43:34	9:20:06	283.45	307.23	317.42	340.10
	AIB4x	5:52:11	6:09:35	6:16:32	**6:20:10**	191.06	208.42	**215.31**	**218.70**
90 mol%	RB-bB4x	**2:11:41**	**3:29:05**	**5:12:34**	6:54:01	**87.78**	139.38	208.38	276.01
	NIB4x	5:31:09	6:27:01	6:47:50	7:25:54	139.72	184.18	200.73	222.04
	AIB4x	4:30:08	5:11:08	5:25:48	**5:35:25**	99.35	**132.82**	**144.77**	**151.22**

A.6 Attended Diploma thesis

Pressure swing distillation. *Florian Forner*: Entwicklung eines dynamischen Modells für die Trennung homogener azeotroper Gemische in stofflich und energetisch gekoppelten Destillationskolonnen (Diplomarbeit), 2003, TU-Berlin

Khaled Briki: Experimentelle Validierung des gProms™-Modells zur Simulation der Zweitdruck-Rektifikation (Diplomarbeit), 2004, TU-Berlin

Hans Forster: Experimentelle Validierung eines Modells zur Trennung homogener azeotroper Stoffsysteme mittels inversem Zweidruckbatchverfahren (Studienarbeit), 2005, TU-Berlin

Gabriel Hopfenmüller: Theoretische und experimentelle Analyse des Betriebsverhaltens eines gekoppelten Zweidruckkolonnensystems zur Trennung homogener azeotroper Gemische (Diplomarbeit), 2004, TU-Berlin

Stefan Platzk: Experimentelle Validierung regulärer und inverser Zweidruckbatchmodelle zur Trennung homogener azeotroper Stoffgemische (Studienarbeit), 2005, TU-Berlin

Roman Helzyk: Theoretische Untersuchung der regulären und inversen Zweidruckbatchrektifikation zur Trennung homogener azeotroper Stoffgemische (Studienarbeit), 2005, TU-Berlin

Dennis v. Ahnen: Entwicklung von Anfahrstrategien für das energetisch und stofflich gekoppelte Zweidruckkolonnensystem (Diplomarbeit), 2006, TU-Berlin

Manuel Behmer: Wirtschaftlichkeitsanalyse des Zweidruckverfahrens zur Trennung homogener azeotroper Gemische (Studienarbeit), 2007, TU-Berlin

Hybrid prozess. *Peter Mues*: Planung einer Hybridanlage zur Trennung azeotroper Gemische (Studienarbeit), 2006, TU-Berlin

Nikolai Jiltsov: Planung und Inbetriebnahme einer Hybridanlage (Studienarbeit), 2007, TU-Berlin

e-learning. *Alexander Grote*: Entwicklung von Methoden zur Erstellung und Implementierung von multimedialen Lernumgebungen für die Prozesswissenschaften (Diplomarbeit), 2003 TU-Berlin

Diethmar Richter: Planung, Aufbau und Inbetriebnahme einer Bodenkolonne für Lehrzwecke (Studienarbeit), 2003, TU-Berlin

Stefan Siedler: Programmierung eines Java basierten Web-front-ends zur Steuerung und Beobachtung einer Online-Kolonne (Diplomarbeit), 2004, TU-Berlin

Hendrik: Integration der Online-Kolonne in die Lehre des Fachgebiets DBTA (Diplomarbeit), 2003, TU-Berlin

B. References

[Abu-Eishah 1984] Abu-Eishah, S. I. & Luyben, W. L., 1984, Design and Control of a Two-Column Azeotropic Distillation System, Ind. Eng. Chem. Process Des. Dev. 24, pp. 132 - 140

[v. Ahnen 2006] v. Ahnen, Entwicklung von Anfahrstrategien für das energetisch und stofflich gekoppelte Zweidruckverfahren, TU-Berlin, 2006, Diplom Thesis

[Barakat 2006] Barakat, T., Fraga, F. & Sørensen, E., 2006, Multi-objective Optimisation of Hybrid Batch Distillation/ Pervaporation Processes, AIChE Annual Meeting San Francisco, USA

[Barolo 1993] Barolo, M. & Trotta, A., 1993, Computer Control of a Distillation Column Startup: Development of Two Process-model-based Controllers, The first Conference on Chemical and Process Engineering, Firenze (Italy)

[Barolo 1994] Barolo, M., Guarise, G. B., Rienzi, S. A. & Trotta, A., 1994, Nonlinear Model Based Start-up and Operation of a Distillation Column: An Experimental Study, Ind. Eng. Chem. Res., Vol. 33, pp. 3160 - 3167

[Betlem 1998] Betlem, B. H. L., Rijnsdorp, J. E. & Azink, R. F., 1998, Influence of the Tray Hydraulics on Tray Column Dynamics, Chem. Eng. Science, Vol. 53, No. 23, pp. 3991 - 4003

[Bernot 1991] Bernot, C., Doherty, M. F. & Malone, M. F., 1991, Feasibility and Separation Sequencing in Multicomponent Batch Distillation, Chem. Eng. Sci., Vol. 46, No. 5/6, 1311 - 1326

[Beste 2005] Beste, Y. A., Eggersmann, M. & Schoenmakers, H., 2005, Extraktivdestillation mit ionische Flüssigkeiten, Chem. Ing. Tech., 77, No.11, pp. 1800 - 1808

[Braun 1993] Braun, H.-H., Eckwert, K. & Reins, G., 1993, Validierung nutzt Energiereserven im Industriekraftwerk, BWK, Bd. 45, Nr. 7/8, pp. 359 - 361

[Briki 2004] Briki, K., 2004, Experimentelle Validierung des gProms™ - Modells zur Simulation der Zweitdruck-Rektifikation, TU-Berlin, Diplomathesis

[Buckley 1964] Buckley, Techniques of process control, Wiley, 1964

[Chem 2000] ChemCAD 5.1.4 by Chemstation, Simulation and Properties Package

[CurveExp 2005] http://curveexpert.webhop.biz/, checked 13. August 2007

[Darton 1992] Darton, R. C., 1992, Distillation and Absorption Technology: Current Market and New Developments, Trans IchemE Vol. 70. Part A. Sept 1992 U.S. Department of energy, Washington DC, pp. 435 - 438

[DIN-1319 1995] DIN 1319-1, DIN 1319-3, 1995, Grundlagen der Meßtechnik, Deutsche Norm

[Doherty 1985] Doherty, M F. & Caldarola, G. A., 1985, Design and Synthesis of Homogeneous Azeotropic Distillation. 3. The Sequencing of Columns for Azeotropic and Extractive Distillations, Ind. Eng. Chem. Fundam. 24, pp. 474 - 485

[Düssel 1998] Düssel, R., Weidlich, U., Warter, M. & Stichlmair, J., 1998, Systematisierung der Azeotroprektifikation und thermodynamische Kriterien zur Entrainerauswahl, GVC-Jahrestagung '98, Freiburg, 30.9.-2.10.1998

[Düssel 2000] Düssel, R. & Warter, W., 2000, Batch-Rektifikation azeotroper Gemische in Verstärker- und Abtriebskolonnen, Chem. Ing. Tech., Vol. 72, No. 7, pp. 675 - 682

[Fabro 2005] Fabro, J. A., Arruda, L. V. R., & Neves Jr., F.N., 2005, Startup of a Distillation Column Using Intelligent Control Techniques, Comp. Chem. Engng., Vol. 30, pp. 309 - 320

[Flender 1997] Flender, M., Li, P., Wozny, G. & Fieg, G., 1997, Modellgestützte Entwicklung einer zeitoptimalen Produktwechselstrategie für Rektifikationskolonnen. VDI Jahrbuch Verfahrenstechnik und Chemieingenieurwesen, pp. 86 - 101

[Flender 1998] Flender, M., Zeitoptimale Strategien für Anfahrvorgänge und Produktwechselvorgängen an Rektifizieranlagen, VDI Fortschritts-berichte Reihe 3, Nr. 610, VDI-Verlag GmbH Düsseldorf

[Forner 2006] Forner, F., Meyer, M., Repke, J.-U. & Wozny, G., 2006, Comparison of the Start-up of Reactive Distillation in Packed and Tray Towers, in Proceedings of 16th ESCAPE and 9th Int. Sym. on Proc. Sys. Eng., W. Marquardt, C. Pantelides (Editors), pp. 137 - 142

[Forner 2007] Forner, F., Döker, D., Gmehling, J., Repke, J.-U. & Wozny, G., 2007, Anfahrstrategien für die Reaktivrektifikation in Boden- und Packungskolonnen, Chemie Ingenieur Technik, 79, No. 4, pp. 367 - 376

[Forster 1955] Forster, H.K & Zuber, N, 1955, Dynamics of Vapour Bubbles and Boiling Heat Transfer. AIChE Journal 5, pp. 531 - 535

[Frank 1997] Frank, T.C., 1997, Break Azeotropes with Pressure - Swing Sensitive Distillation, Chem. Eng. Prog., Apr., pp. 52 - 63

[Furlonge 1999] Furlonge, H.I., Pantelides, C.C. & Sørensen E., 1999, Optimal Operation of Multivessel Batch Distillation Columns, AIChE Journal April 1999, Vol. 45, No. 4, pp. 781 - 801

[Furter 1972] Furter W., 1972, Extractive Distillation by Salt Effect, Adv. Chem. Series 115, 35

[Ganguly 1993] Ganguly, S. & Saraf, D. N., 1993, Start-up of a Distillation Column using Nonlinear Analytical Model Predictive Contro, Ind. Eng. Chem. Res. 32, Nr. 8, pp. 1667 - 1675

[Gani 1987] Gani, R., Ruiz, A. & Cameron, I., 1987, Studies in the Dynamic of Start-up and Shut-down Operations of Distillation Columns, Proceedings of XVIII Congress "The use of computers in chemical Engineering", Italy, pp. 541 - 546

[Gani 1992] Gani, R. & Cameron, I.T., 1992, Modelling for Dynamic Simulation of Chemical Processes: The Index Problem, Chem. Eng. Sci., Vol. 47, No.5, pp. 1311 - 1315

[Gmehling 1996] Gmehling, J. & Brehm, A., 1996, Grundoperationen: Lehrbuch der technischen Chemie, Band 2. Georg Thieme Verlag, Stuttgart

[Gmehlling 1981] Gmehling, J., Onken, U. & Arlt, W., 1981, Vapour-Liquid Equilibrium Data Collection, Part 1a Aqueous-Organic Systems (Supplement 1), DECHEMA

[Gmehling 1992] Gmehling, J. & Kolbe, J., 1992, Thermodynamik, VCH Verlag Weinheim

[Gmehling 2004] Gmehling, J., 2004, Azeotropic data, Wiley-VCH Verlag

[Gnielinski 1994] Gnielinski, V., 1994, Wärmeübergang bei der Strömung durch Rohre, Kap. Gb, VDI Wärmeatlas, 7. Auflage, VDI-Verlag, Düsseldorf

[Grassmann 1997] Grassmann P., Widmer F. & Sinn H., 1997, Einführung in die Thermische Verfahrenstechnik, 3.Auflage, Walter de Gruyter, Berlin, New York

[Gruetzmann 2006] Gruetzmann, S., Kapala, T. & Fieg G., 2006, Dynamic Modelling of Complex Batch Distillation Starting from Ambient Conditions, in Proceedings of 16th ESCAPE and 9th Int. Sym. on Proc. Sys. Eng., W. Marquardt, C. Pantelides (Editors), pp. 865 - 870

[Gruetzmann 2007] Gruetzmann, S. & Fieg G., 2007, Integrale Analyse der Batch-Rektifikation mit Mittelbehälter, Chemie Ingenieur Technik, 79, No. 10, pp. 1613 - 1624

[Güttinger 1997] Güttinger, T.E., Morari, M. & Dorn, C., 1997, Experimental Study of Multiple Steady States in Homogenous Azeotropic Distillation, Ing. Eng. Chem. Res. Vol. 36, pp. 794 - 802

[Hamad 2002] Hamad, A. & Dunn, R.D., 2002, Energy Optimization of Pressure-Swing Azeotropic Distillation, Ing. Eng. Chem. Res. Vol. 41, pp. 6082 - 6093

[Hasebe 1992] Hasebe, S., Abdul Aziz, B., Hashimoto, I. & Watanbe, T., 1992, Optimal Design and Operation of Complex Batch Distillation Column, Proceeding of the IPAC Workshop, London

[Hasebe 1996] Hasebe, S., Kurooka, T., Aziz, B. A. & Hashimoto, I., 1996, Simultaneous Separation of light and heavy Impurities by a Complex Batch Distillation Column, J. of Chem. Eng. of Japan, Vol. 29, No. 6, pp. 1000 - 1006

[Hasebe 1999] Hasebe, S., Noda, M. & Hashimoto, I., 1999, Optimal Operation Policy for Total Reflux and Multi-effect Batch Distillation Systems, Comp. Chem. Engng. Vol 23, pp. 523 - 532

[Hoffmann 1964] Hoffmann E. J., 1964, Azeotropic and Extractive Distillation, Wiley, New York

[Horsley 1973] Horsley, L.H., & Gould, R.F. (eds.), 1973, Advances in Chemistry 116, American Chemical Society, Washington

[Horwitz 1997] Horwitz, B. A., 1997, Optimize Pressure-Sensitive Distillation, Chem. Eng. Prog. April, pp. 47 - 51

[Humphrey 1992] Humphrey, J. L. & Seibert, A. F., 1992, New Horizons in Distillation, Chem. Eng., Vol. 99, No. 12, pp. 86 - 98

[Jacobsen 1990] Jacobsen, E. W. & Skogestad, S., 1990, Dynamics and Control of Unstable Distillation Columns, Presented at 40th Canadian Chemical Engineering Conference, Halifax, July 15 - 21

[Jork 2004] Jork, C., Seiler, M., Beste, J. A. & Arlt, W., 2004, Influence of Ionic Liquids on the phase behavior of aqueous azeotropic systems, J. Chem. Eng. Data, 49, pp. 852 - 857

[King 1987] King, C. J., 1987, Separation & Purification - Critical Needs and Opportunities, National Research Council, National Academy Press, Washington DC

[Kister 1990] Kister, H. Z., 1990, Distillation Operation. McGraw Hill, New York, New York

[Klein 2006] Klein, A., del Pozo - Gómez, M. T., Repke, J.-U. & Wozny, G., 2006, Hybrid-Pervaporation-Distillation Processes - a Novel Heat -Integration Approach, AIChE Annual Meeting San Francisco, USA

[Knapp 1990] Knapp, J.P. & Doherty, M.F., 1990, Thermal Integration of Homogeneous Azeotropic Distillation Sequences, AIChE Journal, Vol. 36, No. 7, pp. 969 -984

[Knapp 1992] Knapp, J.P. & Doherty, M.F., 1992, A New Pressure-Swing Distillation Process for Separating Homogenous Azeotropic Mixtures, Ind. Eng. Chem. Res., Vol. 31, pp. 346 - 357

[Kreis 2005] Kreis, P. & Górak, A., 2005, Prozessanalyse hybrider Trennverfahren am Beispiel der Kopplung von Rektifikation und Membrantrennung, Chem. Ing. Tech. 77, No. 11, pp. 1737 - 1748

[Kreis 2006] Kreis, P.; Górak, A., 2006, Process Analysis of Hybrid Separation Processes - Combination of Distillation and Pervaporation, Chem. Eng. Res. Design, Trans IChemE, Part A, 84(A7), pp. 595 - 600

[Kreul 1998] Kreul, L.U., Górak, A., Dittrich, C. & Barton, P. I., 1998, Dynamic Catalytic Distillation: Advanced Simulation and Experimental Validation, Comp. Chm. Eng., Vol. 22 Suppl., pp. S371 - S378

[Kruse 1995a] Kruse, C., 1995, Theoretische und experimentelle Entwicklung zeitoptimaler Anfahr- und Produktwechselstrategien für die Rektifikation. Fortschritt-Berichte Reihe 3, Nr. 420, VDI- Verlag

[Kruse 1995b] Kruse, C., Fieg, G., & Wozny, G., 1996, A New Time-optimal Strategy for Column Sart-up and Product Changeover, Journal of Process Control 6, pp. 187 - 193

[Lang 1996] Lang L., 1996, Dynamic Behavior and Operational Aspects of Heat-Integrated Distillation Processes, Chem. Eng. Technol. 19, pp. 489 - 497

[Lee 1999] Lee, M., Morari, M., Lee, M., Dorn, C. & Meski, G. A., 1999, Limit Cycle in Homogenous Azeotropic Distillation, Ing. Eng. Chem. Res., Vol. 38, pp. 2021 - 2027

[Lei 2005] Lei, Z., Biaohua, C. & Ding, Z., 2005, Special Distillation Processes, Elsevier

[Lelkes 1998] Lelkes, Z., Lang, P. & Otterbein, M., 1998, Feasibility and Sequencing Studies for Homoazeotropic Distillation in a Batch Rectifier with Continuous Entrainer Feeding, 1998, Comp. Chem. Eng., Vol 22, Suppl., pp. S653 -S656

[Lipnizki 1999] Lipnizki, F., Field, R.W. & Ten, P.-K., 1999, Pervaporation-based Hybrid Process: a Review of Process Design, Applications and Economics, Journal of Membrane Science, vol. 153, pp. 183-210

[Lipnizki 2001] Lipnizki, F. & Trägårdh, 2001, Modelling of Pervaporation: Models to Analyze and Predict the Mass Transfer in Pervaporation, Separation and Purifikation Methods, 30 (1), pp. 49 - 125

[Lockett 1986] Lockett, M. J., 1986, Distillation Tray Fundamentals, Cambridge University Press Cambridge, U.K.

[Lockhardt 1949] Lockhart, R.W & Martinelli, R.C., 1949, Proposed Correlation of Data for Isothermal Two-Phase, Two Component Flow in Pipes, Chem. Eng. Prog. 45(1), pp. 39 - 48

[Low 2005] Low, K.H. & Sørensen, E., 2005, Simultaneous Optimal Configuration, Design and Operation of Batch Distillation, AIChE Journal, Vol. 51, No. 6, pp. 170 - 1713

[Löwe 1999] Löwe, K., Wozny, G. & Gelbe, H., 1999, Startup of Heat- and Mass-Integrated Distillation Columns: An Experimental Study, Pres'99, 31.05 - 02.06. 1999, Budapest, Hungary, pp. 415 - 420

[Löwe 2001a] Löwe, K. & Wozny, G., 2001, A new Strategy for Product Switchover and Startup for a Heat- and Mass- Integrated Distillation System, Chem. Eng. and Proc. 40, pp. 295-302

[Löwe 2001b] Löwe, K., 2001, Theoretische und experimentelle Untersuchungen über das Anfahren und die Prozessführung energetisch und stofflich gekoppelter Destillationskolonnen, Fortschritt-Berichte Reihe 3, Nr. 678, VDI Verlag

[Luyben 1985] Luyben, W. L. & Cheng, H. C., 1985, Heat-Integrated Distillation Columns for Ternary Separations, Ind. Eng. Chem. Process Des. Dev., 24, pp. 707-713

[Luyben 2005] Luyben, W. L., 2005 Comparision of Pressure-Swing and Extractive-Distillation Methods for Methanol-Recovery Systems in the TAME Reactive-Distillation Process, Ind. Eng. Chem. Res., 44, pp. 5715 - 5725

[Matlab] www.mathworks.com

[Mutjaba 2004] Mutjaba, I.M., 2004, Batch Distillation - design and operation, Series on chemical engineering, Vol. 3, Imperial College Press, ISBN 1 86094 437

[Niggemann 2006] Niggemann, G., Gruetzmann, S. & Fieg, G., 2006, Distillation start-up of fully thermally coupled distillation columns: theoretical examinations, IChemE, Distillation & Absorption, Symposiums Series, No. 152, pp. 800 - 808

[Nusselt 1916] Nusselt, W., 1916, Die Oberflächenkondensation des Wasserdampfs, VDI Z. 60, pp. 542-546

[Onken 1975] Onken U., 1975, Thermische Verfahrenstechnik, Carl Hanser Verlag, München

[Oppenheimer 1997] Oppenheimer, O. & Sørensen, E., 1997, Comparative Energy Consumption in Batch and Continuous Distillation, Comp. Chem Eng, Vol. 21 Suppl., pp. S529 - S534

[Ozokwelu 2002] Ozokwelu, D., 2002, Chemicals-Projekt Fact Sheet, Office of Industrial Technologies

[OPC] OPC, OLE for Process control, www.opcfoundation.com

[Phimister 2000] Phimister, J. R. & Seider, W. D., 2000, Semi-continuous, Pressure- Swing Distillation, Ind. Eng. Chem. Res., 39, pp. 122-130

[Phimister 2001] Phimister, J. R. & Seider, W.D., 2001, Bridge the Gap with Semicontinuous Distillation, Chem. Eng. Proc., pp. 72 - 78

[Ponton 2007] Chemical Engineers Toolkit, *http://eweb.chemeng.ed.ac.uk/chemeng/*, checked 10.4.2007

[Porter 1995] Porter, K.E., 1995, Why Research is needed in Distillation, Trans IChemE, Vol. 73, Part A, May, pp. 357 - 362

[Pressly 1998] Pressly, T. G. & Ng, K.M., 1998, A Break-Even Analysis of Distillation - Membrane Hybrids, AIChE Journal, Vol. 44, No. 1, January, pp. 93 - 105

[PSE 2006] PSE (2006), gProms™ - Introductory User Guide, Process Systems Enterprise Ltd.

[Rautenbach 1996] Rautenbach, R. & Vier, J., 1996, Aufbereitung methanolhaltiger organischer Mischungen durch Kombination von Pervaporation und Rektifikation, GVC Jahrbuch, pp. 270 - 285

[Reepmeyer 2002] Reepmeyer, F., Repke, J.-U, Wozny, G., 2002, Analyse des Anfahrprozesses bei der Reaktivrektifikation, Chemie Ingenieur Technik, 74, No. 9, pp. 1253 - 1258

[Reepmeyer 2003] Reepmeyer, F., Repke, J.-U., Wozny, G., 2003, Analysis of the Startup Process for Reactive Distillation, Chem. Eng. Technol. (26), 1, pp. 81 - 86

[Reepmeyer 2004a] Reepmeyer, F., 2004, Dynamik und Anfahren Reaktiver Destillations-prozesse, Shaker Verlag Aachen

[Reepmeyer 2004b] Reepmeyer, F., Repke, J.-U. & Wozny, G., 2004, Time Optimal Start-up Strategies for Reactive Distillation Columns, Chem. Eng. Sci. Vol. 59, pp. 4339 - 4347

[Repke 2002] Repke, J.-U., 2002, Experimentelle und theoretische Analyse der Dreiphasenrektifikation in Packungs- und Bodenkolonnen, VDI-Fortschrittsberichte, Nr. 751, VDI - Verlag, ISBN 0178-9503

[Repke 2005a] Repke, J.-U., Forner, F. & Klein, A., Trennung homogener Azeotrope mittels Zweidruckrektifikation - eine Analyse des Betriebsverhaltens, Chemie Ingenieur Technik (77) No. 6, pp. 763 - 771

[Repke 2005b] Repke, J.-U., Forner, F. & Klein, A., 2005, Separation of Homogeneous Azeotropic Mixtures by Pressure Swing Distillation - Analysis of the Operation Performance, Chemical Engineering & Technology, 28(10), pp. 1151 - 1157

[Rev 2003] Rév, E., Lelkes, Z., Varga, V., Stéger, C. & Fonyó, Z., 2003, Separation of a Minimum Boiling Azeotrope in a Batch Extractive Rectifier with an Intermediate-boiling Entrainer, Ind. Eng. Chem. Res., Vol. 42, pp. 162 - 174

[Rix 1998] Rix, A., 1998, Modellierung und PRozessführung wärmeintegrierter Destillationskolonnen, VDI-Fortschrittsberichte, Nr. 549, VDI - Verlag, ISBN 0178-9503

[Robinson 1950] Robinson, C. S. & Gilliland, E. R., 1950, Elements of Fractional Distillation, 4th edn., McGraw-Hill, New York

[Rohsenow 1973] Rohsenow, W. M. & Hartnett, J. H., 1973, Handbook of Heat Transfer. McGraw Hill, New York

[Rowlinson 1969] Rowlinson, J. S., 1969, Liquids and Liquid Mixtures, Buttworth London

[Ruiz 1988] Ruiz, A., Cameron, I. & Gani, R., 1988, A Generalized Model for Distillation Columns - III, Study of Startup Operations, Comput. Chem. Engng., 12, No.1, pp. 1 - 14

[Sattler 1995] Sattler, K. & Feindt, H. J., 1995, Thermal Separation Prozesses, Principles and Design., VCH Verlagsgesellschaft mbH, Weinheim

[Scenna 2004] Scenna, N. J., Benz, S. J., Francesconi, J. A. & Rodriguez, N. H., 2004, Start-up of Homogeneous Azeotropic Distillation Columns with Multiple Steady States, Ind. Eng. Chem. Res., Vol. 43, pp. 553 - 565

[Seiler 2004] Seiler, M., Jork, C., Kavarnou, A., Arlt, W. & Hirsch, R., 2004, Separation of Azeotropic Mixtures Using Hyperbranched Polymers or Ionic Liquids, AIChE Journal October 2004, Vol. 50, No. 100, pp. 2439 - 2454

[Shinskey 1997] Shinskey, G., 1977, Distillation Control., McGraw-Hill, New York

[Skogestad 1992] Skogestad, S., 1992, Dynamics and Control of Distillation Columns - a Critical Survey, IFAC-Smposium DYCORD 1992, Maryland, Apr. 27-29

[Sloley 2001] Sloley, A. W., 2001, Effectively Control Column Pressure, Chem. Eng. Prog., January 2001, pp. 38 - 48

[Smith 1996] Smith, J. M., Van Ness, H. C. & Abbott, M. M., 1996, Introduction to Chemical Engineering Thermodynamics, McGraw-Hill

[SOP 2007] KLein, A., Barz, T., Skupin, M. & Wozny, G., 2007, Standard operation procedure (SOP) - Two Pressure Column System, Department of proscess and plant technology, TU-Berlin

[Sørensen 1994] Sørensen, E., 1994, Studies on optimal Operation and Control of Batch Distillation Columns, PhD Thesis, The Norwegian Institut of Technology, Universitiy of Trondheim, Norway

[Sørensen 1996] Sørensen, E. & Skogestad, S., 1996, Comparison of Regular and Inverted Batch Distillation, Chem. Eng. Sci., Vol. 51, No. 22, pp. 4949 - 4962

[Sørensen 1996] Sørensen, E. & Skogestad, S., 1996, Optimal Startup Procedure for Batch Distillation, Comp. Chem. Engng., Vol. 20 Suppl., pp. S1257 - S1262

[Sørensen 1997] Sørensen, E. & Prenzler, M., 1997, A Cyclic Operation Policy for Batch Distillation - Theory and Practice, Comp. Chem.. Eng., Vol. 21, Suppl., pp. S1215 - S1220

[Stichlmair 1978] Stichlmair, J. G., 1978, Grundlagen der Dimensionierung des Gas/ Flüssigkeits-Kontaktapparates Bodenkolonne, Verlag Chemie, Weinheim

[Stichlmair 1998] Stichlmair, J. G. & Fair, J. R., 1998, Distillation Principles and Practice, Wiley-VCH, Canada

[Strube 2004] Strube, J., Bäcker, W., Olf, G., Dikow, E., Gorak, A. & Franke, M., 2004, Thermodynamik im Prozessdesign: Trennprozesse/Gesamtprozess, Chemie Ingenieur Technik, 76, No. 9, p. 1344

[Tran 2005] Tran, T. K., 2005, Analyse des Anfahrens von Dreiphasenrektifikations-kolonnen, Shaker Verlag Aachen

[Unger 1995] Unger, J., Kröner, A. & Marquardt, W., 1995, Structural Analysis of Differential-algebraic Equation Systems - Theory and Applications, Comp. Chem. Eng., Vol 19, No. 8, pp. 867 - 882

[Varbanov 2006] Varbanov P., Klein A., Repke J.-U. & Wozny G.,2006, Startup Simulation of Heat-Integrated Two-Column System for Separation of Acetonitrile-Water Mixtures, IChemE, Distillation & Absorption, Symposiums Series, No. 152, pp. 945 - 953

[Varbanov 2006b] Varbanov P., Klein A., Repke J.-U., Wozny G., 2006, Optimal Startup of Mass- and Heat-integrated Two-column Distillation Systems, 11-th Workshop on Transport Phenomena in Two-Phase Flow", Sunny Beach Resort, Bulgaria

[Varbanov 2007] Varbanov P., Klein A., Repke J.-U., Wozny G., 2007, Optimisation of the Startup of Mass- and Heat-integrated Two-Column Distillation Systems, Chemical Engineering & Processing, submitted

[VCI 2006] Chemie in Zahlen, 2006, *http://www.vci.de/template_downloads/tmp_0/CHIZ_2006~DokNr~81447~p~101.pdf*, checked at 10.4.2007

[Wang 2003] Wang, L., Li, P., Wozny, G. & Wang, S., 2003, A Startup Model for Simulation of Batch Distillation Starting from a Cold State, Comp. Chem.. Eng., Vol. 27, pp. 1485 - 1497

[Warter 2002] Warter, M. & Stichlmair, J., 2002, Batchrektifikation mit Mittelbehälter, Chem. Ing. Tech., Vol. 74, No. 9, pp. 1195 - 1206

[Warter 2004] Warter, M. Demicoli, D. & Stichlmair, J., 2004, Operation of a **B**atch Distillation Column with a Middle Vessel: Experimental Results for the Separation of Zeotropic and Azeotropic Mixtures, Chem. Eng. And Proc., 43, pp. 273 - 289

[Wasylkiewicz 2003] Wasylkiewicz, S. K., Kobylka, L. C. & Castillo, F. J. L., 2003, Pressure Sensitive Analysis of Azeotrops, Ind. Eng. Chem. Res., 42 pp. 207 - 213

[Widagdo 1996] Widagdo, S. & Seider, W. D., 1996, Azeotropic Distillation, AIChE Journal, Vol. 42, No.1, pp 96 - 130

[Wijmans 1993] Wijmans, J. G. & Baker, R. W., 1993, A Simple Predictive Treatment of the Permeation Process in Pervaporation, Journal of Membrane Science, Vol. 79, pp. 101 - 113

[Wittgens 2000] Wittgens, B. & Skogestad, S., 2000, Closed Operation of Multivessel batch distillation: Experimental Verification, AIChE Journal, Vol. 46, No. 6, pp. 1209 - 1217

[Wozny 2004] Wozny, G. & Li, P., 2004, Optimization and Experimental Verification of Start-up Policies for Distillation Columns, Comp. and Chem. Eng., 28, pp. 253 - 265

[Wusterhausen 2004] Wusterhausen, M., 2004, Modellierung und Simulation eines aus Rektifikation in Kombination mit Pervaporation bestehenden hybriden Trennprozesses, TU-Berlin, Diplomathesis

[Yamada 1981] Yamada, M., Fukui, H., Hokazono, Z. & Adica, O., 1981, Automatic by Computer, Comp. Aided Op. of Chem Proc., pp. 2859 - 2846

[Yasuoka 1987] Yasuoka, H., Nakanisshi, E. & Kunugita, E., 1987, Design of an On-line Startup System for a Distillation Column Based on a Simple Algorithm, Ind. Chem. Eng., 27, No. 3, pp. 466 - 472

[Zerry 2005] Zerry, R., Repke, J.-U., Wusterhausen, M. & Wozny, G, 2005, Novel heat integration concepts for hybrid distillation/pervaporation processes. PRES 05, 15.-18.05.2005, Giardini di Naxos, Italy; Chemical Engineering Transactions, pp. 219 - 224, Vol. 7, 2005, Proceedings of 8th Conference on PRES 05, ISBN 88-900775-8-1